

Bangor University

DOCTOR OF PHILOSOPHY

Synthesis and characterisation of organometallic compounds of B, Mn and Re

Brassington, David Steven

Award date:
2001

Awarding institution:
University of Wales, Bangor

[Link to publication](#)

General rights

Copyright and moral rights for the publications made accessible in the public portal are retained by the authors and/or other copyright owners and it is a condition of accessing publications that users recognise and abide by the legal requirements associated with these rights.

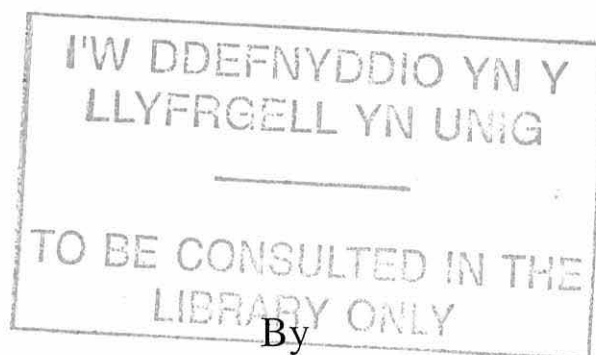
- Users may download and print one copy of any publication from the public portal for the purpose of private study or research.
- You may not further distribute the material or use it for any profit-making activity or commercial gain
- You may freely distribute the URL identifying the publication in the public portal ?

Take down policy

If you believe that this document breaches copyright please contact us providing details, and we will remove access to the work immediately and investigate your claim.

Synthesis and characterisation of organometallic compounds of B, Mn and Re.

A thesis submitted in accordance with the requirements for the degree of Doctor of Philosophy.



David Steven Brassington

Department of Chemistry
University of Wales, Bangor

November 2001



Putting on the spectacles of science in expectation of finding the answer to everything looked at signifies inner blindness.

J. Frank Dobie

Abstract

This thesis describes the synthesis and characterisation of some new organometallic compounds of manganese, rhenium and boron, with the emphasis on attempts to develop new aspects of boron chemistry. Chapter 1 is written as an introduction to the topics of *arachno*-metallatetraboranes, and the co-ordination chemistry of unsaturated boron containing heterocycles, and Mn and Re(I) carbonyl derivatives.

Chapter 2 is concerned with the synthesis of a series of new $[MBr(CO)_3L_2]$ {M = Mn and Re, L = P(C_6H_4Cl-4)₃, P(C_6H_4OMe-4)₃, P(CH₂Ph)₃, 1/2dppp, 1/2dppb; M = Mn, L = 1/2dppfc} and previously reported {M = Mn and Re, L = PPh₃, 1/2dppm, 1/2dppe; M = Re, L = 1/2dppfc} organometallic derivatives. These complexes were characterised by spectroscopic (³¹P - NMR, IR) and single-crystal X-ray diffraction methods {M = Mn, L = P(C_6H_4Cl-4)₃, 1/2dppe, 1/2dppfc; M = Re, L = P(CH₂Ph)₃, P(C_6H_4OMe-4)₃, 1/2dppfc}. The Mn(I) derivatives of monodentate ligands were *mer,trans*- isomers whereas all other derivatives were *fac,cis*- isomers.

Chapter 3 reports the reactions of the complexes described in Chapter 2 with [NBu₄][B₃H₈] and the synthesis and characterisation of several *arachno*-2-metallatetraborane derivatives: [M(CO)₂L₂(B₃H₈)] (M = Re, L = PPh₃, P(C_6H_4Cl-4)₃, P(C_6H_4OMe-4)₃, P(CH₂Ph)₃; M = Mn and Re, L = 1/2dppm, 1/2dppp, 1/2dppb, 1/2dppfc; M = Mn, L = 1/2dppe). Of these derivatives only [Mn(CO)₂(dppe)(B₃H₈)] has been previously reported. All *arachno*-2-metallatetraboranes were characterised by NMR (¹¹B, ³¹P, ¹H) and IR spectroscopy and [Mn(CO)₂(dppe)(B₃H₈)] and [Re(CO)₂(dppfc)(B₃H₈)] were further characterised by single-crystal X-ray diffraction studies.

Chapter 4 describes the synthesis of a series of 1:1 adducts of the Lewis acid B(C₆F₅)₃ with phosphoryl Lewis bases {Et₃PO, ⁿPr₃PO, ⁿOct₃PO, Ph₃PO, (MeO)₃PO, (EtO)₃PO, (PhO)₃PO, (EtO)₂PHO, (nBuO)₂PHO, (PhO)₂PHO, (MeO)₂MePO, (EtO)₂MePO, (EtO)₂PhPO, (MeO)Me₂PO, (EtO)Me₂PO} and their subsequent characterisation by spectroscopic (¹H, ¹³C, ¹⁹F, ³¹P - NMR, IR) and single-crystal diffraction studies (Et₃PO, Ph₃PO). The Lewis acidity of B(C₆F₅)₃ has been measured by Gutmann's NMR and Lappert's IR methods, and the synthesis and characterisation of B(C₆F₅)₃EtOAc is also reported.

Chapter 5 reports the synthesis and a determination of the Lewis acidity of a number of previously reported ArBBr₂ compounds (Ar = Ph, 2-MeC₆H₄, 3-MeC₆H₄, 4-MeC₆H₄, 4-EtC₆H₄, 3,5-Me₂C₆H₃) and unsuccessful attempts to prepare unsaturated 4-membered ring and 6-membered ring B-P heterocyclic compounds by reactions of ArBBr₂ (Ar = Ph, 4-MeC₆H₄) with Li[P(SiMe₃)₂] or by thermolysis of preformed ArBBr₂PhPH₂ adducts.

Chapter 6 describes full experimental details of the reactions detailed in Chapters 2 to 5 with crystallographic data for all compounds which were characterised by single-crystal X-ray diffraction methods given in the appendices.

Contents

Acknowledgements	1
Abbreviations	2

Chapter One

1.1 Introduction	6
1.2 Aims of research	6
1.3 Boron - the element and its chemistry	7
1.3.1 Boron - elemental forms	7
1.3.2 The chemistry of boron	10
(a) Boranes and borane anions	11
(b) Boron containing inorganic heterocycles and their metal complexes	
	16
(c) Boron NMR spectroscopy	22
1.4 Rhenium(I) and manganese(I) co-ordination chemistry	22
1.4.1 Rhenium(I) compounds	25
1.4.2 Manganese(I) compounds	27

Chapter Two

2.1 Introduction	32
2.1.1 Dimanganese and dirhenium decacarbonyl	33
2.1.2 Structures of $[\text{Mn}_2(\text{CO})_{10}]$ and $[\text{Re}_2(\text{CO})_{10}]$	34
2.1.3 Manganese and rhenium pentacarbonyl halides	35
2.1.4 Substituted complexes of $[\text{MX}(\text{CO})_5]$	36
2.1.5 Formation of $[\text{MX}(\text{CO})_3\text{L}_2]$ complexes	39

2.2 Aims	40
2.3 Results and Discussion	40
2.3.1 Synthesis of [MBr(CO) ₅] (M= Mn or Re)	40
2.3.2 Synthesis of [MBr(CO) ₃ L ₂] and [MBr(CO) ₃ (L~L)]	40
2.3.3 ³¹ P NMR spectroscopy	44
2.3.4 Infrared Spectroscopy	47
2.3.5 X-Ray Crystallography	51
2.4 Conclusions	65

Chapter Three

3.1 Introduction	67
3.2 Aims	69
3.3 Results and Discussion	69
3.3.1 Synthesis of the [B ₃ H ₈] ⁻ anion.	69
3.3.2 Attempted synthesis of 2-metallatetraboranes from <i>mer,trans</i> -[MnBr(CO) ₃ (L) ₂]	70
3.3.3 Synthesis of 2-metallatetraboranes from <i>fac,cis</i> -[MBr(CO) ₃ (L) ₂] and <i>fac,cis</i> -[MBr(CO) ₃ (L~L)]	70
3.3.4 Infrared spectroscopy	75
3.3.5 ¹¹ B NMR spectroscopy	76
3.3.6 ³¹ P NMR spectroscopy	81
3.3.7 ¹ H NMR spectroscopy	83
3.3.8 X-Ray crystallography	85
3.3.9 Reactions of [Mn(CO) ₂ (dppe)(B ₃ H ₈)]	92
3.4 Conclusions	93

Chapter Four

4.1 Introduction	95
4.1.1 Lewis acidity of boron compounds	97
4.2 Aims	99
4.3 Results and Discussion	100
4.3.1 Preparation and characterisation of $B(C_6F_5)_3$ (4a)	100
4.3.2 Lewis acidity of $B(C_6F_5)_3$	101
4.3.3 Preparation of adducts of $B(C_6F_5)_3$ with organophosphoryl ligands	104
4.3.4 X-ray Crystallography	110
4.4 Conclusions	117

Chapter Five

5.1 Introduction	119
5.1.1 Three-membered rings	119
5.1.2 Four-membered rings	120
5.1.3 Six-membered rings	123
5.2 Aims	124
5.3 Results and discussion	124
5.3.1. Preparation of the arylborondibromides	124
5.3.2 Synthesis of tris(trimethylsilyl)phosphine	126
5.3.3 Attempted synthesis of diphosphadiboretanes and triphosphatriboriranes using lithium reagents	128
5.3.4 Synthesis and thermolysis of $ArBBr_2PhPH_2$ adducts	129
5.4 Conclusions	131

Chapter Six

6.1 General	133
6.2 Experimental for Chapter 2	134
6.2.1 Preparation of [MBr(CO) ₅] species (M = Mn, Re)	134
6.2.2 Synthesis of <i>mer,trans</i> -[MnBr(CO) ₃ L ₂] and <i>fac,cis</i> -[MnBr(CO) ₃ L]	135
6.2.3 Synthesis of <i>fac,cis</i> -[ReBr(CO) ₃ L ₂]	137
6.3 Experimental for Chapter 3	140
6.3.1 Synthesis of [ⁿ Bu ₄ N][B ₃ H ₈]	140
6.3.2 Synthesis of <i>arachno</i> -[M(CO) ₂ (L) _x (B ₃ H ₈)]	141
6.3.3 Thermolysis of [Mn(CO) ₂ (dppe)(B ₃ H ₈)]	144
6.3.4 Photolysis of [Mn(CO) ₂ (dppe)(B ₃ H ₈)]	144
6.3.5 Reaction between [Mn(CO) ₂ (dppe)(B ₃ H ₈)] and PPh ₃	144
6.4 Experimental for Chapter 4	145
6.4.1 Synthesis of tris(pentafluorophenylborane)	145
6.4.2 Synthesis of R ₂ (R' ¹ O)P=O Lewis bases	146
6.4.3 Synthesis of Lewis base adducts of tris(pentafluorophenyl)borane	147
6.5 Experimental for Chapter 5	157
6.5.1 Synthesis of Aryltrimethylsilanes	157
6.5.2 Synthesis of Arylborondibromides from ArSiMe ₃	160
6.5.3 Synthesis of piperidino phosphorous dichloride	161
6.5.4 Attempted synthesis of tris(trimethylsilyl)phosphine	162
6.5.5 Synthesis of tris(trimethylsilyl)phosphine	162
6.5.6 Attempted synthesis of the diphosphadiboretanes	163
6.5.7 Adducts of ArBBr ₂ with phenylphosphine	163

Acknowledgements

I would like to take this opportunity to thank my supervisor, Dr Mike Beckett, for his support throughout the research and his advice in the preparation of this thesis. I would also like to express my thanks to the technical staff at Bangor, in particular Mr Denis Williams and Mr Glyn Connolly. Also I would like to thank the secretarial staff at Bangor, past and present, especially Mrs Barbara Kinsella and Miss Caroline Naylor without whom the department would grind to a halt.

Thanks also to all of my colleagues in the department especially past and present members of Group 103, but in particular Mr Edward “I’ll start writing next week” Cavanagh, Mr Dafydd “the human fly” Thomas and Dr Patrick “what a catch” Murphy.

I would like to thank the EPSRC for their funding which ultimately made the research possible and the X-ray crystallographic service and staff at Southampton for collecting data and solving the crystallographic structures contained within this thesis, and to my parents for their love, support and for being there.

Finally, I would like to thank Sue, who has put up with me over the last four years. We showed them that it would last, and you mean the world to me.

Abbreviations

Å	Angstrom(s)
atm	atmosphere(s)
Ar	aryl
B. Pt.	boiling point
br	broad
Bu	butyl
calc.	calculated
cm ⁻¹	wavenumber(s)
conc.	concentrated
Cp	cyclopentadiene
°	degrees
°C	Celsius
d	doublet
dppb	bis(diphenylphosphino)butane
dppe	bis(diphenylphosphino)ethane
dppf	bis(diphenylphosphino)ferrocene
dppm	bis(diphenylphosphino)methane
dppp	bis(diphenylphosphino)propane
δ	chemical shift
Δδ	difference in chemical shift
Eq.	equation
Et	ethyl

Fc	ferrocenyl
Fig.	Figure
g	gram(s)
h	hour(s)
Hz	Hertz
IR	infrared
J	coupling constant
Lit.	literature
<i>m</i>	meta
m	multiplet; medium
Me	methyl
Mes	mesityl
Mesityl	2,4,6-trimethylphenyl
MHz	MegaHertz
Min	minute
MmHg	millimetre(s) Hg
Mmol	millimole
MO	molecular orbital
Mol	mole
M. Pt	melting point
n	normal
NMR	Nuclear Magnetic Resonance
<i>o</i>	ortho
<i>p</i>	para
q	quartet

Ph	phenyl
ppm	part(s) per million
Pr	propyl
Ref.	reference
s	singlet; strong
Str.	stretch(es)
t	triplet; tertiary
THF	tetrahydrofuran
Tmp	2,2,6,6-tetramethylpiperidino
TMS	tetramethylsilane
w	weak

Chapter 1

Introduction

1.1 Introduction.

This thesis consists of six chapters and describes original research into boranes and aspects of their co-ordination chemistry. This chapter contains a literature overview of the chemistry of boron, the co-ordination chemistry of rhenium and manganese carbonyl halides, the synthesis and reactions of boron hydrides and unsaturated inorganic heterocycles which contain three co-ordinate boron centres. Chapters Two and Three are concerned with the synthesis, characterisation and reactions of the species $[M(CO)_3X(PR_3)_2]$ and $[M(CO)_2(PR_3)_2(B_3H_8)]$ ($M = Mn, Re; X = Br$). Chapter Four concentrates on the preparation of a series of Lewis base adducts of the borane $B(C_6F_5)_3$ whilst Chapter Five is concerned with the attempted synthesis of diphosphadiboretanes and triphosphatriborinanes, their co-ordination chemistry and associated boron-phosphorus adduct chemistry. A detailed experimental section is given in Chapter Six.

1.2 Aims of research

The first aim of the research work described within this thesis, was to synthesise and investigate the spectroscopic and structural properties of some new and some previously described rhenium(I) and manganese(I) halo carbonyl phosphines derivatives. Such a study was desirable since previous research into these species was limited and structural characterisation was often left incomplete or ambiguous. Spectroscopic data were to be correlated with benchmark crystallographically determined structures.

The second aim was to use these manganese(I) and rhenium(I) halo carbonyl phosphine derivatives and explore their reactions with the octohydrotriborate anion, $[B_3H_8]^-$. With a few notable exceptions [1,2] this area has been frequently overlooked.

The chemistry of the metallatetraborane obtained in the highest yield was further investigated as representative of this class of compounds.

A third aim of the work detailed was to compare various methods of determining Lewis acidity. The Lewis acidity of tris(pentafluorophenylborane), $B(C_6F_5)_3$, was determined and its reactions with various phosphine oxides ligands with this acceptor was explored.

A final aim of the research was to prepare a series of diphosphadiboretanes and triphosphatriboriranes and to react them with the manganese(I) and rhenium(I) halocarbonyl phosphine derivatives described in Chapter Two in order to prepare novel complexes of these ligands.

1.3 Boron - the element and its chemistry

The chemistry of boron and its compounds is well reviewed in many undergraduate textbooks [3,4], and the following few paragraphs contain a brief overview of the chemistry of this element.

1.3.1 Boron - elemental forms

Boron, in an impure form, was first isolated independently by J. L. Gay Lussac and L. J. Thenard of France, and Humphry Davy of Great Britain in 1806. It was not until later in the 19th century that H. Moissan obtained a relatively pure (95 – 98%) sample of boron by reducing B_2O_3 with magnesium. The name boron was proposed by Davy, who joined the first three letters of its parent ore '*borax*' with the last two letters of '*carbon*', the element that displays a similar chemistry. Boron is not a particularly abundant element, but, it does exist in large localised deposits of borax, $Na_2B_4O_7 \cdot 10H_2O$ and kernite $Na_2B_4O_7 \cdot 4H_2O$, both of which are commercially viable for the preparation

of elemental boron. Difficulties arise in trying to obtain high purity boron, due to the high melting point and the corrosive nature of molten boron [5]. There are several commercial methods for the isolation of elemental boron, with all bulk methods leading to a reduction of the purity of the final material. An example of such a process is the reduction of B_2O_3 with magnesium, which yields boron as a black solid of 95-98% purity (Eq. 1.1) [6].



Boron maybe prepared in large quantities by this method. The element can be obtained in a pure form on a smaller scale (i.e. less than 1Kg), using, for example, the Van Arkel method which involves the pyrolysis of boron triiodide, or the thermal decomposition of diborane or other boron hydrides (Eq. 1.2 and Eq. 1.3) [6].



There are several different allotropes of boron and all of which contain the B_{12} icosahedron unit (Figure 1.1). This cluster shape is also known to occur in metal borides and in boron hydride clusters.

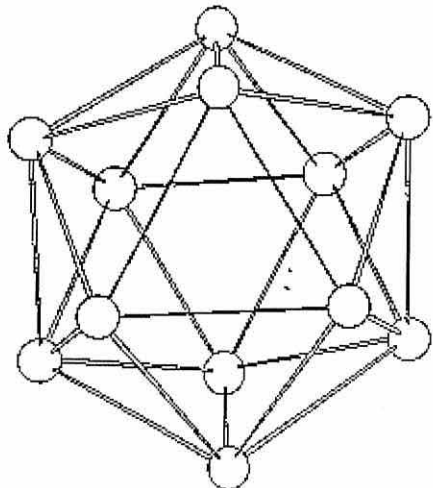


Figure 1.1. A B₁₂ icosahedron.

The α -rhombohedral allotrope, with 37% space filled, is the densest form of elemental boron. This is low in comparison to the 74% for the close packing of the spheres. The β -rhombohedral form is the most stable allotrope and its complicated structure is given in Figure 1.2.

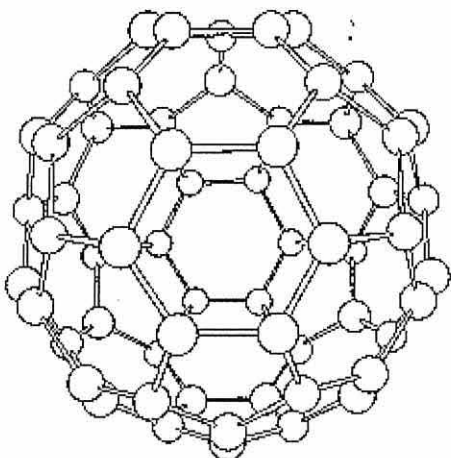


Figure 1.2. The β -rhombohedral form of boron.

Boron, the only non-metallic element in Group 13 of the periodic table has the valence electronic configuration of 2s² 2p¹. The ionisation energies of these electrons

are high (first ionisation energy is 801 kJ mol⁻¹) and as such covalent rather than ionic bonds are favoured [6]. Boron typically forms trivalent compounds and unlike the heavier elements of the group, does not display a tendency to form monovalent compounds [6]. Three co-ordinate boron centres are sp² hybridised, with hybrid orbitals lying in the same plane at angles of 120° to one another. However, trigonal planar boron centres have an insufficient number of electrons to fill their valence shell, after forming three σ-bonds, and are invariably Lewis acids.

1.3.2 The chemistry of boron

At elevated pressures and temperatures boron will react with most metals and non-metals but at ambient temperatures boron is relatively inert. However, it will spontaneously react with fluorine to form BF₃ (Eq. 1.4) and will also react with O₂ to slowly form a surface layer of B₂O₃ (Eq. 1.5).

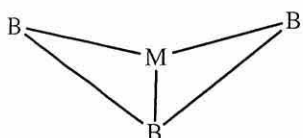


The chemistry of boron is extensive and diverse but may be conveniently subdivided into six main categories, with each category showing differing structures and properties. These categories are metal borides, boron hydrides and their derivatives, boron trihalides their adducts and derivatives, oxo compounds including metaborate esters, polyborates and borosilicates, organoboron compounds with B-C bonds, and lastly inorganic heterocyclic species. Aspects of the chemistry of boron pertinent to this thesis are described below. Detailed discussion of boron trihalides and their adducts, B-P rings and boron hydrides are reserved for Chapters 3, 4 and 5.

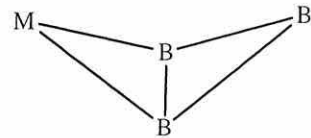
1.3.2 (a) Boranes and borane anions

Boron hydrides were first prepared in a pure form by Alfred Stock in 1912 [7]. He prepared these hydrides by the action of acid on magnesium boride and isolated the volatile compounds using vacuum line techniques. In general boranes are colourless, diamagnetic, molecular compounds of low thermal stability. The lowest members are gases at room temperature but with increasing molecular weight they become volatile liquids or solids. Boranes are extremely reactive and several are spontaneously flammable in air. Boranes may be readily converted into anions and the co-ordination chemistry of one such anion, $[B_3H_8]^-$, is described in this thesis. The synthesis of the $[B_3H_8]^-$ anion will be discussed in detail in Chapter Three.

The $[B_3H_8]^-$ anion can form two different classes of butterfly complexes when reacted with a metal species. They can be described as the 1-metallatetraboranes (the body isomer) and the 2-metallatetraboranes (the wingtip isomer) of the butterfly structure. Both are shown in Figure 1.3 below.



1-Metallatetraborane (Body isomer)



2-Metallatetraborane (Wingtip isomer)

Figure 1.3. The two possible isomers of the butterfly structure of metallatetraboranes.

The 1-metallatetraboranes are relatively uncommon in comparison to the 2-metallatetraboranes, but, iridium, platinum and palladium complexes readily form such complexes (Eq. 1.6) [8].



During the course of the reaction there is a transfer of a hydrogen atom from the borane moiety to the terminal Ir-H position. The molecular structure of this complex is shown in Figure 1.4 below [9].

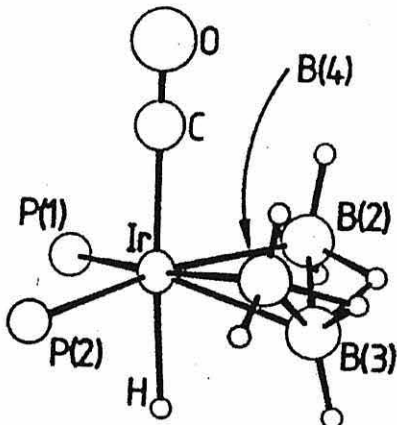
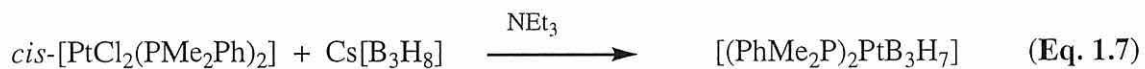
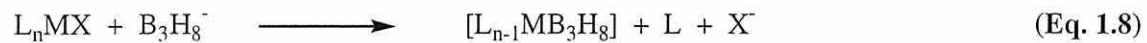


Figure 1.4. Molecular structure of an iridium 1-metallatetraborane.

The corresponding Pt and Pd derivatives $[\text{L}_2\text{MB}_3\text{H}_7]$ are prepared by the reaction between a bis(phosphine) metal dihalide complex and the *arachno*- $[\text{B}_3\text{H}_8]^-$ anion in the presence of a base (Eq. 1.7) [10,11].



The *arachno*-2-metallatetraboranes are more commonly encountered in the literature. They can be prepared by the displacement of a halide from a metal species by the $[B_3H_8]^-$ anion (Eq. 1.8).

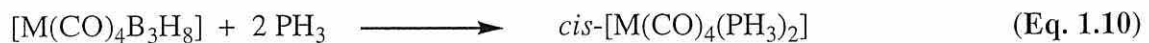


This reaction may occur spontaneously but more often it is induced by thermolysis or photolysis. s-Block and p-block elements also form MB_3 complexes, however these tend to be very volatile compounds that readily decompose in air and they are also thermally unstable.

Complexes containing Cr, W, Mo, Re, Mn, Fe, Ru and Os have been widely studied, with great number of 2-metallatetraboranes having been produced. The direct reaction between $[M(CO)_6]$ ($M = Cr, Mo$ and W) with $Cs[B_3H_8]$ produces compounds of the type $[M(CO)_4(B_3H_8)]^-$. These anions can be stabilised by adding a tetraalkylammonium salt into the reaction mixture (Eq. 1.9) [12].



These compounds can then undergo further reactions. One reaction involves the substitution at the metal centre of $[B_3H_8]^-$ by PH_3 (Eq. 1.10) [13].



Similarly the manganese and rhenium species are readily prepared by the direct reaction between $[B_3H_8]^-$ with $[(CO)_5MX]$ ($M = Mn$ and Re) (Eq. 1.11) [2].

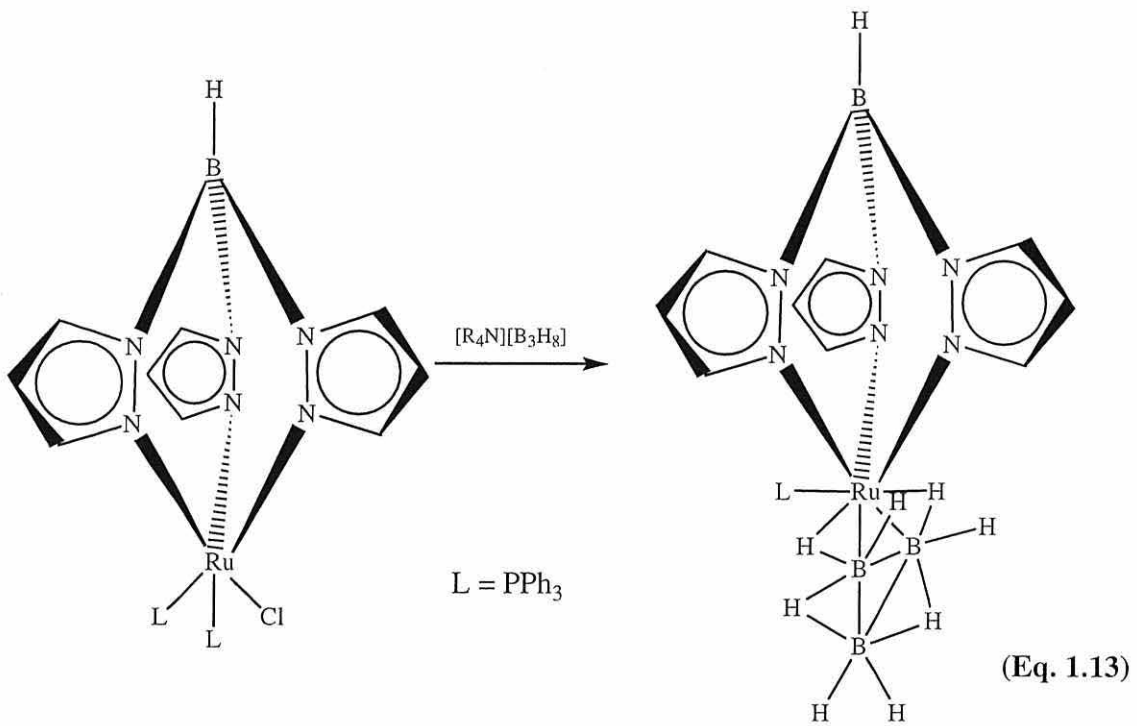


As was evident with the Cr, Mo and W borane, the $[\text{B}_3\text{H}_8]^-$ ligand attached to the Mn and Re centres, will undergo further reactions once attached to the metal centre. One such reaction is shown below (Eq. 1.12) [2].



These Mn(I) and Re(I) tetraboranes will be discussed in greater depth in Chapter Three.

More recently there has been interest shown in the synthesis and subsequent reactions of the ruthenatetraboranes. The reaction of $[\text{RuClH}(\text{CO})(\text{PPh}_3)_3]$ with $[\text{R}_4\text{N}][\text{B}_3\text{H}_8]$ produces the colourless complex $[\text{RuH}(\text{B}_3\text{H}_8)(\text{CO})(\text{PPh}_3)_2]$ in a high yield. The $[\text{B}_3\text{H}_8]$ unit is readily cleaved from this complex by an excess of tert-butylisonitrile producing $[\text{RuHCl}(\text{CN}^t\text{Bu})_2(\text{PPh}_3)_2]$. However, the treatment of $[\text{RuH}(\text{B}_3\text{H}_8)(\text{CO})(\text{PPh}_3)_2]$ with *N*-halogenosuccinimide leads to the selective cleavage of the Ru-H bond. The reaction between a Ru “half-sandwich” and $[\text{B}_3\text{H}_8]^-$ has been reported and is shown in (Eq. 1.13) [14].



This complex can then be reacted with *N*-halogenosuccinimides to produce the chloro, bromo or iodo substituted species.

The coinage metals also produce 2-metallatetraboranes. Metallatetraborane's containing copper are less sensitive to air and water than the corresponding silver species. The copper complexes are relatively straight forward to prepare and tend to follow the routes described above (the replacement of a halide by the $[B_3H_8]^-$ anion). The triphenyl phosphine, arsine and stibine derivatives have all been prepared by this method (Eq. 1.14) [15,16].



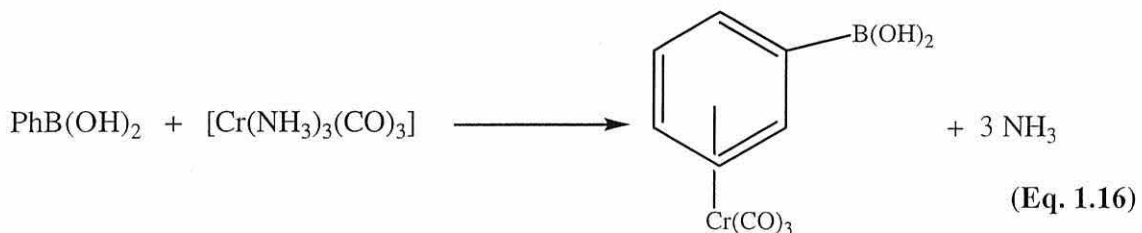
Similarly, the argentatetraboranes can be prepared in an analogous manner. Another route produces the metallatetraborane directly from the $AgNO_3$ precursor (Eq. 1.15) [12].



1.3.2 (b) Boron containing inorganic heterocycles and their metal complexes

Extensive research has been undertaken on the boron containing heterocycles with elements of the second row, and the synthesis and reactivity of the $\text{R}_2\text{N}_2\text{B}_2\text{R}_2^+$, $\text{R}_3\text{B}_3\text{O}_3$ (boroxine) and $\text{R}_3\text{B}_3\text{N}_3\text{R}_3^+$ (borazene) are well documented.

Relatively little work has been described on metal complexes involving boroxines. However, Razuvaev *et al*, in 1976, reported the isolation of $[(\text{CO})_3\text{CrC}_6\text{H}_5\text{B}(\text{OH})_2]$ from the following reaction (Eq. 1.16) [17].



This chromium-boronic acid complex was then dehydrated *in vacuo* to produce the corresponding boroxine $[(\text{CO})_3\text{Cr}(\text{C}_6\text{H}_5\text{BO})_3]$, shown in Figure 1.5, where it is clear that the $\{\text{Cr}(\text{CO})_3\}$ moieties remain bound to the aryl rather than the boroxine ring.

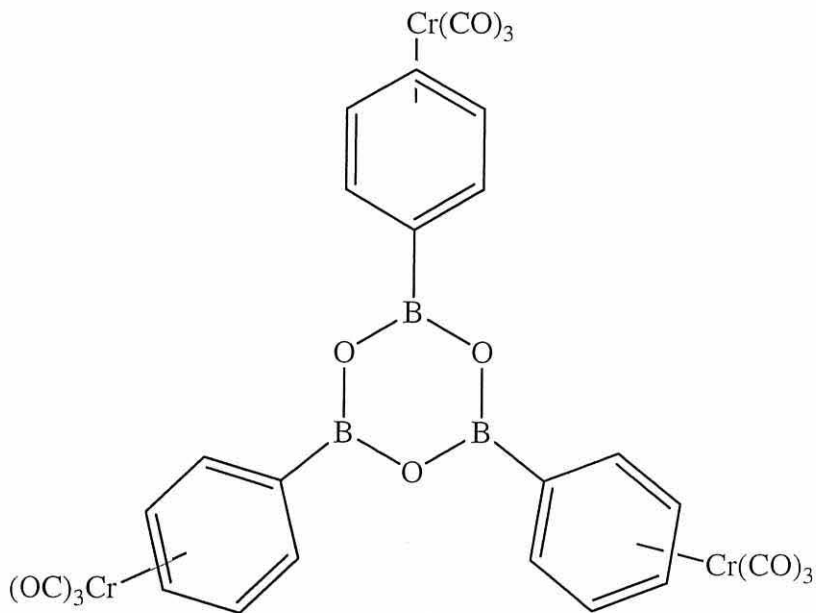


Figure 1.5. Chromium tricarbonyl complex of triphenylboroxine.

The metal complexes of borazines that have been reported generally have alkyl substituents on the annular atoms. Borazines are potential π -ligands and as such will react preferentially with d^6 metal ligand fragments such as $\{\text{Cr}(\text{CO})_3\}$ to form 18 valence electron compounds [18]. Many half-sandwich compounds $[\text{R}_3\text{B}_3\text{N}_3\text{R}^1{}_3\text{ML}_3]$ have been prepared ($\text{M} = \text{Cr, W, Mo}$), although there have been no confirmed preparations of the corresponding full sandwich derivatives of the type $[(\text{R}_3\text{B}_3\text{N}_3\text{R}^1{}_3)_2\text{M}]$. The best method of preparation of these half-sandwich compounds is when the $\{\text{M}(\text{CO})_3\}$ moiety carries a labile ligand such as acetonitrile (Eq. 1.17) [19-22].



It has been shown that the B_3N_3 ring in half-sandwich complexes is labile and can be displaced by other borazine, phosphine and phosphite ligands [23]. Crystallographic data on hexaethylborazine chromiumtricarbonyl has shown that the heterocyclic ring is slightly puckered Figure 1.6 [23]. Infrared studies have shown that the B-N vibrational bands lie at lower energy in relation to uncomplexed borazines. This suggests that the lone pairs on nitrogen have become fully localised owing to the formation of N-Cr dative σ -bonds [23]. The nitrogen atoms effectively gain a formal positive charge and become four co-ordinate, adopting an approximate tetrahedral configuration, which leads to this puckering of the ring.

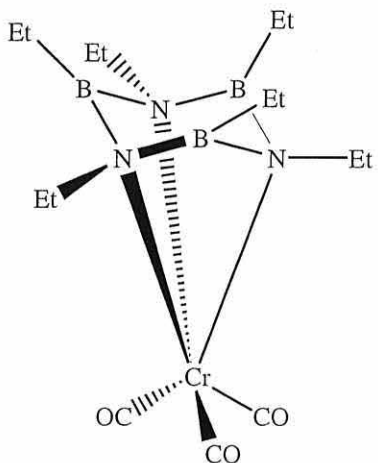


Figure 1.6. The structure of $[(Et_3B_3N_3Et_3)Cr(CO)_3]$.

A second class of metalloborazine complexes exist. In these the metal atoms are bound *via* a σ -bond to either boron or nitrogen within the B_3N_3 system. One of the few examples of these N-substituted metallo-borazines is the N-lithioborazine, which can be prepared by a method shown in Eq. 1.18.



There is only one example of metal complex co-ordination by borthiin ring systems. Noth and Schuchardt [24] reported that the reaction between $[M(CO)_3(CH_3CN)_3]$ (where $M = Mo$, Cr and W) with triphenylborthiin in dioxane produced species of the type $[(PhBS)_3M(CO)_3 \cdot 1.5C_4H_8O_2]$. A postulated structure of these compounds is shown in Figure 1.7, with the $\{M(CO)_3\}$ moieties bound to the heterocyclic B_3S_3 rings.

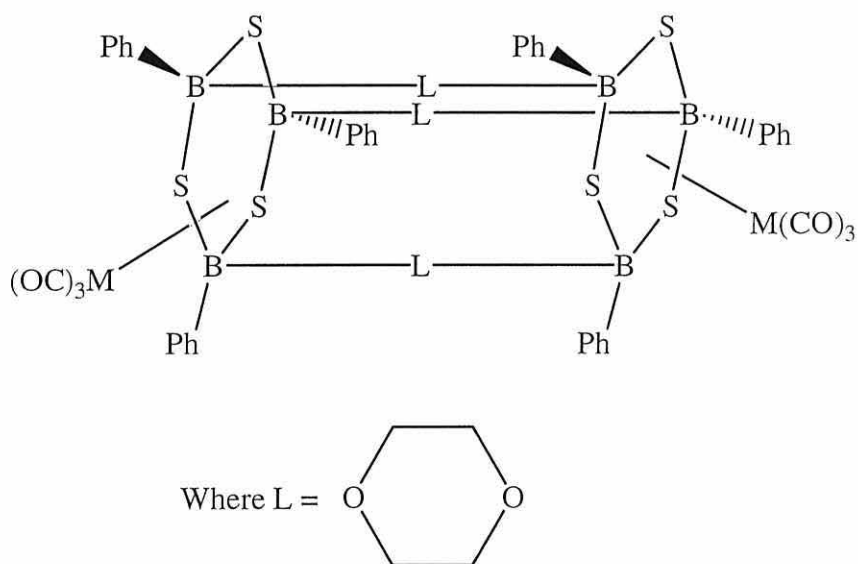
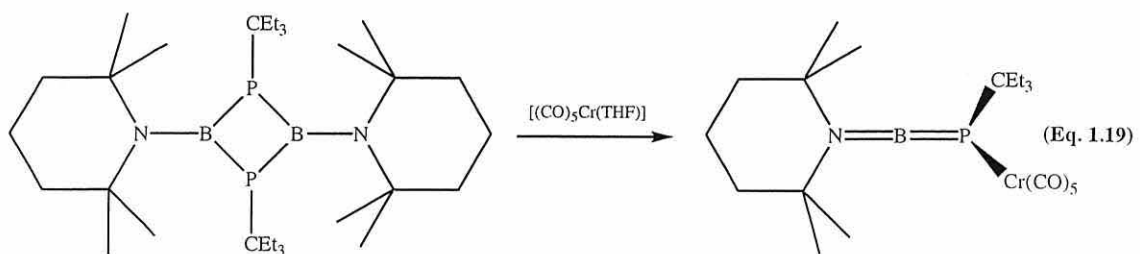


Figure 1.7. Structure of $[(PhBS)_3M(CO)_3 \cdot 1.5C_4H_8O_2]$, where $M = Cr$, Mo or W .

Attempts to remove the dioxane under vacuum resulted in decomposition of the compound.

Reactions of the diphosphadiboretanes have also been investigated by Noeth and co-workers [25,26], where $R_2B_2P_2R^1_2$ rings with sterically hindered groups bound to boron were treated with $[Cr(CO)_5(THF)]$. This led to the dissociation of the $R_2B_2P_2R^1_2$ ring but produced 1,1-diethylpropyl-(Tmp)boranylidene phosphane (Eq. 1.19).



The reaction of diphosphadiborethanes, having less hindered substituents, with $[\text{Cr}(\text{CO})_5(\text{THF})]$ resulted in the formation of mononuclear or binuclear metal carbonyl complexes Figure 1.8.

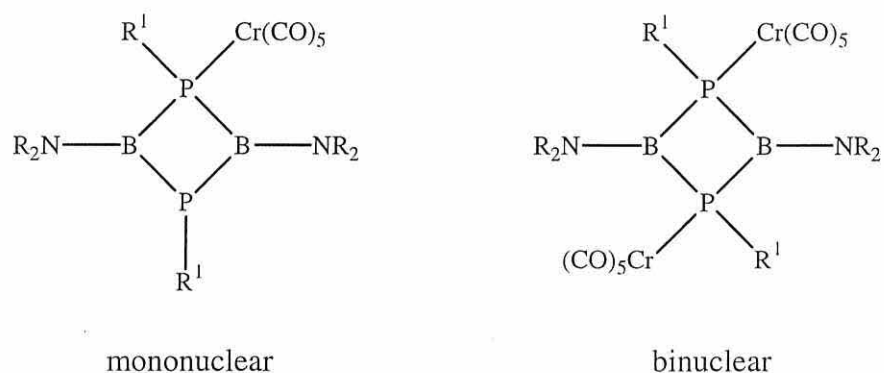


Figure 1.8. Mononuclear and binuclear bonding with diphosphadiborethanes.

However, when $(\text{MesBP}^{\text{t}}\text{Bu})_2$ was reacted with $[\text{Cr}(\text{CO})_5(\text{THF})]$, a complex with a different structure, in which the ring system is retained was produced, Figure 1.9.

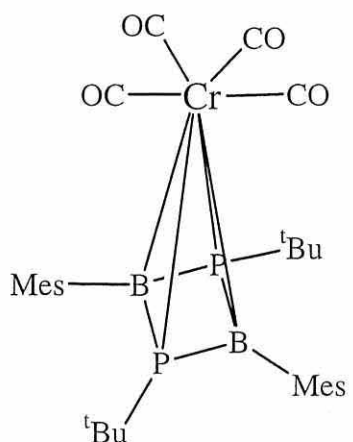


Figure 1.9. Diphosphadiboretane bound to a chromium tetracarbonyl centre.

The reaction of $(\text{MesBPPh}_3)_3$ with $[\text{Cr}(\text{CO})_3(\text{MeCN})_3]$ has been performed to see if the triphosphatriborinane was able to act as a η^6 ligand [27]. A metal carbonyl complex was produced, in which the chromium was bound to all atoms in the heterocyclic ring (see Figure 1.10).

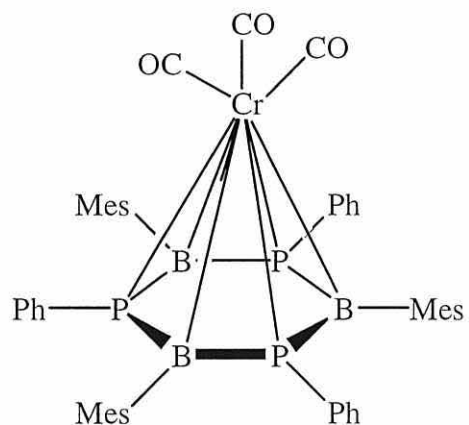


Figure 1.10. Structure of chromium tricarbonyl(η^6 -1,3,5-triphenyl-2,4,6-trimesityl-1,3,5,2,4,6-triphosphaborinane)

1.3.2 (c) Boron NMR spectroscopy

Boron NMR spectroscopy generally deals with the ^{11}B isotope rather than that of ^{10}B , due to its high natural abundance (81% ^{11}B compared with 19% ^{10}B), its better sensitivity in the NMR experiment and its smaller quadrupolar moment [28]. However, measurements of boron-10 NMR spectra can be performed quite easily and are important in isotopic labelling studies where reaction mechanisms are of interest. Both isotopes possess large quadrupoles ($^{10}\text{B} = 8.46 \times 10^{26} \text{ Q/m}^2$, $^{11}\text{B} = 4.06 \times 10^{26} \text{ Q/m}^2$ at 10.75 and 32.1 MHz respectively) [29] since they both have a nuclear spin $I > 1$. Large quadrupole moments generally lead to short relaxation times (T), during which the nuclei in the experiment return to the ground state quickly [28]. Due to the relationship between relaxation time and the line width of the signal, $\nu_{1/2} \propto 1/T$ (at half height $\nu_{1/2}$), broadening of the peaks occurs.

The chemical shift range of ^{11}B covers approximately 200 ppm and chemical shifts can generally be determined with an accuracy of ± 0.5 ppm [28]. The peak area of a ^{11}B NMR signal is related to the number of boron atoms in each chemical environment and the location of the resonance signals for trivalent boron compounds can be explained in terms of a contribution of σ - and π - effects [28]. Basic donor solvents may cause an upfield shift of the NMR signal due to co-ordination (see Chapter Four for further details).

1.4 Rhenium(I) and manganese(I) co-ordination chemistry

The organometallic chemistry of manganese(I) and rhenium(I), unlike the organometallic chemistry of most transition metals, does not have a particularly extensive history. Organometallic species of manganese and rhenium were first

prepared in the 1940's. Since this time research into the organometallic chemistry of manganese and rhenium has grown rapidly.

There is such a large quantity of literature available on compounds of this type, and the reader is directed to texts like Comprehensive Organometallic Chemistry or the annual reviews in the Journal of Organometallic Chemistry for detailed discussions. This section will concentrate solely on the co-ordination chemistry of metal carbonyl derivatives exhibited by both manganese(I) and rhenium(I).

Transition metal carbonyls are very useful and readily available starting materials for the synthesis of low valent metal complexes. However, before any in-depth discussion of carbonyl chemistry begins, it is worthwhile understanding the basic bonding arrangement around the metal centres.

The bonding of a ligand to a metal does not normally just involve a σ -bond, invariably there are π -interactions governing the co-ordination of the ligand. The energy level diagram in Figure 1.11 shows a molecular orbital splitting diagram for a first row transition metal (3d, 4s, 4p). Carbon monoxide is a π acceptor ligand, where the triple bond is made up of a σ bond and two π bonds. The π orbitals are filled, but the π^* orbitals (anti-bonding orbitals) are empty.

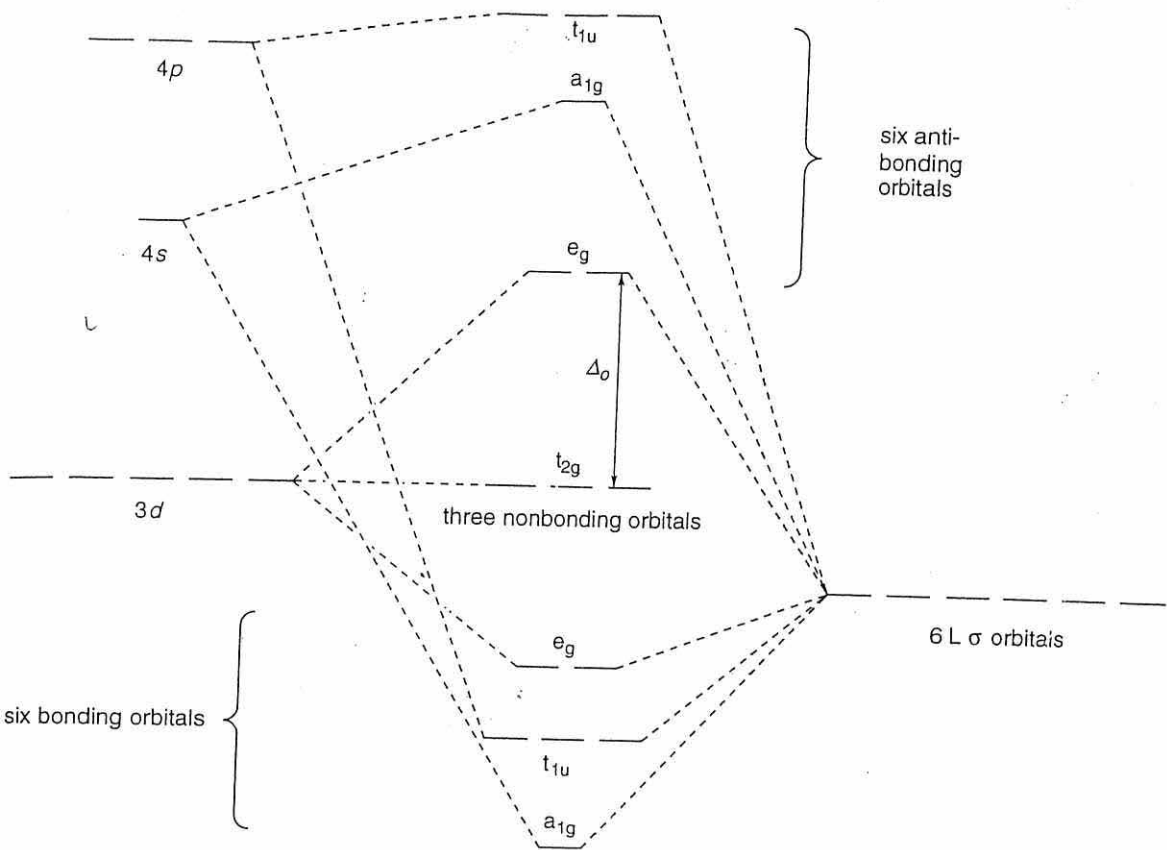


Figure 1.11. Molecular orbital splitting diagram for a transition element.

These empty π^* orbitals are of the correct symmetry to overlap with the filled t_{2g} orbitals of the metal (d_{xy} , d_{xz} and d_{yz}). This is illustrated in Figure 1.12.

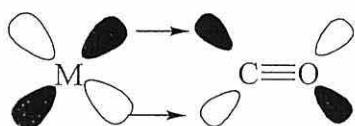


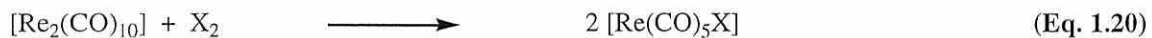
Figure 1.12. Overlap of the t_{2g} orbitals of the metal with the π^* orbitals of CO.

The interaction between the metal t_{2g} orbitals and the linear co-ordination to the CO π^* orbitals effectively means that there is a flow of electron density from the metal to the ligand. This donation of electrons is referred to as back-bonding.

There are several different reactions that metal carbonyls can undergo, substitution, reduction, oxidation and attack on co-ordinated CO. Carbonyl groups can be substituted by other ligands, thermally or photochemically in a dissociative process. Substitution can proceed to the point that there are equal numbers of ligand (L) and carbonyl groups, however, replacement of the remaining carbonyl groups requires the use of quite severe chemical methods (due to the strength of the M-CO back donation).

1.4.1 Rhenium(I) compounds

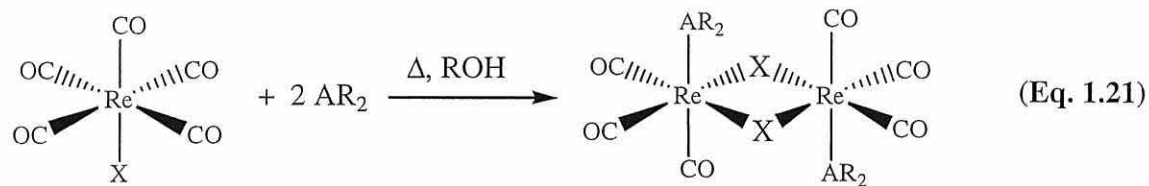
As will be discussed in Chapter Two, the major starting material in low valent organorhenium chemistry is dirhenium decacarbonyl, $[\text{Re}_2(\text{CO})_{10}]$. Oxidation of $[\text{Re}_2(\text{CO})_{10}]$ with halogens produces $[\text{Re}(\text{CO})_5\text{X}]$ and this reaction and the substitution reactions of rhenium halocarbonyls with phosphines will be discussed in detail in Chapter Two. However, it is worthwhile describing some other substitution reactions Eq. 1.20.



Monosubstitution of $[\text{Re}(\text{CO})_5\text{X}]$ is achieved by treatment of one equivalent of donor ligand in a refluxing solvent. Cleavage of the bridged dihalides $[\{\text{ReX}(\text{CO})_4\}_2]$ with donor ligands is also an efficient method for generating *cis*- $[\text{ReX}(\text{CO})_4\text{L}]$ species [30]. Cleavage of the zero valent disubstituted dinuclear complexes $[\{\text{Re}(\text{CO})_4\text{L}\}_2]$ with X^- or X_2 generates *cis*- $[\text{ReX}(\text{CO})_4\text{L}]$. However under certain conditions the *trans* isomer can be isolated. This will on heating generally yield the more stable *cis* isomer.

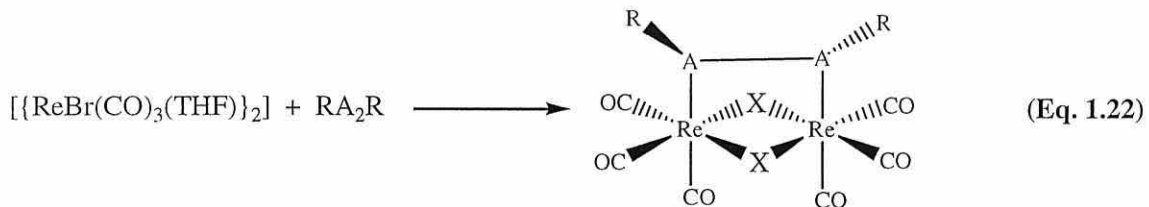
The dialkyl and diaryl O, S, Se and Te ligands AR_2 act as two electron donors and as such exhibit similar properties to other two electron donors i.e. tertiary

phosphines, N-heterocycles. Hence, in a refluxing alcohol $[ReX(CO)_5]$ will react with AR_2 to yield either the mononuclear species $[ReX(AR_2)_2(CO)_3]$ or dinuclear $\{[ReX(AR_2)(CO)_3]\}_2$ (shown in Eq. 1.21) [31].

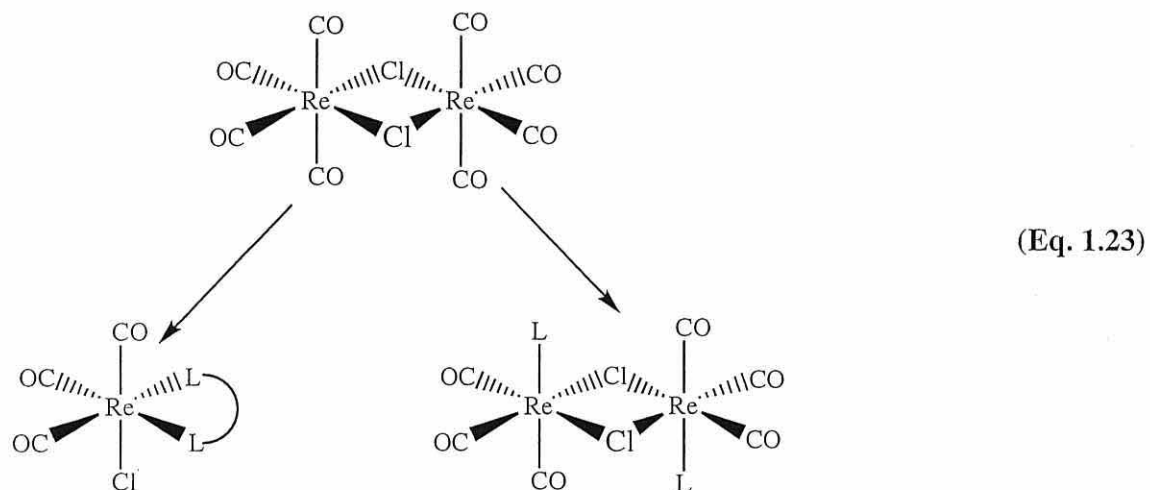


This dinuclear species is normally isolated when A is either sulfur or selenium and R is an aryl group. The mononuclear species are obtained when R is an alkyl group.

Related dinuclear complexes $[Re_2Br_2(CO)_6(RA_2R)]$ have been prepared from the THF adduct $\{[ReBr(CO)_3(THF)]_2\}$ and the appropriate ligand (Eq. 1.22) [32, 33].



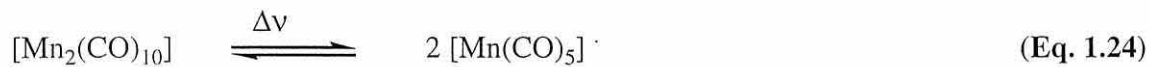
The chloro-bridged species $\{[ReCl(CO)_4]\}_2$ acts as a precursor to complexes containing oxygen donor ligands, for example OH_2 , $OCMe_2$, $HOCH_2CH_2OH$. Thus upon warming $\{[ReCl(CO)_4]\}_2$ with an appropriate quantity of ligand the dinuclear chloro-bridged species (monodentate ligands) or mononuclear *fac* complexes (with bidentate ligands) are formed (Eq. 1.23) [34].



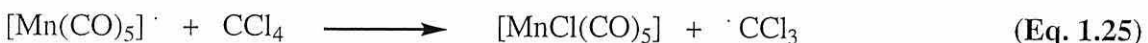
Complexes of rhenium with weakly co-ordinating anions (OSO_2CF_3) or organohalide ligands (RX , CHCl_3) have been studied as organometallic Lewis acids. Beck has developed the chemistry of $[\text{Re}(\text{CO})_5(\text{FBF}_3)]$ [35] in which the BF_4^- ligand is readily substituted by a number of anionic and neutral species [36-39].

1.4.2 Manganese(I) compounds

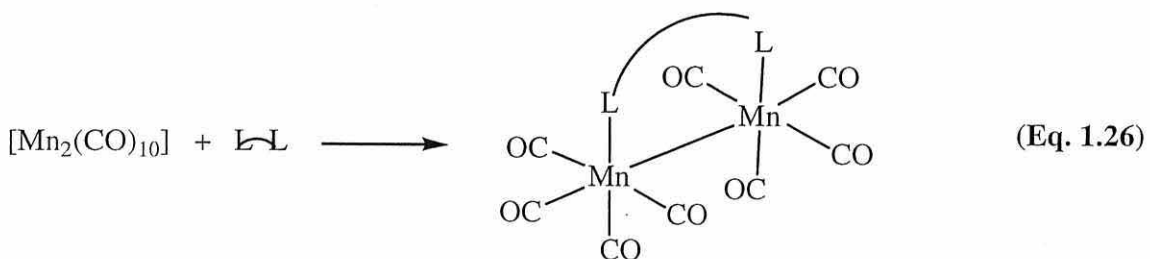
As was seen to be the case for rhenium, the major synthetic precursor in organomanganese carbonyl chemistry is dimanganese decacarbonyl $[\text{Mn}_2(\text{CO})_{10}]$. In the majority of cases, the manganese compounds produced all obey the 18 electron rule. However, one notable exception is the photolytic reaction of $[\text{Mn}_2(\text{CO})_{10}]$ producing a $17e^-$ species (Eq. 1.24).



If the photolytic reaction is performed in a haloalkane, abstraction of the halogen atom occurs [40] (Eq. 1.25).



Reactions of $[\text{Mn}_2(\text{CO})_{10}]$ with both mono and bidentate ligands have been widely studied. Monosubstitution of $[\text{Mn}_2(\text{CO})_{10}]$ generally produces compounds of the formula $[\text{Mn}_2(\text{CO})_9\text{L}]$ where the substituent group is in the axial position [41, 42]. However, disubstitution using bidentate ligands can produce two different geometries. The nitrogen bidentate ligand bipy substitute on a single metal giving an unsymmetrical complex $[(\text{CO})_5\text{MnMn}(\text{CO})_3(\text{L}^\wedge\text{L})]$. Reactions of dppm or dppe with $[\text{Mn}_2(\text{CO})_{10}]$ produced a symmetric species in which the bidentate ligand co-ordinates to equatorial positions on adjacent metals, therefore bridging two metal centres (Eq. 1.26) [43].



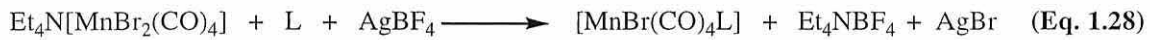
Manganese pentacarbonyl iodide was the first halo manganese compound to be prepared. It was obtained, along with $[\text{Mn}_2(\text{CO})_{10}]$, by carbonylation of MnI_2 . It can also be prepared by the reaction of $[\text{Mn}_2(\text{CO})_{10}]$ with iodine in a sealed tube at 140°C [44]. Other halide complexes have been prepared by halogen cleavage of the Mn-Mn bond in $[\text{Mn}_2(\text{CO})_{10}]$, and this is discussed in greater detail in Chapter Two.

The substitution of carbonyl groups in $[\text{MnX}(\text{CO})_5]$ complexes by neutral ligands have been widely studied. In general, only mild conditions are required to produce the species $[\text{MnX}(\text{CO})_{5-n}\text{L}_n]$ (where $n = 1$ or 2) whilst harsher conditions are employed to produce $[\text{MnX}(\text{CO})_{5-n}\text{L}_n]$ (where $n \geq 3$). The same reactions as detailed in

section 1.5.1 occur with manganese. However, manganese carbonyl halides undergo reactions that the analogous rhenium species do not. For example the reaction between $[\text{MnX}(\text{CO})_5]$ with tetra alkylammonium halides produced the anionic complex *cis*- $[\text{MnX}_2(\text{CO})_4]^-$ (Eq. 1.27) [45, 46].



At the same time the reaction between KCN and $[\text{MnBr}(\text{CO})_5]$ was carried out, giving $[\text{Mn}(\text{CN})_2(\text{CO})_4]^-$. The displacement of a halide ion in $[\text{MnX}_2(\text{CO})_4]^-$ may be assisted by using a halide acceptor such as silver tetrafluoroborate. This provides a convenient route to the monosubstituted tetracarbonyl halide compounds [47] (Eq. 1.28).



Reactions between $[\text{MnX}(\text{CO})_5]$ and secondary phosphine oxides, secondary phosphine sulphides and secondary phosphine selenides have produced some interesting results. Different products are formed when phosphine sulphides react with $[\text{MnX}(\text{CO})_5]$ at varying temperatures. Below 45°C , monosubstituted complexes of the ligand co-ordinated *via* the sulphide lone pair are produced (Eq. 1.29) [48, 49].



At higher temperatures a different product is formed which has the isomeric thiophosphonous acid as a ligand, with co-ordination to the metal occurring *via* the phosphorus atom (Eq. 1.30) [49].



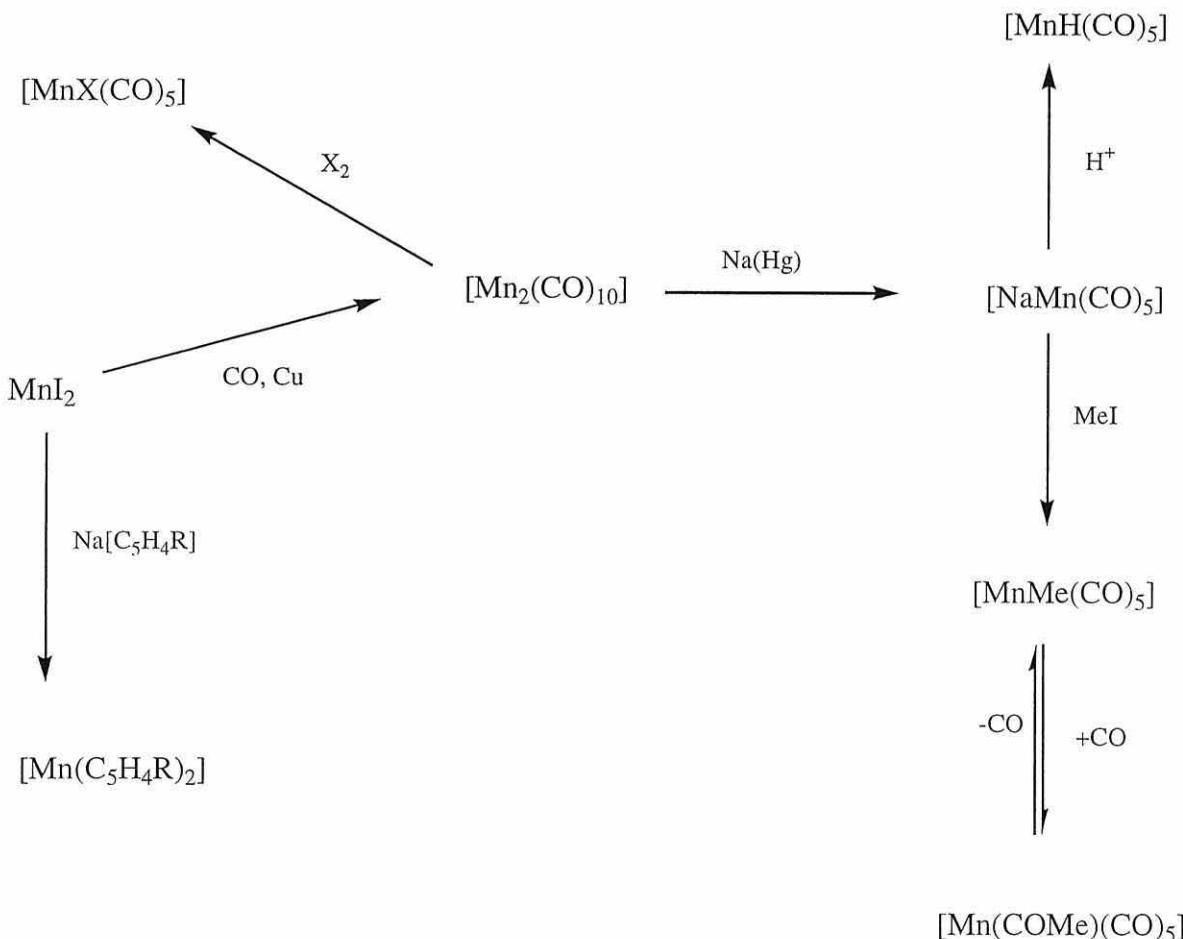
Heating the product shown in Eq. 1.29 produces the product shown in Eq. 1.30. Secondary phosphine oxides produce species analogous to that shown in Eq. 1.29 whilst secondary phosphine selenides produce species analogous to that shown in Eq. 1.30.

Chapter 2

Synthesis and characterisation of triorganophosphine derivatives of $[MBr(CO)_5]$ ($M = Mn$ or Re).

2.1 Introduction

The development of the organometallic chemistry of manganese dates back to 1954 [44] whilst rhenium dates back to 1941 [50]. The organometallic chemistry of rhenium has been less extensively explored than manganese. This lack of attention is not surprising when considering the availability of rhenium and thus its associated cost. As previously mentioned in Chapter One, the dimetal decacarbonyls are the key starting materials in this chemistry [51] and key aspects of the chemistry of $[\text{Mn}_2(\text{CO})_{10}]$ are depicted in scheme 2.1, and expanded upon in the following sections [52].

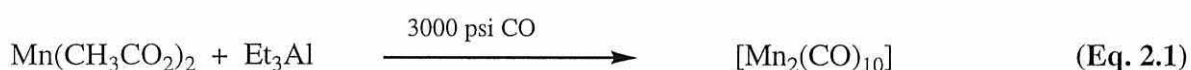


Scheme 2.1. Important aspects of the chemistry of $[\text{Mn}_2(\text{CO})_{10}]$.

2.1.1 Dimanganese and dirhenium decacarbonyl

The first report of dimanganese decacarboyl [$\text{Mn}_2(\text{CO})_{10}$] appeared in 1949 [53], however full characterisation of the compound did not appear until 1954 [44]. The product was prepared by carbonylation of MnI_2 in diethyl ether and gave [$\text{Mn}_2(\text{CO})_{10}$] in a yield of 1%. Obviously, improved methods of synthesis of [$\text{Mn}_2(\text{CO})_{10}$] were required if further work on this compound were to be carried out efficiently and rapidly.

In 1960 Podall *et al* [54] reported a more efficient preparation of [$\text{Mn}_2(\text{CO})_{10}$], this is shown below in (Eq. 2.1). This produced the desired yellow crystalline product in a 55% yield.



Similarly, dirhenium decacarbonyl [$\text{Re}_2(\text{CO})_{10}$] was first reported in 1941 [50] by Hieber, Schuh and Fuchs. Their synthesis, shown in (Eq. 2.2) relied on high temperatures and pressures but yielded [$\text{Re}_2(\text{CO})_{10}$] in over 90%.



In 1963 Wilkinson *et al* [55] showed that reduction of anhydrous ReCl_3 or ReCl_5 by sodium in THF at 130°C and 250 atm CO allowed the isolation of [$\text{Re}_2(\text{CO})_{10}$] in 70% yield (Eq. 2.3).



2.1.2 Structures of $[\text{Mn}_2(\text{CO})_{10}]$ and $[\text{Re}_2(\text{CO})_{10}]$

X-Ray crystal structure determinations of $[\text{Mn}_2(\text{CO})_{10}]$ and $[\text{Re}_2(\text{CO})_{10}]$ [56] have shown that these species are structurally isomorphous, with a metal–metal bond joining two $\{\text{M}(\text{CO})_5\}$ units whose radial carbonyl groups are in staggered conformation (Figure 2.1).

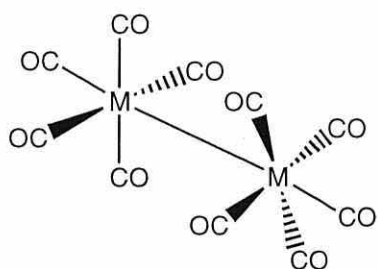


Figure 2.1. Structure of $[\text{M}_2(\text{CO})_{10}]$ ($\text{M} = \text{Mn}$ or Re).

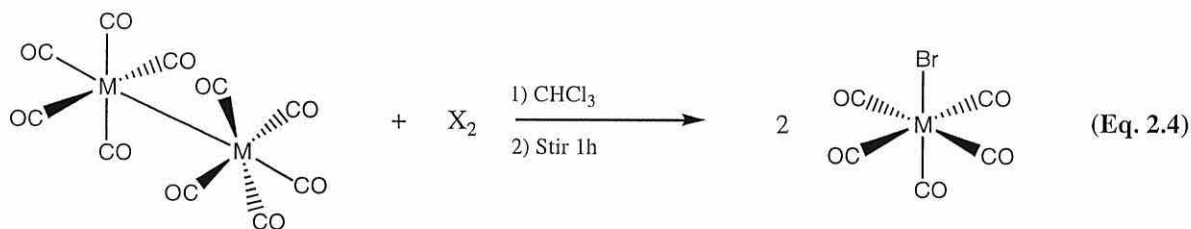
This gives rise to a molecule of approximately D_{4d} symmetry. In these $[\text{M}_2(\text{CO})_{10}]$ structures, the radial carbonyl groups are bent away from the metal–metal bond with $\text{M}-\text{M-C}$ angles of around 95° . This larger than expected angle has been explained as a result of an intrinsic property of an $[\text{M}(\text{CO})_5]$ unit rather than an effect due to the ligands or the metal–metal bond [57].

There have been a number of studies of the IR spectrum [58-62] and the Raman spectrum [63], of $[\text{Mn}_2(\text{CO})_{10}]$ in which assignments have been made and CO force constants calculated. The IR spectrum of $[\text{Mn}_2(\text{CO})_{10}]$ consists of three major absorptions at 2046 , 2015 and 1984 cm^{-1} each with the symmetry designations B_2 , E_1 and B_2 , respectively. Similarly, assignments of the carbonyl region of the IR and Raman spectra of $[\text{Re}_2(\text{CO})_{10}]$ have been produced, and force constants have been

determined [62, 64, 65]. The IR spectrum of $[\text{Re}_2(\text{CO})_{10}]$, as with $[\text{Mn}_2(\text{CO})_{10}]$, consists of three major absorptions at 2070, 2014 and 1976 cm^{-1} , each with the same symmetry designation as for $[\text{Mn}_2(\text{CO})_{10}]$. As was described in Scheme 2.1, the metal-metal bond is readily cleaved producing, amongst other product types the pentacarbonyl halides.

2.1.3 Manganese and rhenium pentacarbonyl halides

The pentacarbonyl rhenium halides, first prepared by Hieber [50, 66] are convenient starting materials for many rhenium carbonyl compounds. Similarly, the pentacarbonyl manganese halides were first prepared by Brimm [44] with more comprehensive studies undertaken by Abel and Wilkinson in 1959 [67]. Both of these compounds exhibit interesting photochemical [68, 69], vibrational [70-72] and kinetic properties [73-75]. They are prepared by the direct reaction of a halogen with the dimetal decacarbonyl species (shown in Eq. 2.4) [76].



Cleavage of the metal to metal bond by halogens giving $[\text{MX}(\text{CO})_5]$ (where $\text{X}=\text{Cl}, \text{Br}$ and I) has been proposed to go *via* a rate limiting ‘end-on’ attack of X_2 at the metal-metal bond. This gives a halogenium intermediate (Figure 2.2a) which dissociates X^- to give a halogenium ion (Figure 2.2b) [77].

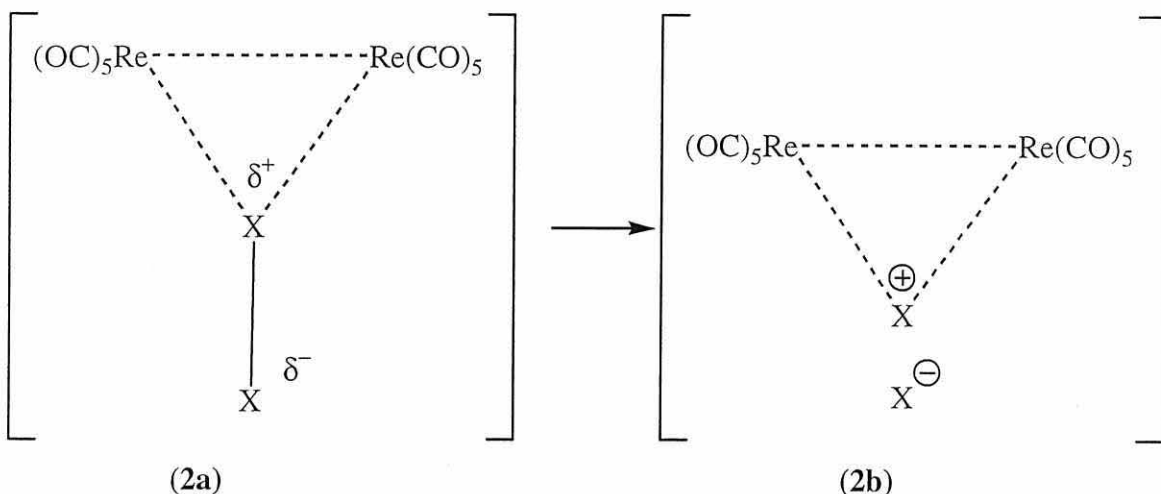


Figure 2.2. Cleavage of the metal-metal bond by a halogen.

Further replacement of the remaining carbonyls by neutral ligands (L) has been studied and results produced have formed the basis of a number of publications over the years. Section 2.1.4 discusses this chemistry in further detail.

2.1.4 Substituted complexes of $[MX(CO)_5]$

Carbonyl substitution in rhenium halocarbonyls $[ReX(CO)_5]$ is generally 1 to 2 orders of magnitude slower than in the corresponding manganese complexes; however in both cases the reaction has been shown to follow a first order rate law in which $[MX(CO)_5]$ has no dependence on the incoming ligand [73]. It has been suggested that this is due to dissociation of a *cis* carbonyl group resulting from *cis* labilisation [73]. This has been confirmed by a study in which ^{13}CO exchange showed *cis* labilisation increased in the order $X = I < Br < Cl$ *i.e.* in the order of decreasing σ -donor character of the halide [78].

Monosubstitution of $[MX(CO)_5]$ can be accomplished by treatment with one equivalent of donor ligand in refluxing solvent. Cleavage of the metal-metal bonded

species $\{\text{ReX}(\text{CO})_4\}_2$ with 2 equivalents of donor ligand is also an efficient method for generating *cis*- $[\text{ReX}(\text{CO})_4\text{L}]$ compounds [79]. It is also possible to take the metal-metal bonded species $\{\text{Mn}(\text{CO})_4\text{L}\}_2$, with halogen to produce the monosubstituted species [80] (Eq. 2.5).



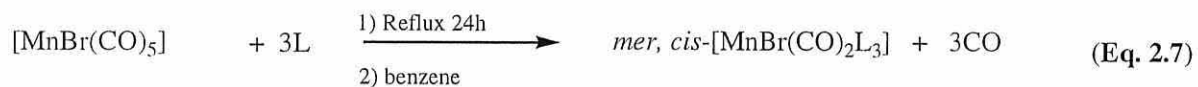
Purification and isolation of these monosubstituted compounds however is difficult, since invariably a mixture of the monosubstituted and disubstituted compounds are formed. This lack of specificity is a commonly encountered problem in carbonyl substitution chemistry [81]. One procedure which has been used to overcome this problem is to employ PdO as a catalyst [82] (Eq. 2.6).



This produces the desired tetracarbonyl species in yields $> 75\%$. However this process is only applicable when Tolmman's cone angle for the organophosphine is below 150° [83] and ligands with a larger cone angle do not react. It has been shown that the mechanism for the substitution reaction is quite different to that of the thermal reaction (which has been established as occurring via an $\text{S}_{\text{N}}1$ mechanism [78]). Furthermore, it is believed that the reaction proceeds *via* a radical chain-type mechanism [84]. This process has no effect on substitution reactions of $[\text{MnX}(\text{CO})_5]$.

The species $[\text{MnX}(\text{CO})_4\text{L}]$ can be produced by a number of different synthetic routes. For example, by the cleavage of $[\text{Mn}_2(\text{CO})_8\text{L}_2]$ by halogens [80]; by halogen-

hydrogen exchange reactions starting with $[\text{MnH}(\text{CO})_4\text{L}]$ [85]; or by photolysis of $[\text{Mn}_2(\text{CO})_8\text{L}_2]$ species in chlorinated solvents. With both manganese and rhenium, the most common complexes by far are the disubstituted species, and this is discussed in section 2.1.5. For manganese, it is also possible to prepare dicarbonyl and monocarbonyl complexes (Eq. 2.7) whereas these dicarbonyl species are rare in rhenium chemistry.



However, quite harsh conditions are necessary to achieve these dicarbonyl manganese products [86], and a recent publication has shown that the rhenium dicarbonyl species can be prepared but requires even harsher conditions and the use of perchloric acid. Monocarbonyl complexes are relatively uncommon apart from complexes formed from isocyanide precursors. Species with chelating diphosphines are generated by taking $[\text{MnX}(\text{CO})_5]$ with excess ligand and subjecting the mixture to UV photolysis [87]. An alternative method is shown in Figure 2.3 below [88, 89].

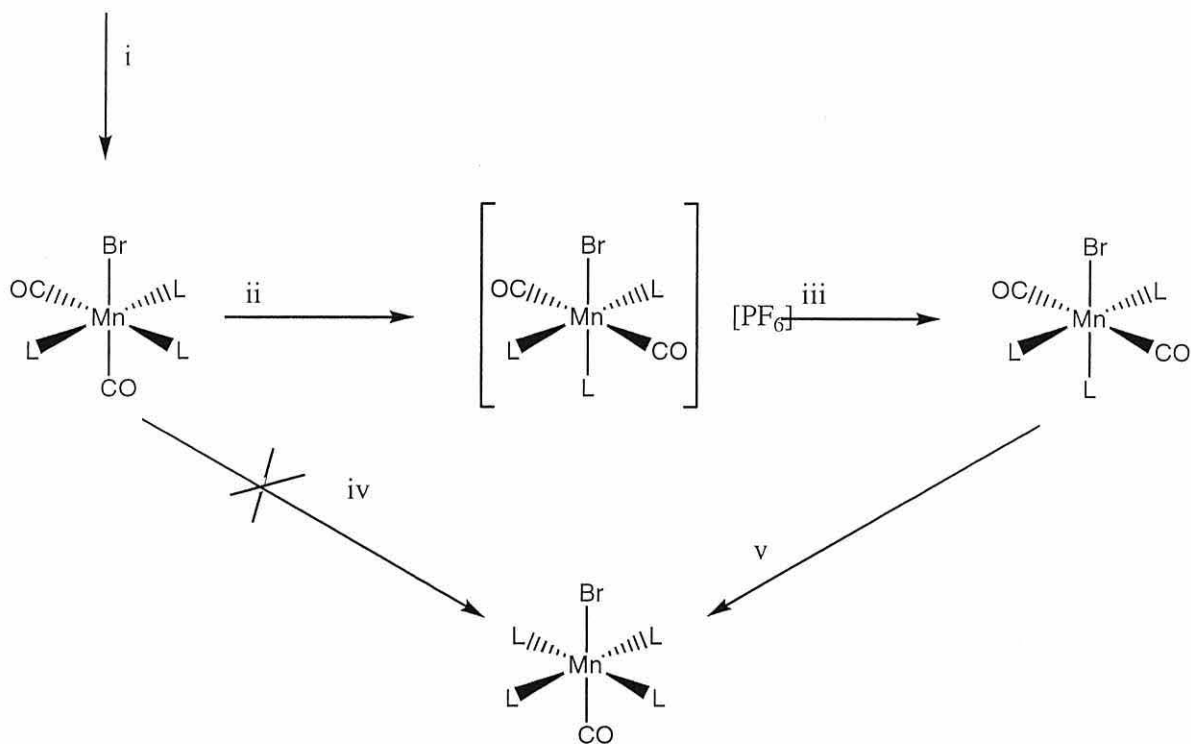
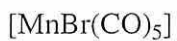


Figure 2.3. Preparation of tetrakis(OMe)₃-substituted monocarbonyl manganese halide ($\text{L} = \text{P}(\text{OMe})_3$). Conditions are (i) excess L , (ii) $[\text{NO}][\text{PF}_6]$, (iii) N_2H_4 , (iv) L and heat, (v) L and $\text{h}\nu$

2.1.5 Formation of $[\text{MX}(\text{CO})_3\text{L}_2]$ complexes

Carbonyl substituted complexes are readily obtained from $[\text{MX}(\text{CO})_5]$ which goes *via* intermediate monosubstitution products. The substitution of the second carbonyl is considerably slower than the initial substitution, but will occur at elevated temperatures to form the disubstituted species $[\text{MX}(\text{CO})_3\text{L}_2]$. Since the first paper on substitution of manganese and rhenium pentacarbonyl halides appeared in 1958, the area has hardly been out of press. The reader is pointed in the direction of Comprehensive Organometallic chemistry (I and II) [90, 91] and the Annual reviews of Manganese and Rhenium in Journal of Organometallic chemistry [92-94] for details.

2.2 Aims

The aims of this research were to prepare a series of new triorganophosphine derivatives of $[MBr(CO)_5]$ ($M = Mn$ and Re) and to unambiguously determine their stereochemistry. The new complexes will be characterised by ^{31}P NMR and IR spectroscopy and by single crystal X-ray diffraction studies of suitable crystals. The X-ray structures will serve as benchmarks for the spectroscopic data. These new complexes will also be used as organometallic reagents in the synthesis of metallaborane derivatives, as discussed in Chapter 3.

2.3 Results and Discussion

2.3.1 Synthesis of $[MBr(CO)_5]$ ($M = Mn$ or Re)

$[MnBr(CO)_5]$ and $[ReBr(CO)_5]$ were prepared by the literature methods [76], in yields varying from 60 to 90%, (Eq. 2.8). The physical and spectroscopic properties of $[MnBr(CO)_5]$ and $[ReBr(CO)_5]$ were in good agreement with literature values.



2.3.2 Synthesis of $[MBr(CO)_3L_2]$ and $[MBr(CO)_3(L\sim L)]$

Direct reaction of $[MBr(CO)_5]$ with various triorganophosphine ligands, in a 1:2 ratio for monodentate phosphines or 1:1 ratio for bidentate phosphines, produced complexes of the type $[MBr(CO)_3L_2]$ and $[MBr(CO)_3(L\sim L)]$ (Eq. 2.9 and 2.10). The $Mn(I)$ complexes were prepared in yields varying from 51 to 91% by refluxing in $CHCl_3$ for 3-8 h. The $Re(I)$ complexes were prepared by refluxing in $CHCl_3$ for 24 h and produced in yields ranging from 49 to 85%.



L= PPh₃, P(C₆H₄Cl)₃, P(C₆H₄OMe)₃, P(CH₂C₆H₅)₃

M = Mn: **2a**, **2b**, **2c**, **2d**.
 M = Re: **2e**, **2f**, **2g**, **2h**.



L= dppm, dppe, dppp, dppb, dppfc

M = Mn: **2i**, **2j**, **2k**, **2l**, **2m**.
 M = Re: **2n**, **2o**, **2p**, **2q**, **2r**.

All complexes were analysed *via* elemental analysis, melting point, ³¹P NMR and infra-red spectroscopy. The yield, elemental analysis and melting point data is summarised in Table 2.1 for Mn(I) complexes and Table 2.2 for Re(I) complexes. Compounds **2a**, **2e**, **2i**, **2j**, **2n**, **2o** and **2r** have been reported previously. However, these compounds were not fully characterised in the relevant reports. The remaining complexes are new to this study. All complexes were purified by recrystallisation from a CHCl₃ / hexane mixture (1:4), and they all gave satisfactory elemental analysis.

No	Compound	Analytical data		M.Pt (°C)	Yield (%)
		C(%) Found (Calc)	H(%) Found (Calc)		
	[MnBr(CO) ₅]	21.7 (21.9)	-	169 (Lit 171°C [77])	50
2a	[MnBr(CO) ₃ (PPh ₃) ₂]	63.2 (63.0)	4.0 (4.1)	166	82
2b	[MnBr(CO) ₃ {P(C ₆ H ₄ Cl-4) ₃ } ₂]	45.4 (45.2)	2.4 (2.4)	139	51
2c	[MnBr(CO) ₃ {P(C ₆ H ₄ OMe-4) ₃ } ₂]	58.7 (58.6)	4.6 (4.6)	138	77
2d	[MnBr(CO) ₃ {P(CH ₂ C ₆ H ₅) ₃ } ₂]	65.6 (65.4)	5.1 (5.1)	163	89
2i	[MnBr(CO) ₃ (dppm)]	48.2 (48.3)	3.1 (3.2)	178 (Lit 174°C [89])	91
2j	[MnBr(CO) ₃ (dppe)]	48.5 (49.0)	3.3 (3.4)	184 (Lit 183°C [89])	78
2k	[MnBr(CO) ₃ (dppp)]	56.7 (57.1)	4.2 (4.2)	210	76
2l	[MnBr(CO) ₃ (dppb)]	56.9 (57.7)	4.3 (4.4)	215	91
2m	[MnBr(CO) ₃ (dppfc)]	57.7 (57.5)	3.8 (3.7)	191	60

Table 2.1. Analytical data, M.Pt. and yields of Mn(I) tricarbonyl bromide complexes.

No	Compound	Analytical data		M.Pt. (°C)	Yield (%)
		C(%) Found (Calc)	H(%) Found (Calc)		
	[ReBr(CO) ₅]	14.8 (14.8)	-	182	94
2e	[ReBr(CO) ₃ (PPh ₃) ₂]	53.5 (53.6)	3.3 (3.45)	182 (Lit 181°C [95])	49
2f	[ReBr(CO) ₃ {P(C ₆ H ₄ Cl-4) ₃ } ₂]	43.1 (43.4)	2.5 (2.2)	172	67
2g	[ReBr(CO) ₃ {P(C ₆ H ₄ OMe-4) ₃ } ₂]	51.2 (51.2)	4.1 (4.0)	180	70
2h	[ReBr(CO) ₃ (P(CH ₂ C ₆ H ₅) ₃) ₂]	55.9 (56.4)	4.3 (4.4)	179	59
2n	[ReBr(CO) ₃ (dppm)]	45.9 (45.8)	3.1 (3.0)	225	70
2o	[ReBr(CO) ₃ (dppe)]	47.0 (46.5)	3.3 (3.2)	210	82
2p	[ReBr(CO) ₃ (dppp)]	47.2 (47.2)	3.4 (3.4)	292	76
2q	[ReBr(CO) ₃ (dppb)]	46.9 (47.2)	3.3 (3.6)	134	85
2r	[ReBr(CO) ₃ (dppfc)]	49.5 (49.1)	3.3 (3.1)	166	60

Table 2.2. Analytical data, M.Pt and yields of Re(I) tricarbonyl bromide complexes.

When adding two ligands (L) to a pentacarbonyl halide system $[MX(CO)_5]$, three possible isomers maybe potentially formed (Figure 2.4).

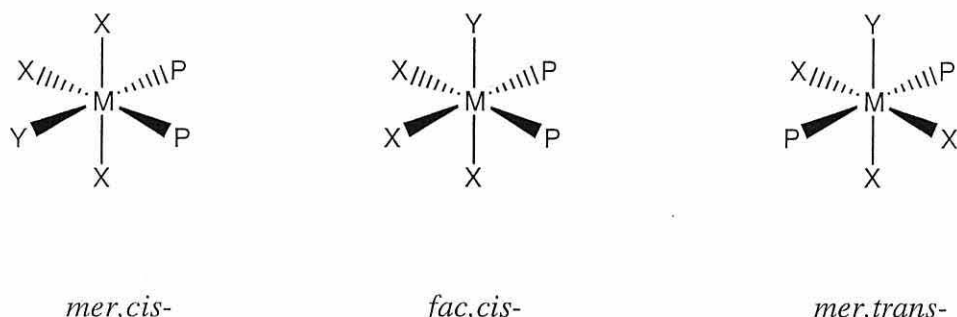


Figure 2.4. Differing stereo arrangements for disubstituted metal tricarbonyl centres.

In the cases of both the *fac,cis*- and *mer,trans*- isomers, only one peak would be expected in the phosphorus NMR since both phosphorus atoms are in equivalent environments. However, the *mer,cis*- isomer would show two phosphorus signals since both phosphorus nuclei are in differing environments. All of Mn(I) and Re(I) complexes gave, only one signal and it can be deduced that the compounds produced must have either *fac,cis*- or *mer,trans*- stereochemistry. The complexes with bidentate ligands must adopt a *fac,cis*- geometry whereas those with monodentate ligands may be in either of these two geometries. ^{31}P NMR, infrared spectroscopy and X-ray crystal data will be used to distinguish the stereochemistry of these complexes.

2.3.3 ^{31}P NMR spectroscopy

During the early 70's research was beginning into the use of ^{31}P NMR as a tool for structural elucidation [96]. Merriwether in 1961 described the ^{31}P NMR chemical shifts of a series of nickel carbonyl-phosphine complexes [97] and several authors have since used the chemical shift changes upon co-ordination as a diagnostic tool [98-100].

The ^{31}P NMR values of free phosphine (δ_f), co-ordinated phosphine (δ_c) and $\Delta\delta$ (calculated from subtracting the coordinated value from the free phosphine ^{31}P value) for all of the Mn(I) and Re(I) triorganophosphine complexes produced are shown in Tables 2.3 and 2.4 respectively. A downfield shift is indicated by a negative $\Delta\delta$ value.

No.	Compound	δ_f / ppm	δ_c / ppm	$\Delta\delta = \delta_f - \delta_c$
2a	[MnBr(CO) ₃ (PPh ₃) ₂]	-6.0	+53.3	-59.3
2b	[MnBr(CO) ₃ {P(C ₆ H ₄ Cl-4) ₃ } ₂]	-9.15	+52.8	-61.95
2c	[MnBr(CO) ₃ {P(C ₆ H ₄ OMe-4) ₃ } ₂]	-10.8	+44.8	-55.6
2d	[MnBr(CO) ₃ {P(CH ₂ C ₆ H ₅) ₃ } ₂]	-12.4	+41.8	-54.2
2i	[MnBr(CO) ₃ (dppm)]	-23.0	+11.8 (+10.9 [101])	-34.8
2j	[MnBr(CO) ₃ (dppe)]	-13.3	+69.5 (+67.6 [101])	-82.8
2k	[MnBr(CO) ₃ (dppp)]	-18.1	+27.6	-45.7
2l	[MnBr(CO) ₃ (dppb)]	-16.8	+32.9	-49.7
2m	[MnBr(CO) ₃ (dppfc)]	-17.9	+37.1	-55.0

Table 2.3. ^{31}P NMR data for Mn(I) tricarbonyl bromide complexes.

No.	Compound	δ_f / ppm	δ_c / ppm	$\Delta\delta = \delta_f - \delta_c$
2e	[ReBr(CO) ₃ (PPh ₃) ₂]	-6.0	-1.0	-5
2f	[ReBr(CO) ₃ {P(C ₆ H ₄ Cl-4) ₃ } ₂]	-9.15	-2.8	-6.35
2g	[ReBr(CO) ₃ {P(C ₆ H ₄ OMe-4) ₃ } ₂]	-10.8	-4.6	-6.2
2h	[ReBr(CO) ₃ {P(CH ₂ C ₆ H ₅) ₃ } ₂]	-12.4	-18.1	+5.7
2n	[ReBr(CO) ₃ (dppm)]	-23.0	-38.3 (-38.5 [101])	+15.3
2o	[ReBr(CO) ₃ (dppe)]	-13.3	+31.0 (+30.0 [101])	-44.3
2p	[ReBr(CO) ₃ (dppp)]	-18.1	-15.9	-2.2
2q	[ReBr(CO) ₃ (dppb)]	-16.8	-4.0	-12.8
2r	[ReBr(CO) ₃ (dppfc)]	-17.9	-0.7	-17.2

Table 2.4. ^{31}P NMR data for Re(I) tricarbonyl bromide complexes.

As would be expected, all of the phosphines upon complexation move downfield i.e. they become deshielded by the central metal atom, with the exception of **2n** and **2h**. The Mn(I) complexes appear to shift further downfield than the analogous Re(I) complexes, this may be due to the difference in size and electron distribution of Mn(I) compared with Re(I). The Mn(I) and Re(I) complexes with the largest $\Delta\delta$ value had dppe as ligand. The phosphorus environments in complexed dppe derivatives with 5-membered rings are strongly deshielded by the metal, whereas such deshielding is a lot less pronounced for the 4-membered ring (dppm) and 6-membered ring (dppp) chelates [102]. Indeed, the $\Delta\delta$ value for the rhenium (I) derivative [ReBr(CO)₃(dppm)] **2n** is positive, indicative of overall shielding at phosphorus.

Although both *mer,trans*- and *fac,cis*- complexes have been prepared previously, there has been no reported ^{31}P NMR data making any discussion of the results difficult.

IR and X-ray crystallographic data (see later) strongly suggest that the bis(monodentate) Mn(I) derivatives have the *mer,trans*-configuration whereas the analogous Re(I) derivatives have the *fac,cis*-configuration. Inspection of $\Delta\delta$ values for the derivatives would indicate that these values are not diagnostic of configuration.

2.3.4 Infra-red Spectroscopy

As with ^{31}P NMR, this is potentially an important diagnostic tool for the solution of stereochemical problems. Infrared spectroscopy is a powerful technique for detecting the presence of metal-carbonyl bonds. The stretching frequencies of manganese and rhenium carbonyls range from 2150 cm^{-1} to 1850 cm^{-1} and are in the region expected for terminal metal carbonyl derivatives. This section will be concerned only with the metal carbonyl stretching region in an IR spectrum.

The number of bands that appear in this region of the infrared spectrum can indicate the different isomers present. Table 2.5 shows the number of expected IR absorption bands for the different isomers of $[\text{MBr}(\text{CO})_3\text{L}_2]$ with equivalent L environments, based on the symmetry of the carbonyl ligands.

Isomer	Approx. Point Group	Expected No of Bands.
<i>Fac, cis</i> $[\text{MBr}(\text{CO})_3\text{L}_2]$	C_s	$3 (2\text{A}' + \text{A}'')$
<i>Mer, trans</i> $[\text{MBr}(\text{CO})_3\text{L}_2]$	C_{2v}	$3 (2\text{A}_1 + \text{B}_2)$

Table 2.5. Expected number of bands for each isomer in the metal carbonyl region.

The symmetry stretches and bends associated with each of the symmetry operators A_1 , B_2 , A' and A'' are shown in Figure 2.5 below.

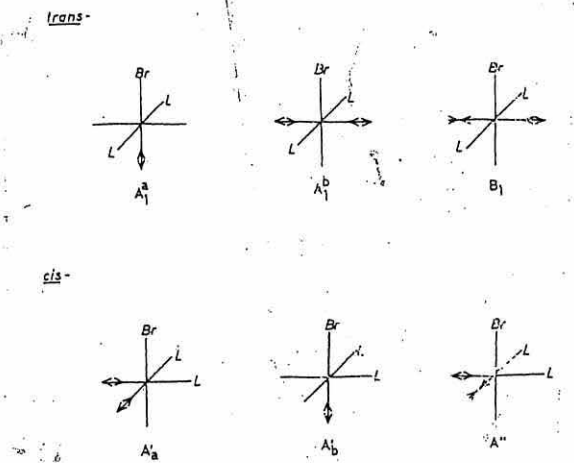


Figure 2.5. Symmetry stretches and bends associated with the operators A_1 , B_2 , A' and A'' .

The values of the stretches observed in both the Mn(I) and Re(I) complexes are shown in Tables 2.6 and 2.7, respectively.

No	Compound	ν (CO) stretches
2a	[MnBr(CO) ₃ (PPh ₃) ₂]	2040(m), 1943(s), 1918(s)
2b	[MnBr(CO) ₃ {P(C ₆ H ₄ Cl-4) ₃ } ₂]	2033(w), 1951(s), 1901(s)
2c	[MnBr(CO) ₃ {P(C ₆ H ₄ OMe-4) ₃ } ₂]	2031(w), 1946(s), 1908(s)
2d	[MnBr(CO) ₃ {P(CH ₂ C ₆ H ₅) ₃ } ₂]	2031(w), 1945(s), 1912(s)
2i	[MnBr(CO) ₃ (dppm)]	2026(s), 1957(s), 1919(s) (2025(s), 1955(s), 1920(s) [88])
2j	[MnBr(CO) ₃ (dppe)]	2008(s), 1935(s), 1915(s) (2023(s), 1956(s), 1917(s) [88])
2k	[MnBr(CO) ₃ (dppp)]	2028(s), 1961(s), 1909(s)
2l	[MnBr(CO) ₃ (dppb)]	2028(s), 1962(s), 1910(s)
2m	[MnBr(CO) ₃ (dppfc)]	2025(s), 1959(s), 1909(s)

Table 2.6. IR stretches of Mn(I) tricarbonyl bromide complexes (KBr disc).

No.	Compound	IR Stretches in Carbonyl region
2e	[ReBr(CO) ₃ (PPh ₃) ₂]	2028(s), 1950(s), 1892(s) (2037(s), 1960(s), 1899(s) [95])
2f	[ReBr(CO) ₃ {P(C ₆ H ₄ Cl-4) ₃ } ₂]	2035(s), 1956(s), 1912(s)
2g	[ReBr(CO) ₃ {P(C ₆ H ₄ OMe-4) ₃ } ₂]	2022(s), 1954(s), 1915(s)
2h	[ReBr(CO) ₃ {P(CH ₂ C ₆ H ₅) ₃ } ₂]	2033(s), 1952(s), 1899(s)
2n	[ReBr(CO) ₃ (dppm)]	2026(s), 1943(s), 1893(s)
2o	[ReBr(CO) ₃ (dppe)]	2026(s), 1948(s), 1913(s)
2p	[ReBr(CO) ₃ (dppp)]	2034(s), 1955(s), 1904(s)
2q	[ReBr(CO) ₃ (dppb)]	2032(s), 1953(s), 1904(s)
2r	[ReBr(CO) ₃ (dppfc)]	2036(s), 1958(s), 1901(s)

Table 2.7. Carbonyl stretches for Re(I) complexes.

As can be seen for this data, there are evidently two types of complexes produced. One of them has three equal intensity carbonyl stretches (see Figure 2.6) whilst the other has only two strong absorptions with one weak one (see Figure 2.7)

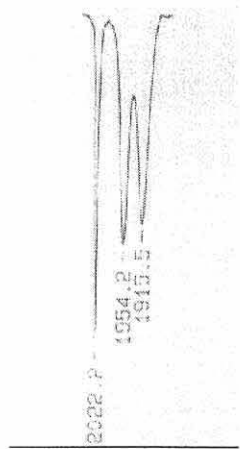


Figure 2.6

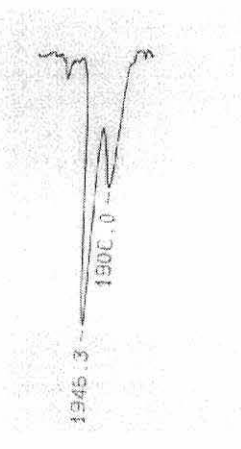


Figure 2.7

The literature is not clear on the identification of which isomer is which. Clearly, the complexes of the bidentate ligands must be *fac,cis*- and these all have spectra similar to Figure 2.6. The remaining rhenium(I) derivatives have similar spectra and are likely to also be *fac,cis*- whereas the manganese(I) derivatives, **2a – 2e**, are of a different type (Fig. 2.7) and are presumably *mer,trans*- . To confirm this, it has been possible to benchmark these IR absorptions against crystal structures as described in the next section.

2.3.5 X-Ray Crystallography

This section reports single crystal crystallographic data for the compounds [ReBr(CO)₃{P(C₆H₄OMe)₃}₂] **2g**, [ReBr(CO)₃{P(CH₂C₆H₅)₃}₂] **2h**, [ReBr(CO)₃(dppfc)] **2r**, [MnBr(CO)₃{P(C₆H₄Cl)₃}₂] **2b**, [MnBr(CO)₃(dppe)] **2j** and [MnBr(CO)₃(dppfc)] **2m**. Full crystallographic data for the compounds is presented in Appendices A-F. Compound **2r**, was determined to have three independent conformational isomers present in the unit cell, but for convenience only the one isomer will be discussed here, compound **2b** was a disordered structure, but data are described for the highest occupancy structure.

Tables 2.8, 2.9 and 2.10 contain selected bond lengths for compounds **2b**, **2g**, **2h**, **2j**, **2m** and **2r** whilst Tables 2.11, 2.12 and 2.13 contain selected bond angles for the above compounds. Figure 2.8 to Figure 2.13 show the molecular structures for **2b**, **2g**, **2h**, **2j**, **2m** and **2r** respectively. Atoms are numbered as in the diagrams and arranged in the tables as to be comparable.

	2g (Å)		2h (Å)		2r (Å)
Re – P(1)	2.527(9)	Re – P(1)	2.500(5)	Re – P(1)	2.5180(18)
Re – P(2)	2.547(10)	Re – P(2)	2.494(6)	Re – P(2)	2.5520(16)
Re – Br	2.631(6)	Re – Br	2.650(3)	Re – Br	2.586(3)
Re – C(1)	1.926(4)	Re – C(1)	1.917(2)	Re – C(1)	1.855(19)
Re – C(2)	1.941(4)	Re – C(2)	1.946(3)	Re – C(2)	1.930(7)
Re – C(3)	1.950(4)	Re – C(3)	1.935(2)	Re – C(3)	1.943(8)

Table 2.8. Selected bond lengths (Å) about the *fac,cis*- rhenium(I) centres in **2g**, **2h** and **2r**.

	2j (Å)		2m (Å)
Mn – P(1)	2.519(10)	Mn - P(1)	2.507(8)
Mn – P(2)	2.321(17)	Mn - P(2)	2.400(11)
Mn – Br	2.333(17)	Mn – Br	2.378(11)
Mn – C(1)	1.818(7)	Mn – C(35)	1.821(4)
Mn – C(2)	1.827(6)	Mn – C(36)	1.824(4)
Mn – C(3)	1.953(9)	Mn – C(37)	1.938(5)

Table 2.9. Selected bond lengths (Å) about the *fac,cis*- manganese(I) centres in **2j** and **2m**.

	2b (Å)
Mn – P(1)	2.3260(11)
Mn – P(2)	2.3275(10)
Mn – Br	2.5458(7)
Mn – C(37)	1.7986(8)
Mn – C(38)	1.7986(7)
Mn – C(39)	1.804(4)

Table 2.10. Selected bond lengths about the *mer,trans-* manganese(I) centre.

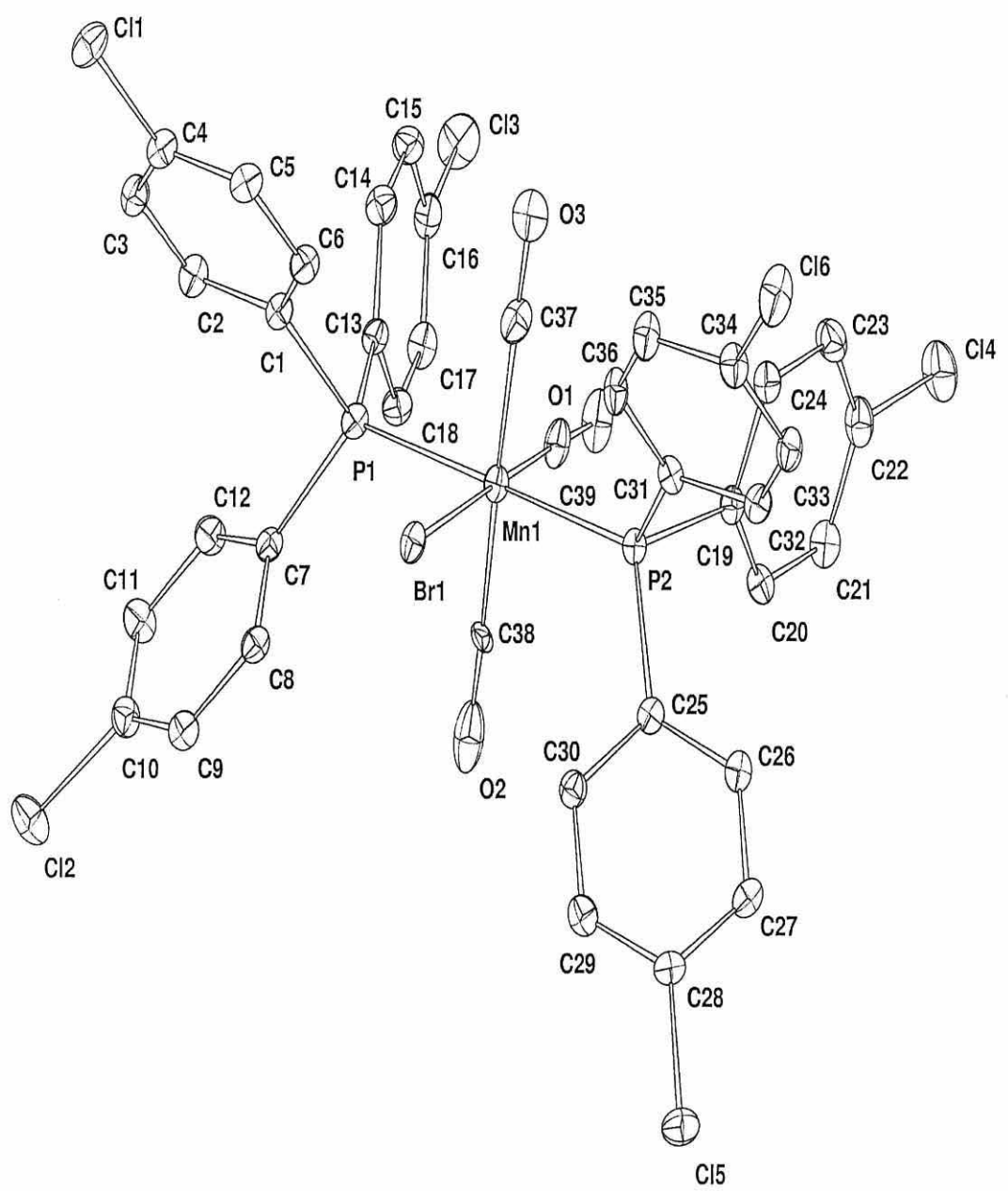


Figure 2.8. Molecular structure of **2b**.

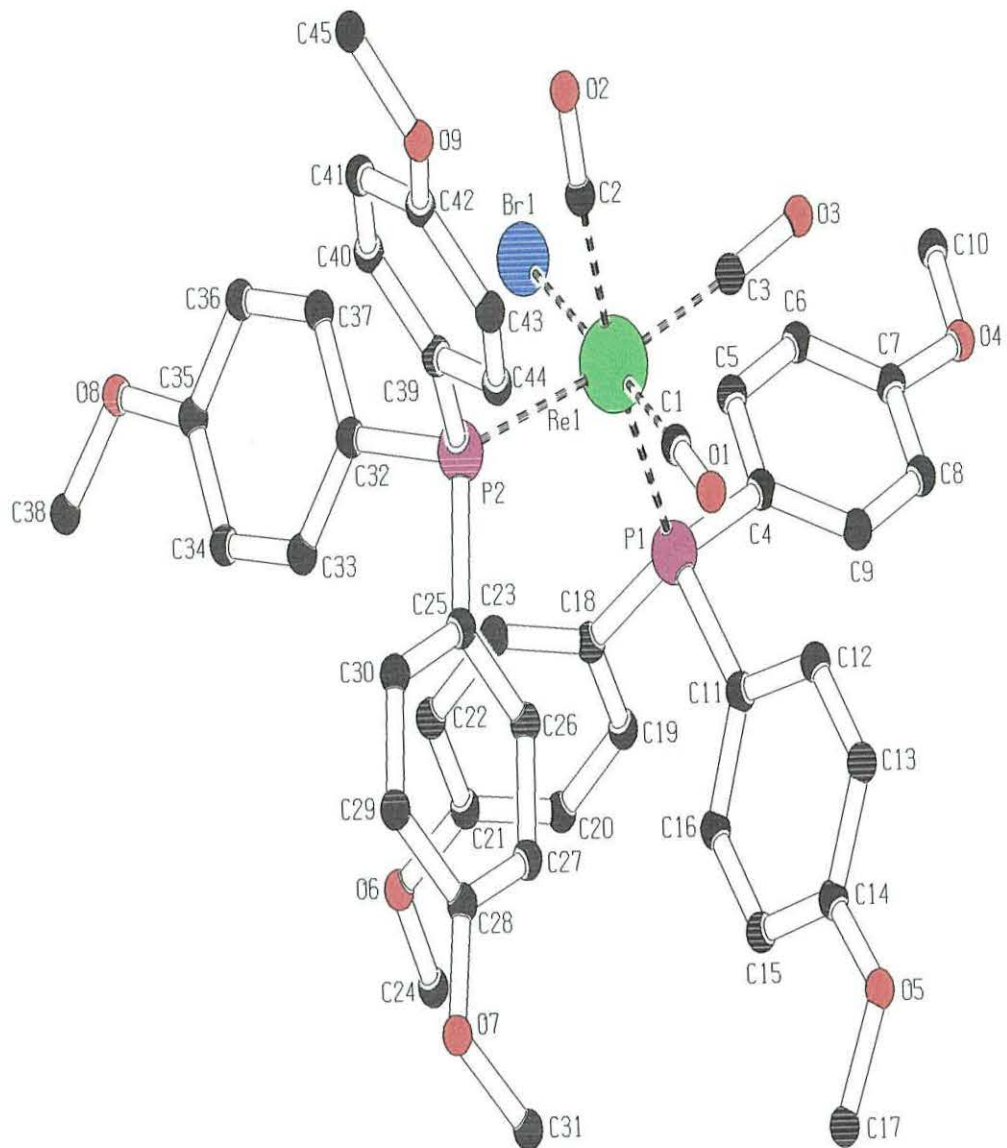


Figure 2.9. Molecular structure of **2g**

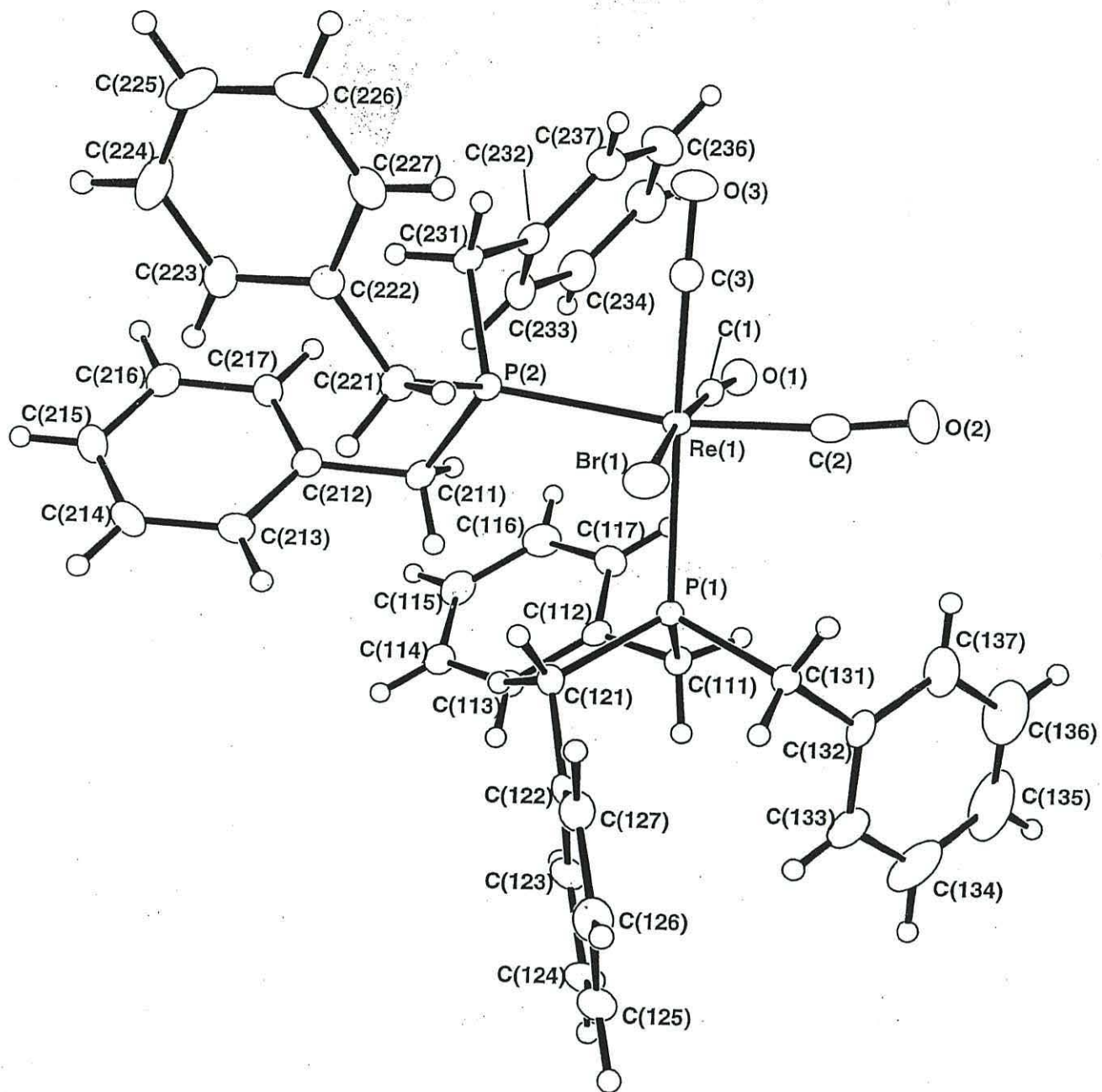


Figure 2.10. Molecular structure of **2h**.

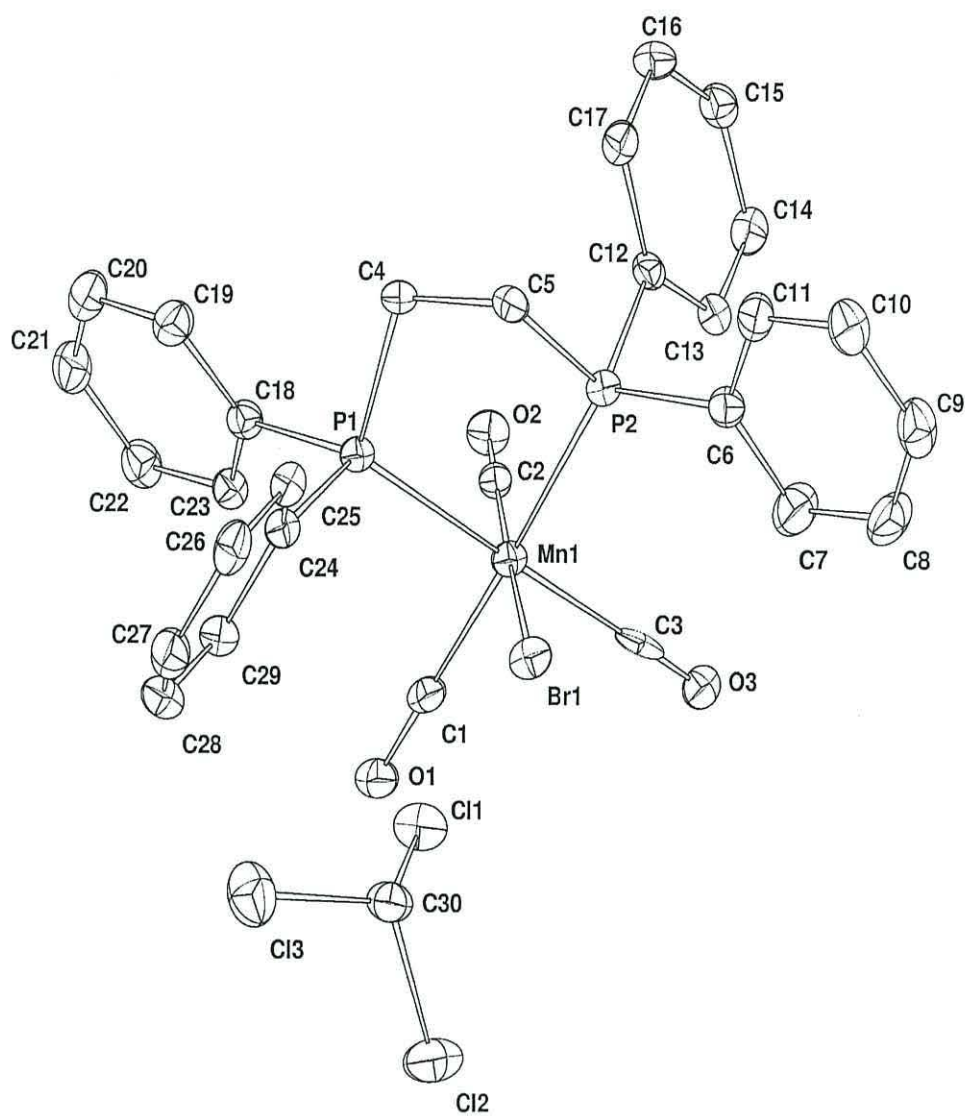


Figure 2.11. Molecular structure of **2j**.

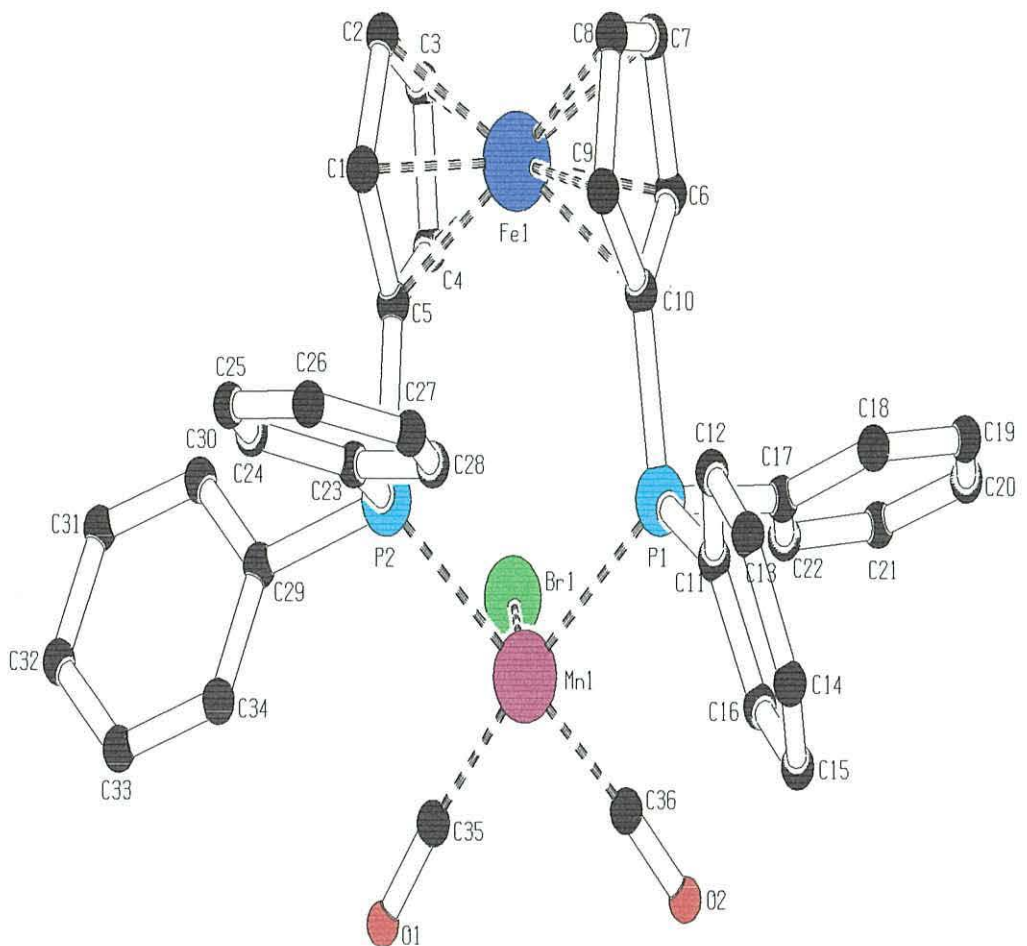


Figure 2.12. Molecular structure of **2m**, viewed down the OC-Mn-Br axis. The Mn1 and C37 are obscured in this view.

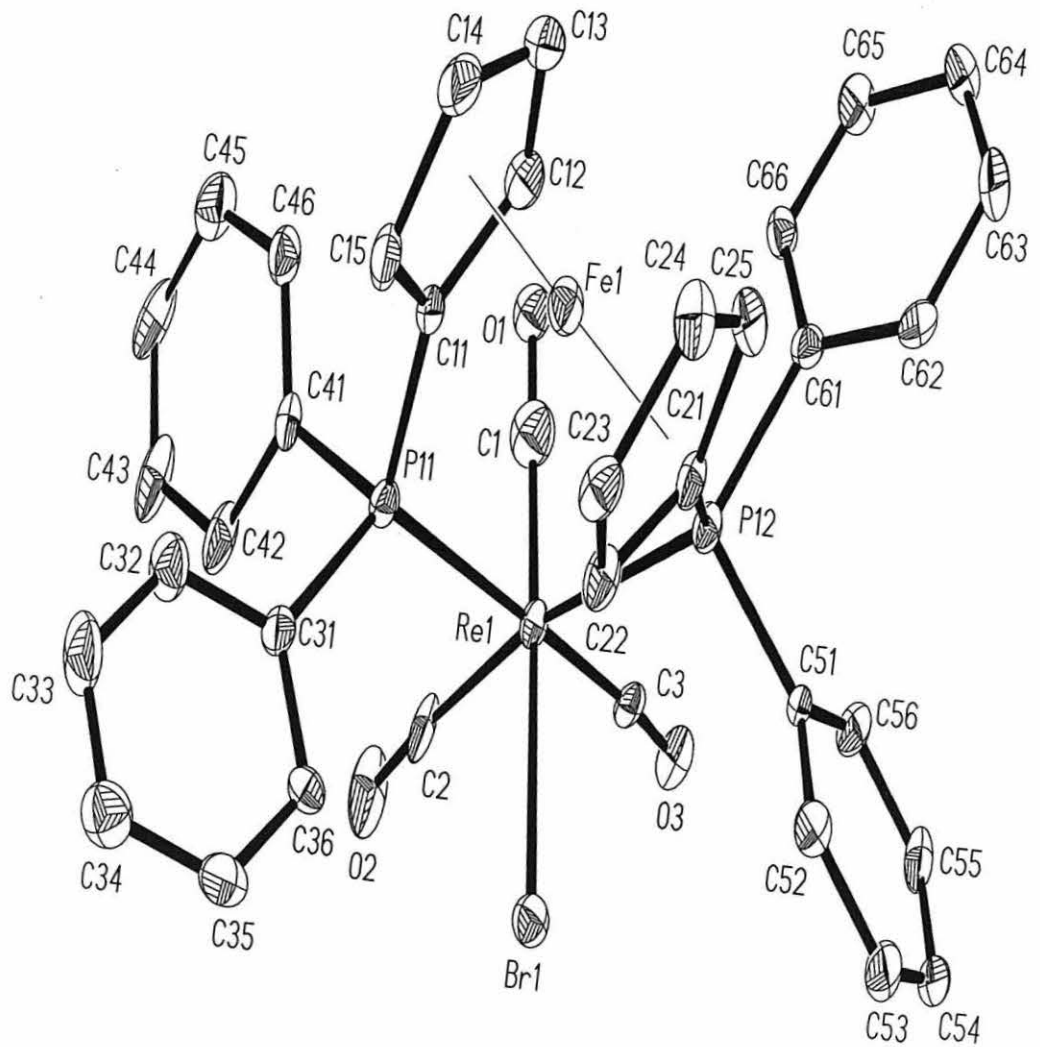


Figure 2.13. Molecular structure of **2r**.

	2g (°)		2h (°)		2r (°)
C1–Re–C3	91.21(15)	C1–Re–C3	93.78(10)	C1–Re–C3	91.0(5)
C1–Re–C2	92.88(15)	C1–Re–C2	85.67(10)	C1–Re–C2	90.6(5)
C3–Re–C2	86.48(15)	C3–Re–C2	86.18(10)	C3–Re–C2	86.7(3)
C1–Re–P1	92.91(10)	C1–Re–P1	96.38(7)	C1–Re–P1	84.6(5)
C2–Re–P1	168.79(11)	C2–Re–P1	169.06(7)	C2–Re–P1	87.7(2)
C3–Re–P1	83.82(10)	C3–Re–P1	90.57(2)	C3–Re–P1	172.76(19)
C1–Re–P2	85.66(10)	C1–Re–P2	92.59(7)	C1–Re–P2	97.4(4)
C2–Re–P2	84.11(11)	C2–Re–P2	85.19(7)	C2–Re–P2	169.6(2)
C3–Re–P2	169.91(10)	C3–Re–P2	171.07(7)	C3–Re–P2	86.42(19)
P1–Re–P2	105.89(3)	P1–Re–P2	98.34(2)	P1–Re–P2	99.79(6)
C1–Re–Br	177.98(10)	C1–Re–Br	173.99(7)	C1–Re–Br	175.4(5)
C2–Re–Br	87.36(11)	C2–Re–Br	88.44(7)	C2–Re–Br	85.4(2)
C3–Re–Br	90.80(11)	C3–Re–Br	88.91(8)	C3–Re–Br	86.7(2)
P1–Re–Br	87.19(2)	P1–Re–Br	81.05(14)	P1–Re–Br	97.33(6)
P2–Re–Br	92.37(2)	P2–Re–Br	93.16(14)	P2–Re–Br	86.41(6)

Table 2.11. Selected bond angles (°) about the rhenium(I) centre.

	2j (°)		2m (°)
C1 – Mn – C3	90.70(2)	C35 – Mn – C36	85.85(16)
C1 – Mn – C2	93.00(2)	C35 – Mn – C37	87.71(17)
C3 – Mn – C2	90.10(2)	C36 – Mn – C37	91.62(15)
C1 – Mn – P1	90.56(18)	C37 – Mn – P1	93.72(12)
C2 – Mn – P1	90.06(17)	C36 – Mn – P1	87.62(11)
C3 – Mn – P1	178.69(17)	C35 – Mn – P1	173.36(11)
C1 – Mn – P2	172.58(19)	C36 – Mn – P2	174.17(12)
C2 – Mn – P2	92.72(17)	C35 – Mn – P2	91.50(11)
C3 – Mn – P2	93.96(17)	C37 – Mn – P2	93.46(10)
P1 – Mn – P2	84.74(6)	P1 – Mn – P2	94.88(4)
C1 – Mn – Br	89.26(18)	C35 – Mn – Br	81.56(12)
C2 – Mn – Br	177.56(17)	C37 – Mn – Br	169.25(12)
C3 – Mn – Br	90.70(16)	C36 – Mn – Br	86.90(12)
P1 – Mn – Br	89.05(5)	P1 – Mn – Br	96.85(3)
P2 – Mn – Br	84.94(5)	P2 – Mn – Br	87.58(3)

Table 2.12. Selected bond angles (°) about the manganese(I) centre.

	2b (°)
C37 – Mn – C38	171.03(8)
C38 – Mn – C39	85.66(17)
C37 – Mn – C39	85.58(17)
C37 – Mn – P1	88.41(12)
C38 – Mn – P1	89.82(12)
C39 – Mn – P1	91.27(13)
C37 – Mn – P2	91.48(12)
C38 – Mn – P2	90.59(11)
C39 – Mn – P2	90.71(13)
P1 – Mn – P2	178.01(4)
C37 – Mn – Br	94.76(8)
C38 – Mn – Br	94.03(7)
C39 – Mn – Br	178.87(12)
P1 – Mn – Br	89.82(3)
P2 – Mn – Br	88.21(3)

Table 2.13. Selected bond lengths around the *mer,trans-* isomer.

There have been relatively few crystallographically determined Mn(I) or Re(I) tricarbonyl halide compounds containing two phosphines or related ligands. Those that have are limited to $[\text{MnCl}(\text{CO})_3(\text{Et}_2\text{PCH}_2\text{CH}_2\text{PEt}_2)]$ [103], $[\text{MnBr}(\text{CO})_3(\text{PPhH}_2)_2]$ [104], $[\text{MnCl}(\text{CO})_3\{\text{C}_6\text{H}_4(\text{PH}_2)_2\}]$ [104], $[\text{MnCl}(\text{CO})_3\{\text{C}_6\text{H}_4(\text{PPh}_2)_2\}]$ [104], $[\text{MnBr}(\text{CO})_3(\text{dppe})]$ [104], $[\text{MnBr}(\text{CO})_3(\text{triphos})\text{Cr}(\text{CO})_5]$ [105], $[\text{Mn}(\text{CO})_3(\text{dppe})(\text{NCO})]$ [106], $[\text{Mn}(\text{CO})_3(\text{dppp})\text{C}(\text{O})\text{OEt}]$ [106], $[\text{MnBr}(\text{CO})_3(\text{CNPh})_2]$

[107], *fac,cis*-[MnBr(CO)₃(P(OMe)₂Ph)₂] [108] and *mer,trans*-[MnBr(CO)₃(P(OMe₂)Ph)₂] [108], [MnBr(CO)₃{P(OMe)₂O}₂SiMe₂] [109] whilst there are fewer determined structures for Re(I), [ReCl(CO)₃(SbPh₃)₂] [110], [Re(CO)₃(dppp)C(O)OD] [111] and [ReBr(CO)₃(L_c)₂] (where L_c = *cis*-3,4-dihydro-2,3,4,5-tetraphenyl-2*H*-1,2,3-diazaphosphole) [112].

For the *fac,cis*- Mn(I) complex **2j**, the Mn-C bond length *trans* to Br is shorter than the Mn-C bond lengths *trans* to the tertiary phosphines. This has been observed previously with the [MnBr(CO)₃(triphos)Cr(CO)₅] [105] complex. However, with compound **2m**, the Mn-C bond length *trans* to Br is significantly longer, the corresponding structure in the literature has all three Mn-C bond lengths the same [104].

The Mn-Br bond lengths for **2j** and **2m** are shorter than the corresponding bond lengths found in *fac*-[MnBr(CO)₃(MeNC)₂] (2.54Å) , [MnBr(CO)₃(CNPh)₂] (2.527Å) [107], [MnBr(CO)₃(P(OMe)₂Ph)₂] (2.532Å) [108], [MnBr(CO)₃(dppe)] (2.504Å) [104], the two isomers of [MnBr(CO)₃(triphos)Cr(CO)₅] (2.537Å and 2.534Å) [105] and [MnBr(CO)₃{P(OMe₂)₂O}₂SiMe₂] (2.528Å) [109]. Whilst the Mn-P lengths in compounds **2j** and **2m** are longer than those previously reported [MnBr(CO)₃(PPhH₂)₂] (2.305Å and 2.322Å) [104], [MnCl(CO)₃(C₆H₄(PPh₂)₂)] (2.325Å and 2.320Å) [104], [Mn(CO)₃(dppe)(NCO)] (2.341Å and 2.329Å) [106], [Mn(CO)₃(dppp)C(O)OEt] (2.346Å and 2.340Å) [106], *fac,cis*-[MnBr(CO)₃(P(OMe)₂Ph)₂] (2.296Å and 2.303Å) [108] and [MnBr(CO)₃{P(OMe₂)₂O}₂SiMe₂] (2.258Å and 2.255Å) [109].

There has only been one previous example of a *mer,trans*- Mn(I) tricarbonyl halide complex analysed by X-ray crystallography, [MnBr(CO)₃(P(OMe)₂Ph)₂] [108]. Comparison of compound **2b** with this reported structure shows a good correlation. The Mn-C bond lengths are very similar (1.7968(8)Å to 1.804(4)Å for **2b** *cf.* 1.80(2)Å to 1.80(3)Å for [MnBr(CO)₃(P(OMe)₂Ph)₂]) as are the Mn-Br bond length (2.524(7)Å for

$[\text{MnBr}(\text{CO})_3(\text{P}(\text{OMe})_2\text{Ph})_2]$ cf. 2.5458(7) \AA for compound **2b**). The Mn-P bond lengths however are different, with those in compound **2b** being longer than those found in $[\text{MnBr}(\text{CO})_3(\text{P}(\text{OMe})_2\text{Ph})_2]$ (2.360(1) \AA and 2.3275(10) \AA for **2b** cf. 2.179(8) \AA and 2.260(8) \AA for $[\text{MnBr}(\text{CO})_3(\text{P}(\text{OMe})_2\text{Ph})_2]$).

There is also a good correlation between the three Re(I) crystal structures presented here and those published in the literature [110-112]. Compounds **2g**, **2h** and **2r** all have Re-P bond lengths in the range 2.494(6) \AA to 2.5520(16) \AA , which are in the same range as those found for *fac*- $[\text{Re}(\text{CO})_3(\text{dppp})\text{C}(\text{O})\text{OD}]$ (Re-P 2.472(3) \AA and 2.454(3) \AA [111]) and $[\text{ReBr}(\text{CO})_3(\text{L}_c)_2]$ (Re-P 2.481(3) \AA and 2.497(3) \AA [112]). The Re-C bond lengths in *fac*- $[\text{Re}(\text{CO})_3(\text{dppp})\text{C}(\text{O})\text{OD}]$ range from 1.927(13) \AA to 1.945(14) \AA [111], in $[\text{ReCl}(\text{CO})_3(\text{SbPh}_3)_2]$ they are 1.92(1) \AA to 1.97(1) \AA [110] and in $[\text{ReBr}(\text{CO})_3(\text{L}_c)_2]$ they range from 1.898(13) \AA to 1.956(14) \AA these values are encompassed by the Re-C bond lengths shown for compounds **2g**, **2h** and **2r** (range from 1.855(19) \AA to 1.950(4) \AA). Compounds **2g**, **2h** and **2r** all exhibit Re-Br bond lengths, in the range 2.586(3) \AA to 2.650(3) \AA , again in agreement with the Re-Br bond length found in $[\text{ReBr}(\text{CO})_3(\text{L}_c)_2]$ 2.622(1) \AA [112].

The single crystal diffraction studies confirm that there are two different isomers. With the bidentate phosphines attached to both Mn(I) and Re(I), only the *fac,cis*- isomer is observed (this would be expected as the phosphines need to be mutually *cis* to bond with the metal centre). However, in the case of the monodentate phosphines, a *fac,cis*- isomer is observed for Re(I), but a *mer,trans*- isomer is observed for Mn(I). This agrees with the IR spectroscopic data, where all the monodentate phosphine complexes of Mn(I) showed three absorptions (two strong and one weak), whilst for the Re(I) complexes again three absorptions were observed but all three were of equal intensity.

2.4 Conclusions

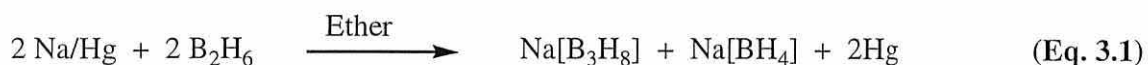
In conclusion, a range of Mn(I) and Re(I) (bis)triorganophosphine complexes have been prepared. These have been characterised by ^{31}P NMR, IR spectroscopy, melting point and elemental analysis. Suitable crystals have been solved via X-ray crystal diffraction. It has been shown that the monodentate phosphines form *mer,trans*-isomers with Mn(I) with Re(I) monodentate and bidentate phosphines form only the *fac,cis*- isomer.

Chapter 3

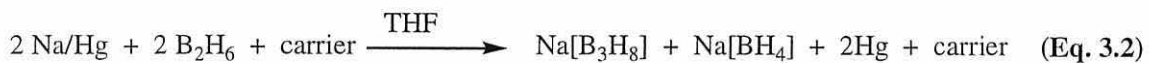
Synthesis and characterisation of octahydrotriborate
derivatives of $[M(CO)_3(L)_2Br]$ ($M = Mn$ or Re).

3.1 Introduction

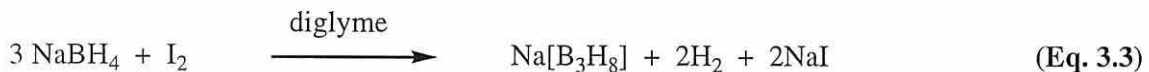
Alfred Stock first prepared the octahydrotriborate anion, $[B_3H_8]^-$, by the reaction of a sodium mercury amalgam with diborane. However he incorrectly characterised the product as $Na_2[B_2H_6]$ [113], and it was not until later that Hough, Edwards and McElroy determined that the product from the reaction was $Na[B_3H_8]$ (Eq. 3.1) [114, 115].

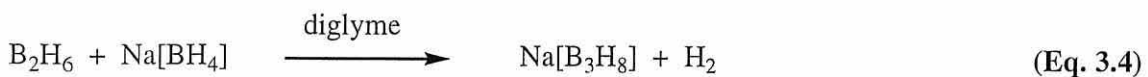


By addition of a carrier species, for example naphthalene, the rate of reaction is increased allowing the synthesis to be completed within a few seconds in THF (Eq. 3.2) [116]. Sodium amalgam has also been found to react with B_4H_{10} and B_5H_{11} in diethyl ether to produce $Na[B_3H_8]$ [117].



A more convenient synthesis of $[B_3H_8]^-$ however involves the reaction of sodium borohydride with iodine (Eq. 3.3) [118]. A mechanism for this has been postulated, and is thought to involve the oxidation of $[BH_4]^-$ to B_2H_6 , followed by a subsequent reaction between diborane and $[BH_4]^-$ producing $[B_3H_8]^-$ (Eq. 3.4) [118].





Alternatively the reaction between boron trifluoride diethyl etherate and $\text{Na}[\text{BH}_4]$ also produces $[\text{B}_3\text{H}_8]^-$ (Eq. 3.5) [119].



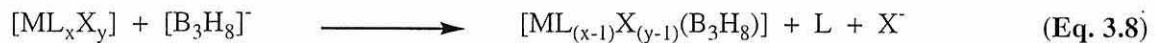
The reactions illustrated in Eq. 3.3 and Eq. 3.5 produce sodium octahydrotriborate, which has a limited air stability. A number of other cations can be used which produce salts with enhanced stability, for example the preparation of an air-stable caesium salt is available by a metathesis reaction (Eq. 3.6) [118, 119, 120].



Tetraalkylammonium salts have proved to be useful due to their high thermal and air-stability whilst also having a low moisture sensitivity. They are also soluble in organic solvents which makes them valuable as starting materials for metathesis to other $[\text{B}_3\text{H}_8]^-$ salts. The general method of their preparation involves the addition of a saturated aqueous solution of tetraalkylammonium halide to a diethyl ether solution of $\text{Na}[\text{B}_3\text{H}_8]$ (Eq. 3.7) [116].



The most general preparation of metal-B₃H₈ complexes involves the reaction of an organometallic halide with [R₄N][B₃H₈] in a dichloromethane solution (Eq. 3.8). Most reactions proceed at room temperature, although thermal or photolytic induction is required in some cases.



L = Neutral donor ligand, X = Halide

3.2 Aims

The aim of this chapter was to use the manganese(I) and rhenium(I) halo carbonyl phosphine derivatives prepared in Chapter 2 and explore their reactions with the octohydrotriborate anion. With a few exceptions [1, 2] this area has been frequently overlooked. The chemistry of the complex obtained in the highest yield was to be further investigated as representative of the chemistry of the class.

3.3 Results and Discussion

3.3.1 Synthesis of the [B₃H₈]⁻ anion.

[ⁿBu₄N][B₃H₈] was prepared by the literature method [118], in yields varying from 70 to 80%, (Eq. 3.9 and Eq. 3.10). The physical and spectroscopic properties of [ⁿBu₄N][B₃H₈] so obtained were in good agreement with literature values.



3.3.2 Attempted synthesis of 2-metallatetraboranes from *mer,trans*-[MnBr(CO)₃(L)₂].

The reaction between compounds **2a-2d** and [ⁿBu₄N][B₃H₈], in a 1:1 ratio, were attempted under both thermal and photolytic conditions. In all cases a white solid formed which was insoluble and was difficult to identify. NMR spectra of the residual solids and solution did not indicate formation of any metallatetraborane species.

3.3.3 Synthesis of 2-metallatetraboranes from *fac,cis*-[MBr(CO)₃(L)₂] and *fac,cis*-[MBr(CO)₃(L~L)].

The reaction between [ⁿBu₄N][B₃H₈] with compounds **2e – 2r**, in a 1:1 ratio, produced complexes of the type [M(CO)₂(L)₂(B₃H₈)] and [M(CO)₂(L~L)(B₃H₈)] (Eq. 3.11 and Eq. 3.12). The Mn(I) complexes were prepared in yields ranging from 17 to 59% by UV photolysis in CHCl₃ for 20h. Similarly, the Re(I) complexes were prepared in yields ranging from 17 to 46% under the same conditions as Mn(I).



L~L = dppm, dppe, dppp, dppb, dppfc

M = Mn: **3a**, **3b**, **3c**, **3d**, **3e**.
M = Re: **3j**, N/A, **3k**, **3l**, **3m**.



L = PPh₃, P(C₆H₄Cl)₃, P(C₆H₄OMe)₃, P(CH₂C₆H₅)₃

M = Re: **3f**, **3g**, **3h**, **3i**.

All complexes were analysed by elemental analysis, melting point, ¹H, ¹¹B and ³¹P NMR and infrared spectroscopy. The yield, elemental analysis and melting point data is summarised in Table 3.1 for Mn(I) complexes and Table 3.2 for Re(I) complexes. Only compound **3b** has been reported previously, however this compound was not completely characterised at the time, all other complexes are previously unreported. All complexes decomposed if left in solution for more than 24h, and gradually decomposed in the solid state. All complexes were purified by column chromatography, using hexane and chloroform as eluents on a Florisil column.

No	Compound	Analytical data		M.Pt (°C)	Yield (%)
		C(%) Found (Calc)	H(%) Found (Calc)		
3a	[Mn(CO) ₂ (dppm)(B ₃ H ₈)]	60.2 (60.5)	5.4 (5.6)	187	28
3b	[Mn(CO) ₂ (dppe)(B ₃ H ₈)]	60.9 (61.1)	6.0 (5.9)	243	59
3c	[Mn(CO) ₂ (dppp)(B ₃ H ₈)]	61.7 (61.7)	6.4 (6.1)	85	17
3d	[Mn(CO) ₂ (dppb)(B ₃ H ₈)]	62.6 (62.3)	6.0 (6.3)	157	24
3e	[Mn(CO) ₂ (dppfc)(B ₃ H ₈)]	61.3 (61.3)	5.4 (5.1)	138	36

Table 3.1. Analytical data, M.Pt and yields of Mn(I) B₃H₈ complexes.

No	Compound	Analytical data		M.Pt (°C)	Yield (%)
		C(%) Found (Calc)	H(%) Found (Calc)		
3f	[Re(CO) ₂ (PPh ₃) ₂ (B ₃ H ₈)]	56.1 (56.4)	4.7 (4.7)	175	20
3g	[Re(CO) ₂ {P(C ₆ H ₄ Cl-4)} ₂ (B ₃ H ₈)]	44.9 (45.0)	3.0 (3.2)	129	36
3h	[Re(CO) ₂ {P(C ₆ H ₄ OMe-4)} ₂ (B ₃ H ₈)]	53.4 (53.5)	5.4 (5.1)	109	31
3i	[Re(CO) ₂ {P(CH ₂ C ₆ H ₅) ₃ } ₂ (B ₃ H ₈)]	59.5 (59.3)	5.4 (5.7)	210	17
3j	[Re(CO) ₂ (dppm)(B ₃ H ₈)]	48.9 (48.6)	4.7 (4.5)	164	28
3k	[Re(CO) ₂ (dppp)(B ₃ H ₈)]	50.5 (50.1)	5.1 (4.9)	77	32
3l	[Re(CO) ₂ (dppb)(B ₃ H ₈)]	50.9 (50.8)	5.0 (5.1)	183	39
3m	[Re(CO) ₂ (dppfc)(B ₃ H ₈)]	51.5 (51.5)	4.2 (4.3)	193	46

Table 3.2. Analytical data, M.Pt and yields of Re(I) B₃H₈ complexes.

The product of formula $[M(CO)_2(L)_2(B_3H_8)]$ may exist in a number of isomeric forms (Figure 3.1).

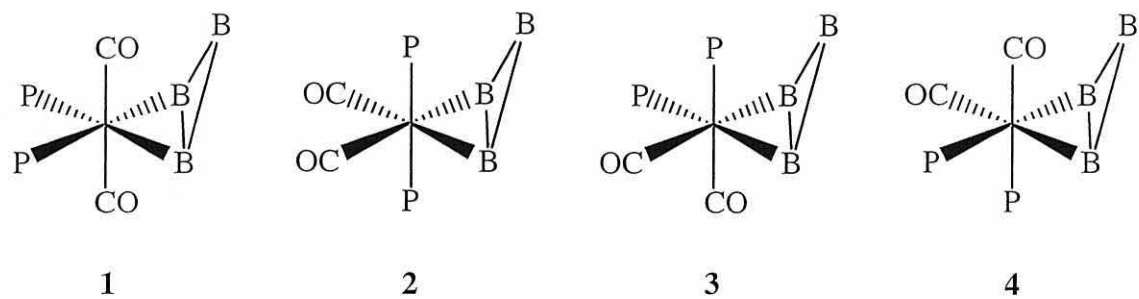


Figure 3.1. Differing isomeric forms of $[M(CO)_2(L)_2(B_3H_8)]$.

Previous work has [2] shown that $[Mn(CO)_2(dppe)(B_3H_8)]$ has structure **1** and the use of chelating phosphine ligands excludes the possibility of **2**. In the case of isomer **1**, only one peak would be expected in the ^{31}P NMR since both phosphorus nuclei are in equivalent environments. However, in isomer **3** and **4**, two phosphorus signals of equal intensity would be observed due to the nuclei being in differing environments. The same argument holds true for the ^{11}B NMR, where in isomer **1** two signals would be seen of a 2:1 ratio (2 M-H-B environments and 1 terminal BH_2 environment). But in isomers in **3** and **4**, all three boron atoms are in differing environments and hence three signals of equal intensity would be seen. All isomers would be expected to show two carbonyl stretches in their respective infrared spectra. ^{11}B , ^{31}P NMR, infrared spectroscopy and X-ray crystallography will be used to confirm that isomer **1** is formed in all cases.

3.3.4 Infra-red spectroscopy

As was demonstrated in chapter 2, infrared spectroscopy is an important diagnostic tool for the determination of stereochemical phenomena. However, unlike the compounds **2a – 2r**, only two carbonyls are present in the molecules **3a – 3m**. Symmetry considerations would indicate that two carbonyl stretches would be observed for all possible isomers of $[M(CO)_2(L)_2(B_3H_8)]$. This was found to be the case with the exception of compound **3b**, which presumably has coincidental overlap of the vibrational stretches. The values of the stretches observed in both the Mn(I) and Re(I) complexes are shown in Table 3.3 and 3.4 respectively.

No	Compound	ν (CO) stretches
3a	$[Mn(CO)_2(dppm)(B_3H_8)]$	1961(s), 1901(s)
3b	$[Mn(CO)_2(dppe)(B_3H_8)]$	1922(s) (Lit 1915(s) [2])
3c	$[Mn(CO)_2(dppp)(B_3H_8)]$	1960(s), 1907(s)
3d	$[Mn(CO)_2(dppb)(B_3H_8)]$	1960(s), 1907(s)
3e	$[Mn(CO)_2(dppfc)(B_3H_8)]$	1959(s), 1882(s)

Table 3.3. Infrared stretches of $[Mn(CO)_2(L)_2(B_3H_8)]$ (KBr disc).

No	Compound	ν (CO) stretches
3f	[Re(CO) ₂ (PPh ₃) ₂ (B ₃ H ₈)]	1945(s), 1915(s)
3g	[Re(CO) ₂ {P(C ₆ H ₄ Cl-4) ₃ } ₂ (B ₃ H ₈)]	1971(s), 1913(s)
3h	[Re(CO) ₂ {P(C ₆ H ₄ OMe-4) ₃ } ₂ (B ₃ H ₈)]	2049(s), 1972(s)
3i	[Re(CO) ₂ {P(CH ₂ C ₆ H ₅) ₃ } ₂](B ₃ H ₈)]	1948(s), 1901(s)
3j	[Re(CO) ₂ (dppm)(B ₃ H ₈)]	1966(s), 1902(s)
3k	[Re(CO) ₂ (dppp)(B ₃ H ₈)]	1967(s), 1912(s)
3l	[Re(CO) ₂ (dppb)(B ₃ H ₈)]	1965(s), 1900(s)
3m	[Re(CO) ₂ (dppfc)(B ₃ H ₈)]	1964(s), 1912(s)

Table 3.4. Infrared stretches of [Re(CO)₂(L)₂(B₃H₈)] (KBr disc).

As can be clearly seen, all complexes exhibit two strong signals in the carbonyl stretching region. In other reports of metallatetraboranes, values for the B-H stretching frequency have been given. Only small amounts of each compound were available for IR spectroscopic studies, it proved difficult to produce KBr discs of sufficient strengths. Hence all of the B-H data were effectively masked in the background of the IR spectra. B-H stretching data is however, no more diagnostic of structure than the carbonyl stretching data.

3.3.5 ^{11}B NMR spectroscopy

a) Solution state NMR

Performing solution state ^{11}B NMR gives a rapid indication as to the progress of the reaction and also provides evidence for the structure of the complexes. The high boron content of the multinuclear NMR probe available for this study, meant that the signal

for the terminal boron nucleus was often hidden by the signal from the borosilicate glass of the NMR probe. A sample of $[\text{Mn}(\text{CO})_2(\text{dppe})(\text{B}_3\text{H}_8)]$ was sent to Leeds University to be examined on a high field ‘low boron content’ multinuclear NMR probe. The ^{11}B spectra obtained in Bangor is shown in Figure 3.2 whilst the ^{11}B obtained from Leeds on the same sample is shown in Figure 3.3.

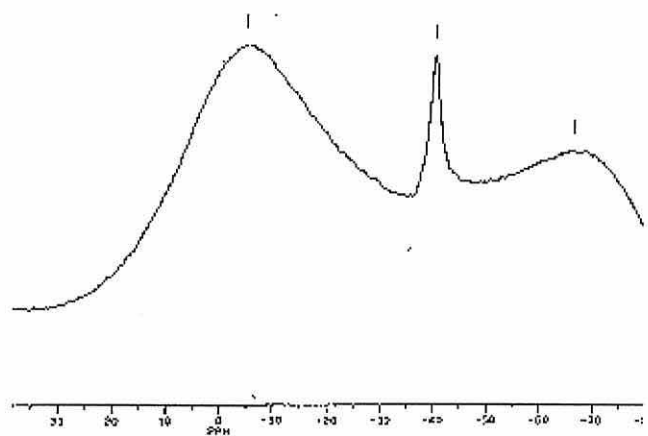


Figure 3.2. ^{11}B NMR of $[\text{Mn}(\text{CO})_2(\text{dppe})(\text{B}_3\text{H}_8)]$ at 250MHz (Bangor).

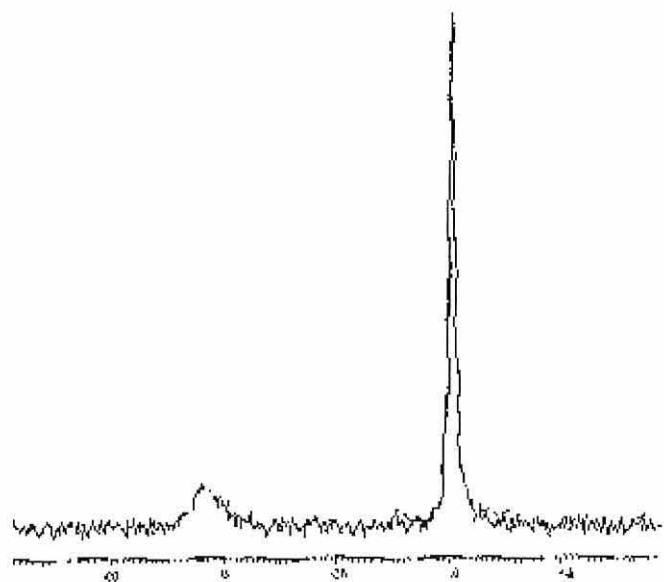


Figure 3.3. ^{11}B NMR of $[\text{Mn}(\text{CO})_2(\text{dppe})(\text{B}_3\text{H}_8)]$ at 400MHz (Leeds).

As can be seen there is only one diagnostic signal in the sample run in Bangor (-40.7 ppm), whilst the same sample run at Leeds clearly shows two signals, one of intensity two (-40.6 ppm) and one of intensity one (+3 ppm). These relate to the M-H-B boron environments (intensity two) and the terminal BH_2 boron environments (intensity one), and the values obtained are in close agreement with those reported by Gaines *et al* [2].

All of the remaining manganese and rhenium derivatives produced were only analysed on the instrument in Bangor, hence only the higher intensity signal relating to the metal bound boron was clearly discerned and are reported here. ^{11}B values obtained for the manganese derivatives are reported in Table 3.5, whilst the rhenium derivatives values are shown in Table 3.6.

No.	Compound	M-H-B $\delta(^{11}\text{B})$ /ppm
3a	[Mn(CO) ₂ (dppm)(B ₃ H ₈)]	-40.1
3b	[Mn(CO) ₂ (dppe)(B ₃ H ₈)]	-40.6 (Lit -40.6 [2])
3c	[Mn(CO) ₂ (dppp)(B ₃ H ₈)]	-40.1
3d	[Mn(CO) ₂ (dppb)(B ₃ H ₈)]	-40.1
3e	[Mn(CO) ₂ (dppfc)(B ₃ H ₈)]	-40.6

Table 3.5. ^{11}B NMR values for Mn(I) complexes.

No.	Compound	M-H-B $\delta(^{11}\text{B})$ /ppm
3f	[Re(CO) ₂ (PPh ₃) ₂ (B ₃ H ₈)]	-40.9
3g	[Re(CO) ₂ {P(C ₆ H ₄ Cl-4)} ₂ (B ₃ H ₈)]	-40.2
3h	[Re(CO) ₂ {P(C ₆ H ₄ OMe-4)} ₂ (B ₃ H ₈)]	-41.6
3i	[Re(CO) ₂ {P(CH ₂ C ₆ H ₅) ₃ } ₂](B ₃ H ₈)]	-41.9
3j	[Re(CO) ₂ (dppm)(B ₃ H ₈)]	-40.9
3k	[Re(CO) ₂ (dppp)(B ₃ H ₈)]	-41.0
3l	[Re(CO) ₂ (dppb)(B ₃ H ₈)]	-41.3
3m	[Re(CO) ₂ (dppfc)(B ₃ H ₈)]	-40.6

Table 3.6. ^{11}B NMR values for Re(I) complexes.

These values are in accord with those published in the literature, $[(\text{CH}_3)_4\text{N}][\text{Cr}(\text{CO})_4(\text{B}_3\text{H}_8)]$ (BH_2 -3.6, MHB -42.1), $[(\text{CH}_3)_4\text{N}][\text{W}(\text{CO})_4(\text{B}_3\text{H}_8)]$ (BH_2 -4.7, MHB -42.6) and $[(\text{CH}_3)_4\text{N}][\text{Mo}(\text{CO})_4(\text{B}_3\text{H}_8)]$ (BH_2 -6.5, MHB -42.2) [12]. This indicates that the borane moiety is not fluxional on the NMR time scale. Also, the similarity of the ^{11}B spectra of all complexes with that of $[\text{Mn}(\text{CO})_2(\text{dppe})(\text{B}_3\text{H}_8)]$ indicates that they are all of the same structure. The ^{11}B NMR data effectively excludes structures **3** and **4** since these would have (unless coincidental) two high field resonances at *ca.* -40 ppm.

b) Solid state NMR

Previously there has only been the one reported solid state study of metallatetraboranes [121] all other studies have been restricted to solution ^1H , ^{11}B and ^{31}P NMR as well as infrared spectroscopy and X-ray crystallography. Isotropic

chemical shift data from solid state MAS-NMR spectra normally requires simulation of spectra to account for quadrupolar effects. However, the spectra reported here gave strong relatively sharp signals and hence simulation was unnecessary.

One would expect to see two signals in the solid state NMR spectra for the metallatetraboranes discussed in this chapter, with a 2:1 ratio. Indeed, two signals are observed, with a 2:1 ratio, with the upfield signal (*ca.* -40 ppm) being associated with the resonance of the 2 M-H-B boron environments whilst the signal observed downfield (*ca.* 0 ppm) is the resonance associated with the terminal boron nucleus. The ^{11}B solid state MAS-NMR chemical shifts obtained for compounds **3e** and **3j** are given in Table 3.7, whilst the spectra of **3e** is given in Figure 3.4.

No	Compound	M-H- B $\delta(^{11}\text{B})$	Terminal BH ₂ $\delta(^{11}\text{B})$
3e	[Mn(CO) ₂ (dppfc)(B ₃ H ₈)]	-41.38	-3.4
3j	[Re(CO) ₂ (dppm)(B ₃ H ₈)]	-44.37	-3.9

Table 3.7. Solid state ^{11}B MAS-NMR data for complexes **3e** and **3j**.

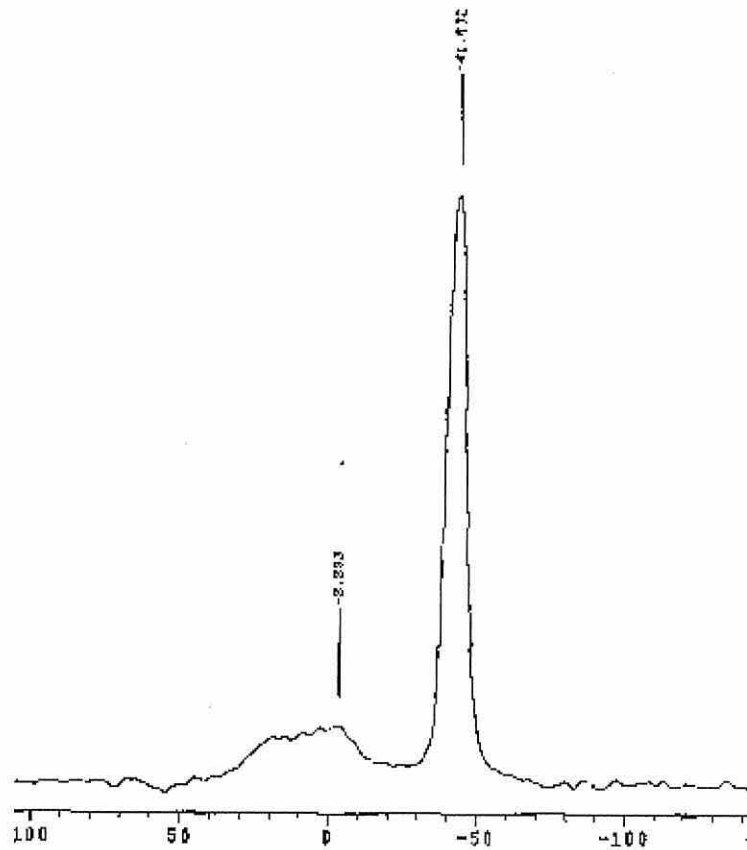


Figure 3.4. Solid state ^{11}B MAS-NMR spectra of complex **3e**.

These spectra indicate that like the previously reported Cr and W metallatetraboranes, and unlike the Ag and Cu metallatetraboranes, that the Mn and Re derivatives are not fluxional at room temperature in the solid state.

3.3.6 ^{31}P NMR spectroscopy

The ^{31}P NMR values for the metallatetraborane complexes δ , and $\Delta\delta$ (calculated from subtracting the chemical shift of the starting organometallic phosphine halide from δ) are given in Tables 3.8 and 3.9. A downfield shift is indicated by a negative $\Delta\delta$

value. Literature data for the previously prepared compound **3b** is unavailable for comparison.

No.	Compound	δ / ppm	$\Delta\delta$
3a	[Mn(CO) ₂ (dppm)(B ₃ H ₈)]	+49.6	-37.8
3b	[Mn(CO) ₂ (dppe)(B ₃ H ₈)]	+100.1	-30.6
3c	[Mn(CO) ₂ (dppp)(B ₃ H ₈)]	+63.4	-32.9
3d	[Mn(CO) ₂ (dppb)(B ₃ H ₈)]	+68.9	-36.0
3e	[Mn(CO) ₂ (dppfc)(B ₃ H ₈)]	+14.6	+22.5

Table 3.8. ^{31}P NMR data for Mn(I) metallatetraborane complexes.

No.	Compound	δ / ppm	$\Delta\delta$
3f	[Re(CO) ₂ (PPh ₃) ₂ (B ₃ H ₈)]	+31.8	-32.8
3g	[Re(CO) ₂ {P(C ₆ H ₄ Cl-4)} ₃ ₂ (B ₃ H ₈)]	+16.6	-19.4
3h	[Re(CO) ₂ {P(C ₆ H ₄ OMe-4)} ₃ ₂ (B ₃ H ₈)]	+11.5	-16.1
3i	[Re(CO) ₂ {P(CH ₂ C ₆ H ₅) ₃ } ₂ (B ₃ H ₈)]	+7.9	-26.0
3j	[Re(CO) ₂ (dppm)(B ₃ H ₈)]	-21.2	-17.1
3k	[Re(CO) ₂ (dppp)(B ₃ H ₈)]	+0.0	-15.9
3l	[Re(CO) ₂ (dppb)(B ₃ H ₈)]	-6.8	+2.8
3m	[Re(CO) ₂ (dppfc)(B ₃ H ₈)]	+2.0	-2.7

Table 3.9. ^{31}P NMR data for Re(I) metallatetraborane complexes.

The ^{31}P NMR chemical shifts of the Mn and Re metallatetraboranes are all, with the exception of compounds **3e** and **3l**, shifted downfield relative to the starting organometallic phosphine halide complexes. In general, the Mn(I) complexes (**3a – 3d**) had a $\Delta\delta$ value in the region of -35 ppm whilst the Re(I) complexes exhibit a $\Delta\delta$ of approximately -18 ppm. This may be a result of the different size and electron distribution of Mn(I) compared with Re(I).

The observation of only one phosphorus signal in the ^{31}P NMR of the metallatetraboranes, confirm that isomer **1** (Figure 3.1) is present.

3.3.7 ^1H NMR spectroscopy

Gaines *et al* reported the presence of five distinct hydrogen environments for the $[\text{B}_3\text{H}_8]^-$ protons in these static bidentate complexes [2]. However, when the samples reported in this study were analysed by solution state ^1H NMR, only two of the five reported environments were clearly distinguishable and these were upfield of TMS. This is in part due to masking the downfield resonances by the protons on the phosphine ligands and also due to the presence of a tetraalkylammonium salt impurity that proved difficult to remove from the samples. Hence, ^1H spectral data are only reported for the range 0 to -20 ppm. In all complexes two distinct proton environments were evident, those of H(5, 6) and H(7, 8) (see Figure 3.5 for numbering scheme).

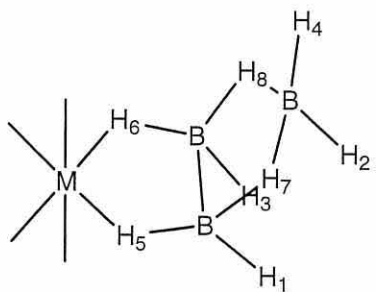


Figure 3.5. Numbering of the ^1H in $[\text{B}_3\text{H}_8]^-$.

The proton shifts obtained are in Tables 3.10 and 3.11 for the Mn(I) and Re(I) metallatetraborane species respectively.

No	Compound	H (5, 6)	H (7, 8)
3a	$[\text{Mn}(\text{CO})_2(\text{dppm})(\text{B}_3\text{H}_8)]$	-12.7	-0.9
3b	$[\text{Mn}(\text{CO})_2(\text{dppe})(\text{B}_3\text{H}_8)]$	-12.9	-0.8
3c	$[\text{Mn}(\text{CO})_2(\text{dppp})(\text{B}_3\text{H}_8)]$	-12.7	-0.2
3d	$[\text{Mn}(\text{CO})_2(\text{dppb})(\text{B}_3\text{H}_8)]$	-12.9	-0.7
3e	$[\text{Mn}(\text{CO})_2(\text{dppfc})(\text{B}_3\text{H}_8)]$	-9.8	-0.2

Table 3.10. ^1H NMR data for the Mn(I) metallatetraboranes.

No	Compound	H (5, 6)	H (7, 8)
3f	[Re(CO) ₂ (PPh ₃) ₂ (B ₃ H ₈)]	-8.5	-1.1
3g	[Re(CO) ₂ {P(C ₆ H ₄ Cl-4) ₃ } ₂ (B ₃ H ₈)]	-9.0	-1.1
3h	[Re(CO) ₂ {P(C ₆ H ₄ OMe-4) ₃ } ₂ (B ₃ H ₈)]	-9.0	-0.4
3i	[Re(CO) ₂ {P(CH ₂ C ₆ H ₅) ₃ } ₂ (B ₃ H ₈)]	-8.8	-0.2
3j	[Re(CO) ₂ (dppm)(B ₃ H ₈)]	-8.5	-0.2
3k	[Re(CO) ₂ (dppp)(B ₃ H ₈)]	-9.2	-0.5
3l	[Re(CO) ₂ (dppb)(B ₃ H ₈)]	-9.0	-0.1
3m	[Re(CO) ₂ (dppfc)(B ₃ H ₈)]	-9.4	-0.3

Table 3.11. ¹H NMR data for the Re(I) metallatetraboranes.

These values are consistent with those reported by Gaines for similar metallatetraboranes. The Mn(I) species exhibit lower field proton environments than those exhibited by the Re(I) complexes for the bridging M-H-B's. This is again in agreement with what has been reported in the literature, where the H(5, 6) chemical shift for [Mn(CO)₄(B₃H₈)] was -12.05 ppm, and the corresponding rhenium complex [Re(CO)₄(B₃H₈)] has a chemical shift was -9.33 ppm [2]. Again the H(7, 8) chemical shift of compounds **3a** – **3m** is in close agreement with that reported *c.f.* [Mn(CO)₄(B₃H₈)] -0.88 ppm, and [Re(CO)₄(B₃H₈)] -1.42 ppm.

3.3.8 X-Ray crystallography

This section reports the single-crystal crystallographic data for the compounds [Mn(CO)₂(dppe)(B₃H₈)] **3b** (Figure 3.6) and [Re(CO)₂(dppfc)(B₃H₈)] **3m** (Figure 3.7). Full crystallographic data for the compounds is presented in Appendices G and H.

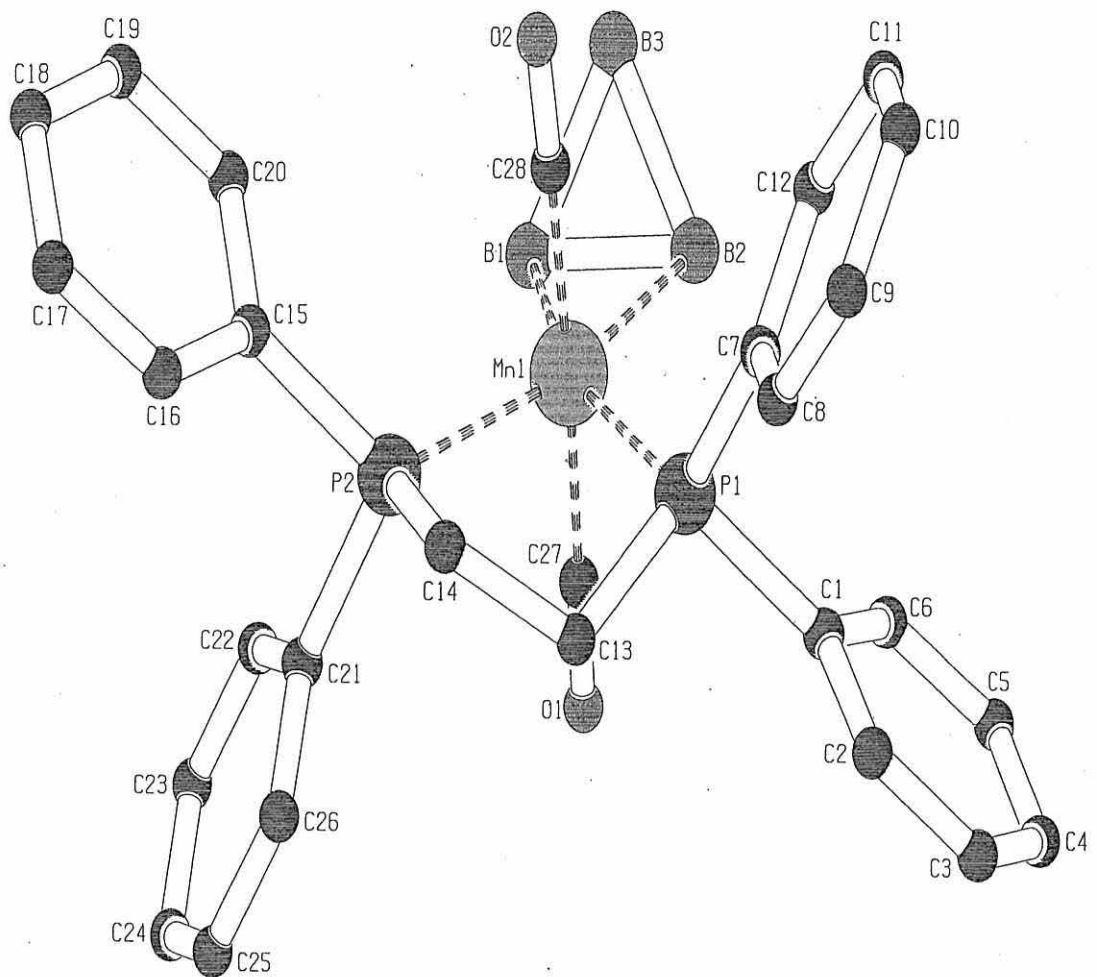


Figure 3.6. Molecular structure of **3b**.

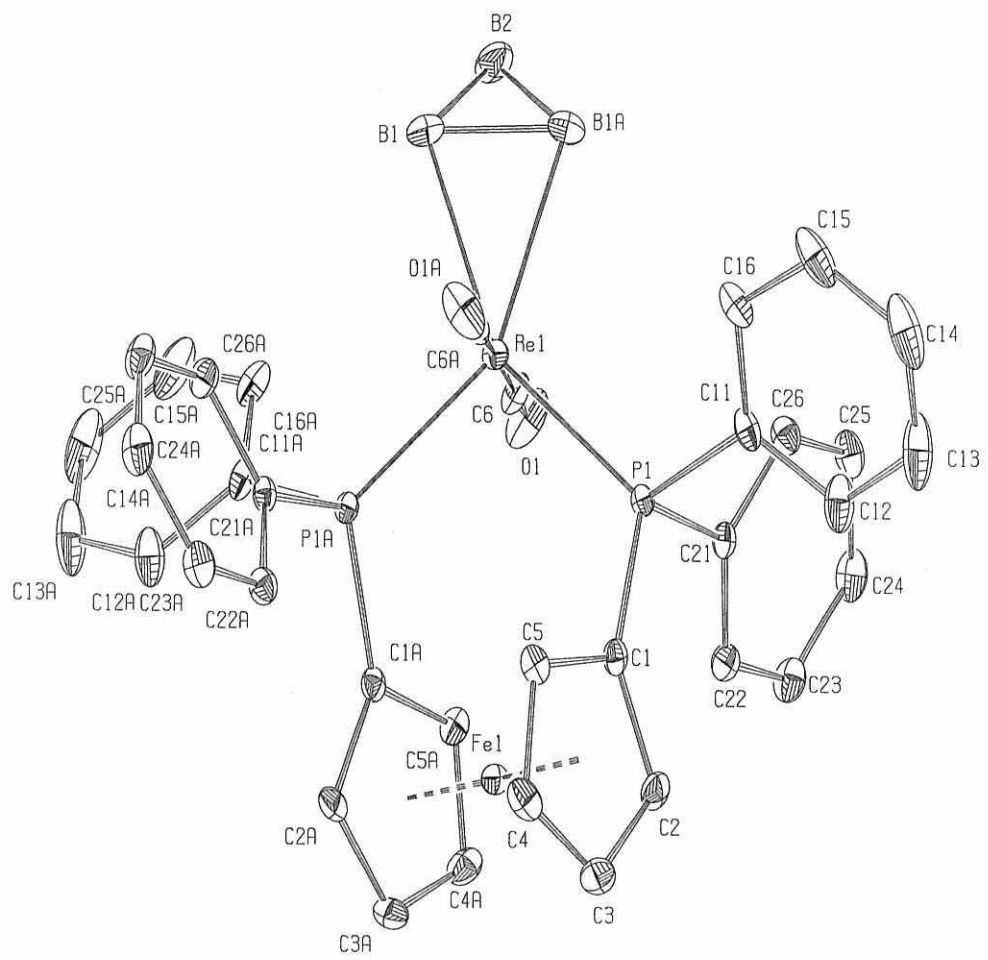


Figure 3.7. Molecular structure of **3m**.

Table 3.12 contains selected bond lengths for compounds **3b** and **3m** whilst

Table 3.13 contains selected bond angles for these compounds.

	3b		3m
Mn – C(27)	1.844(3)	Re – C(6A)	1.968(4)
Mn – C(28)	1.835(3)	Re – C(6)	1.968(4)
Mn – P(1)	2.240(8)	Re – P(1A)	2.3911(7)
Mn – P(2)	2.2495(7)	Re – P(1)	2.3911(7)
Mn – B(1)	2.330(3)	Re – B(1A)	2.432(4)
Mn – B(2)	2.336(3)	Re – B(1)	2.432(4)

Table 3.12. Selected bond lengths (\AA) in **3b** and **3m**.

	3b		3m
C28-Mn-C27	176.96(10)	C6A-Re-C6	177.17(17)
C28-Mn-P1	91.99(7)	C6A-Re-P1A	88.57(9)
C27-Mn-P1	88.55(7)	C6-Re-P1A	89.64(10)
C28-Mn-P2	87.10(7)	C6A-Re-P1	89.64(10)
C27-Mn-P2	89.95(7)	C6-Re-P1	88.57(9)
P1-Mn-P2	86.34(3)	P1A-Re-P1	101.34(3)
C28-Mn-B1	96.76(11)	C6A-Re-B1A	92.19(17)
C27-Mn-B1	83.86(11)	C6-Re-B1A	90.45(17)
P1-Mn-B1	156.69(8)	P1A-Re-B1A	150.46(12)
P2-Mn-B1	115.57(8)	P1-Re-B1A	108.2(12)
C28-Mn-B2	95.84(11)	C6A-Re-B1	90.45(17)
C27-Mn-B2	86.69(11)	C6-Re-B1	92.19(17)
P1-Mn-B2	113.50(8)	P1A-Re-B1	108.2(12)
P2-Mn-B2	159.75(8)	P1A-Re-B1	150.46(12)
B1-Mn-B2	44.22(11)	B1A-Re-B1	42.30(2)

Table 3.13. Selected bond angles ($^{\circ}$) about the manganese (I) and rhenium (I) centres.

There have only been two Mn(I) complexes containing the $[B_3H_8]$ moiety previously determined by X-ray crystallography, the *nido*- $[Mn(CO)_3(B_3H_8)]$ [2] and the *arachno*- $[Mn(CO)_4(B_3H_7Br)]$ [1], whilst there have been no previous reports of Re(I) $[B_3H_8]$ complexes. Other metallatetraborane complexes which have been characterised crystallographically include $[(Cu\{PPh_3\}_2)(B_3H_8)]$, $[NMe_4][\{Cr(CO)_4\}B_3H_8]$, $[\{WH_3(PMe_3)_3\}B_3H_8]$, $[\{NbCp_2\}B_3H_8]$, $[\{RuH(CO)(PPh_3)_2\}B_3H_8]$,

$[\{\text{Ru}(\text{C}_6\text{Me}_6)\text{Cl}\}\text{B}_3\text{H}_8]$, $[\{\text{Ru}(\text{PPh}_3)(\text{HB}\{\text{pz}\}_3)\text{B}_3\text{H}_8]$ and $[\{\text{OsH}(\text{CO})(\text{PPh}_3)_2\}\text{B}_3\text{H}_8]$ [14, 121-127]. Bond lengths and bond angles for these Mn(I) metallatetraboranes are shown in Table 3.14 and Table 3.15 respectively (with numbering scheme for the compounds in Table 3.14 and 3.15 being shown in Fig 3.8).

Complex	Interatomic bond distances (M-B) (\AA)				
	M-B1	M-B3	B1-B3	B1-B2	B2-B3
$[\text{Mn}(\text{CO})_4(\text{B}_3\text{H}_7\text{Br})]$	2.356(9)	2.356(9)	1.75(2)	1.71(2)	1.71(2)
$[\text{Mn}(\text{CO})_3(\text{B}_3\text{H}_8)]$	2.281(7)	2.273(7)	1.748(9)	1.713(9)	1.737(9)

Table 3.14. Selected interatomic distances for structurally characterised metallatetraboranes.

Complex	Interbond angles ($^{\circ}$)	
	B1-M-B3	B1-B2-B3
$[\text{Mn}(\text{CO})_4(\text{B}_3\text{H}_7\text{Br})]$	43.5(4)	61.5(8)
$[\text{Mn}(\text{CO})_3(\text{B}_3\text{H}_8)]$	45.1(2)	60.9(4)

Table 3.15. Selected intermolecular bond angles for structurally characterised Mn(I) metallatetraboranes.

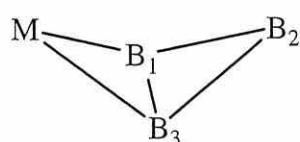


Figure 3.8. Atom labelling for Tables 14 and 15.



Figure 3.9. Atom labelling for compounds **3b** and **3m**.

The Mn-B bond lengths in **3b** (Mn-B1 2.330(3) \AA and Mn-B2 2.336(3) \AA) are in close agreement with those shown by $[\text{Mn}(\text{CO})_4(\text{B}_3\text{H}_7\text{Br})]$ (Mn-B1 2.356(9) \AA and Mn-B2 2.356(9) \AA) whilst they are longer than those exhibited by the *nido*- $[\text{Mn}(\text{CO})_3(\text{B}_3\text{H}_8)]$ (Mn-B1 2.281(7) \AA and Mn-B3 2.273(7) \AA). The Re-B bond lengths in compound **3m** are longer than those found in **3b** (Re-B1 2.432(4) \AA , Re-B1A 2.432(4) \AA).

The bond lengths in the B-B bridge for **3b** (B1-B2 1.756(4) \AA) are, within error, the same as those observed for $[\text{Mn}(\text{CO})_3(\text{B}_3\text{H}_8)]$ (B1-B3 1.748(9) \AA) and $[\text{Mn}(\text{CO})_4(\text{B}_3\text{H}_7\text{Br})]$ (B1-B3 1.75(2) \AA) and in **3m**, (B1-B1A 1.754(10) \AA). The bond lengths between the B-B bridge and the terminal BH_2 in **3b** (B1-B3 1.788(4) \AA , B2-B3 1.815(5) \AA) are slightly longer than those found in $[\text{Mn}(\text{CO})_4(\text{B}_3\text{H}_7\text{Br})]$ (B1-B2 1.71(2) \AA , B2-B3 1.71(2) \AA) and $[\text{Mn}(\text{CO})_3(\text{B}_3\text{H}_8)]$ (B1-B2 1.713(9) \AA , B2-B3 1.737(9) \AA) but these differences may not be significant.. In **3m** the situation is not as clear cut. One side of the B1-B1A-B2 triangle is shorter than the other with the B1-B2 bond length being 1.653(11) \AA and the B1A-B2 bond length being 1.784(12) \AA .

The B1-Mn-B2 bond angle ($44.22(11)^\circ$) in compound **3b** shows close agreement with $[\text{Mn}(\text{CO})_3(\text{B}_3\text{H}_8)]$ (B1-Mn-B3 $45.1(2)^\circ$) and $[\text{Mn}(\text{CO})_4(\text{B}_3\text{H}_7\text{Br})]$ (B1-Mn-B3 $43.5(4)^\circ$). Similarly the B1-B3-B2 bond angle in **3b** ($58.34(17)^\circ$) is slightly smaller than those observed for $[\text{Mn}(\text{CO})_3(\text{B}_3\text{H}_8)]$ (B1-B2-B3 $60.9(4)^\circ$) and $[\text{Mn}(\text{CO})_4(\text{B}_3\text{H}_7\text{Br})]$ (B1-B2-B3 $61.5(8)^\circ$). In compound **3m**, a similar observation may be made, where the B1A-Re-B1 bond angle is ($42.30(2)^\circ$) and the B1-B2-B1A bond

angle is $(61.3(5)^\circ)$. The precursors of complexes **3b** and **3m** (**2j** and **2r** respectively) have had their structures determined by X-ray crystallography. In compound **3m**, the Mn-P bond lengths ($2.240(8)\text{\AA}$ and $2.2495(7)\text{\AA}$) are shorter than those of **2j** ($2.519(10)\text{\AA}$ and $2.321(17)\text{\AA}$). Similarly, in compound **3m**, the Re-P bond lengths ($2.3911(7)\text{\AA}$ and $2.3911(7)\text{\AA}$) are shorter than those of its precursor, **2r**, ($2.5180(18)\text{\AA}$ and $2.5520(16)\text{\AA}$). This would indicate that the *trans*- influence of $[\text{B}_3\text{H}_8]^-$ is less than that of a *cis*-combination of Br^- and CO.

Conversely, the P-Mn-P bond angle of **3b** ($86.34(3)^\circ$) is larger than that found in **2j** ($84.74(6)^\circ$). The same is found for **3m** where the P-Re-P bond angle ($101.34(3)^\circ$) is larger than that of its precursor, **2r**, ($99.79(6)^\circ$). This may be due to the release of steric constraints due to the removal of the halide.

3.3.9 Reactions of $[\text{Mn}(\text{CO})_2(\text{dppe})(\text{B}_3\text{H}_8)]$

Reactions of $[\text{Mn}(\text{CO})_2(\text{dppe})(\text{B}_3\text{H}_8)]$ were attempted as representative of this class of compounds. This compound was chosen as it was readily available and obtained in highest yield. Preliminary reactions included thermal (with and without Me_3NO) and photolytic reactions in benzene and CHCl_3 , in attempts to remove a carbonyl and generate a *nido*- complex. Thermal and photolytic CO substitution reactions with PPh_3 were also attempted. In all cases, reactions did occur, but these reactions were not clean and complex mixtures resulted from which it was difficult to isolate pure materials. For example, the photolytic decarbonylation of $[\text{Mn}(\text{CO})_2(\text{dppe})(\text{B}_3\text{H}_8)]$ produced a pink solid. ^{31}P and ^{11}B NMR of the crude products were performed and the results indicate a possible *nido*-structure. The ^{11}B NMR showed one signal at -47.1ppm (close to the value obtained for the *nido*-

[Mn(CO)₃(B₃H₈)] species), whilst the ³¹P NMR showed two sets of signals, one at +99.3 ppm (unreacted [Mn(CO)₂(dppe)(B₃H₈)] and a multiplet of peaks at +72 ppm.

In all cases separation of products proved difficult and time consuming and this area of research was not pursued further.

3.4 Conclusion

This chapter reports the synthesis and characterisation of twelve new and one previously reported Mn(I) and Re(I) *arachno*-2-metallatetraboranes. All compounds were characterised by NMR and IR studies and two compounds, [Mn(CO)₂(dppe)(B₃H₈)] and [Re(CO)₂(dppfc)(B₃H₈)], were characterised by single crystal X-ray diffraction studies. The chemistry of [Mn(CO)₂(dppe)(B₃H₈)] has been further explored but reaction products were not isolated nor characterised.

Chapter 4

Lewis acidity and organophosphoryl adducts of
tris(pentafluorophenyl)borane.

4.1 Introduction

It was not until the 1960s that the first reports of pentafluorophenylborane derivatives were published [129]. These included the synthesis of $\text{Cl}_2\text{B}(\text{C}_6\text{F}_5)$, $\text{ClB}(\text{C}_6\text{F}_5)_2$ and $\text{B}(\text{C}_6\text{F}_5)_3$ [130]. The strong Lewis acid properties of $\text{B}(\text{C}_6\text{F}_5)_3$ (**4a**) were acknowledged at the time although they were not put to practical use. This area of research lay dormant for about 20 years, when further applications of pentafluorophenylborane reagents were described [131].

Compared to the boron trihalides, tris(pentafluorophenyl)borane is an ideal boron-based Lewis acid since it possesses both high Lewis acid strength and good stability. It is thermally robust, being able to withstand temperatures of up to 270°C, and it is also resistant towards oxidation by dioxygen. However it is slowly hydrolysed with elimination $\text{C}_6\text{F}_5\text{H}$, under ambient conditions. The compound forms strong and stable adducts with water [132, 133] which have been analysed by X-ray crystallographic techniques. It is its reaction with zirconium alkyls that have lead to the resurgence of interest in this compound. Some of these reactions are described below.

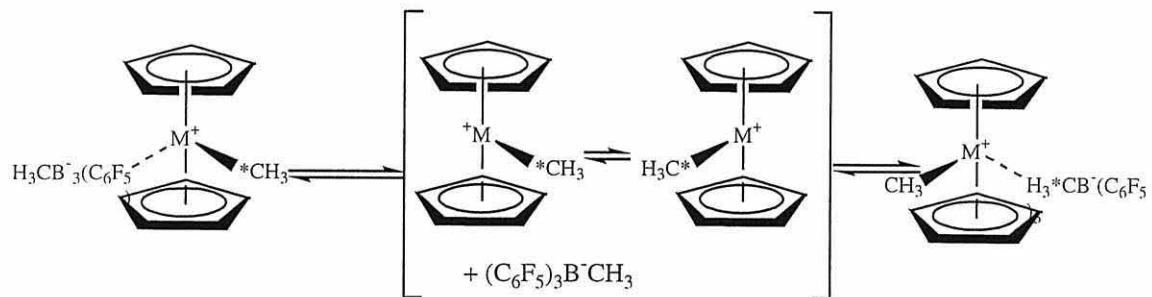
Treatment of dimethylzirconocenes with $\text{B}(\text{C}_6\text{F}_5)_3$ lead to what was initially described as “cation like” species, with the general formula $[\text{Cp}'_2\text{Zr}(\text{CH}_3)]^+[\text{CH}_3\text{B}(\text{C}_6\text{F}_5)_3]^-$ (Eq. 4.1) [131]. Several of these species have since been structurally characterised [134].



Where $\text{Cp}' = \eta^5\text{-C}_5\text{H}_5, \eta^5\text{-C}_5\text{Me}_5$

Analysis of these species in solution by NMR have shown that there are two dynamic processes occurring in these species (Figure 4.1) [135].

(a)



(b)

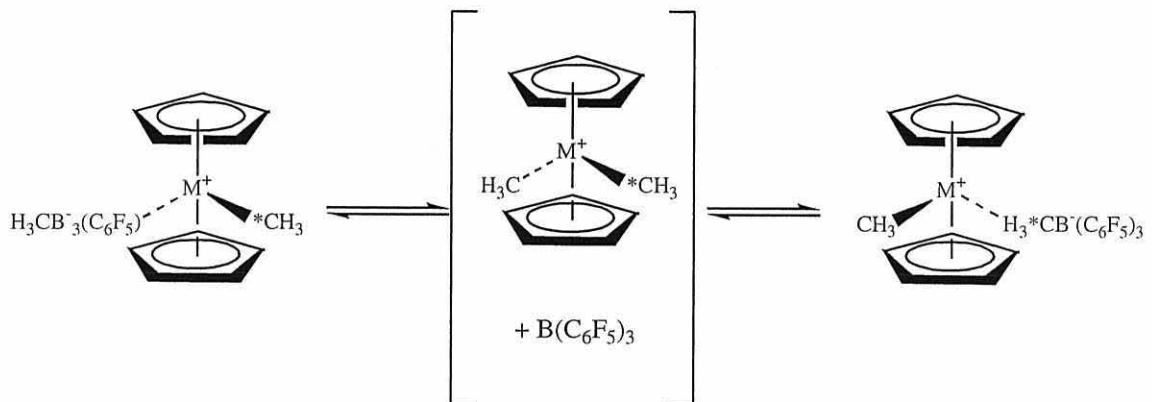


Figure 4.1. Dynamic processes occurring in solution for “ $\text{MCp}_2\text{Me}_2\text{B}(\text{C}_6\text{F}_5)_3$ ”.

The first process exchanges the diastereotopic ring substituents and involves separation of the anion from the cation, flipping of the terminal $\text{Zr}-\text{CH}_3$ from one side of the metallocene to the other followed by reassociation of the ion pair (Fig. 4.1(a)). The second process involves the initial dissociation of free $\text{B}(\text{C}_6\text{F}_5)_3$ through $\mu-\text{H}_3\text{C}-\text{B}$ bond cleavage followed by abstraction of the other zirconocene methyl group (Fig. 4.1(b))). The process in Fig. 4.1(a) is predominant when $\text{M} = \text{Zr}$ whilst the process in Fig. 4.1(b) is predominant when $\text{M} = \text{Hf}$. This type of process is not just limited to methyl groups; benzyl groups are readily abstracted forming zirconium cations stabilised by benzyl ligands [136] (Figure 4.2).

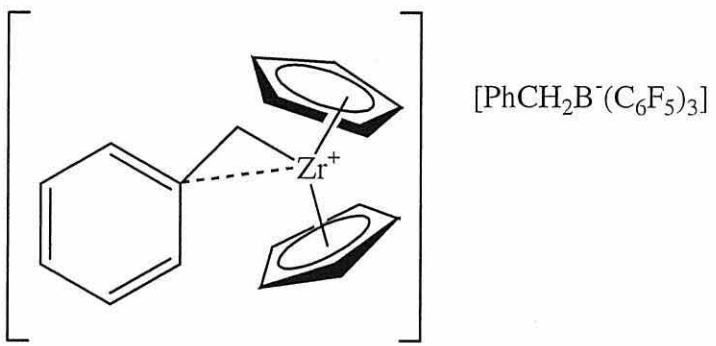


Figure 4.2. Zirconium cation stabilised by a benzyl ligand.

4.1.1 Lewis acidity of boron compounds

Boron shows many similarities to its neighbours in the periodic table, carbon and silicon, with its preference to form covalent bonds. However, boron has one fewer valence electrons than its number of valence orbitals. Boron species that are trigonal planar use three sp^2 orbitals, to form three covalent σ -bonds. The boron atom has two electrons short of an octet and, as such, possesses a vacant p_z orbital (which lies perpendicular to the sp^2 plane). This electron deficiency is responsible for the Lewis acidity of sp^2 hybridised boron compounds.

When a Lewis base is added to a Lewis acid a complex is formed which involves the rearrangement of molecular structure of the starting materials. Boron trihalides change from being trigonal planar, in which the boron atom is sp^2 hybridised, to being tetrahedral, upon co-ordination, in which the boron atom is sp^3 hybridised. The process requires energy for orbital re-hybridisation, for overcoming the loss of σ -bonding in the original molecule, for overcoming increased electron pair repulsion's between halogen atoms and for overcoming any steric crowding due to a decrease in the X-B-X bond angle. This is offset by the energy gained on formation of the B-L bond.

A major factor in determining Lewis acidity of trigonal boron compounds is the extent of σ -bonding to adjacent atoms, and this may be described by using the boron trihalides as examples. The boron trihalides are trigonal planar molecules with D_{3h} symmetry. The relative order of Lewis acidity of the boron trihalides is $\text{BBr}_3 > \text{BCl}_3 > \text{BF}_3$, which is the opposite to what would be expected from electronegativity arguments or on steric grounds. The mean energy of the B-F bond is 646 kJ mol^{-1} which makes it one of the strongest known ‘single’ bonds. This bond energy is considerably greater than those found in other boron-halide bonds and is stronger than a B-O bond. Evidence for this strong bond is observed if the reaction between water with BF_3 is compared to the reaction between water and other boron trihalides. Boron trifluoride reacts to produce hydrated species $\text{BF}_3\text{H}_2\text{O}$ and $\text{BF}_3\text{2H}_2\text{O}$, whereas the other boron trihalides are hydrolysed to produce orthoboric acid, B(OH)_3 (Eq. 4.2).



The weaker Lewis acidity, relative to the other boron trihalides, found in BF_3 is attributed to the $p_\pi-p_\pi$ back bonding between the filled fluorine p -orbital and the vacant boron $2p_z$ orbital. This effect is found in all BX_3 compounds, but the strength of the π -bonding is dependent on the overlap between the p -orbitals. The π -bond strength of BF_3 is due to a favourable energy match, and a good overlap between the $2p$ orbital fluorine and the $2p_z$ orbital on boron atom. The overlap becomes progressively less favourable for the larger and more diffuse $3p$ and $4p$ orbitals on the chlorine and bromine atoms respectively.

An efficient and simple method for determining the Lewis acidity of boron containing compounds has been reported by Beckett *et al* [137]. The method is based

upon a quantitative parameter which is known as an acceptor number (AN), which was described first by Gutmann [138] and Mayer *et al* [139]. These AN values were derived from $^{31}\text{P}-\{\text{H}\}$ NMR chemical shifts produced in triethylphosphine oxide (TEPO) by electrophilic solvent interactions. These lead to deshielding of the phosphorus atoms in TEPO by perturbation of the ^{31}P chemical shift tensor which has a vector along the P-O axis. These AN values, known as Gutmann's scale, has arbitrary fixed points of hexane at zero and antimony pentachloride at 100.

The AN values of numerous boron containing compounds can be estimated from the δ ^{31}P NMR shift of TEPO dissolved in the boron containing species using the equation below. The values 86.1 and 41.0 relate to the δ ^{31}P of TEPO in antimony pentachloride and hexane solutions, respectively.

$$\text{AN} = 100 \times (\delta^{31}\text{P}_{(\text{sample})} - 41.0) / \{86.1 - 41.0\}$$

4.2 Aims

The primary aim of the research was to measure the Lewis acidity of tris(pentafluorophenyl)borane by Gutmann's method, and to this method with other reported means of Lewis acidity determination. A second aim of the research was to examine the spectroscopic properties, associated with the phosphoryl bond in a range of organophosphoryl ligands co-ordinated to the $\text{B}(\text{C}_6\text{F}_5)_3$ moiety.

4.3 Results and Discussion

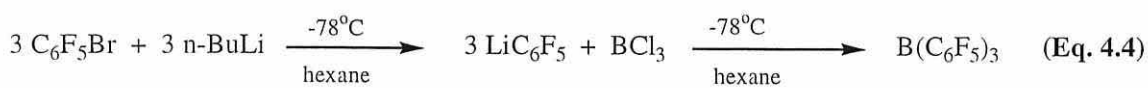
4.3.1 Preparation and characterisation of $B(C_6F_5)_3$ (**4a**)

Tris(pentafluorophenyl)borane (**4a**) was first prepared many years ago [130], however the reported syntheses have a few disadvantages. The first method was to treat a pentane solution of pentafluorophenyl bromide with n-BuLi at low temperature in order to generate $Li(C_6F_5)$. The latter is thermally sensitive and will detonate at *ca* -20°C. The resulting lithium salt was then treated with boron trichloride to produce LiCl and $B(C_6F_5)_3$ (Eq. 4.3).



The reported yield of the crude product was between 30-50% but, when this method was attempted we found it was only possible to isolate $B(C_6F_5)_3$ (**4a**) in 10% yield after purification. The compound can also be prepared [140] by reacting the Grignard reagent $Mg(C_6F_5)Cl$ in diethyl ether with $BF_3\cdot Et_2O$. This preparation is experimentally also not very satisfactory since there is difficulty in removing co-ordinated diethyl ether from the crude product.

It was decided to follow the preparation reported by Green *et al* [141] whereby the entire system is kept at -78°C. This has been shown to be an essential feature of this synthesis [142]. This method, which is described in detail in Chapter 6, gave $B(C_6F_5)_3$ in 52% yield (Eq. 4.4).



The tris(pentafluorophenyl)borane (**4a**) was analysed by ^{11}B , ^{13}C and ^{19}F NMR spectroscopy, as well as infrared spectroscopy. The ^{11}B NMR showed, as would be expected, a single peak. Its chemical shift (-7 ppm) suggested that the boron nucleus was in a tetrahedral geometry [143] and is significantly different from previous values reported in the literature. This was accounted for by considering water co-ordination to the borane moiety. Upon sublimation of the product, ^{11}B NMR gave a single peak at +59 ppm, which is agreement with the literature values [144]. The water adduct $(\text{C}_6\text{F}_5)_3\text{B}(\text{H}_2\text{O})$ has been characterised by another research group, and their findings agree with a ^{11}B NMR of -7 ppm. There are four different carbon environments present in $\text{B}(\text{C}_6\text{F}_5)_3$ and assuming free rotation about the B-C bond it would be expected that four different peaks should be present in the ^{13}C - $\{{}^1\text{H}\}$ NMR. However, this was not the case, the *ipso* carbon was not seen. Therefore ^{13}C spectra shows three doublets ($^1\text{J}(\text{CF})$ ranging from 235 to 260Hz) for the *ortho*, *meta* and *para* resonances of the perfluoroaryl groups of $\text{B}(\text{C}_6\text{F}_5)_3$ at 148, 137 and 141 ppm, respectively. The ^{19}F NMR spectra showed the expected three resonances, of relative intensity 2:2:1, for *ortho*, *meta* and *para* aryl substituents at -163, -135 and -156 ppm. These values are in close agreement with Massey and Parks' original ^{19}F values of -161, -128 and -146 ppm [145]. The infrared spectra will be discussed in detail in section 4.3.3.

4.3.2 Lewis acidity of $\text{B}(\text{C}_6\text{F}_5)_3$

Yamamoto and co-workers have recently investigated the Lewis acid catalysed aldol type and Michael reactions using $\text{B}(\text{C}_6\text{F}_5)_3$ as the catalyst [133]. Parks and Piers [145] found $\text{B}(\text{C}_6\text{F}_5)_3$ to be an efficient catalyst for the hydrosilylation of carbonyl functions. The reactivity and regioselectivity of these Lewis acid catalysed reactions

will depend on the details of the reaction mechanism and kinetics. Hence, knowledge of the relative Lewis acidity of the catalyst is of great importance.

Reported methods for the experimental determination of Lewis acidity are based on spectroscopic techniques (IR, NMR) [138, 139, 146-148]. Childs' ¹H NMR method is based upon the downfield shift ($\Delta\delta$) of the H-(3) resonance in crotonaldehyde upon complexation to the Lewis acid. This method has been theoretically justified through MNDO calculations [149]. Erker and co-workers [150, 151] recently reported the application of Childs' method to B(C₆F₅)₃. Their results indicated that B(C₆F₅)₃ is a slightly weaker Lewis acid than BF₃.

In order to further probe the Lewis acidity of B(C₆F₅)₃ we prepared two new 1:1 Lewis acid / Lewis base complexes: (TEPO·B(C₆F₅)₃ (**4b**) and EtOAc·B(C₆F₅)₃ (**4c**)). They were both prepared in high yield [152] following the procedure of Massey and Parks [130]. Previously reported adducts of B(C₆F₅)₃ include amines and ammonia [130, 140], water [153], *O*-carbonyl donors [154], nitriles and isonitriles [151] and phosphines [130, 140, 151, 155]. Compounds **4b** and **4c** were characterised fully, and **4c** and related phosphoryl derivatives will be discussed in greater detail in section 4.3.3.

As a quantitative measure of Lewis acidity, Lappert [148, 149] used the shift ($\Delta\nu/\text{cm}^{-1}$) to lower wavenumber of the carbonyl stretching frequency of EtOAc upon co-ordination. For the adduct **4b**, $\Delta\nu$ is 93 cm⁻¹ placing the Lewis acidity of B(C₆F₅)₃ significantly lower (Table 4.1) than BCl₃ and lower than that of BF₃ and AlCl₃, in agreement with the result of Erker and co-workers [150, 151].

Acid	$\Delta\nu/\text{cm}^{-1}$
$\text{B}(\text{C}_6\text{F}_5)_3$ (4a)	93
BCl_3	176
BF_3	119
AlCl_3	117

Table 4.1. Lapperts $\Delta\nu/\text{cm}^{-1}$ of EtOAc adducts of various Lewis acids [148, 149].

Gutmann's method has been applied to a range of boron containing Lewis acids by Beckett *et al* [156-158]. The adduct TEPOB(C₆F₅)₃ **4c** showed a single ³¹P resonance in a THF solution at room temperature at 78.0 ppm, with a $\Delta\delta$ of 37.0 ppm and hence an AN of 82. To enable a comparison between Childs' and Gutmann's method, the AN values of the non-boron containing Lewis acids AlCl₃, TiCl₄ and SnCl₄ were also determined.

This confirmed the relative Lewis acidities as $\text{BF}_3 \sim \text{AlCl}_3 > \text{B}(\text{C}_6\text{F}_5)_3$, with TiCl₄ and SnCl₄ being much weaker Lewis acids (Fig. 4.3). The positive correlation ($R^2 = 0.97$) between the ¹H NMR method of Childs and co-workers, and the measured AN values described above confirms the validity of Gutmann's AN method. With the exception of one pair of similar acidity (AlCl₃ and BF₃), the relative Lewis acid strength as determined using either NMR methods is the same.

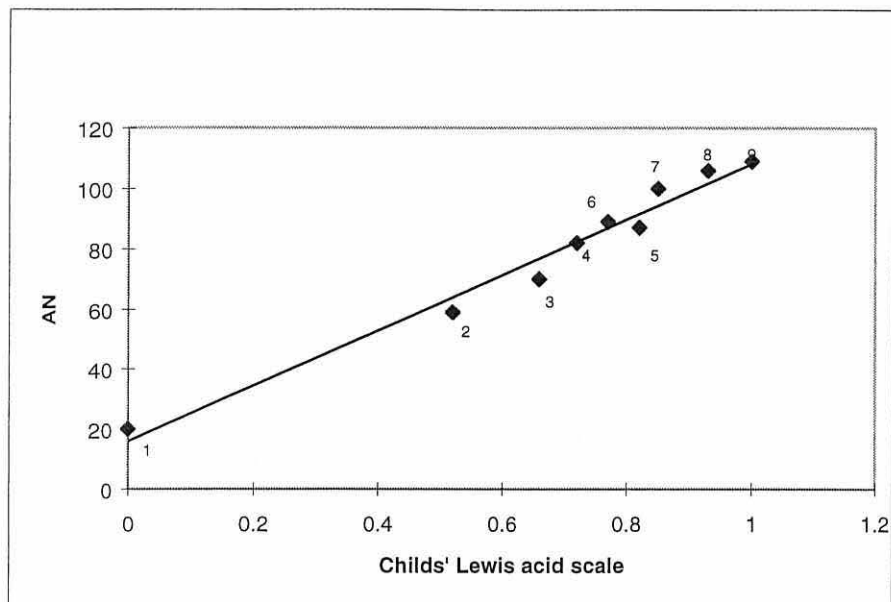
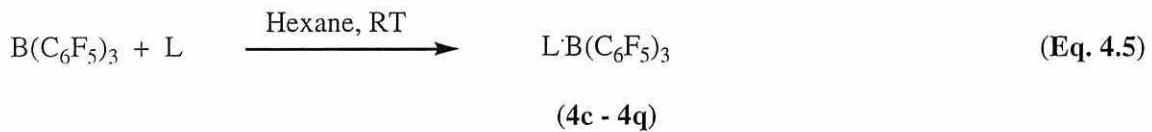


Figure 4.3. A graph showing the correlation between Gutmann's acceptor number and Childs Lewis acid scale. 1 = CH_2Cl_2 , 2 = SnCl_4 , 3 = TiCl_4 , 4 = $\text{B}(\text{C}_6\text{F}_5)_3$, 5 = AlCl_3 , 6 = BF_3 , 7 = SbCl_5 , 8 = BCl_3 and 9 = BBr_3

4.3.3 Preparation of adducts of $\text{B}(\text{C}_6\text{F}_5)_3$ with organophosphoryl ligands.

The reaction of one equivalent of the phosphoryl compound (L) with one equivalent of $\text{B}(\text{C}_6\text{F}_5)_3$ in hexane rapidly produced the new analytically pure adducts L:B(C_6F_5)₃ (Eq. 4.5) in moderate to high yields. The phosphoryl compounds used as Lewis bases were the triorganophosphine oxides (Et_3PO , $^n\text{Pr}_3\text{PO}$, $^n\text{Oct}_3\text{PO}$ and Ph_3PO), the organoesters of phosphoric acid { $(\text{MeO})_3\text{PO}$, $(\text{EtO})_3\text{PO}$, and $(\text{PhO})_3\text{PO}$ }, phosphinic and organophosphonic acids { $(\text{EtO})_2(\text{H})\text{PO}$, $(^n\text{BuO})_2(\text{H})\text{PO}$, $(\text{PhO})_2(\text{H})\text{PO}$, $(\text{MeO})_2\text{MePO}$, $(\text{EtO})_2\text{MePO}$ and $(\text{EtO})_2\text{PhPO}$ }, and two diorganophosphonic acids { $(\text{MeO})\text{Me}_2\text{PO}$ and $(\text{EtO})\text{Me}_2\text{PO}$ }.



All new adducts were characterised by elemental analysis, M.Pt, IR and multi-nuclear NMR (^1H , ^{13}C , ^{11}B , ^{19}F and ^{31}P) and formula and letter names are given in Table 4.2.

All of the adducts were white solids, except for (^nOct) $_3\text{PO}\cdot\text{B}(\text{C}_6\text{F}_5)_3$ (**4e**) which was a viscous liquid, and all were air stable. They were readily soluble in chlorinated solvents, with the exception of $(\text{MeO})\text{Me}_2\text{PO}\cdot\text{B}(\text{C}_6\text{F}_5)_3$ (**4p**), but were insoluble in petroleum ether. The adducts of the phosphinic acids (**4j – 4l**) were very deliquescent.

The formulation of these products as adducts follows from their ^{11}B NMR chemical shifts (in the range -0.2 to -9.3 ppm), upfield from “free” $\text{B}(\text{C}_6\text{F}_5)_3$ (+59 ppm [144]) and in the region normally observed for four co-ordinate tetrahedral boron centres [28]. This was confirmed by the single crystal X-ray crystallographic structures of $\text{TEPO}\cdot\text{B}(\text{C}_6\text{F}_5)_3$ (**4c**) and $\text{Ph}_3\text{PO}\cdot\text{B}(\text{C}_6\text{F}_5)_3$ (**4f**). The room temperature multinuclear NMR spectra were in full agreement with the proposed structures. ^{19}F spectra were obtained for **4c – 4l**. The chemical shifts of the *ortho*, *meta* and *para* fluorines depend on a number of factors such as charge density on the fluorine atom or its neighbouring carbon atom, on paramagnetic contributions and on an “*ortho*” effect. These showed the expected three resonances of relative intensity 2:2:1, for *ortho*, *meta* and *para* aryl substituents at *ca.* -164 , -135 and -157 ppm respectively. The values observed are consistent with previously reported adducts of **4a** [144].

The ^{13}C spectra of the adducts showed in addition to the resonances associated to the phosphoryl ligand [159], doublets ($^1\text{J}(\text{CF})$ *ca.* 240 Hz) for the *ortho*, *meta* and *para* resonances of the perfluoro aryl groups of $\text{B}(\text{C}_6\text{F}_5)_3$ at *ca.* 148, 137 and 140 ppm

respectively [150, 151, 159]. In all cases the *ipso* carbon was not observed. The ¹H spectra of all the adducts showed little change relative to spectra of the uncomplexed phosphoryl ligands, but there was a slight shift towards higher frequency upon adduct formation.

Phosphorus-31 NMR data for all of the adducts is given in Table 4.2. The $\Delta\delta$ values ($\delta_{\text{adduct}} - \delta_{\text{free base}}$) which ranged from -9.2 to +25.9 can also be found in Table 4.2. Rather than reflecting change of electron density at phosphorus, these shifts are a consequence of the Lewis acid perturbing the ³¹P chemical shift tensors, which have a component along the PO axis of the phosphoryl ligand [160]. Due to variations in molecular symmetry, the ³¹P chemical shift tensors will differ for each class of phosphoryl derivative, which will ensure that $\Delta\delta$ values are unlikely to be uniform. The phosphorus atoms in the phosphoryl compounds with alkoxy or aryloxy substituents were slightly shielded upon co-ordination to B(C₆F₅)₃, whilst in compounds with alkyl substituents were deshielded upon co-ordination to B(C₆F₅)₃. This substituent effect appears cumulative with $\Delta\delta$ values roughly following the order trialkylphosphine oxides (~ +24) > dialkylphosphinates (~ +4) > alkylphosphonates (~ -1) > phosphates (~ -5). Burford and co-workers [159, 161] observed deshielding of the phosphorus centre in adducts of Ph₃PO with BF₃, BCl₃, AlCl₃, AlBr₃ and GaCl₃, and slight shielding at phosphorus in (PhO)₃PO·AlCl₃.

No.	Base	δ (free base)	δ (adduct)	$\Delta\delta$ (adduct–free base)
4c	Et ₃ PO	+52.1	+78.0	+25.9
4d	ⁿ Pr ₃ PO	+47.6	+69.3	+21.6
4e	ⁿ Oct ₃ PO	+48.1	+70.6	+22.5
4f	Ph ₃ PO	+28.5	+24.3	-4.2
4g	(MeO) ₃ PO	+1.4	-2.6	-4.0
4h	(EtO) ₃ PO	-1.9	-10.1	-8.2
4i	(PhO) ₃ PO	-18.3	-27.5	-9.2
4j	(EtO) ₂ PHO	+6.4	+3.4	-3.0
4k	(ⁿ BuO) ₂ PHO	+6.9	+5.2	-1.7
4l	(PhO) ₂ PHO	+0.2	-1.2	+1.4
4m	(MeO) ₂ MePO	+32.1	+29.9	-2.2
4n	(EtO) ₂ MePO	+27.6	+27.8	+0.2
4o	(EtO) ₂ PhPO	+10.8	+16.6	+5.8
4p	(MeO)Me ₂ PO	+53.2	+57.2	+4.0
4q	(EtO)Me ₂ PO	+50.7	+54.5	+3.8

Table 4.2. ^{31}P $\Delta\delta$ values (ppm) of $\text{B}(\text{C}_6\text{F}_5)_3$ adducts of phosphoryl ligands (in CDCl_3).

The $\Delta\delta$ values obtained for the $\text{B}(\text{C}_6\text{F}_5)_3$ adducts of phosphonic acid esters (~ -2) were similar to those for alkylphosphonate esters indicating that the effect of H was comparable to an alkyl group. The largest $\Delta\delta$ (^{31}P) values were the trialkylphosphine oxides, with the $\Delta\delta$ value of TEPO being marginally greater than those of $^n\text{Pr}_3\text{PO}$ and $^n\text{Oct}_3\text{PO}$.

No.	Base	$\nu(\text{PO})/\text{cm}^{-1}$ (base)	$\nu(\text{PO})/\text{cm}^{-1}$ (adduct)	$\Delta\nu(\text{PO})/\text{cm}^{-1}$
4c	Et_3PO	1193	1172	-21
4d	$^n\text{Pr}_3\text{PO}$	1157	1131	-26
4e	$^n\text{Oct}_3\text{PO}$	1151	1143	-8
4f	Ph_3PO	1190	1177	-13
4g	$(\text{MeO})_3\text{PO}$	1282	1226	-56
4h	$(\text{EtO})_3\text{PO}$	1275	1208	-67
4i	$(\text{PhO})_3\text{PO}$	1296	1255	-41
4j	$(\text{EtO})_2\text{PHO}$	1258	1180	-78
4k	$(^n\text{BuO})_2\text{PHO}$	1261	1188	-73
4l	$(\text{PhO})_2\text{PHO}$	1279	1249	-30
4m	$(\text{MeO})_2\text{MePO}$	1242	1190	-52
4n	$(\text{EtO})_2\text{MePO}$	1243	1190	-55
4o	$(\text{EtO})_2\text{PhPO}$	1250	1174	-76
4p	$(\text{MeO})\text{Me}_2\text{PO}$	1216	1177	-39
4q	$(\text{EtO})\text{Me}_2\text{PO}$	1210	1187	-23

Table 4.3. $\Delta\nu(\text{PO})$ values (cm^{-1}) for $\text{B}(\text{C}_6\text{F}_5)_3$ adducts of phosphoryl ligands, $\Delta\nu(\text{PO}) = \nu(\text{PO})$ (adduct) - $\nu(\text{PO})$ (base).

It has been noted [162] that the phosphoryl stretch of TEPO was solvent dependent $\Delta\nu(\text{PO})$ has been correlated with Gutmann's [138, 139] AN solvent scale.

Lappert used $\Delta\nu(\text{CO})$ of ethyl acetate upon adduct formation as a measure of Lewis acidity and this has been discussed in section 4.3.2. The $\nu(\text{PO})$ stretching data for the adducts is shown in Table 4.3 along with the $\Delta\nu(\text{PO})$ values. The negative $\Delta\nu(\text{PO})$ values indicate that the $\nu(\text{PO})$ is shifted to lower wavenumber upon co-ordination to $\text{B}(\text{C}_6\text{F}_5)_3$. The $\Delta\nu(\text{PO})$ values for the adducts ranged from -8 to -78 cm^{-1} . Detailed examination of the data reveals that the magnitude of $\Delta\nu(\text{PO})$ was lowest for triorganophosphine oxides and greatest for species with OR or OAr groups at P. The $\Delta\nu(\text{PO})$ ranges associated with the various classes of compounds, arranged in decreasing order of P-C bonds, were -8 to -26 (phosphine oxides), -23 (phosphinate esters), -52 to -78 (phosphonate esters), and -41 to -67 (phosphate esters). The adducts of phosphonate esters had similar $\Delta\nu(\text{PO})$ ranges irrespective of whether H or alkyl were bound to P, although a smaller shift was observed for $(\text{PhO})_2(\text{H})\text{PO}\cdot\text{B}(\text{C}_6\text{F}_5)_3$, **4i**. A theoretical study [151] has demonstrated that $\text{B}(\text{C}_6\text{F}_5)_3$ is a hard acid and that its bonding is dominated by electrostatic effects. The phosphoryl bond can be drawn as a resonance hybrid of two limiting canonical forms (Figure 4.4) with (I) having a heavier weighting than (II). An electrostatic interaction with $\text{B}(\text{C}_6\text{F}_5)_3$ would favour the former and effectively reduce the PO bond order, and hence $\nu(\text{PO})$.



Figure 4.4. Resonance hybrids of the phosphoryl bond.

The absolute value of $\nu(\text{PO})$ in phosphoryl derivatives may be accurately calculated [163] using an empirical relationship involving additive electronegativities of substituents at phosphorus (inductive effects). The $\Delta\nu(\text{PO})$ values are greatest where π -resonance from a substituent is possible indicating that structures such as $(\text{PhO})_2(\text{PhO}^+)=\text{P}-\text{O}^-$ may be important in lowering the PO bond order upon adduct formation.

4.3.4 X-ray Crystallography

Two of these adducts ($\text{TEPO}^+\text{B}(\text{C}_6\text{F}_5)_3$ (**4c**) and $\text{Ph}_3\text{PO}^+\text{B}(\text{C}_6\text{F}_5)_3$ (**4f**)) were characterised by a single crystal X-ray diffraction study. Crystals suitable for X-ray diffraction were given from a layered $\text{CHCl}_3/\text{hexane}$ solution. These two structures are the only crystallographically characterised structures of phosphoryl adducts of $\text{B}(\text{C}_6\text{F}_5)_3$. A drawing of the molecular structure of **4c** is shown in Figure 4.5 whilst a drawing of the molecular structure of **4f** is shown in Figure 4.6. Selected bond lengths are shown in Table 4.4 and selected bond angles in Table 4.5.

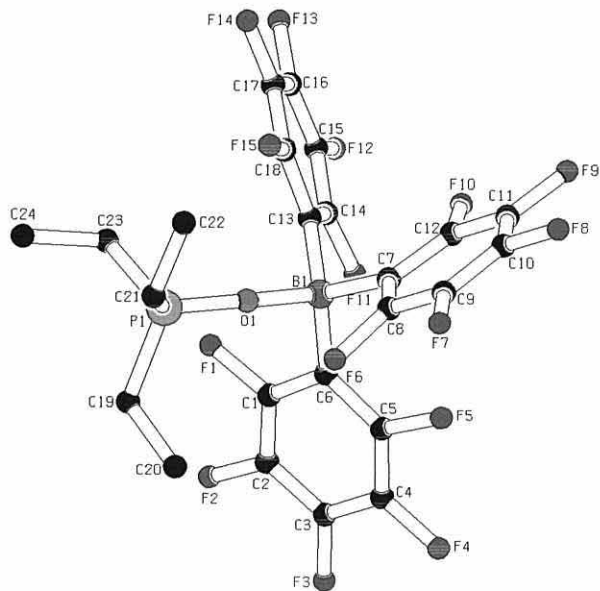


Figure 4.5. Molecular structure of $\text{B}(\text{C}_6\text{F}_5)_3\text{OPEt}_3$, **4c**.

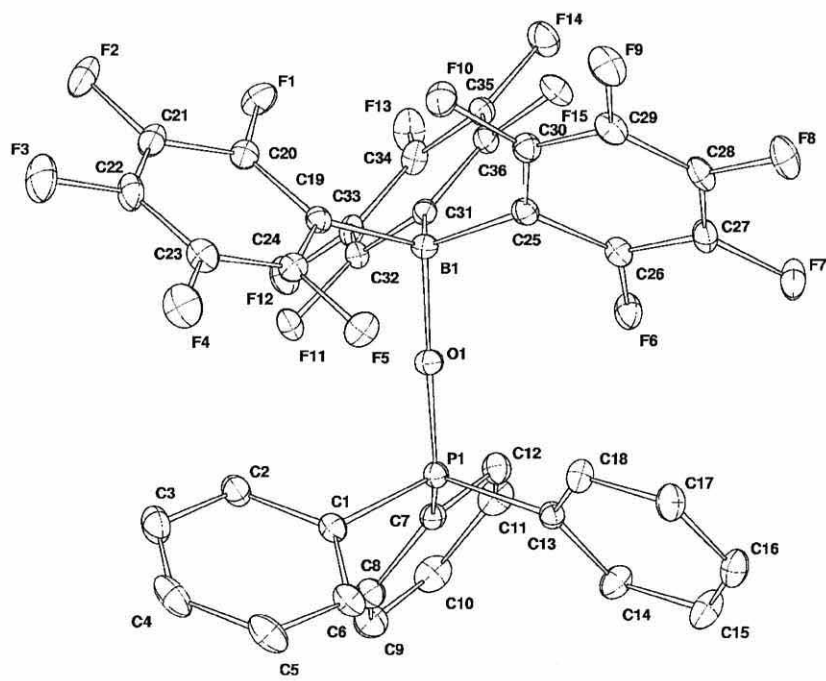


Figure 4.6. Molecular structure of $\text{B}(\text{C}_6\text{F}_5)_3\text{OPPh}_3$, **4f**.

4c	Bond Angle (°)	4f	Bond Angle (°)
P(1)-O(1)-B(1)	161.04(16)	P(1)-O(1)-B(1)	178.7(2)
O(1)-P(1)-C(19)	110.97(13)	O(1)-P(1)-C(1)	109.6(1)
O(1)-P(1)-C(21)	109.81(13)	O(1)-P(1)-C(7)	109.6(1)
O(1)-P(1)-C(23)	111.50(12)	O(1)-P(1)-C(13)	109.9(1)
O(1)-B(1)-C(6)	105.70(19)	O(1)-B(1)-C(19)	104.9(2)
O(1)-B(1)-C(7)	105.30(18)	O(1)-B(1)-C(25)	105.1(2)
O(1)-B(1)-C(13)	106.79(18)	O(1)-B(1)-C(31)	105.1(2)
C(6)-B(1)-C(7)	114.79(19)	C(19)-B(1)-C(25)	113.7(2)
C(6)-B(1)-C(13)	113.8(2)	C(19)-B(1)-C(31)	112.7(2)
C(7)-B(1)-C(13)	109.66(19)	C(25)-B(1)-C(31)	114.2(2)
C(19)-P(1)-C(21)	106.86(15)	C(1)-P(1)-C(7)	110.2(1)
C(19)-P(1)-C(23)	107.07(15)	C(1)-P(1)-C(13)	108.9(1)
C(21)-P(1)-C(23)	110.52(15)	C(7)-P(1)-C(13)	108.7(1)

Table 4.5. Selected bond angles for **4c** and **4f**.

4c	Bond Length Å	4f	Bond Length Å
P(1)-O(1)	1.4973(13)	P(1)-O(1)	1.497(2)
P(1)-C(19)	1.811(3)	P(1)-C(1)	1.791(2)
P(1)-C(21)	1.763(3)	P(1)-C(7)	1.791(2)
P(1)-C(23)	1.776(3)	P(1)-C(13)	1.783(2)
O(1)-B(1)	1.533(3)	O(1)-B(1)	1.538(3)
B(1)-C(6)	1.632(4)	B(1)-C(19)	1.632(3)
B(1)-C(7)	1.636(4)	B(1)-C(25)	1.639(3)
B(1)-C(13)	1.645(3)	B(1)-C(31)	1.643(3)

Table 4.4. Selected bond length's of **4c** and **4f**.

As might be expected the molecular structures are essentially what might be found from the precursors with the acid $\text{B}(\text{C}_6\text{F}_5)_3$ and the base (TEPO or Ph_3PO) joined together *via* a O→B co-ordinate bond. The overall structure of **4c** is similar to that of **4f** except for the angle at O in the B-O-P linkage being bent in **4c** ($161.04(16)^\circ$) and linear in **4f** ($178.66(16)^\circ$).

In **4f** the B-C bonds of the borane are almost eclipsed with respect to the P-C bonds of the phosphine oxide (Figure 4.7).

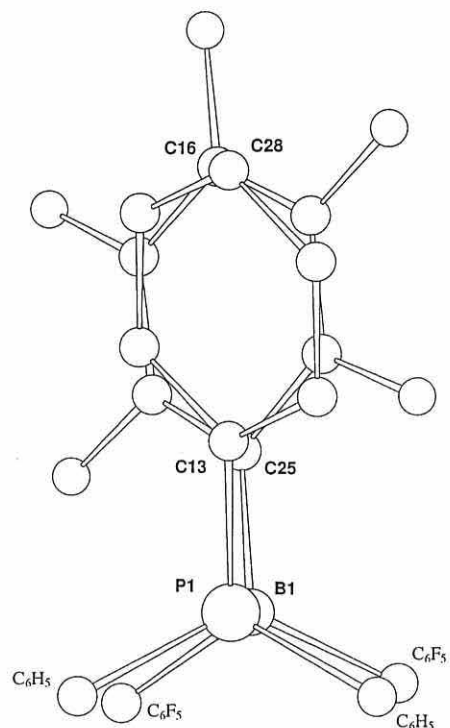


Figure 4.7. A view down the P(1)-O(1) bond of **4f** showing the eclipsed conformation of the phenyl groups of the phosphine oxide and the C₆F₅ groups of the borane.

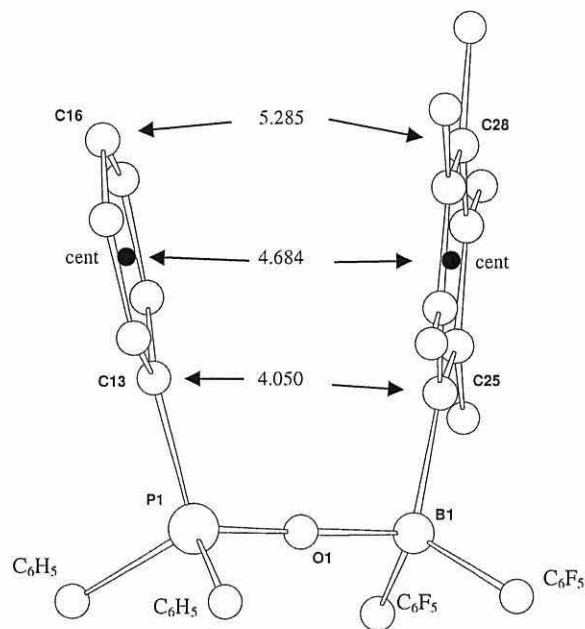


Figure 4.8. A view of **4f** showing the aryl π -interactions between a C_6F_5 and a C_6H_5 unit.

There are weak intramolecular π -stacking interaction between the three C_6F_5 groups of the borane and the three Ph groups of the phosphine oxide (Figure 4.8). This π -stacking interaction has been observed previously where the bent B-O-C system of $B(C_6F_5)_3PhC(X)O$ ($X = OEt, N^iPr_2$) [154] enables a strong interaction between the Ph ring of the base and the C_6F_5 ring of the acid. Similarly the hydroxy bridged borate anion $[(C_6F_5)_3BO(H)B(C_6F_5)_3]$, with a B-O-B angle of $139.6(5)^\circ$ and a staggered confirmation, has a strong π -interaction between two of its C_6F_5 rings [153].

Previously determined structures of TEPO adducts have been confined to the following transition metal complexes: $[Mo_2(OAc)_3(OPEt_3)(S_2CPEt_3)][BF_4]$ [164], *mer*- $[VCl_3(OPEt_3)_3]$ [165], $[Ba_2Cu_4(O^tBu)_8(OPEt_3)_2] \cdot 0.5C_7H_8 \cdot 1.5THF$ [166] and $[\{MoCl_2(OPEt_3)(NO)_2\}_2]$ [167].

The B and P atoms in both **4c** and **4f** are 4 co-ordinate with angles subtended at these atoms close to those expected for σ framework sp^3 hybridisation (Table 4.6).

Compound	Angle at B ($^{\circ}$) av.	Angle at P ($^{\circ}$) av.
TEPO·B(C ₆ F ₅) ₃ , 4c	109.3	109.45
Ph ₃ PO·B(C ₆ F ₅) ₃ , 4f	109.3	109.5

Table 4.6. Angle at B and P for **4c** and **4f**.

The detailed deviation of angles at B suggest back strain in the acid upon adduct formation with larger C-B(1)-C angles and smaller O(1)-B(1)-C angles (Table 4.7).

Compound	C-B(1)-C ($^{\circ}$) av.	O-B(1)-C ($^{\circ}$) av.
TEPO·B(C ₆ F ₅) ₃ , 4c	112.7	105.7
Ph ₃ PO·B(C ₆ F ₅) ₃ , 4f	113.5	105.1

Table 4.7. Average angles for **4c** and **4f**

The deviation at idealised tetrahedral angles at B is less marked than has been observed previously in other adducts [151, 152, 154, 155]. The B(1)-O(1) bond length for **4c** at 1.533(3) \AA is similar to that found in **4f** at 1.538(3) \AA and BF₃·B(C₆F₅)₃ 1.516(3) \AA [161], shorter than that in BF₃·PhC(H)O 1.591(6) \AA [168] and at the lower end of the range (1.52(1) – 1.610(8) \AA) observed for B(C₆F₅)₃·PhC(X)O complexes [154]. Shorter B-O distances have been reported in metal-oxo adducts of B(C₆F₅)₃ e.g. [WO{OB(C₆F₅)₃}₃]²⁻ (1.491(3)–1.508(3) \AA) [169] and [(Me₅Cp)₂Zr{OB(C₆F₅)₃}]

(1.460(6)) [170]. As noted above, the B-O-P angles for **4c** and **4f** differ. P-O-M angles in Ph₃PO complexes are variable and range from 123.0(4) (in SeOCl₂Ph₃PO [171]) to 180 (in AlCl₃Ph₃PO [159]). The same is observed with TEPO complexes with P-O-M angles in the range from 141.02(46) to 180 [164-170, 172]. An explanation of this phenomena has been offered in terms of the relative π -acceptor properties of the acid [173]. In view of the large difference in this angle for **4c** and **4f** it is clear that other factors must also be in operation. The angle at O when bound to main group atoms (X) from the second row is renowned for its flexibility, and intermolecular crystal packing forces are sufficient to cause a difference in B-O-X angles [174]. The intramolecular π -stacking interaction for **4f** are maximised with a linear B-O-P linkage and it is this that might be a factor in the energetics of the system. The P-O bond length at 1.497(2) \AA for **4f** and 1.4973(17) \AA for **4c** are similar to that found for BF₃·Ph₃PO (1.523(3) \AA [161]) and slightly longer than that found for Ph₃PO (1.483(2) \AA [175]) indicating a reduction of bond order upon adduct formation.

4.4 Conclusions

A series of 15 new phosphoryl adducts of B(C₆F₅)₃ (**4a**) have been prepared and characterised by satisfactory elemental analysis, M.Pt., IR and NMR (¹H, ¹¹B, ¹³C, ¹⁹F, ³¹P) spectroscopy. The new ethyl acetate complex of B(C₆F₅)₃ has also been synthesised and characterised. Δv (P=O) of the phosphoryl adducts have been analysed in terms of substituent effects at P. The Lewis acidity of **4a** has been determined by Gutmann's and Lappert's methods and these measurements indicate a Lewis acidity order of TiCl₄ < B(C₆F₅)₃ < AlCl₃ ~ BF₃.

Chapter 5

Attempts to prepare unsaturated boron-phosphorus
heterocycles.

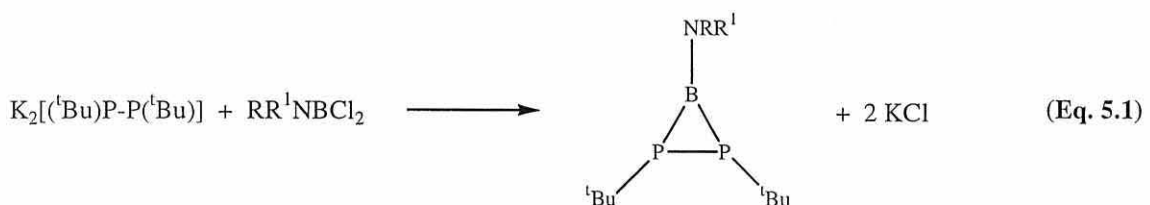
5.1 Introduction

The study of unsaturated B-P ring compounds is a relatively recent area of heterocyclic boron chemistry. It has not been exploited to the same extent as the analogous B-N systems due to the mistaken belief that the π -bonding between boron and phosphorus would be too weak to allow for the formation of such heterocycles.

It was discovered that the presence of bulky substituents on or near the reactive centres stabilise these systems, hence reports of these elusive unsaturated ring systems became increasingly common. Comprehensive reviews of B-P chemistry have been written by Noth and Paine [176] and by Power [177, 178].

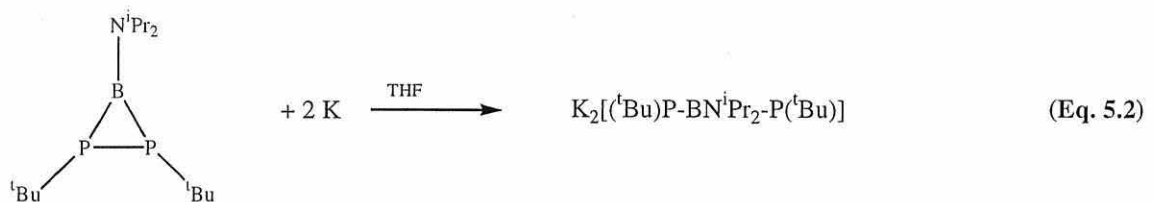
5.1.1 Three-membered rings

The first compound to be analysed by X-ray crystallography, containing bonding between three co-ordinate boron and phosphorus atoms was that of the diphosphaborirane $\text{Et}_2\text{NB}(\text{P}^t\text{Bu})_2$ [179]. This and analogous compounds can be prepared in good yields by treatment of $\text{K}_2[(^t\text{Bu})\text{P}-\text{P}(^t\text{Bu})]$ with a diorganylaminoborondichloride (Eq. 5.1) [180].

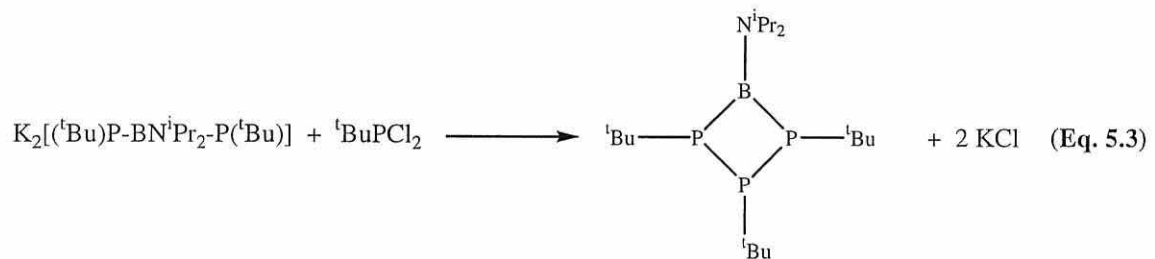


These compounds are relatively stable towards dimerisation to the related B_2P_4 six-membered rings, although the process is influenced by electronic and steric effects of the substituents [180].

The diphosphaboriranes react with potassium in DME to produce the monometallated three membered ring [181], where one of the phosphorus substituents is replaced. If the same reaction is performed in THF it causes cleavage of the P-P bond (Eq. 5.2).



If the non-cyclic product produced from the reaction in Eq. 5.2 is treated with ^tBuPCl_2 , a [3+1] cyclocondensation occurs to produce the four membered triphosphaboretane (Eq. 5.3) [182, 183].

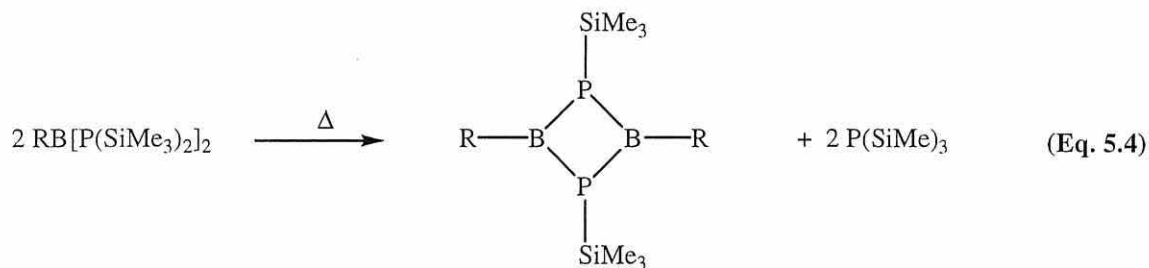


Similarly the five-membered tetraphosphaborolidine ring can be prepared from a [4+1] cyclocondensation of $\text{K}_2[(\text{tBu})\text{P}-(\text{tBu})\text{P}_2-\text{P}(\text{tBu})]$ with $\text{^iPr}_2\text{NCl}_2$ [183].

5.1.2 Four-membered rings

A diphosphadiboretane ring was first prepared by thermolysis of $\text{RB[P(SiMe}_3)_2]_2$ at 150°C (Eq. 5.4) [184]. Other syntheses have since been discovered,

one such synthesis involves the treatment of tmpBCl₂ with an equivalent of Li[P(SiMe)₃R] to produce a diphosphadiboretane (Eq. 5.5) [177].



The first reported X-ray structures of the diphosphadiboretanes were of (tmpBPCEt₃) and (tmpBPMes)₂ [185, 186]. The heterocyclic rings were found to be planar with trigonal planar geometries being observed at both boron and exocyclic nitrogen, whilst the phosphorus centres were pyramidal. The B-N bond distances suggested strong exocyclic π -bonding however, crystallographic data and MO calculations indicated the absence of dative P B π -bonding and a lack of any ring delocalisation [177].

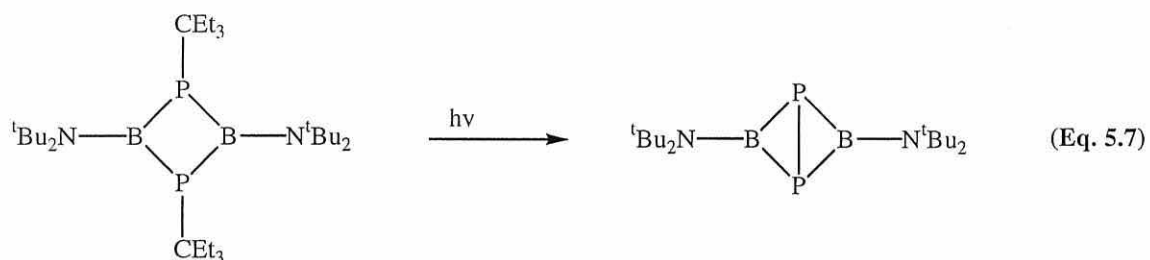
Diphosphadiboretanes with aryl or alkyl substituents, rather than amino substituents, have also been prepared [177, 178, 187]. These are readily formed by reactions of organoborondihalides with a lithiated primary phosphine, RPHLi, as shown in Eq. 5.6 [178].



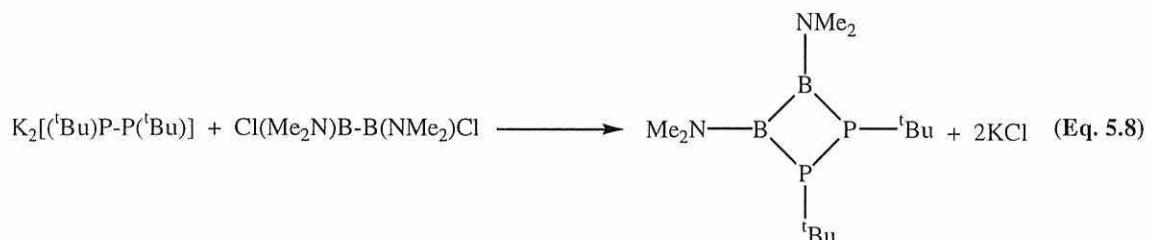
Where R / R¹ = Thexyl / Mes

These systems have also been found to possess a planar B_2P_2 ring [178], with the B-P bond lengths being similar to those observed for the diphosphadiboretanes with amino substituents on boron.

Photolysis of a diphosphadiboretane has been reported to produce a fused three membered ring (Eq. 5.7) [188].



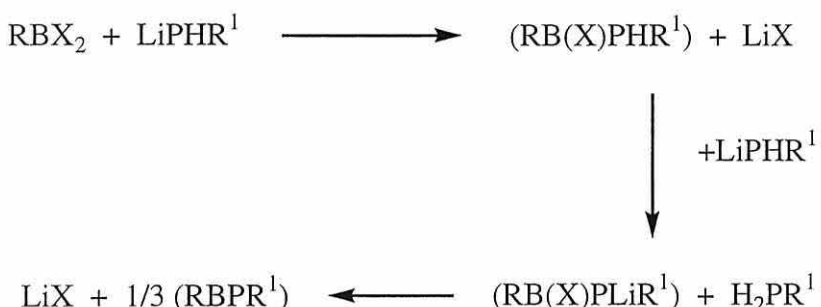
Isomers of the diphosphadiboretane with non-alternating B and P atoms have also been prepared by a [2+2] cyclocondensation of $K_2[(^t\text{Bu})\text{P}-\text{P}(^t\text{Bu})]$ with $\text{Cl}(\text{Me}_2\text{N})\text{B}-\text{B}(\text{NMe}_2)\text{Cl}$, as shown in Eq. 5.8 [189].



These were reported to be planar and readily decomposed in the presence of water or oxygen [189].

5.1.3 Six-membered rings

The first B_3P_3 rings were isolated during an unsuccessful attempt to prepare the related diphosphadiboretane species (scheme 5.1) [178]. It was later found that steric hindrance was an important feature of the synthesis and accordingly several triphosphatriborinanes have been prepared. They have been shown to exhibit less sensitivity towards the atmosphere than the corresponding diphosphadiboretanes, reacting only slowly with water to produce a primary phosphine and boron-oxygen compounds [178].



Scheme 5.1. Synthetic strategy to produce six-membered rings.

Two competing mechanisms have been suggested to operate during the addition of R^1PHLi to RBX_2 and these dictate the identity of the heterocycle so produced [187]. The formation of the four membered ring requires the association of two molecules of a $RB(PHR^1)_2$ intermediate, with the subsequent elimination of R^1PH_2 . Bulkier substituents, especially at boron, impede the reaction and the six-membered ring is favoured. Some ligand combinations have been found to afford mixtures of both six- and four-membered rings [187].

X-ray studies of the triphosphatriboriranes have shown that the B_3P_3 ring has a planar configuration, in which all B-P bond lengths are shorter (1.84\AA) than those observed for a single B-P bond, suggesting the presence of some double bond character [187].

5.2 Aims

The aims of the research detailed in this chapter were to prepare a series of new diphosphadiboretanes and triphosphatriboriranes, with various aryl substituents at boron, and to examine their co-ordination reactions with metal carbonyl complexes.

5.3 Results and discussion

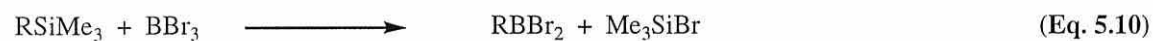
The preferred route to the heterocyclic species was by the reaction of arylboron dibromides with tris(trimethylsilyl)phosphine, and the preparation of these compounds (section 5.3.1 and 5.3.2) and their reactions (section 5.3.3) are discussed first. The synthesis of PhPH_2 adducts of the arylboron dibromides and their subsequent thermolysis, as an alternative route to B-P heterocycles, is discussed in section 5.3.4.

5.3.1. Preparation of the arylborondibromides

Previous syntheses of the arylborondibromides have involved the use of $HgBr$, which was found to be a convenient preparation though unfavorable toxicity considerations hinder the work up [190]. Another route to the arylborondibromides is by reaction of borontribromide with an aryltrimethylsilane [191].

The aryltrimethylsilanes have been prepared in good yields by use of a Grignard approach (Eq. 5.9). All compounds were colourless volatile liquids which were analysed by 1H NMR, IR and M.Pt / B.Pt., and all were in good agreement with

literature values [191]. These compounds prove valuable precursors for the preparation of the arylborondibromides. Reacting an aryltrimethylsilane with one equivalent of borontribromide produces the required arylborondibromide in good yield (Eq. 5.10).



All the arylboron dibromides were colourless volatile liquids that rapidly decompose in contact with water, and all compounds were authenticated by ^1H and ^{11}B NMR by comparison with literature values (Table 5.1)

ArBBR_2	^{11}B NMR shift
PhBBR_2 [192]	+56.4 [+56.2]
$2\text{-MeC}_6\text{H}_4\text{BBR}_2$ [193]	+57.6 [+57.7]
$3\text{-MeC}_6\text{H}_4\text{BBR}_2$ [192]	+56.8 [+56.9])
$4\text{-MeC}_6\text{H}_4\text{BBR}_2$ [192]	+55.9 (+55.9]
$4\text{-EtC}_6\text{H}_4\text{BBR}_2$ [193]	+56.0 [+56.1]
$3,5\text{-Me}_2\text{C}_6\text{H}_3\text{BBR}_2$ [193]	+56.8 [+56.7]
MesBBR_2 [194]	+62.1 [+62.2]

Table 5.1. ^{11}B NMR values for the arylborondibromides literature values in parenthesis (ppm).

Gutmann's AN values can be used as a measure of Lewis acidity [138, 139]. Measurement of Lewis acidity of arylboron dibromides has not been previously reported. The AN values of the arylborondibromides are shown in Table 5.2 below. All values are calculated in accordance with the method described in Chapter 4.

ArBBr ₂	AN Value
PhBBr ₂	67.8
2-MeC ₆ H ₄ BBr ₂	68.7
3-MeC ₆ H ₄ BBr ₂	71.2
4-MeC ₆ H ₄ BBr ₂	68.2
3,5-Me ₂ C ₆ H ₃ BBr ₂	65.6
4-EtC ₆ H ₄ BBr ₂	66.5

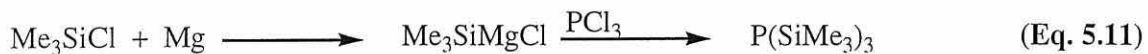
Table 5.2. Acceptor numbers of the arylborondibromides.

Gutmann's AN scale runs from 100 for the strong Lewis acid SbCl₅ to 0 for hexane. As might be expected, all are quite strong Lewis acids, being between SnCl₄ (AN = 59) and TiCl₄ (AN = 70) in strength, but considerably weaker than BF₃ (AN = 89) and BBr₃ (AN = 109).

5.3.2 Synthesis of tris(trimethylsilyl)phosphine

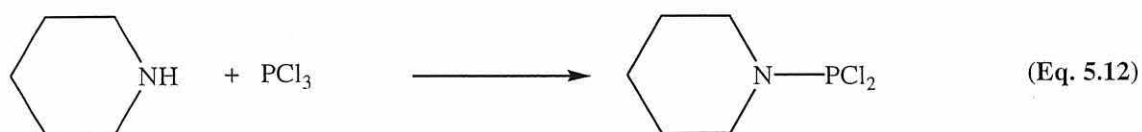
Due to the very high commercial cost of tris(trimethylsilyl)phosphine it became necessary to prepare this tertiary phosphine. The initial attempt used a Grignard approach with trimethylsilyl chloride (Eq. 5.11) generating trimethylsilylmagnesium

chloride, which was quenched with phosphorus trichloride and left refluxing for 7 days [195].



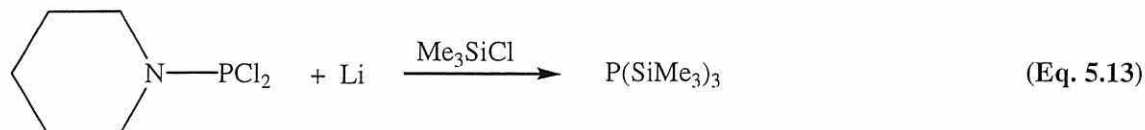
After the seven day reflux, crude ^{31}P NMR samples showed a plethora of signals covering the range of +13 to -153 ppm. There was however, no evidence for formation of $\text{P}(\text{SiMe}_3)_3$ (-253 ppm), and upon working up the reaction, a yellow malodorous solid was obtained. Thus it became necessary to find an alternative synthesis for tris(trimethylsilyl)phosphine. One possible method [196] involved the addition of a potassium and sodium alloy to white phosphorus, however this was not attempted due to safety considerations.

A more recent reported preparation of $\text{P}(\text{SiMe}_3)_3$ involved the reaction of piperidinophosphorus dichloride [197], with lithium powder, followed by quenching the reaction with PCl_3 . The piperidinophosphorus dichloride was readily prepared by adding PCl_3 to piperidine in diethyl ether (Eq. 5.12) at 0°C. The compound was distilled, and was a colourless liquid. All data obtained agreed with the literature values.



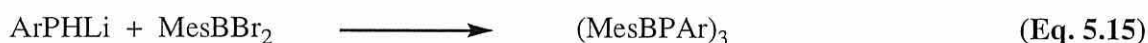
Subsequently reacting the piperidinophosphorus dichloride with lithium powder, and quenching with Me_3SiCl , as illustrated in Eq. 5.13, produced the desired compound

in a 59% yield. Tris(trimethylsilyl)phosphine spontaneously combusts in contact with air / moisture, all spectroscopic data for the compound agreed with the literature values.



5.3.3 Attempted synthesis of diphosphadiboretanes and triphosphaboriranes using lithium reagents

In 1977, Fritz and Holderich produced a diphosphadiboretane from lithiated tris(trimethylsilyl)phosphine and PhBBr₂ (Eq. 5.14) and in 1989 Power published the preparation of 6-membered rings B₃P₃ rings by reactions of lithium salts of primary phosphines with (Mes)BBr₂ (Eq. 5.15) [187].



Ar = Mes, ^tBu, C₆H₁₁, Ph

It was the aim of this research to generate some new 4 and 6-membered BP ring derivatives by repeating the above reactions with the various arylboron dibromides synthesised in section 5.3.1. Mono-lithiation of tris(trimethylsilyl)phosphine with methyl lithium, produced the desired product Li[P(SiMe₃)₂] in good yields (around 60%). The 1:1 reaction between this lithiated phosphine and PhBBr₂ should have produced the diphosphadiboretane (PhBPSiMe₃)₂. However, this was not the case, a

yellow solid was obtained, which gave an array of weak signals in the ^{31}P NMR and only several broad signal in the ^{11}B NMR. Similar results were obtained from using 4-MeC₆H₄BBr₂ as the boron source.

It has been reported that under similar reaction conditions, polymeric materials are produced. For example, Livingstone and Coates [198] suggested that the reaction of PhBCl₂ with PhPH₂ at reflux temperatures generated a number of products, and one of which was a yellow polymeric material. Their work was later repeated by Tevebaugh and he reported that the reaction products were a white, waxy, trimeric compound and a low molecular weight polymer [199]. It appears that we were also likely to be forming polymeric materials rather than the anticipated BP ring systems.

The unsuccessful nature of this area of research is not entirely understood. It is possible that the reactions performed here were on too large a scale to enable isolation. Diaz and Power worked with smaller quantities and isolated single crystals. It is also possible that the optimum reaction conditions to obtain these compounds were not fully reported in their original communication.

5.3.4 Synthesis and thermolysis of ArBBr₂·PhPH₂ adducts

An alternative strategy to obtain the BP ring systems was to attempt a thermolysis of preformed adducts of ArBBr₂ and PhPH₂ (Eq. 5.16 and 5.17).



A number of previously unreported adducts of PhPH₂ with ArBBr₂ (Ar = Ph, 2MeC₆H₄, 3-MeC₆H₄, 4-MeC₆H₄, 3,5-Me₂C₆H₃ and 4-EtC₆H₄) were prepared in hexane at 0°C.

The adducts were characterised by ^{11}B and ^{31}P NMR (Table 5.3). The boron nuclei were shielded by \sim 65 ppm upon co-ordination by the primary phosphine, whilst the ^{31}P nuclei are shifted downfield by \sim 80 ppm by co-ordination to B (Table 5.4) $\Delta\delta$ (^{31}P) for $\text{BBr}_3\text{PhPH}_2$ is reported at 56.1 ppm [200]. Attempted thermolysis of these adducts did not lead to clean reactions and presumably led again to polymeric materials.

ArBBr_2	$\delta(^{11}\text{B})$	$\delta(^{31}\text{P})$
PhBBr_2	-4.6	-42.1
$2\text{-MeC}_6\text{H}_4\text{BBr}_2$	-5.1	-50.3
$3\text{-MeC}_6\text{H}_4\text{BBr}_2$	-3.8	-45.4
$4\text{-MeC}_6\text{H}_4\text{BBr}_2$	-3.9	-44.1
$3,5\text{-Me}_2\text{C}_6\text{H}_3\text{BBr}_2$	-4.8	-46.3
$4\text{-EtC}_6\text{H}_4\text{BBr}_2$	-4.9	-44.1

Table 5.3. NMR shifts of ArBBr_2 adducts of PhPH_2 .

ArBBr ₂	³¹ P Δδ	¹¹ B Δδ
PhBBr ₂	-80.5	+61.0
2-MeC ₆ H ₄ BBr ₂	-72.3	+62.7
3-MeC ₆ H ₄ BBr ₂	-77.2	+60.6
4-MeC ₆ H ₄ BBr ₂	-78.5	+59.8
3,5-Me ₂ C ₆ H ₃ BBr ₂	-76.3	+60.8
4-EtC ₆ H ₄ BBr ₂	-78.5	+61.7

Table 5.4. Δδ NMR values of adducts of PhPH₂.

5.4 Conclusions

Attempts to prepare the B₂P₂ and B₃P₃ heterocycles by the literature methods proved unsuccessful. An alternate route involving the synthesis of a series of 1:1 adducts of ArBBr₂ with PhPH₂ was also attempted but again these reactions did not yield the desired heterocycles. Accordingly, their co-ordination chemistry could not be examined.

Chapter 6

Experimental

6.1 General

All reactions were performed using standard Schlenk line techniques under a dinitrogen atmosphere and all solvents were dried, distilled and degassed prior to use.

A variety of chemicals employed for the following experiments were obtained from commercial sources and used as supplied. Infrared spectra were recorded on a Perkin-Elmer FT-IR 1600 spectrometer, as KBr disks unless otherwise stated. Melting points were measured on an Electrothermal Melting Point apparatus. Multi-element NMR spectra were obtained on a Bruker AC 250 CP / MAS NMR spectrometer (operating at 250 MHz for ^1H , 63 MHz for ^{13}C -{ ^1H }, 80 MHz for ^{11}B -{ ^1H }, 49 MHz for ^{29}Si -{ ^1H } and 101 MHz for ^{31}P -{ ^1H }). ^{11}B -{ ^1H } (solid state) MAS NMR spectra were recorded on a 350 MHz instrument (EPSRC solid state service, Durham) operating at 96.234 MHz, whilst ^{19}F NMR spectra were recorded on a Bruker 350 operating at 328 MHz. Chemical shifts (δ) are given in ppm with positive values towards high frequency (downfield) from tetramethylsilane for ^1H , ^{13}C -{ ^1H } and ^{29}Si -{ ^1H }, from $\text{BF}_3\cdot\text{OEt}_2$ for ^{11}B -{ ^1H }, from H_3PO_4 for ^{31}P and from CFCl_3 for ^{19}F . All samples were dissolved in CDCl_3 unless otherwise stated. Elemental analysis was performed using a Carbo Erba CHNS-O Ea1108 instrument using helium as the carrier gas.

The experimental details concerned with Chapter 2, 3, 4 and 5 are shown in sections 6.2, 6.3, 6.4 and 6.5 respectively.

6.2 Experimental for Chapter 2

6.2.1 Preparation of [MBr(CO)₅] species (M = Mn, Re).

The metal pentacarbonylbromides were produced from [M₂(CO)₁₀](where M= Mn, Re) using a synthetic strategy published by Quick and Angelici [201].

[ReBr(CO)₅]

Dirhenium decacarbonyl (0.86 g, 1.32 mmol) was dissolved in dichloromethane (30 cm³). To this was added bromine (0.21 g, 1.32 mmol) and the resulting mixture was left to stir at room temperature for 1h after which time a precipitate had formed. The solvent was removed by vacuum and the precipitate recrystallised from acetone and methanol (0.43 g, 88%).

IR (KBr disk, CO region):- 2152s, 2035s, 1965s (Lit. 2154w, 2048s, 2018s, 1987m [76])

M.Pt:- 182°C

[MnBr(CO)₅]

To a solution of dimanganese decacarbonyl (2.0 g, 5.13 mmol) in dichloromethane (50 cm³) was added bromine (0.81 g, 5.13 mmol) drop wise. The resulting mixture was left to stir for 1h at room temperature before the solvent was removed to produce a yellow powder. The powder was then re-dissolved in dichloromethane (60 cm³) and filtered. The resulting liquid was layered with hexane (60 cm³). Crystals appeared on leaving and were filtered off (0.7 g, 50%).

IR (KBr disk, CO region):- 2137w, 2050s, 2007m (Lit. 2133w, 2049s, 2004m [201])

M.Pt:- 169°C (Lit. 171°C [201])

6.2.2 Synthesis of *mer*, *trans*-[MnBr(CO)₃L₂] and *fac*, *cis*-[MnBr(CO)₃L₂].

The [MnBr(CO)₃L₂] compounds were produced from [Mn(CO)₅Br] using a route developed by Abel and Wilkinson [202]. The preparation of *mer,trans*-[MnBr(CO)₃{P(C₆H₄Cl-4)₃}₂] (**2b**) is reported in its entirety; other derivatives were synthesised by a similar method. Analytical and spectroscopic for the following compounds are given in Chapter two. Additional data, is listed here.

Mer,trans-[MnBr(CO)₃{P(C₆H₄Cl-4)₃}₂] (**2b**)

To chloroform (30 cm³) was added [MnBr(CO)₅] (0.5 g, 1.82 mmol). The resulting mixture was stirred before tris(4-chlorophenyl)phosphine (1.33 g, 3.64 mmol) was added. The resulting mixture was stirred for 12h before the solvent was removed. The crude product was recrystallised from a 1:4 chloroform / hexane mixture (0.85 g, 51%).

IR (KBr disk): 3041w, 2034w, 1951m, 1901m, 1480s, 1386s, 1186w, 1080s, 816s, 745s, 706w, 636s

Mer,trans-[MnBr(CO)₃(PPh₃)₂] (**2a**)

Yield: 82%

IR (KBr disk): 3052s, 2040m, 1943s, 1918s, 1482s, 1433s, 1311m, 1189m, 1159m, 1089s, 1074sh, 1026w, 999s, 747s, 694s, 636s, 618sh

Mer,trans-[MnBr(CO)₃{P(C₆H₄OMe-4)₃}₂] (2c)

Yield: 77%

IR (KBr disk): 3053s, 2024w, 1945s, 1911s, 1595s, 1500s, 1265s, 1217s, 1182m, 1094m, 1029m, 896w, 742s

Mer,trans-[MnBr(CO)₃{P(CH₂Ph)₃}₂] (2d)

Yield: 89%

IR (KBr disk): 3020s, 2031w, 1949s, 1896s, 1493s, 1072s, 1011s, 912s, 855s, 767s

Fac,cis-[MnBr(CO)₃(dppm)] (2i)

Yield: 91%

IR (KBr disk): 3019s, 2026s, 1957s, 1919s, 1436m, 1215s, 1099m, 1026w, 929w, 750s

Fac,cis-[MnBr(CO)₃(dppe)] (2j)

Yield: 78%

IR (KBr disk): 3018s, 2024s, 1958s, 1916s, 1435s, 1216s, 1097m, 1028w, 929w, 770s, 670m

Fac,cis-[MnBr(CO)₃(dppp)] (2k)

Yield: 76%

IR (KBr disk): 3019s, 2028s, 1961s, 1909s, 1334s, 1218s, 1097m, 971m, 929m, 832w, 752s, 669m

Fac,cis-[MnBr(CO)₃(dppb)] (2l)

Yield: 91%

IR (KBr disk): 3052s, 2015s, 1958s, 1899s, 1483s, 1434s, 1310s, 1218w, 1089s, 999s, 909s, 855m, 812s, 738s, 691s

Fac,cis-[MnBr(CO)₃(dppfc)] (2m)

Yield: 60%

IR (KBr disk): 3018s, 2026s, 1960s, 1910s, 1434m, 1214s, 1091w, 1038w, 929m, 739s, 669s

6.2.3 Synthesis of *fac, cis-[ReBr(CO)₃L₂]*.

The *fac,cis-[ReBr(CO)₃L₂]* compounds were produced from [ReBr(CO)₅] using an approach developed by Abel and Wilkinson [202]. The preparation of *fac,cis-[ReBr(CO)₃{P(C₆H₄OMe-4)₃}₂]* (**2g**) is reported in its entirety; other derivatives were synthesised by a similar method. Analytical and spectroscopic for the following compounds are given in Chapter Two. Additional data, is listed here.

Fac,cis-[ReBr(CO)₃{P(C₆H₄OMe-4)₃}₂] (**2g**)

To chloroform (30 cm³) was added [ReBr(CO)₅] (0.5 g, 1.23 mmol). The resulting mixture was stirred before tris(4-methoxyphenyl)phosphine (0.866 g, 2.46 mmol) was added. The resulting solution was heated to reflux for 12h before the solvent was removed. The crude product was recrystallised from a 1:4 chloroform / hexane mixture. (0.91 g, 70%).

IR (KBr disk): 2958m, 2033s, 1953s, 1899s, 1595s, 1501s, 1287s, 1255s, 1215s, 1182s, 1095m, 1031m, 756s

Fac,cis-[ReBr(CO)₃(PPh₃)₂] (2e)

Yield: 49%

IR (KBr disk): 2889s, 2026s, 1948s, 1889s, 1459s, 1376s, 1155w, 1089w, 971w, 736s, 722s

Fac,cis-[ReBr(CO)₃{P(C₆H₄Cl-4)₃}₂] (2f)

Yield: 67%

IR (KBr disk): 3010s, 2035s, 1956s, 1912s, 1567s, 1495s, 1451s, 1229m, 1154w, 1098w, 950w, 735s, 723s

Fac,cis-[ReBr(CO)₃{P(CH₂Ph)₃}₂] (2h)

Yield: 59%

IR (KBr disk): 3026s, 2022s, 1938s, 1904s, 1598s, 1494s, 1451s, 1236m, 1068s, 1028s, 916s, 837s, 776s

Fac,cis-[ReBr(CO)₃(dppm)] (2n)

Yield: 70%

IR (KBr disk): 3059s, 2026s, 1943s, 1893s, 1483m, 1436s, 1360m, 1099s, 1026w, 801m, 728s, 691s

Fac,cis-[ReBr(CO)₃(dppe)] (**2o**)

Yield: 82%

IR (KBr disk): 3053s, 2026s, 1948s, 1913s, 1421m, 1265s, 896w, 738s, 705sh, 696s

Fac,cis-[ReBr(CO)₃(dppp)] (**2p**)

Yield: 76%

IR (KBr disk): 3019s, 2035s, 1956s, 1904s, 1524w, 1434w, 1215s, 1093w, 1017w, 929m, 767s, 669s

Fac,cis-[ReBr(CO)₃(dppb)] (**2q**)

Yield: 85%

IR (KBr disk): 3019s, 2032s, 1953s, 1904s, 1426m, 1215s, 1095w, 929m, 760s

Fac,cis-[ReBr(CO)₃(dppfc)] (**2r**)

Yield: 60%

IR (KBr disk): 3018s, 2036s, 1958s, 1901s, 1482m, 1434m, 1216s, 929m, 764s, 669s

6.3 Experimental for Chapter 3

6.3.1 Synthesis of [ⁿBu₄N][B₃H₈]

A three necked 1L round bottom flask was equipped with a sealed mechanical stirrer, a pressure equalising funnel (the tip of which was extended below the surface of the reaction mixture) and a bubbler containing 4-picoline. A slurry of sodium borohydride (17 g, 0.45 mol) in diglyme (250 cm³) was added to the flask. A solution of iodine (20.6 g, 81 mmol) in diglyme (115 cm³) was poured into the pressuring equalising funnel. The reaction system was purged with nitrogen before being placed into a pre-heated oil bath of ~100°C. The iodine solution was slowly added to the sodium borohydride solution over a period of 1 to 2 hours. The resulting mixture was left to stir at ~100°C for a further two hours before being left to cool overnight. The volume was then reduced to approx 100 cm³ before the addition of water (50 cm³). The mixture was filtered to remove the grey byproduct, and the solution transferred to a 2L beaker. To this was added a solution of saturated tetra-n-butylammonium iodide (1 L). The white precipitate produced was filtered and washed with water (900 cm³), and the resulting solid was dried under vacuum. (12.0 g, 72%).

The crude product was purified by the following method. A sample of the crude product (5.2 g) was dissolved in dichloromethane (30 cm³), filtered and then washed with dichloromethane (30 cm³). To the resulting solution was added diethyl ether (400 cm³), the white precipitate that forms was filtered and then dried in vacuum. (4.8 g)

δ (¹¹B): -30.4 ppm

M.pt: 203°C (Lit 208°C [118])

6.3.2 Synthesis of *arachno*-[M(CO)₂(L)_x(B₃H₈)]

Following a similar method to that reported by Gaines *et al* [2]. . The preparation of *arachno*-[Mn(CO)₂(dppe)(B₃H₈)] (**3b**) is described in detail; all other derivatives were made in a similar manner. Analytical and spectroscopic for the following compounds are given in Chapter Two. Additional data, is listed here.

Arachno-[Mn(CO)₂(dppe)(B₃H₈)] (**3b**)

To a Carius tube containing dried and degassed dichloromethane (20 cm³) was added *fac,cis*-[MnBr(CO)₃(dppe)] (0.5 mmol, 351 mg) and [ⁿBu₄N][B₃H₈] (0.5 mmol, 141 mg). The tube was cooled to -198°C and evacuated before being sealed. The resulting sealed tube was irradiated for 20h by UV. After this time the tube was opened and the solvent removed *in vacuu*. The product was purified by column chromatography using CH₂Cl₂ / hexane (1:4) on Florisil. (0.16 g, 59%).

IR (KBr disk): 3018s, 2957s, 2927m, 2871m, 1923s, 1522m, 1457m, 1421m, 1378w, 1216s, 929m, 770s, 669s, 624w

Arachno-[Mn(CO)₂(dppm)(B₃H₈)] (**3a**)

Yield: 28%

IR (KBr disk): 3021s, 2959s, 1961s, 1901s, 1466m, 1389w, 1215s, 1030m, 930m, 789s

Arachno-[Mn(CO)₂(dppp)(B₃H₈)] (**3c**)

Yield: 17%

IR (KBr disk): 3053s, 2985m, 1960m, 1907m, 1421s, 1265s, 1067w, 896m, 738s, 705s

Arachno-[Mn(CO)₂(dppb)(B₃H₈)] (**3d**)

Yield: 24%

IR (KBr disk): 3011w, 1960s, 1907s, 1793m, 1469s, 1382s, 1097s, 908s, 734s, 651s

Arachno-[Mn(CO)₂(dppfc)(B₃H₈)] (**3e**)

Yield: 36%

IR (KBr disk): 3053s, 2985s, 1960m, 1882m, 1436w, 1421m, 1265s, 1174m, 1107m, 1062m, 1029m, 896s, 738s, 704s

Arachno-[Re(CO)₂(PPh₃)₂(B₃H₈)] (**3f**)

Yield: 20%

IR (KBr disk): 2965s, 2877w, 2388w, 1945m, 1915w, 1634s, 1482s, 1436m, 1382m, 919s, 746s, 650s

Arachno-[Re(CO)₂{P(C₆H₄Cl-4)}₂(B₃H₈)] (**3g**)

Yield: 36%

IR (KBr disk): 2966s, 1971s, 1913s, 1515w, 1460m, 1382w, 1216w, 1088m, 908s, 736s, 650s

Arachno-[Re(CO)₂{P(C₆H₄OMe-4)}₂(B₃H₈)] (**3h**)

Yield: 31%

IR (KBr disk): 3020m, 2959s, 2049m, 1972m, 1466s, 1378s, 1264s, 1216s, 1181w, 1097w, 1030w, 766s

Arachno-[Re(CO)₂{P(CH₂Ph)₃}₂(B₃H₈)] (3i)

Yield: 17%

IR (KBr disk): 3019s, 1948s, 1901m, 1496m, 1390m, 1214s, 929s, 768s, 669s

Arachno-[Re(CO)₂(dppm)(B₃H₈)] (3j)

Yield: 28%

IR (KBr disk): 3053s, 2985s, 1966m, 1902m, 1420s, 1265s, 1072m, 895s, 741s, 705s

Arachno-[Re(CO)₂(dppp)(B₃H₈)] (3k)

Yield: 32%

IR (KBr disk): 3053s, 2986s, 1967m, 1912m, 1654w, 1421s, 1265s, 896s, 740s, 705s

Arachno-[Re(CO)₂(dppb)(B₃H₈)] (3l)

Yield: 39%

IR (KBr disk): 3053, 2986s, 1965m, 1900m, 1421s, 1265s, 896s, 744s, 705s

Arachno-[Re(CO)₂(dppfc)(B₃H₈)] (3m)

Yield: 46%

IR (KBr disk): 3054s, 2987m, 1964s, 1912s, 1421s, 1265s, 896m, 738s, 705s

6.3.3 Thermolysis of [Mn(CO)₂(dppe)(B₃H₈)]

To a round bottomed flask was added [Mn(CO)₂(dppe)(B₃H₈)] (100 mg, 1.82 mmol) and chloroform (30 cm³). The resulting mixture was refluxed for 24hr. Due to the low yields only crude data was available.

δ (¹¹B): -47.1 ppm

δ (³¹P): +72 ppm, +99.3 ppm

6.3.4 Photolysis of [Mn(CO)₂(dppe)(B₃H₈)]

To a carius tube was added [Mn(CO)₂(dppe)(B₃H₈)] (100 mg, 1.82 mmol) and chloroform (30 cm³). The resulting mixture was irradiated for 24hr. Due to the low yields only crude data was available.

δ (¹¹B): -46.9 ppm

δ (³¹P): +28.7 ppm, +75 ppm, +98.2 ppm

6.3.5 Reaction between [Mn(CO)₂(dppe)(B₃H₈)] and PPh₃

To a round bottomed flask was added PPh₃ (47.7 mg, 1.82 mmol) and [Mn(CO)₂(dppe)(B₃H₈)] (100 mg, 1.82 mmol). To this was added chloroform (30 cm³) and the resulting mixture was refluxed for 24hr. The crude products produced were insoluble in chlorinated and unchlorinated solvents.

6.4 Experimental for Chapter 4

6.4.1 Synthesis of tris(pentafluorophenyl)borane (**4a**).

A solution of bromopentafluorobenzene (53.5 g, 217 mmol) in hexane (500 cm³), at -78°C, was treated with n-butyllithium in hexane (86.8 cm³, 2.5 mol dm⁻³, 217 mmol). The resulting white suspension was stirred for 1h and then added to a solution of boron tribromide (72 cm³, 1 mol dm⁻³, 72 mmol) in hexane (300 cm³). After stirring for 24h the mixture was filtered through a bed of celite to give a colourless liquid. A white crystalline material was obtained after reducing the solvent volume to *ca.* 30 cm³. The supernatant liquid was decanted off and the resulting white solid dried *in vacuo*. (19.1 g, 52%).

δ (¹³C): 137.1 (d) ¹J (CF) 235Hz *meta*, 141.1 (d) ¹J (CF) 258Hz *para*, 147.7 (d) ¹J (CF) 239Hz *ortho, ipso* C not seen.

δ (¹¹B): +59.1

δ (¹⁹F): -134.9 (2F, *ortho*), -153.6 (1F, *para*), -162.3 (2F, *meta*)

IR (KBr Disk/cm⁻¹): 1649, 1519, 1466, 1378, 1284, 1104, 980, 867, 803, 773, 738, 676, 615, 587.

M.Pt: 126-128°C.

Elemental Analysis: for C ₁₈ F ₁₅ B	Calc.	C, 42.2; H, 0.0%
---	-------	------------------

Found	C, 42.1; H, 0.0%
-------	------------------

6.4.2 Synthesis of R₂(R¹O)P=O derivatives.

Me₂(MeO)P=O

A solution of dimethylphosphinic acid chloride (500 mg, 4.4 mmol) in benzene (50 cm³) was added dropwise to a stirring solution of sodium methoxide (240 mg, 4.4 mmol) in methanol (50 cm³). The resulting solution was stirred until a white precipitate had formed. This mixture was then filtered and the solvents were removed *in vacuo*. The crude product was subsequently purified via bulb to bulb distillation. (0.28 g, 58%)

δ (¹H): 1.4 (d, 6H) ²J (HP) 14Hz, 3.6 (d, 3H) ³J (HP) 11Hz.

δ (¹³C): 14.8 (d) ¹J (CP) 94Hz, 50.4 (d) ²J (CP) 6.7Hz.

δ (³¹P): +53.2

IR (Thin Film): 2986, 2916, 1465, 1422, 1300, 1216, 1042, 938, 875, 769, 753, 683.

B.Pt: 77°C /12mm Hg

Me₂(EtO)P=O

Yield 61%.

δ (¹H): 1.0 (t, 3H) ³J (HH) 7Hz, 1.1 (d, 6H) ²J (HP) 14Hz, 3.7 (p, 2H) ³J (HH) 7Hz.

δ (¹³C): 15.2 (d) ¹J (CP) 94Hz, 16.2 (d) ³J (CP) 5.7Hz, 59.5 (d) ²J (CP) 5.7Hz

δ (³¹P): +50.7

IR (Thin Film): 2982, 2917, 1421, 1393, 1300, 1209, 1098, 1040, 959, 874, 754, 688

B.Pt: 88°C /15mm Hg

6.4.3 Synthesis of Lewis base adducts of tris(pentafluorophenyl)borane.

A typical synthesis is described below for EtOAc·B(C₆F₅)₃ and Et₃PO·B(C₆F₅)₃. All other adducts were produced in a similar manner.

EtOAc·B(C₆F₅)₃ (**4c**)

To a stirred solution of B(C₆F₅)₃ (200 mg, 0.39 mmol) in pentane (30 cm³) was added EtOAc (34 mg, 0.39 mmol). The product which precipitated as a white solid in an analytically pure form was isolated by filtration, washed with pentane at 0°C and subsequently dried *in vacuo*. (0.135 g, 58%).

δ (¹H): 1.37 (t, 3H) ³J (HH) 7.5Hz, 2.09 (s, 3H), 4.37 (q, 2H) ³J (HH) 7.5 Hz.

δ (¹³C): 13.4, 20.6, 66.6, 136.9 (d) ¹J (CF) 261 Hz *meta*, 140.5 (d) ¹J (CF) 252 Hz *para*, 147.7 (d) ¹J (CF) 246 Hz *ortho, ipso* C not seen, 180.9.

δ (¹¹B): -0.7.

δ (¹⁹F): -135.2 (2F, *ortho*), -155.9 (1F, *para*), -163.3 (2F, *meta*).

M.Pt: 98-100°C.

Elemental Analysis for C ₂₂ H ₈ BF ₁₅ O ₂	Calc.	C, 44.0; H, 1.3%
	Found	C, 43.9; H, 1.3%.

Et₃P=O·B(C₆F₅)₃ (**4b**)

To a stirred solution of B(C₆F₅)₃ (200 mg, 0.39 mmol) in pentane (30 cm³) was added TEPO (52.2 mg, 0.39 mmol). The product which precipitated as a white solid in an analytically pure form was isolated by filtration, washed with pentane at 0°C and subsequently dried *in vacuo*. (0.116 g, 46%).

δ (¹H): 1.1 (dt, 3H) ³J (HP) 17.5Hz, ³J (HH) 7.5 Hz, 1.94 (dq, 2H) ²J (HP) 12.5Hz, ³J (HH) 7.5Hz.

δ (^{13}C): 5.6 (d) ^2J (CP) 4.5Hz, 17.6 (d) ^1J (CP) 67.9Hz, 136.9 (d) ^1J (CF) 245Hz *meta*,
139.6 (d) ^1J (CF) 264Hz *para*, 147.7 (d) ^1J (CF) 235Hz *ortho, ipso* C not seen.

δ (^{11}B): -2.6.

δ (^{19}F): -134.7 (2F, *ortho*), -158.3 (1F, *para*), -164.6 (2F, *meta*).

IR (KBr disk): 3000, 1646, 1518, 1465, 1371, 1283, 1172, 1098, 980, 851, 774, 738,
678, 616.

M.Pt: 188-190°C.

Elemental analysis for $\text{C}_{24}\text{H}_{15}\text{BF}_{15}\text{OP}$	Calc.	C, 44.6; H, 2.3%
	Found	C, 44.7; H, 2.1%.

$\text{nPr}_3\text{P=O}^-\text{B}(\text{C}_6\text{F}_5)_3$ (**4d**)

Yield 54%.

δ (^1H): 1.0 (dt, 3H) ^3J (HH) 7.0Hz ^4J (HP) 1.5Hz, 1.5 (m, 2H), 1.83 (m, 2H).

δ (^{13}C): 14.9 (d) ^3J (CP) 4.0Hz, 15.5 (d) ^2J (CP) 17.0Hz, 27.1 (d) ^1J (CP) 65.0Hz, 137 (d)
 ^1J (CF) 252Hz *meta*, 140.0 (d) ^1J (CF) 255 Hz *para*, 147.7 (d) ^1J (CF) 238 Hz *ortho,*
ipso C not seen.

δ (^{11}B): -2.6

δ (^{19}F): -134.5 (2F, *ortho*), -158.4 (1F, *para*), -164.6 (2F, *meta*).

IR (KBr disk): 3000, 1519, 1461, 1373, 1284, 1132, 1102, 979, 861, 797, 767, 738, 679,
615, 579.

M.Pt: 140-141°C.

Elemental analysis for $\text{C}_{27}\text{H}_{21}\text{BF}_{15}\text{OP}$	Calc.	C, 47.1; H, 3.0%
	Found	C, 47.1; H, 2.8%.

(ⁿOct)₃P=O·B(C₆F₅)₃ (**4e**)

Yield 51%.

δ (¹H): 0.9 (t, 3H) ³J (HH) 6.4Hz, 1.25 (m, 12H), 1.85 (m, 2H).

δ (¹³C): 13.9, 21.05 (d) J (CP) 3.8Hz, 22.5, 25.3 (d) ¹J (CP) 65.8Hz, 28.7, 28.8, 30.6, 30.7 (d) ²J (CP) 15.7Hz, 31.6, 137.1 (d) ¹J (CF) 238Hz *meta*, 139.6 (d) ¹J (CF) 258Hz *para*, 147.8 (d) 240Hz *ortho, ipso* C not seen.

δ (¹¹B): -3.8

δ (¹⁹F): -134.5 (2F, *ortho*), -158.7 (1F, *para*), -164.6 (2F, *meta*).

IR (Thin Film): 2929, 1644, 1517, 1467, 1376, 1284, 1143, 1100, 981, 912, 742, 650.

Elemental analysis for C ₄₂ H ₅₁ BF ₁₅ OP	Calc.	C, 56.1; H, 5.7%
	Found	C, 56.1; H, 5.5%.

Ph₃P=O·B(C₆F₅)₃ (**4f**)

Yield 37%.

δ (¹H): 7.6 (m).

δ (¹³C): (major) 128.8 (d) J (CP) 2.8Hz, 129.0 (d) J (CP) 2.7Hz, 131.8 (d) J (CP) 10.5Hz, (minor) 132.6 (d) J (CP) 11.5Hz, 133.2 (d) J (CP) 2.9Hz, 133.9 J (CP) 2.9Hz, 136.7 (d) ¹J (CF) 237Hz *meta*, 139.2 (d) ¹J (CF) 254Hz *para*, 147.8 (d) ¹J (CF) 241Hz *ortho, ipso* C not seen in both cases.

δ (¹¹B): -0.4

δ (¹⁹F): (major) -134.9 (*ortho*), -158.7 (*para*), -164.9 (*meta*); (minor) -133.1 (*ortho*), -158.2 (*para*), -164.4 (*meta*).

IR (KBr disk): 3010, 1684, 1646, 1517, 1464, 1376, 1285, 1177, 1126, 1102, 978, 848, 793, 773, 750, 684, 616, 575, 532.

M.Pt: 278-280°C.

Elemental analysis for C ₃₆ H ₁₅ BF ₁₅ OP	Calc.	C, 54.7; H, 1.9%
	Found	C, 54.7; H, 1.8%.

(MeO)₃P=O·B(C₆F₅)₃ (4g)

Yield 48%.

δ (¹H): 3.68 (d) ³J (HP) 10.7Hz.

δ (¹³C): 56.0 (d) ²J (CP) 132Hz, 136.9 (d) ¹J (CF) 254Hz *meta*, 139.8 (d) ¹J (CF) 245Hz *para*, 147.8 (d) ¹J (CF) 241Hz *ortho, ipso* C not seen.

δ (¹¹B): -1.7.

δ (¹⁹F): -135.1 (2F, *ortho*), -157.8 (1F, *para*), -164.6 (2F, *meta*).

IR (KBr disk): 2995, 1648, 1510, 1470, 1378, 1284, 1226, 1104, 1075, 984, 865, 775, 738, 678, 618, 576, 512

M.Pt: 210-212°C.

Elemental analysis for C ₂₁ H ₉ BF ₁₅ O ₄ P	Calc.	C, 38.7; H, 1.4%
	Found	C, 38.7; H, 1.4%.

(EtO)₃P=O·B(C₆F₅)₃ (4h)

Yield 47%.

δ (¹H): 1.3 (t, 3H) ³J (HH) 7.3Hz, 3.9 (quint, 2H) ³J (HH) 7.3Hz ³J (HP) 7.3Hz.

δ (¹³C): 15.8 (d) ³J (CP) 6.7Hz, 63.7 (d) ²J (CP) 5.7Hz, 136.5 (d) ¹J (CF) 240Hz *meta*, 139.3 (d) ¹J (CF) 269Hz *para*, 148.1 (d) ¹J (CF) 231Hz *ortho, ipso* C not seen.

δ (¹¹B): -3.7.

δ (¹⁹F): -135.6 (2F, *ortho*), -157.7 (1F, *para*), -164.9 (2F, *meta*).

IR (KBr disk): 2995, 1647, 1521, 1472, 1378, 1287, 1208, 1106, 1049, 981, 774, 739, 677, 617.

M.Pt: 150-151°C.

Elemental analysis for C ₂₄ H ₁₅ BF ₁₅ O ₄ P	Calc.	C, 41.5; H, 2.2%
	Found	C, 41.3; H, 2.1%.

(PhO)₃P=O·B(C₆F₅)₃ (4i)

Yield 35%.

δ (¹H): 7.3 (m).

δ (¹³C): 119.8 (d) ³J (CP) 4.7Hz *ortho*, 126.1 *para*, 129.9 *meta*, 136.7 (d) ¹J (CF) 244Hz *meta*, 141.4 (d) ¹J (CF) 251Hz *para*, 147.9 (d) ¹J (CF) 255Hz *ortho, ipso* C's not seen.

δ (¹¹B): -1.2.

δ(¹⁹F): -135.4 (2F, *ortho*), -157.1 (1F, *para*), -164.1 (2F, *meta*).

IR (KBr disk): 3050, 1646, 1590, 1464, 1376, 1287, 1255, 1158, 1106, 1040, 982, 911, 764, 736, 686, 675, 616.

M.Pt: 185-186°C.

Elemental analysis for C ₃₆ H ₁₅ BF ₁₅ O ₄ P	Calc.	C, 51.6; H, 1.8%
	Found	C, 51.3; H, 1.5%.

(EtO)₂(H)P=O·B(C₆F₅)₃ (4j)

Yield 48%.

δ (¹H): 1.3 (s, 6H), 4.1 (s, 4H), 6.5 (d, 1H) ¹J (HP) 700Hz.

δ (¹³C): 15.8 (d) ³J (CP) 6.7Hz, 63.6 (d) ²J (CP) 6.8Hz, 137.0 (d) ¹J (CF) 253Hz *meta*, 140.6 (d) ¹J (CF) 264Hz *para*, 147.9 (d) ¹J (CF) 247Hz *ortho, ipso* C not seen.

$\delta(^{11}\text{B})$: -2.1

$\delta(^{19}\text{F})$: -135.5 (2F, *ortho*), -157.5 (1F, *para*), -164.3 (2F, *meta*).

IR (KBr disk): 2997, 1647, 1521, 1472, 1380, 1288, 1180, 1107, 1043, 970, 772, 682,

551

M.Pt: 120-122°C.

Elemental analysis for $\text{C}_{22}\text{H}_{11}\text{BF}_{15}\text{O}_3\text{P}$

Calc. C, 40.7; H, 1.7%

Found C, 40.5; H, 1.7%.

$(^n\text{BuO})_2(\text{H})\text{P}=\text{O}^\cdot\text{B}(\text{C}_6\text{F}_5)_3$ (**4k**)

Yield 37%

$\delta(^1\text{H})$: 0.9 (q, 6H) ^3J (HH) 6.7Hz, 1.3 (m, 4H) ^3J (HH) 7.6Hz, 1.6 (m, 4H) ^3J (HH) 7.3Hz, 4.1 (m, 4H), 6.9 (d, 1H) ^1J (HP) 750Hz.

$\delta(^{13}\text{C})$: 15.3, 15.4, 15.5, 15.6, 64.8, 64.9, 67.5, 67.6, 137.0 (d) $^1\text{J}(\text{CF})$ 245Hz *meta*, 140 (d) $^1\text{J}(\text{CF})$ 245Hz *para*, 147.8 (d) $^1\text{J}(\text{CF})$ 239Hz *ortho*, *ipso* C not seen

$\delta(^{11}\text{B})$: -2.2.

$\delta(^{19}\text{F})$: -135.4 (2F, *ortho*), -157.3 (1F, *para*), -164.3 (2F, *meta*).

IR (Thin Film): 3000, 1692, 1646, 1598, 1518, 1469, 1379, 1289, 1237, 1188, 1104, 976, 907, 734, 650.

M.Pt: 44-46°C

Elemental analysis for $\text{C}_{24}\text{H}_{15}\text{BF}_{15}\text{O}_3\text{P}$

Calc. C, 44.2; H, 2.7%

Found C, 43.9; H, 2.7%.

(PhO)₂(H)P=O·B(C₆F₅)₃ (4I)

Yield 55%.

δ (¹H): 7.1 (2H) ³J (HH) 7.35Hz *ortho*, 7.3 (1H) ³J (HH) 7.35Hz *para*, 7.4 ³J (HH) 7.95Hz *meta*.

δ (¹³C): 120.1 ³J (CP) 4.77Hz *ortho*, 126.4 *para*, 130.2 *meta*, 137.1 ¹J (CF) 254Hz *meta*, 139.9 ¹J (CF) 249Hz *para*, 147.8 ¹J (CF) 238Hz *ortho*, *ipso* C not seen in both cases.

δ (¹¹B): -0.25.

δ (¹⁹F): -135.5 (2F, *ortho*), -156.7 (1F, *para*), -163.7 (2F, *meta*).

IR (KBr disk): 3000, 1649, 1596, 1519, 1472, 1373, 1290, 1249, 1190, 1102, 1025, 961, 861, 761, 685, 611, 579.

M.Pt: 130-132°C.

Elemental analysis for C ₃₀ H ₁₁ BF ₁₅ O ₃ P	Calc.	C, 48.2; H, 1.5%
	Found.	C, 47.9; H, 1.4%.

Me(MeO)₂P=OB(C₆F₅)₃ (4m)

Yield 42%.

$\delta(^1\text{H})$: 1.3 d ^2J (PH) 17.7Hz, 3.6 d ^3J (PH) 11.6Hz.

$\delta(^{13}\text{C})$: 8.7 d ^1J (CP) 146 Hz; 52.9 d ^2J (CP) 6.7 Hz; 136.9

$\delta(^{11}\text{B})$: -1.2.

$\delta(^{19}\text{F})$: -135.5 (2F, *o*), -157.2 (1F, *p*), -164.1 (2F, *m*).

IR (KBr disk): 2997, 1642, 1554, 1519, 1472, 1373, 1313, 1278, 1190, 1103, 982, 855,

797, 774, 738, 678, 618

M.Pt: 226-228°C.

Elemental analysis for C ₂₁ H ₉ BF ₁₅ O ₃ P	Calc.	C, 39.7; H, 1.4%
---	-------	------------------

Found	C, 39.4; H, 1.4%.
-------	-------------------

Me(EtO)₂P=OB(C₆F₅)₃ (4n)

Yield 47%.

$\delta(^1\text{H})$: 1.2 (t, 6H) ^3J (HH) 7.0Hz, 1.6 (d, 3H) ^2J (HP) 18Hz, 4.1 (m, 4H)

$\delta(^{13}\text{C})$: 9.8 (d) ^1J (PC) 162Hz, 15.6 (d) ^3J (CP) 7.6Hz, 15.9 (d) ^3J (CP) 6.7Hz, 63.0 (d)

^2J (CP) 4.8Hz, 65.8 (d) ^2J (CP) 8.6Hz, 137.0 (d) ^1J (CF) 252Hz *meta*, 139.8 (d) ^1J (CF)

261Hz *para*, 147.7 (d) ^1J (CF) 231Hz *ortho, ipso* C not seen.

$\delta(^{11}\text{B})$: -8.2.

IR (KBr disk): 3002, 1647, 1518, 1462, 1397, 1376, 1321, 1285, 1190, 1107, 1031, 968,

905, 851, 824, 792, 774, 740, 674

M.Pt: 145-147°C.

Elemental analysis for C ₂₃ H ₁₃ BF ₁₅ O ₃ P	Calc.	C, 41.6; H, 1.9%
--	-------	------------------

Found	C, 41.6; H, 1.7%.
-------	-------------------

(EtO)₂PhP=O·B(C₆F₅)₃ (4o)

Yield 49%.

δ (¹H): 1.2 (t, 6H) ³J (HH) 6.5Hz, 3.91 (t, 4H) ³J (HH) 7.3Hz, 7.44 (m, 5H).

δ (¹³C): 15.9, 63.5, 128.9 (d) ²J (CP) 12.5Hz *ortho*, 131.2 (d) ³J (CP) 10.1Hz *meta*, 133.6 (d) ⁴J (CP) 4.8Hz *para*, 137.0 (d) ¹J (CF) 252Hz *meta*, 139.9 (d) ¹J (CF) 258Hz *para*, 147.4 (d) ¹J (CF) 273Hz *ortho*.

δ (¹¹B): -1.56.

δ (³¹P): +16.55.

IR (KBr disk): 3001, 2995, 1734, 1684, 1654, 1560, 1522, 1456, 1291, 1174, 1096, 1027, 976, 804, 749, 694, 560, 534

M.Pt: 170-172°C.

Elemental analysis for C ₂₈ H ₁₅ BF ₁₅ O ₃ P	Calc.	C, 46.3; H, 2.1%
	Found	C, 46.3; H, 1.8%.

Me₂(MeO)P=O·B(C₆F₅)₃ (4p)

Yield 36%

δ (¹¹B): -1.6.

IR (KBr disk): 2978, 1717, 1648, 1519, 1466, 1417, 1396, 1375, 1320, 1310, 1283, 1177, 1102, 1057, 980, 895, 848, 795, 773, 739, 678, 617, 576

M.Pt: 243-245°C

Elemental analysis for C ₂₁ H ₉ BF ₁₅ O ₂ P	Calc.	C, 40.6; H, 1.5%
	Found	C, 40.3; H, 1.4%.

Me₂(EtO)P=O·B(C₆F₅)₃ (4q)

Yield 42%.

δ (¹H): 1.27(q, 3H) ³J (HH) 7.0Hz, 1.7 (d, 6H) ²J (PH) 14Hz, 4.1 (m, 4H)

δ (¹³C): 13.4 (d) ¹J (CP) 99Hz, 15.6 (d) ³J (PC) 7.6Hz, 64.4 (d) ²J (CP) 7.6Hz, 137.1 (d)

¹J (CF) 254Hz *para*, 139.7 (d) ¹J (CF) 251Hz *meta*, 147.8 (d) ¹J (CF) 236Hz *ortho, ipso*

C not seen

δ (¹¹B): -9.3

IR (KBr disk): 3002, 1648, 1559, 1540, 1458, 1399, 1375, 1319, 1284, 1187, 1102, 1042, 971, 890, 853, 797, 772, 743, 681, 616, 576, 538, 480

M.Pt: 168-170°C

Elemental analysis for C ₂₂ H ₁₁ BF ₁₅ O ₂ P	Calc.	C, 41.6; H, 1.7%
	Found	C, 41.6; H, 1.8 %.

6.5 Experimental for Chapter 5

6.5.1 Synthesis of Aryltrimethylsilanes

The general strategy used to synthesise the aryltrimethylsilanes was from a method developed by Clark and co-workers [191]. The preparation of PhSiMe₃ is discussed in detail; all other derivatives were made in a similar manner.

PhSiMe₃

Phenyl bromide (15.70 g, 0.1 mol) was added to dry THF (80 cm³) containing dried magnesium turnings (2.43 g, 0.1 mol) and one iodine crystal. After refluxing for 24h, the mixture was cooled to room temperature before trimethylchlorosilane (10.90 g, 0.1 mol) was added. The mixture was then heated to reflux for another 24h. After this time, the solvent was removed under vacuum and the residue heated for approximately 1h at *ca.* 90°C. The resulting solid was then broken up in diethyl ether (50 cm³) and transferred into a flask containing cold water (40 g), ice (40 g) and conc. HCl (1 cm³). The organic layer was separated and washed first with distilled water and then distilled water containing sodium bicarbonate. The organic phase was dried over anhydrous sodium sulphate overnight and filtered before the diethyl ether was removed *via* a rotary evaporator. This left a pale yellow liquid which was subsequently distilled to give a colourless liquid (10.30 g, 69 %).

δ (¹H): 0.5 (s, 9H); 7.4 - 7.6 (m, 5H)

IR (Thin film): 3068m, 2955s, 1949w, 1877w, 1815w, 1590w, 1425s, 1310m, 1249s, 1113s, 837s, 726s, 697s

B.Pt: 168°C

2-MeC₆H₄SiMe₃

Yield 65%

δ (¹H): 0.7 (s, 9H); 2.8 (s, 3H); 7.45 – 7.85 (m, 4H)

IR (Thin film): 3054m, 2954s, 1802w, 1684w, 1588m, 1445s, 1284w, 1248s, 1128s, 1079s, 842s, 740s, 689s

B.Pt: 185°C

3-MeC₆H₄SiMe₃

Yield 70%

δ (¹H): 0.6 (s, 9H); 2.7 (s, 3H); 7.4 – 7.7 (m, 4H)

IR (Thin film): 3017m, 2955s, 1868w, 1593w, 1575w, 1452m, 1402m, 1311w, 1248s, 1118s, 1054m, 874s, 837s, 778m, 751s, 690s

B.Pt: 186°C

4-MeC₆H₄SiMe₃

Yield 60%

δ (¹H): 0.45 (s, 9H); 2.5 (s, 3H); 7.35(d, 2H); 7.6(d, 2H)

IR (Thin film): 3010w, 2955s, 1904w, 1804w, 1742w, 1604s, 1502w, 1446m, 1392m, 1312w, 1248s, 1191w, 1107s, 839s, 799s, 754s, 691m

B.Pt: 190°C

3,5-Me₂C₆H₃SiMe₃

Yield 72%

δ (¹H): 0.7(s, 9H); 2.75(s, 6H); 7.4(s, 1H); 7.6(s, 2H)

IR (Thin film): 3014s, 2955s, 1935w, 1852w, 1597m, 1448m, 1401m, 1141s, 878s, 835s, 754s, 689s

B.Pt: 212°C

4-EtC₆H₄SiMe₃

Yield 85%

δ (¹H): 0.5(s, 9H); 1.45(t, 3H); 2.8(q, 2H); 7.35(d, 2H); 7.65(d, 2H)

IR(Thin film): 3010w, 2960s, 1907m, 1660w, 1602s, 1502m, 1458m, 1397s, 1248s, 1191w, 1109s, 1059m, 966w, 841s, 754s, 720m, 692m, 641s

B.Pt: 205°C

MesSiMe₃

Yield 65%

δ (¹H): 0.4(s, 9H); 2.5(m, 9H); 7.0(s, 2H)

IR (Thin film): 2960s, 2740m, 1610m, 1444s, 1248s, 1070s, 962m, 841s, 739s, 687m

B.Pt: 231°C

6.5.2 Synthesis of Arylborondibromides from ArSiMe₃

These were all prepared from the aryltrimethylsilanes described above, following a procedure of Haubold and co-workers [192]. All compounds were prepared using the same conditions, as typified by the experimental of 4-MeC₆H₄BBr₂ unless otherwise stated. Crude products were distilled by bulb-to-bulb distillation.

4-MeC₆H₄BBr₂

Boron tribromide (6.30 g, 25.1 mmols) was placed into a 100 cm³ two-necked round-bottomed flask and cooled to 0°C. 4-MeC₆H₄SiMe₃ (4.12 g, 25.1 mmols) was added dropwise and the mixture was then stirred at room temperature for 1h and at 60°C for a further 2h. The mixture was later distilled to give a colourless liquid (5.39 g, 82%)

δ (¹H): 2.4 (s, 3H); 7.3 (m, 2H); 8.1 (m, 2H)

B.Pt: 135°C / 2mmHg

C₆H₅BBr₂

Yield 69%

δ (¹H): 7.0–8.2 (m)

M.Pt: 45°C

2-MeC₆H₄BBr₂

Yield 38%

δ (¹H): 2.6 (s, 3H); 7.2–7.6 (m, 4H); 7.8 (d, 4H)

B.Pt: 65°C / 0.15mmHg

3-MeC₆H₄BBBr₂

Yield 68%

δ (¹H): 2.5 (s, 3H); 7.4-7.6 (m, 2H); 8.2 (d, 2H)

B.Pt: 90°C / 0.30mmHg

4-EtC₆H₄BBBr₂

Yield 77%

δ (¹H): 1.2 (t, 3H); 2.7 (q, 2H); 7.2 (d, 2H); 8.1 (d, 2H)

B.Pt: 140°C / 0.5mmHg

3,5-Me₂C₆H₃BBBr₂

Yield 65%

δ (¹H): 2.3 (s, 6H); 7.2 (m, 1H); 7.9 (m, 2H)

M.Pt: 60°C

6.5.3 Synthesis of piperidino phosphorous dichloride

To a three necked 1L round bottomed flask equipped with a mechanical stirrer and a pressure equalising dropping funnel was added a mixture of diethyl ether (250 cm³) and phosphorus trichloride (68.6 g, 0.5 mol) . This was subsequently cooled to 0°C before piperidine (42.5 g, 0.5 mol) was added dropwise. The resulting mixture was stirred for 24hr, before the mixture was filtered. The diethyl ether solution remaining was distilled to generate the product (62.8 g, 69%)

δ (¹³C): 24.1, 26.2, 47.4 (d) ²J (CP) 18Hz

δ (³¹P): +156.4ppm

6.5.4 Attempted synthesis of tris(trimethylsilyl)phosphine

To a stirring and refluxing suspension of magnesium turnings (12.2 g, 0.5 mol) in THF (250 cm³) was added trimethylsilylchloride (54.3 g, 0.5 mol) with bromine (1 cm³). The resulting mixture was left refluxing for 5h before phosphorus trichloride (22.6 g, 0.165 mol) was added drop wise. This mixture was left refluxing for 160h. After this time the reaction was cooled, ³¹P NMR of the crude mixture showed there to be no tris(trimethylsilyl)phosphine present hence no work up was carried out.

6.5.5 Synthesis of tris-trimethylsilylphosphine

To a refluxing mixture of trimethylsilyl chloride (43.46 g, 0.4 mol) and lithium powder (4.86 g, 0.7 mol) in THF (250 cm³) was added drop wise a solution of piperidino phosphorusdichloride (18.59 g, 0.1 mol) in THF (50 cm³). The resulting mixture was left to stir overnight at room temperature. The solvent was removed *in vacuu* and the residue washed with pentane (300 cm³). The resulting mixture is then filtered and the precipitate washed with pentane (3 x 50 cm³). The filtrate is concentrated and then distilled under vacuum (14.7 g, 59%).

δ (¹H): 0.3ppm

δ (³¹P): -252ppm

B.Pt: 55°C / 0.5mmHg

6.5.6 Attempted synthesis of the diphosphadiboretanes

To LiP(SiMe₃)₂ (1.0 g, 5.4 mmol) in pentane (50 cm³) was added PhBBr₂ (1.3 g, 5.4 mmol) dropwise. The resulting solution was stirred for 24hr, before the solvent was removed *in vacuo* leaving a yellow waxy solid.

6.5.7 Adducts of ArBBr₂ with phenylphosphine

The method for the preparation of PhPH₂PhBBr₂ is described below in detail, all other adducts were prepared in a similar manner.

PhPH₂PhBBr₂

PhBBr₂ (0.59 g, 2.4 mmol) in hexane (30 cm³) was added to PhPH₂ (0.26 g, 2.4 mmol). The resulting solution was stirred for 1hr at 0°C, before the solvent was removed. A white air sensitive solid was produced (0.38 g, 45%).

References

1. M. W. Chen, J. C. Calabrese, D. F. Gaines and D. F. Hillenbrand, *J. Am. Chem. Soc.*, 1980, **102**, 4928
2. D. F. Gaines and S. J. Hildebrandt, *Inorg. Chem.*, 1978, **17**, 794
3. N. N. Greenwood, *Comprehensive Inorganic Chemistry*, (Pergamon Press, London 1973), Vol. 2, 665
4. N. N. Greenwood and A. Earnshaw, *Chemistry of the Elements*, (Pergamon Press, London, 1984), Ch 6, 155
5. F. A. Cotton and G. Wilkinson, *Advanced Inorganic Chemistry*, (Wiley Interscience, 1988), Ch 6, 162
6. J. D. Lee, *Concise Inorganic Chemistry*, (Chapman and Hall, 1991), Ch 12, 329
7. A. Stock, *Z. Angew. Chem.*, 1926, **39**, 461
8. N. N. Greenwood, J. D. Kennedy and J. Staves, *J. Chem. Soc. Dalton Trans.*, 1978, 1146
9. J. Bould, N. N. Greenwood, J. D. Kennedy and W. S. McDonald, *J. Chem. Soc. Dalton Trans.*, 1985, 1843
10. L. J. Guggenberger, A. R. Kane and E. L. Muetterties, *J. Am. Chem. Soc.*, 1972, **94**, 5665
11. J. Bould, N. N. Greenwood and J. D. Kennedy, *J. Chem. Soc. Dalton Trans.*, 1984, 2477
12. F. Klanberg, E. L. Muetterties and L. J. Guggenberger, *Inorg. Chem.*, 1968, **7**, 2272
13. F. Klanberg and E. L. Muetterties, *J. Am. Chem. Soc.*, 1968, **90**, 3296
14. N. W. Alcock, I. D. Burns, K. S. Claire and A. F. Hill, *Inorg. Chem.*, 1992, **31**, 2906
15. S. J. Lippard and D. A. Ucko, *Inorg. Chem.*, 1968, **7**, 1051

16. C. H. Bushweller, H. Beall and W. J. Dewkett, *Inorg. Chem.*, 1976, **15**, 1739
17. G. A. Razuvaev, A. N. Artemov, A. A. Aladjin and N. I. Sirotkin, *J. Organomet. Chem.*, 1976, **111**, 131
18. W. Siebert, *Adv. Organomet. Chem.*, 1980, **18**, 301
19. R. Prinz and H. Werner, *Angew. Chem. Int. Ed. Engl.*, 1967, **6**, 91
20. J. L. Adcock and J. J. Lagowski, *Inorg. Chem.*, 1973, **12**, 2533
21. M. Scotti and H. Werner, *Helv. Chim. Acta*, 1974, **57**, 1234
22. K. Deckelmann and H. Werner, *Helv. Chim. Acta*, 1971, **54**, 2189
23. J. J. Lagowski, *Coord. Chem. Revs.*, 1977, **22**, 185
24. H. Noth and U. Schuchardt, *J. Organomet. Chem.*, 1977, **134**, 297
25. B. Kaufmann, H. Noth, R. T. Paine, K. Polborn and M. Thomann, *Angew. Chem. Int. Ed. Engl.*, 1993, **32**, 1446
26. G. Linti, H. Noth, R. T. Paine and K. Polborn, *Angew. Chem. Int. Ed. Engl.*, 1990, **29**, 682
27. B. Kaufmann, N. Metzler, H. Noth and R. T. Paine, *Chem. Ber.*, 1994, **127**, 825
28. H. Noth and B. Wrackmeyer, *NMR – Basic Principles and Progress*, (Springer, 1978)
29. R. K. Harris, *Nuclear Magnetic Resonance Spectroscopy*, (Longman Scientific and Technical, 1992), 238
30. D. Baudry, M. Ephritikhine and H. Felkin, *J. Organomet. Chem.*, 1982, **224**, 363
31. M. R. Detty and W. D. Jones, *J. Am. Chem. Soc.*, 1987, **109**, 5666
32. J. K. Hoyano and W. A. G. Graham, *Organometallics*, 1982, **1**, 783
33. W. A. Kiel, W. E. Buhro and J. A. Gladysz, *Organometallics*, 1984, **3**, 879
34. J. I. Seeman and S. G. Davies, *J. Am. Chem. Soc.*, 1985, **107**, 6522
35. W. Beck and K. Sunkel, *Chem. Rev.*, 1988, **88**, 1405

36. E. Fritsch, J. Heidrich, K. Polborn and W. Beck, *J. Organomet. Chem.*, 1992, **441**, 203
37. P. M. Fritz, J. Breimair, B. Wagner and W. Beck, *J. Organomet. Chem.*, 1992, **426**, 343
38. P. Steil, U. Nagel and W. Beck, *J. Organomet. Chem.*, 1988, **339**, 111
39. P. Steil, U. Nagel and W. Beck, *J. Organomet. Chem.*, 1989, **366**, 313
40. M. L. H. Green and D. J. Jones, *Inorg. Chem. Radiochem.*, 1965, **7**, 115
41. M. L. Ziegler, H. Haas and R. K. Sheline, *Chem. Ber.*, 1965, **98**, 2454
42. J. P. Fawcett, A. J. Poe and M. V. Twigg, *J. Organomet. Chem.*, 1973, **61**, 315
43. L. Y. Y. Chan and F. W. B. Einstein, *J. Chem. Soc. Dalton Trans.*, 1973, 111
44. E. O. Brimm, M. A. Lynch and W. J. Sesny, *J. Am. Chem. Soc.*, 1954, **76**, 3831
45. E. W. Abel and I. S. Butler, *J. Chem. Soc.*, 1964, 434
46. R. J. Angelici, *J. Organomet. Chem.*, 1964, **3**, 1099
47. J. A. Connor and G. A. Hudson, *J. Organomet. Chem.*, 1974, **73**, 351
48. E. Linder and H. Dreher, *J. Organomet. Chem.*, 1976, **104**, 331
49. E. Linder and B. Schilling, *Chem. Ber.*, 1977, **110**, 3725
50. W. Hieber, R. Schuh and H. Fuchs, *Z. Anorg. Allg. Chem.*, 1941, **248**, 243
51. E. W. Abel and S. P. Tyfield, *Adv. Organomet. Chem.*, 1970, **8**, 117
52. G. Wilkinson, *Comprehensive organometallic chemistry*, (Elsevier Science, 1989)

Vol 1

53. D. T. Hurd, G. W. Sentell and F. J. Norton, *J. Am. Chem. Soc.*, 1949, **71**, 1899
54. H. E. Podall, J. H. Dunn and H. Shapiro, *J. Am. Chem. Soc.*, 1960, **82**, 1325
55. A. Davison, J. A. McCleverty and G. Wilkinson, *J. Chem. Soc.*, 1963, 1133
56. R. G. Behrens, *J. Organomet. Chem.*, 1976, **121**, C63
57. J. K. Burdett, *J. Chem. Soc. Faraday Trans. 2*, 1974, 1599

58. H. Haas and R. K. Sheline, *J. Chem. Phys.*, 1967, **47**, 2996
59. N. Flitcroft, D. K. Huggins and H. D. Kaesz, *Inorg. Chem.*, 1964, **3**, 1123
60. F. A. Cotton and R. M. Wing, *Inorg. Chem.*, 1964, **4**, 1328
61. G. Bor, *Chem. Comm.*, 1969, 641
62. G. Bor and G. Sbrignadello, *J. Chem. Soc. Dalton Trans.*, 1974, 440
63. D. M. Adams, M. A. Hooper and A. Squire, *J. Chem. Soc. (A)*, 1971, 71
64. G. Sbrignadello, G. Battiston and G. Bor, *Inorg. Chim. Acta*, 1975, **14**, 69
65. W. T. Wozniak, G. O. Evans and R. K. Sheline, *J. Inorg. Nucl. Chem.*, 1975, **37**, 105
66. W. Hieber and H. Schulten, *Z. Anorg. Allg. Chem.*, 1939, **243**, 164
67. E. W. Abel and G. Wilkinson, *J. Chem. Soc.*, 1959, 1501
68. D. R. Tyler and D. P. Petrylak, *Inorg. Chim. Acta*, 1981, **53**, L185
69. D. M. Allen, A. Cox, T. J. Kemp, Q. Sultana and R. B. Pitts, *J. Chem. Soc. Dalton Trans.*, 1976, 1189
70. H. D. Kaesz, R. Bau, D. Hendrickson and J. M. Smith, *J. Am. Chem. Soc.*, 1967, **89**, 2844
71. G. Keeling, S. F. A. Kettle and I. Paul, *J. Chem. Soc. Dalton Trans.*, 1971, 3143
72. F. Zingales, M. Graziani, F. Faraone and U. Belluco, *Inorg. Chim. Acta*, 1967, **1**, 172
73. D. A. Brown and R. T. Sane, *J. Chem. Soc. (A)*, 1971, 2088
74. M. J. Blandamer, J. Burgess, S. J. Cartwright and M. Dupree, *J. Chem. Soc. Dalton Trans.*, 1976, 1158
75. J. Burgess and A. J. Duffield, *J. Organomet. Chem.*, 1979, **177**, 435
76. S. P. Schmit, W. C. Trogler and F. Basolo, *Inorg. Synth.*, **28**, 160
77. S. P. Schmidt, W. C. Trogler and F. Basolo, *J. Am. Chem. Soc.*, 1984, **106**, 1308

78. J. D. Atwood and T. L. Brown, *J. Am. Chem. Soc.*, 1975, **97**, 3380
79. K. Moedritzer, *Synth. React. Inorg. Metal-Org. Chem.*, 1972, **2**, 121
80. F. Zingales and U. Sartorelli, *Inorg. Chem.*, 1967, **6**, 1243
81. J. P. Fawcett and A. Poe, *J. Chem. Soc. Dalton Trans.*, 1977, 1032
82. A. E. Leins and N. J. Coville, *J. Organomet. Chem.*, 1991, **407**, 359
83. C. A. Tolman, *Chem. Rev.*, 1977, **77**, 325
84. N. J. Coville, *Organometallic Radical Processes*, (Elsevier, Amsterdam 1990), 108
85. B. L. Booth and R. N. Hazeldine, *J. Chem. Soc. A*, 1966, 157
86. T. Kruck and A. Engelmann, *Angew. Chem. Int. Ed. Engl.*, 1966, **5**, 836
87. R. H. Reimann and E. Singleton, *J. Organomet. Chem.*, 1972, **38**, 113
88. P. M. Treichel and J. J. Benedict, *J. Organomet. Chem.*, 1969, **17**, P37
89. R. H. Reimann and E. Singleton, *J. Chem. Soc. Dalton Trans.*, 1973, 841
90. P. M. Treichel, *Comprehensive Organometallic Chemistry*, (Pergamon Press, 1981) Ch 29
91. P. M. Treichel, *Comprehensive Organometallic Chemistry II*, (Elsevier Science, 1995) Vol 6, Ch 1-10
92. A. Wojciciki, *J. Organomet. Chem.*, 1972, **45**, 335
93. P. M. Treichel, *J. Organomet. Chem.*, 1973, **58**, 273
94. P. M. Treichel, *J. Organomet. Chem.*, 1980, **189**, 129
95. F. Zingales, U. Sartorelli and A. Trovati, *Inorg. Chem.*, 1967, **6**, 1246
96. B. E. Mann, C. Masters and B. L. Shaw, *J. Chem. Soc. A*, 1971, 1104
97. L. S. Merriwether and J. R. Leto, *J. Am. Chem. Soc.*, 1961, **83**, 3182
98. J. A. Connor, J. J. Day, E. M. Jones and G. K. McEwen, *J. Chem. Soc. Dalton Trans.*, 1973, 347
99. J. A. Connor, G. K. McEwen and C. J. Rix, *J. Chem. Soc. Dalton Trans.*, 1974, 589

100. S. O. Grim, R. Barth, W. Briggs, C. A. Tolman and J. P. Jesson, *Inorg. Chem.*, 1974, **13**, 1095
101. D. A. Edwards and J. Marshalsea, *J. Organomet. Chem.*, 1975, **96**, C50
102. S. Heitkamp, D. J. Stuffken and K. Vrieze, *J. Organomet. Chem.*, 1979, **169**, 107
103. G. Q. Li, J. Feldman, J. A. Krause and M. Orchin, *Polyhedron*, 1997, **16**, 2041
104. S. J. A. Pope and G. Reid, *J. Chem. Soc. Dalton Trans.*, 1999, 1615
105. P. H. Bird, N. J. Coville, I. S. Butler and M. L. Schneider, *Inorg. Chem.*, 1973, **12**, 2902
106. S. K. Mandal, D. M. Ho and M. Orchin, *Polyhedron*, 1992, **11**, 2055
107. D. Bright and O. S. Mills, *J. Chem. Soc. Dalton Trans.*, 1974, 219
108. G. J. Kruger, R. O. Heckrodt, R. H. Reimann and E. Singleton, *J. Organomet. Chem.*, 1975, **87**, 323
109. V. Sum, M. T. Patel, T. P. Kee and M. Thornton-Pett, *Polyhedron*, 1992, **11**, 1743
110. N. J. Holmes, W. Levason and M. Webster, *J. Organomet. Chem.*, 1998, **568**, 213
111. S. K. Mandal, D. M. Ho and M. Orchin, *J. Organomet. Chem.*, 1992, **439**, 53
112. G. Baccolini, L. Busetto, A. Roncaroio, V. G. Albano and F. Demartin, *J. Chem. Soc. Dalton Trans.*, 1987, 21
113. A. E. Stock, *Hydrides of Boron and Silicon*, Cornell University Press, Ithica, New York, 1933
114. W. V. Hough, L. J. Edwards and A. D. McElroy, *J. Am. Chem. Soc.*, 1956, **78**, 689

115. W. V. Hough, L. J. Edwards and A. D. McElroy, *J. Am. Chem. Soc.*, 1958, **80**, 1828
116. D. F. Gaines, R. F. Schaefer and F. Tebbe, *Inorg. Chem.*, 1963, **2**, 526
117. R. M. Adams, *Boron, Metallo-boron Compounds and Boranes*, Interscience, New York, 1964
118. W. J. Dewkett, M. Grace and H. Beall, *Inorg. Synth.*, 1974, **15**, 111
119. W. J. Dewkett, M. Grace and H. Beall, *J. Inorg. Nucl. Chem.*, 1971, **33**, 1279
120. H. Beall, C. H. Bushweller and M. C. Grace, *Inorg. Nucl. Chem. Lett.*, 1971, **7**, 641
121. M. A. Beckett and P. W. Jones, *Synth. React. Inorg. Met.-Org. Chem.*, 1997, **27**, 41
122. S. J. Lippard and K. M. Melmed, *Inorg. Chem.*, 1969, **8**, 2755
123. L. J. Guggenberger, *Inorg. Chem.*, 1970, **9**, 367
124. M. L. H. Green, P. Mountford, P. D. Grebenik, J. B. Leach and J. M. Pounds, *J. Organomet. Chem.*, 1990, **382**, C1
125. P. D. Grebenik, J. B. Leach, M. L. H. Green and N. M. Walker, *J. Organomet. Chem.*, 1988, **345**, C31
126. M. Bown, S. L. Ingham, G. E. Norris and J. M. Waters, *Acta Cryst.*, 1995, **C51**, 1503
127. I. D. Burns, A. F. Hill and D. J. Williams, *Inorg. Chem.*, 1996, **35**, 2685
128. J. Bould, N. P. Rath and L. Barton, *Acta Cryst.*, 1996, **C52**, 1388
129. R. D. Chambers and T. Chivers, *Proc. Chem. Soc.*, 1963, 208
130. A. G. Massey and A. J. Park, *J. Organomet. Chem.*, 1964, **2**, 245
131. X. Yang, C. L. Stern and T. J. Marks, *J. Am. Chem. Soc.*, 1991, **113**, 3623

132. A. R. Siedle, R. A. Newmark and W. M. Lamanna, *Organometallics*, 1993, **12**, 1491
133. K. Ishihara, N. Hanaki, M. Funahashi, M. Miyata and H. Yamamoto, *Bull. Chem. Soc. Japan*, 1995, **68**, 1721
134. X. Yang, C. L. Stern and T. J. Marks, *J. Am. Chem. Soc.*, 1994, **116**, 10015
135. P. A. Deck and T. J. Marks, *J. Am. Chem. Soc.*, 1995, **117**, 6128
136. M. Bochmann, S. J. Lancaster, M. B. Hursthouse and K. M. A. Malik, *Organometallics*, 1994, **13**, 2235
137. M. A. Beckett, G. C. Strickland, J. R. Holland and K. S. Varma, *Polymer*, 1996, **37**, 4629
138. V. Gutmann, *Coord. Chem. Rev.*, 1976, **18**, 225
139. U. Mayer, V. Gutmann and W. Gerger, *Monatshefte fur Chemie*, 1975, **106**, 1235
140. A. G. Massey, A. J. Park and F. G. A. Stone, *Proc. Chem. Soc.*, 1963, 212
141. A. N. Chernenko, A. J. Graham, M. L. H. Green, J. Haggitt, J. Lloyd, C. P. Mehnert, N. Metzler and J. Souter, *J. Chem. Soc. Dalton Trans.*, 1997, 2293
142. H. H. Brintzinger, D. Fischer, R. Mulhaupt, B. Rieger and R. Waymoun, *Angew. Chem. Int. Ed. Engl.*, 1995, **34**, 1143
143. L. H. Doerrer and M. L. H. Green, *J. Chem. Soc. Dalton Trans.*, 1999, 4325
144. A. G. Massey and A. J. Parks, *J. Organomet. Chem.*, 1966, **5**, 218
145. D. J. Parks and W. E. Piers, *J. Am. Chem. Soc.*, 1996, **118**, 9440
146. R. F. Childs, D. L. Mulholland and A. Nixon, *Can. J. Chem.*, 1982, **60**, 801
147. M. F. Lappert, *J. Chem. Soc.*, 1961, 817
148. M. F. Lappert, *J. Chem. Soc.*, 1962, 542
149. P. Laszlo and M. Teston, *J. Am. Chem. Soc.* 1990, **112**, 8750

150. S. Doring, G. Erker, R. Frohlich, O. Meyer and K. Bergander, *Organometallics*, 1998, **17**, 2183
151. H. Jacobsen, H. Berke, S. Doring, G. Kehr, G. Erker, R. Frohlich and O. Meyer, *Organometallics*, 1999, **18**, 1724
152. M. A. Beckett, D. S. Brassington, S. J. Coles and M. B. Hursthouse, *Inorg. Chem. Comm.*, 2000, **3**, 530
153. A. A. Danopoulos, J. R. Galsworthy, M. L. H. Green, S. Cafferkey, L. H. Doerrer and M. B. Hursthouse, *Chem. Comm.*, 1998, 3191
154. D. J. Parks, W. E. Piers, M. Parvez, R. Atencio and M. J. Zaworotko, *Organometallics*, 1998, **17**, 1369
155. D. C. Bradley, I. S. Harding, A. D. Keefe, M. Motavalli and D. -H. Zheng, *J. Chem. Soc. Dalton Trans.*, 1996, 2529
156. M. A. Beckett, D. S. Brassington, P. Owen, M. B. Hursthouse, M. E. Light, K. M. A. Malik and K. S. Varma, *J. Organomet. Chem.*, 1999, **585**, 7
157. M. A. Beckett, P. Owen and K. S. Varma, *J. Organomet. Chem.*, 1999, **588**, 107
158. M. A. Beckett, D. E. Hibbs, M. B. Hursthouse, K. M. A. Malik, P. Owen and K. S. Varma, *J. Organomet. Chem.*, 2000, **595**, 241
159. N. Burford, B. W. Royan, R. E. vH. Spence, T. S. Cameron, A. Linden and R. D. Rogers, *J. Chem. Soc. Dalton Trans.*, 1990, 1521
160. S. Un and M. P. Klein, *J. Am. Chem. Soc.*, 1989, **111**, 5119
161. N. Burford, R. E. vH. Spence, A. Linden and T. S. Cameron, *Acta Crystallogr. Sect. C*, 1990, **46**, 92
162. M. C. R. Symons and G. Eaton, *J. Chem. Soc. Farady I*, 1982, **78**, 3033
163. J. V. Bell, J. Heisler, H. Tannenbaum and J. Goldenson, *J. Am. Chem. Soc.*, 1954, **76**, 5185

164. D. M. Baird, P. E. Fanwich and T. Barwick, *Inorg. Chem.*, 1985, **24**, 3753
165. F. A. Cotton, J. Lu and T. Ren, *Inorg. Chim. Acta*, 1994, **215**, 47
166. B. Borup, J. C. Huffman and K. G. Caulton, *J. Organomet. Chem.*, 1997, **536**, 109
167. G. Philipp, S. Wocadlo, W. Massa, K. Dehnicke, D. Fenske, C. Maichle-Mossmer, E. Niquet and J. Strahle, *Z. Naturforsch Teil B*, 1995, **50**, 1
168. M. T. Reetz, M. Hullmann, W. Massa, S. Berger, P. Rademacher and P. Heymanns, *J. Am. Chem. Soc.*, 1986, **108**, 2405
169. G. Barrado, L. Doerrer, M. L. H. Green and M. A. Leech, *J. Chem. Soc. Dalton Trans.*, 1999, 1061
170. A. R. Siedle, R. A. Newmark, W. M. Lamanna and J. C. Huffman, *Organometallics*, 1993, **12**, 1491
171. Y. Hermodsson, *Ark. Kemi.*, 1969, **30**, 15
172. R. Hauptmann, R. Kliss, J. Schneider and G. Henkel, *Z. Anorg. Allg. Chem.*, 1998, **624**, 1927
173. N. Burford, B. W. Royan, R. E. vH. Spence and R. D. Rogers, *J. Chem. Soc. Dalton Trans.*, 1990, 2111
174. D. Murphy, J. P. Sheehan, T. R. Spalding, G. Ferguson, A. J. Lough and J. F. Gallagher, *J. Mater. Chem.*, 1993, **3**, 1275
175. G. Ruban and V. Zabel, *Cryst. Struct. Commun.*, 1976, **5**, 671
176. R. T. Paine and H. Noeth, *Chem. Rev.*, 1995, **95**, 343
177. P. P. Power, *Angew. Chem. Int. Ed. Engl.*, 1990, **29**, 449
178. P. P. Power, *J. Organomet. Chem.*, 1990, **400**, 49
179. M. Feher, R. Frohlich and K. F. Tebbe, *Z. Anorg. Allg. Chem.*, 1981, **474**, 31
180. M. Baudler and A. Marx, *Z. Anorg. Allg. Chem.*, 1981, **474**, 18

181. M. Baudler and G. Kupprat, *Z. Anorg. Allg. Chem.*, 1986, **533**, 146
182. B. Riegel, A. Pfitzner, G. Heckmann, E. Fluck and H. Binder, *Phosphorus, Sulfur and Silicon*, 1994, **93-94**, 173
183. B. Riegel, A. Pfitzner, G. Heckmann, E. Fluck and H. Binder, *Z. Anorg. Allg. Chem.*, 1994, **620**, 8
184. G. Fritz and W. Holderich, *Z. Anorg. Allg. Chem.*, 1977, **431**, 61
185. A. M. Arif, A. M. Cowley, M. Pakulski and J. M. Power, *J. Chem. Soc. Chem. Comm.*, 1986, 889
186. P. Kolle, H. Noth and R. T. Paine, *Chem. Ber.*, 1986, **109**, 2681
187. H. V. R. Dias and P. P. Power, *J. Am. Chem. Soc.*, 1989, **111**, 144
188. P. Kolle, G. Linti, H. Noth and K. Polborn, *J. Organomet. Chem.*, 1988, **355**, 7
189. M. Baudler and M. Hintze, *Z. Anorg. Allg. Chem.*, 1985, **522**, 184
190. W. Gerrard, M. Howarth, E. F. Mooney and D. E. Pratt, *J. Chem. Soc.*, 1963, 1582
191. H. A. Clark, A. F. Gordon, C. W. Young and M. J. Hunter, *J. Am. Chem. Soc.*, 1951, **73**, 3798
192. W. Haubold, J. Herdtle, W. Gollinger and W. Einholz, *J. Organomet. Chem.*, 1986, **315**, 1
193. M. A. Beckett, P. R. Minto and B. Werschkun, *J. Organomet. Chem.*, 1994, **468**, 37
194. D. Kaufmann, *Chem. Ber.*, 1987, **120**, 853
195. A. J. Leffler and E. G. Teach, *J. Am. Chem. Soc.*, 1960, **82**, 2710
196. H. Schumann and L. Rosch, *J. Organomet. Chem.*, 1973, **55**, 257
197. E. Niecke and H. Westermann, *Synthesis*, 1998, **18**, 330
198. G. E. Coates and J. G. Livingstone, *J. Chem. Soc.*, 1961, 5053

199. A. D. Tevebaugh, *Inorg. Chem.*, 1964, **3**, 302
200. B. Rapp and J. E. Drake, *Inorg. Chem.*, 1973, **12**, 2868
201. M. H. Quick and R. J. Anjelici, *Inorg. Synth.*, 1990, **28**, 126
202. E. W. Abel and G. Wilkinson, *J. Chem. Soc.*, 1959, 1601
203. R. B. King and N. D. Sadanani, *Synth. React. Inorg. Met.-Org. Chem.*, 1985, **15**,

149

Appendix A

Crystal tables for **2b**

Table 1. Crystal data and structure refinement.

Identification code	98SRC289
Empirical formula	C40 H25 Br Cl9 Mn O3 P2
Formula weight	1069.44
Temperature	150(2) K
Wavelength	0.71074 Å
Crystal system	Monoclinic
Space group	P2/n
Unit cell dimensions	a = 15.3638(3) Å b = 14.0991(2) Å c = 20.5356(5) Å beta = 103.9470(10) deg.
Volume	4317.19(15) Å^3
Z	4
Density (calculated)	1.645 Mg/m^3
Absorption coefficient	1.901 mm^-1
F(000)	2128
Crystal size	0.2 x 0.2 x 0.3 mm
Theta range for data collection	2.99 to 23.25 deg.
Index ranges	-17<=h<=17, -15<=k<=15, -22<=l<=22
Reflections collected	57780
Independent reflections	6201 [R(int) = 0.0747]
Refinement method	Full-matrix least-squares on F^2
Data / restraints / parameters	6201 / 34 / 559
Transmission Factors	Min = 0.594 Max = 0.717
Goodness-of-fit on F^2	1.052
Final R indices [I>2sigma(I)]	R1 = 0.0582, wR2 = 0.1513
R indices (all data)	R1 = 0.0742, wR2 = 0.1643
Largest diff. peak and hole	1.374 and -1.495 e.Å^-3

Table 2. Atomic coordinates ($\times 10^4$) and equivalent isotropic displacement parameters ($\text{\AA}^2 \times 10^3$). $U(\text{eq})$ is defined as one third of the trace of the orthogonalized U_{ij} tensor.

	x	y	z	$U(\text{eq})$
P(1)	8035(1)	5356(1)	5691(1)	27(1)
P(2)	6726(1)	2537(1)	4761(1)	26(1)
C1(5)	6155(1)	2024(1)	1613(1)	45(1)
C1(1)	5801(1)	8176(1)	7072(1)	46(1)
C1(6)	2929(1)	1263(1)	5166(1)	62(1)
C1(2)	9076(1)	8554(1)	3844(1)	54(1)
C1(4)	9314(1)	-642(1)	6315(1)	64(1)
C1(3)	11448(1)	4210(1)	7957(1)	68(1)
C(13)	9033(2)	5125(3)	6365(2)	28(1)
C(1)	7375(2)	6160(3)	6090(2)	29(1)
C(8)	7911(2)	6345(3)	4496(2)	31(1)
C(25)	6594(2)	2353(3)	3854(2)	28(1)
C(31)	5610(2)	2216(3)	4870(2)	27(1)
C(19)	7394(2)	1521(3)	5146(2)	29(1)
C(5)	6015(3)	6563(3)	6427(2)	36(1)
C(9)	8115(3)	7050(3)	4090(2)	36(1)
C(20)	8115(3)	1192(3)	4910(2)	34(1)
C(14)	8990(3)	5080(3)	7032(2)	38(1)
C(24)	7281(3)	1175(3)	5756(2)	36(1)
C(6)	6504(3)	5943(3)	6127(2)	34(1)
C(17)	10571(3)	4588(3)	6691(2)	38(1)
C(39)	8376(3)	3280(3)	5678(2)	40(1)
C(30)	6462(3)	3146(3)	3430(2)	33(1)
C(34)	3953(3)	1645(3)	5045(2)	37(1)
C(18)	9830(3)	4863(3)	6198(2)	34(1)
C(29)	6337(3)	3038(3)	2747(2)	37(1)
C(10)	8852(3)	7616(3)	4330(2)	36(1)
C(22)	8571(3)	193(3)	5869(2)	44(1)
C(7)	8433(2)	6193(3)	5140(2)	29(1)
O(1)	8995(2)	2851(2)	5946(2)	57(1)
C(32)	5249(3)	1331(3)	4645(2)	34(1)
C(26)	6590(2)	1452(3)	3572(2)	32(1)
C(23)	7867(3)	509(3)	6117(2)	43(1)
C(36)	5100(3)	2807(3)	5171(2)	37(1)
C(28)	6333(2)	2143(3)	2480(2)	31(1)
C(27)	6451(2)	1350(3)	2882(2)	35(1)
C(33)	4426(3)	1048(3)	4732(2)	37(1)
C(12)	9187(3)	6767(3)	5360(2)	37(1)
C(11)	9400(3)	7469(3)	4962(2)	40(1)
C(15)	9723(3)	4788(3)	7521(2)	43(1)
C(3)	7264(3)	7646(3)	6650(2)	36(1)
C(16)	10503(3)	4551(3)	7344(2)	40(1)
C(4)	6402(3)	7406(3)	6686(2)	34(1)
C(21)	8700(3)	519(3)	5265(2)	40(1)
C(2)	7742(3)	7021(3)	6351(2)	34(1)
C(35)	4278(3)	2530(3)	5263(2)	43(1)
O(2)*	8317(1)	4149(3)	4137(1)	71(2)
O(3)*	6805(1)	3640(3)	6476(1)	79(2)
C(37)*	6989(1)	3763(3)	5973(1)	44(1)
C(38)*	7984(1)	4041(3)	4574(1)	39(1)
Br(2)†	6943(1)	3545(2)	6316(1)	36(1)
Br(3)†	8402(1)	3986(2)	4407(1)	41(1)
Mn(1)	7404(1)	3933(1)	5234(1)	28(1)
Br(1)**	6022(1)	4826(1)	4591(1)	33(1)
C(42)##	6466(1)	4537(1)	4700(1)	79(6)
O(4)##	6051(3)	4927(3)	4237(2)	410(3)
Cl(7)	5490(1)	548(1)	6800(1)	158(1)
Cl(8A)+	5460(2)	2187(2)	7513(1)	184(2)
Cl(8B)+	6087(1)	2256(1)	7360(3)	369(4)
Cl(9)	3946(1)	1488(2)	6972(1)	213(2)

C (40) +	5118 (1)	1557 (1)	7150 (2)	179 (9)
C (41) +	4961 (1)	1655 (1)	6743 (1)	362 (1)

* = 85% occupied; + = 50% occupied; ## = 30% occupied
= 15% occupied; ** = 70% occupied

Table 3. Bond lengths [Å] and angles [deg].

P(1)-C(13)	1.831(3)	P(1)-C(7)	1.839(4)
P(1)-C(1)	1.840(4)	P(1)-Mn(1)	2.3260(11)
P(2)-C(19)	1.828(4)	P(2)-C(31)	1.838(4)
P(2)-C(25)	1.843(4)	P(2)-Mn(1)	2.3275(10)
Cl(5)-C(28)	1.743(4)	Cl(1)-C(4)	1.736(4)
Cl(6)-C(34)	1.737(4)	Cl(2)-C(10)	1.741(4)
Cl(4)-C(22)	1.738(4)	Cl(3)-C(16)	1.744(4)
C(13)-C(14)	1.390(6)	C(13)-C(18)	1.398(6)
C(1)-C(2)	1.391(5)	C(1)-C(6)	1.393(5)
C(8)-C(9)	1.381(6)	C(8)-C(7)	1.388(5)
C(25)-C(26)	1.394(5)	C(25)-C(30)	1.401(5)
C(31)-C(36)	1.387(6)	C(31)-C(32)	1.398(5)
C(19)-C(20)	1.393(6)	C(19)-C(24)	1.393(6)
C(5)-C(4)	1.378(6)	C(5)-C(6)	1.389(6)
C(9)-C(10)	1.376(6)	C(20)-C(21)	1.387(6)
C(14)-C(15)	1.378(6)	C(24)-C(23)	1.386(6)
C(17)-C(16)	1.371(6)	C(17)-C(18)	1.384(5)
C(39)-O(1)	1.149(5)	C(39)-Mn(1)	1.804(4)
C(30)-C(29)	1.378(6)	C(34)-C(33)	1.368(6)
C(34)-C(35)	1.380(6)	C(29)-C(28)	1.374(6)
C(10)-C(11)	1.381(6)	C(22)-C(23)	1.375(7)
C(22)-C(21)	1.382(7)	C(7)-C(12)	1.396(5)
C(32)-C(33)	1.379(6)	C(26)-C(27)	1.388(6)
C(36)-C(35)	1.378(6)	C(28)-C(27)	1.376(6)
C(12)-C(11)	1.373(6)	C(15)-C(16)	1.374(7)
C(3)-C(2)	1.380(6)	C(3)-C(4)	1.386(6)
O(2)-C(38)	1.1464(8)	O(3)-C(37)	1.1478(8)
C(37)-Mn(1)	1.7986(8)	C(38)-Mn(1)	1.7986(7)
Br(2)-Mn(1)	2.5492(9)	Br(3)-Mn(1)	2.5476(9)
Mn(1)-C(42)	1.8001(9)	Mn(1)-Br(1)	2.5458(7)
C(42)-O(4)	1.1500(10)	Cl(7)-C(41)	1.7502(9)
Cl(7)-C(40)	1.7502(10)	Cl(8B)-C(40)	1.7503(9)
Cl(8B)-C(41)	2.063(3)	Cl(9)-C(41)	1.7498(10)
Cl(9)-C(40)	1.7506(8)		
C(13)-P(1)-C(7)	103.71(17)	C(13)-P(1)-C(1)	102.95(17)
C(7)-P(1)-C(1)	100.37(17)	C(13)-P(1)-Mn(1)	110.07(12)
C(7)-P(1)-Mn(1)	118.26(12)	C(1)-P(1)-Mn(1)	119.36(13)
C(19)-P(2)-C(31)	101.37(17)	C(19)-P(2)-C(25)	103.96(17)
C(31)-P(2)-C(25)	102.15(17)	C(19)-P(2)-Mn(1)	109.48(12)
C(31)-P(2)-Mn(1)	119.60(13)	C(25)-P(2)-Mn(1)	118.04(13)
C(14)-C(13)-C(18)	118.9(3)	C(14)-C(13)-P(1)	121.5(3)
C(18)-C(13)-P(1)	119.0(3)	C(2)-C(1)-C(6)	118.5(4)
C(2)-C(1)-P(1)	119.6(3)	C(6)-C(1)-P(1)	121.9(3)
C(9)-C(8)-C(7)	121.5(3)	C(26)-C(25)-C(30)	118.9(4)
C(26)-C(25)-P(2)	122.4(3)	C(30)-C(25)-P(2)	118.6(3)
C(36)-C(31)-C(32)	117.5(3)	C(36)-C(31)-P(2)	123.3(3)
C(32)-C(31)-P(2)	119.1(3)	C(20)-C(19)-C(24)	118.6(3)
C(20)-C(19)-P(2)	121.4(3)	C(24)-C(19)-P(2)	119.0(3)
C(4)-C(5)-C(6)	119.0(4)	C(10)-C(9)-C(8)	119.2(4)
C(21)-C(20)-C(19)	120.9(4)	C(15)-C(14)-C(13)	120.4(4)
C(23)-C(24)-C(19)	120.8(4)	C(5)-C(6)-C(1)	121.0(4)
C(16)-C(17)-C(18)	118.9(4)	O(1)-C(39)-Mn(1)	178.2(4)
C(29)-C(30)-C(25)	120.5(4)	C(33)-C(34)-C(35)	121.2(4)
C(33)-C(34)-Cl(6)	118.6(3)	C(35)-C(34)-Cl(6)	120.2(3)
C(17)-C(18)-C(13)	120.5(4)	C(28)-C(29)-C(30)	119.6(4)
C(9)-C(10)-C(11)	120.8(4)	C(9)-C(10)-Cl(2)	119.6(3)
C(11)-C(10)-Cl(2)	119.6(3)	C(23)-C(22)-C(21)	121.3(4)
C(23)-C(22)-Cl(4)	120.0(4)	C(21)-C(22)-Cl(4)	118.7(4)
C(8)-C(7)-C(12)	117.7(4)	C(8)-C(7)-P(1)	118.9(3)
C(12)-C(7)-P(1)	123.0(3)	C(33)-C(32)-C(31)	121.3(4)
C(27)-C(26)-C(25)	120.2(4)	C(22)-C(23)-C(24)	119.4(4)
C(35)-C(36)-C(31)	121.7(4)	C(29)-C(28)-C(27)	121.3(4)
C(29)-C(28)-Cl(5)	118.7(3)	C(27)-C(28)-Cl(5)	120.0(3)
C(28)-C(27)-C(26)	119.6(4)	C(34)-C(33)-C(32)	119.3(4)
C(11)-C(12)-C(7)	121.5(4)	C(12)-C(11)-C(10)	119.3(4)

C(16)-C(15)-C(14)	119.5(4)	C(2)-C(3)-C(4)	119.0(4)
C(17)-C(16)-C(15)	121.8(4)	C(17)-C(16)-Cl(3)	118.0(3)
C(15)-C(16)-Cl(3)	120.2(3)	C(5)-C(4)-C(3)	121.2(4)
C(5)-C(4)-Cl(1)	119.2(3)	C(3)-C(4)-Cl(1)	119.6(3)
C(22)-C(21)-C(20)	119.0(4)	C(3)-C(2)-C(1)	121.3(4)
C(34)-C(35)-C(36)	118.9(4)	O(3)-C(37)-Mn(1)	173.69(15)
O(2)-C(38)-Mn(1)	176.0(3)	C(37)-Mn(1)-C(38)	171.03(8)
C(37)-Mn(1)-C(42)	100.51(10)	C(38)-Mn(1)-C(42)	88.34(10)
C(37)-Mn(1)-C(39)	85.58(17)	C(38)-Mn(1)-C(39)	85.66(17)
C(42)-Mn(1)-C(39)	173.22(16)	C(37)-Mn(1)-P(1)	88.41(12)
C(38)-Mn(1)-P(1)	89.82(12)	C(42)-Mn(1)-P(1)	91.86(7)
C(39)-Mn(1)-P(1)	91.27(13)	C(37)-Mn(1)-P(2)	91.48(12)
C(38)-Mn(1)-P(2)	90.59(11)	C(42)-Mn(1)-P(2)	86.20(7)
C(39)-Mn(1)-P(2)	90.71(13)	P(1)-Mn(1)-P(2)	178.01(4)
C(37)-Mn(1)-Br(1)	94.76(8)	C(38)-Mn(1)-Br(1)	94.03(7)
C(39)-Mn(1)-Br(1)	178.87(12)	P(1)-Mn(1)-Br(1)	89.82(3)
P(2)-Mn(1)-Br(1)	88.21(3)	C(37)-Mn(1)-Br(3)	163.46(8)
C(42)-Mn(1)-Br(3)	95.91(8)	C(39)-Mn(1)-Br(3)	78.13(16)
P(1)-Mn(1)-Br(3)	89.09(7)	P(2)-Mn(1)-Br(3)	91.58(7)
Br(1)-Mn(1)-Br(3)	101.58(5)	C(38)-Mn(1)-Br(2)	165.23(9)
C(42)-Mn(1)-Br(2)	106.41(8)	C(39)-Mn(1)-Br(2)	79.57(16)
P(1)-Mn(1)-Br(2)	90.56(6)	P(2)-Mn(1)-Br(2)	89.54(6)
Br(1)-Mn(1)-Br(2)	100.74(5)	Br(3)-Mn(1)-Br(2)	157.68(7)
O(4)-C(42)-Mn(1)	158.8(3)	Cl(7)-C(40)-Cl(8B)	102.48(14)
Cl(7)-C(40)-Cl(9)	106.92(13)	Cl(8B)-C(40)-Cl(9)	148.56(15)
Cl(9)-C(41)-Cl(7)	106.95(13)	Cl(9)-C(41)-Cl(8B)	124.0(2)
Cl(7)-C(41)-Cl(8B)	91.03(9)		

Symmetry transformations used to generate equivalent atoms:

Table 4. Anisotropic displacement parameters ($\text{Å}^2 \times 10^3$).
 The anisotropic displacement factor exponent takes the form:
 $2 \pi^2 [h^2 a^{*2} U_{11} + \dots + 2 h k a^* b^* U_{12}]$

	U11	U22	U33	U23	U13	U12
(1)	22(1)	30(1)	29(1)	-4(1)	5(1)	-1(1)
(2)	23(1)	24(1)	31(1)	0(1)	5(1)	0(1)
1(5)	41(1)	62(1)	31(1)	-6(1)	5(1)	-5(1)
1(1)	38(1)	53(1)	46(1)	-15(1)	5(1)	13(1)
1(6)	42(1)	47(1)	108(1)	-19(1)	41(1)	-16(1)
1(2)	49(1)	55(1)	57(1)	17(1)	9(1)	-11(1)
1(4)	56(1)	51(1)	75(1)	19(1)	-5(1)	18(1)
1(3)	64(1)	73(1)	52(1)	1(1)	-16(1)	31(1)
(13)	24(2)	30(2)	26(2)	-5(2)	-1(2)	-2(2)
(1)	25(2)	31(2)	29(2)	-3(2)	4(2)	4(2)
(8)	26(2)	33(2)	33(2)	-7(2)	7(2)	-3(2)
(25)	22(2)	31(2)	32(2)	-2(2)	6(2)	2(2)
(31)	19(2)	28(2)	33(2)	4(2)	2(2)	-1(2)
(19)	25(2)	25(2)	33(2)	-1(2)	1(2)	-1(2)
(5)	26(2)	44(2)	36(2)	-5(2)	6(2)	2(2)
(9)	32(2)	39(2)	35(2)	-1(2)	4(2)	4(2)
(20)	31(2)	32(2)	38(2)	5(2)	8(2)	1(2)
(14)	34(2)	41(2)	40(2)	-2(2)	10(2)	6(2)
(24)	35(2)	32(2)	39(2)	0(2)	7(2)	-1(2)
(6)	30(2)	36(2)	37(2)	-5(2)	10(2)	-5(2)
(17)	26(2)	36(2)	49(2)	-5(2)	4(2)	-1(2)
(39)	34(2)	30(2)	51(3)	-11(2)	-1(2)	-8(2)
(30)	32(2)	32(2)	35(2)	-1(2)	7(2)	2(2)
(34)	27(2)	35(2)	52(2)	1(2)	14(2)	-4(2)
(18)	31(2)	38(2)	31(2)	-3(2)	4(2)	-2(2)
(29)	31(2)	39(2)	38(2)	5(2)	2(2)	1(2)
(10)	33(2)	34(2)	43(2)	0(2)	13(2)	-5(2)
(22)	38(2)	34(2)	52(3)	4(2)	-3(2)	3(2)
(7)	28(2)	30(2)	29(2)	-6(2)	7(2)	-3(2)
(1)	41(2)	41(2)	76(2)	-4(2)	-14(2)	4(2)
(32)	32(2)	32(2)	36(2)	-3(2)	6(2)	1(2)
(26)	24(2)	31(2)	41(2)	-2(2)	7(2)	-1(2)
(23)	46(2)	39(2)	39(2)	8(2)	3(2)	1(2)
(36)	32(2)	25(2)	56(3)	-1(2)	14(2)	-4(2)
(28)	24(2)	44(2)	27(2)	-4(2)	6(2)	-3(2)
(27)	26(2)	41(2)	36(2)	-10(2)	6(2)	-2(2)
(33)	33(2)	29(2)	47(2)	-6(2)	9(2)	-7(2)
(12)	36(2)	40(2)	33(2)	-2(2)	3(2)	-7(2)
(11)	30(2)	46(2)	41(2)	3(2)	1(2)	-12(2)
(15)	56(3)	41(2)	32(2)	3(2)	8(2)	10(2)
(3)	36(2)	32(2)	37(2)	-5(2)	3(2)	1(2)
(16)	42(2)	32(2)	39(2)	-3(2)	-7(2)	4(2)
(4)	27(2)	40(2)	32(2)	-3(2)	1(2)	12(2)
(21)	29(2)	36(2)	52(3)	-2(2)	6(2)	0(2)
(2)	23(2)	37(2)	42(2)	-5(2)	5(2)	-3(2)
(35)	38(2)	31(2)	65(3)	-5(2)	22(2)	-2(2)
(2)	54(2)	40(2)	99(3)	-11(2)	-22(2)	4(2)
(3)	120(4)	55(3)	68(3)	-5(2)	31(3)	-11(3)
(37)	41(3)	42(3)	50(3)	-12(2)	14(2)	-5(2)
(38)	74(3)	22(2)	18(2)	0(2)	7(2)	-26(2)
r(2)	38(1)	33(1)	36(1)	-4(1)	6(1)	0(1)
r(3)	39(1)	35(1)	43(1)	-4(1)	0(1)	0(1)
n(1)	23(1)	26(1)	32(1)	-2(1)	4(1)	-1(1)
r(1)	29(1)	28(1)	42(1)	-8(1)	8(1)	-3(1)
(42)	99(11)	38(9)	129(13)	-32(9)	88(10)	-14(9)
(4)	310(4)	140(2)	590(7)	80(4)	-250(4)	-30(3)
l(7)	206(2)	71(1)	223(2)	-46(1)	101(2)	-3(1)
l(8A)	244(6)	112(3)	219(5)	-95(3)	103(4)	-17(4)
l(8B)	789(10)	190(4)	216(5)	-94(4)	293(6)	-301(5)
l(9)	250(3)	225(3)	166(3)	57(2)	54(2)	123(3)

C(40)	115(11)	75(8)	350(2)	-114(11)	69(14)	18(8)
C(41)	362(1)	362(1)	362(1)	0(1)	87(1)	0(1)

* = 85% occupied; + = 50% occupied; ## = 30% occupied
= 15% occupied; ** = 70% occupied

Appendix B

Crystal tables for **2g**



University of Southampton · Department of Chemistry

EPSRC National Crystallography Service

**Table 1.** Crystal data and structure refinement.

Identification code	00src069		
Empirical formula	$C_{45}H_{42}BrO_9P_2Re$		
Formula weight	1054.84		
Temperature	150(2) K		
Wavelength	0.71073 Å		
Crystal system	Orthorhombic		
Space group	$Pbca$		
Unit cell dimensions	$a = 18.337(4)$ Å	$\alpha = 90^\circ$	
	$b = 20.515(4)$ Å	$\beta = 90^\circ$	
	$c = 22.738(5)$ Å	$\gamma = 90^\circ$	
Volume	8554(3) Å ³		
Z	8		
Density (calculated)	1.638 Mg / m ³		
Absorption coefficient	3.905 mm ⁻¹		
$F(000)$	4192		
Crystal	Prism; colourless		
Crystal size	0.2 × 0.2 × 0.2 mm ³		
θ range for data collection	2.98 – 30.41°		
Index ranges	–25 ≤ h ≤ 25, –24 ≤ k ≤ 28, –26 ≤ l ≤ 30		
Reflections collected	65319		
Independent reflections	11208 [$R_{int} = 0.0588$]		
Completeness to $\theta = 30.41^\circ$	86.7 %		
Absorption correction	Semi-empirical from equivalents		
Max. and min. transmission	0.472 and 0.347		
Refinement method	Full-matrix least-squares on F^2		
Data / restraints / parameters	11208 / 0 / 529		
Goodness-of-fit on F^2	0.821		
Final R indices [$F^2 > 2\sigma(F^2)$]	$RI = 0.0375$, $wR2 = 0.0954$		
R indices (all data)	$RI = 0.0652$, $wR2 = 0.1165$		
Largest diff. peak and hole	1.884 and –2.020 e Å ^{–3}		

Diffractometer: *Enraf Nonius KappaCCD* area detector (ϕ scans and ω scans to fill *Ewald sphere*). **Data collection and cell refinement:** *Denzo* (Z. Otwinowski & W. Minor, *Methods in Enzymology* (1997) Vol. 276: *Macromolecular Crystallography*, part A, pp. 307–326; C. W. Carter, Jr. & R. M. Sweet, Eds., Academic Press). **Absorption correction:** *SORTAV* (R. H. Blessing, *Acta Cryst. A*51 (1995) 33–37; R. H. Blessing, *J. Appl. Cryst.* 30 (1997) 421–426). **Program used to solve structure:** *SHELXS97* (G. M. Sheldrick, *Acta Cryst.* (1990) A46 467–473). **Program used to refine structure:** *SHELXL97* (G. M. Sheldrick (1997), University of Göttingen, Germany).

Further information: <http://www.soton.ac.uk/~xservice/strat.htm>

Special details:

Table 2. Atomic coordinates [$\times 10^4$], equivalent isotropic displacement parameters [$\text{\AA}^2 \times 10^3$] and site occupancy factors. U_{eq} is defined as one third of the trace of the orthogonalized U^{ij} tensor.

Atom	<i>x</i>	<i>y</i>	<i>z</i>	U_{eq}	S.o.f.
Re1	4450(1)	556(1)	6216(1)	19(1)	1
Br1	4077(1)	429(1)	7328(1)	30(1)	1
P1	3280(1)	1190(1)	6077(1)	21(1)	1
P2	5425(1)	1398(1)	6459(1)	21(1)	1
O1	4919(1)	752(1)	4947(1)	29(1)	1
O2	5631(2)	-472(1)	6471(2)	42(1)	1
O3	3536(2)	-644(1)	5870(1)	35(1)	1
O4	657(2)	-553(1)	6245(1)	37(1)	1
O5	3213(2)	2355(2)	3665(1)	47(1)	1
O6	2708(2)	3548(1)	7528(1)	41(1)	1
O7	5474(1)	3862(1)	5058(1)	37(1)	1
O8	5421(2)	2301(1)	8965(1)	40(1)	1
O9	8232(1)	123(1)	5741(1)	34(1)	1
C1	4741(2)	677(2)	5410(2)	26(1)	1
C2	5225(2)	-72(2)	6368(2)	28(1)	1
C3	3850(2)	-187(2)	6004(2)	25(1)	1
C4	2478(2)	669(2)	6129(2)	24(1)	1
C5	2302(2)	375(2)	6663(2)	31(1)	1
C6	1701(2)	-40(2)	6722(2)	31(1)	1
C7	1270(2)	-162(2)	6235(2)	28(1)	1
C8	1439(2)	118(2)	5704(2)	35(1)	1
C9	2028(2)	535(2)	5651(2)	30(1)	1
C10	445(2)	-842(2)	6781(2)	46(1)	1
C11	3187(2)	1561(2)	5345(2)	23(1)	1
C12	3288(2)	1188(2)	4841(2)	27(1)	1
C13	3270(2)	1457(2)	4290(2)	31(1)	1
C14	3177(2)	2131(2)	4221(2)	32(1)	1
C15	3056(2)	2512(2)	4714(2)	29(1)	1
C16	3060(2)	2231(2)	5269(2)	26(1)	1
C17	3202(3)	3050(2)	3589(2)	51(1)	1
C18	3067(2)	1855(2)	6575(2)	23(1)	1
C19	2372(2)	2136(2)	6574(2)	33(1)	1
C20	2231(2)	2698(2)	6893(2)	34(1)	1
C21	2786(2)	2982(2)	7219(2)	30(1)	1
C22	3466(2)	2690(2)	7247(2)	29(1)	1
C23	3600(2)	2130(2)	6923(2)	25(1)	1
C24	2019(2)	3871(2)	7492(2)	56(1)	1
C25	5450(2)	2137(2)	6020(2)	24(1)	1
C26	4831(2)	2345(2)	5735(2)	27(1)	1
C27	4811(2)	2915(2)	5409(2)	30(1)	1
C28	5430(2)	3293(2)	5368(2)	28(1)	1
C29	6072(2)	3094(2)	5650(2)	35(1)	1
C30	6079(2)	2527(2)	5970(2)	35(1)	1
C31	4838(2)	4049(2)	4741(2)	40(1)	1
C32	5483(2)	1699(2)	7212(2)	24(1)	1
C33	5364(2)	2356(2)	7345(2)	27(1)	1
C34	5326(2)	2577(2)	7922(2)	29(1)	1
C35	5426(2)	2141(2)	8382(2)	26(1)	1
C36	5552(2)	1483(2)	8258(2)	27(1)	1
C37	5560(2)	1268(2)	7686(2)	23(1)	1
C38	5309(3)	2975(2)	9107(2)	51(1)	1
C39	6323(2)	1040(2)	6292(2)	22(1)	1
C40	6806(2)	809(2)	6706(2)	26(1)	1
C41	7452(2)	492(2)	6545(2)	26(1)	1
C42	7617(2)	415(2)	5957(2)	26(1)	1
C43	7133(2)	648(2)	5526(2)	28(1)	1
C44	6502(2)	953(2)	5697(2)	29(1)	1
C45	8745(2)	-128(2)	6152(2)	44(1)	1

Table 3. Bond lengths [\AA] and angles [°].

Re1–C1	1.926(4)
Re1–C3	1.941(4)
Re1–C2	1.950(4)
Re1–P1	2.5279(9)
Re1–P2	2.5467(10)
Re1–Br1	2.6308(6)
P1–C18	1.815(3)
P1–C4	1.824(4)
P1–C11	1.838(4)
P2–C25	1.816(4)
P2–C32	1.823(4)
P2–C39	1.842(3)
O1–C1	1.112(5)
O2–C2	1.133(5)
O3–C3	1.142(4)
O4–C7	1.381(5)
O4–C10	1.410(5)
O5–C14	1.348(5)
O5–C17	1.436(5)
O6–C21	1.365(4)
O6–C24	1.430(5)
O7–C28	1.365(4)
O7–C31	1.423(5)
O8–C35	1.366(5)
O8–C38	1.435(5)
O9–C42	1.368(4)
O9–C45	1.423(5)
C4–C9	1.391(5)
C4–C5	1.394(5)
C5–C6	1.399(5)
C6–C7	1.385(5)
C7–C8	1.371(5)
C8–C9	1.384(5)
C11–C12	1.390(5)
C11–C16	1.404(5)
C12–C13	1.369(5)
C13–C14	1.402(5)
C14–C15	1.384(5)
C15–C16	1.387(5)
C18–C23	1.379(5)
C18–C19	1.398(5)
C19–C20	1.386(5)
C20–C21	1.388(5)
C21–C22	1.385(5)
C22–C23	1.386(5)
C25–C26	1.375(5)
C25–C30	1.408(5)
C26–C27	1.385(5)
C27–C28	1.378(5)
C28–C29	1.403(5)
C29–C30	1.371(5)
C32–C33	1.398(5)
C32–C37	1.402(5)
C33–C34	1.390(5)
C34–C35	1.387(5)
C35–C36	1.398(5)
C36–C37	1.375(5)
C39–C40	1.377(5)
C39–C44	1.404(5)

C40-C41	1.399(5)
C41-C42	1.381(6)
C42-C43	1.406(5)
C43-C44	1.372(5)
C1-Re1-C3	91.21(15)
C1-Re1-C2	92.88(15)
C3-Re1-C2	86.48(15)
C1-Re1-P1	92.91(10)
C3-Re1-P1	83.82(10)
C2-Re1-P1	168.79(11)
C1-Re1-P2	85.66(10)
C3-Re1-P2	169.91(10)
C2-Re1-P2	84.11(11)
P1-Re1-P2	105.89(3)
C1-Re1-Br1	177.98(10)
C3-Re1-Br1	90.80(11)
C2-Re1-Br1	87.36(11)
P1-Re1-Br1	87.19(2)
P2-Re1-Br1	92.37(2)
C18-P1-C4	103.10(16)
C18-P1-C11	103.51(15)
C4-P1-C11	103.06(16)
C18-P1-Re1	119.48(12)
C4-P1-Re1	111.98(12)
C11-P1-Re1	113.89(11)
C25-P2-C32	103.36(17)
C25-P2-C39	101.42(16)
C32-P2-C39	106.03(15)
C25-P2-Re1	117.71(12)
C32-P2-Re1	118.32(11)
C39-P2-Re1	108.21(11)
C7-O4-C10	118.9(3)
C14-O5-C17	116.8(3)
C21-O6-C24	117.2(3)
C28-O7-C31	116.3(3)
C35-O8-C38	116.8(3)
C42-O9-C45	117.9(3)
O1-C1-Re1	178.9(3)
O2-C2-Re1	174.2(3)
O3-C3-Re1	175.8(3)
C9-C4-C5	117.3(3)
C9-C4-P1	122.9(3)
C5-C4-P1	119.8(3)
C4-C5-C6	121.9(4)
C7-C6-C5	118.9(4)
C8-C7-O4	116.2(3)
C8-C7-C6	120.0(3)
O4-C7-C6	123.7(3)
C7-C8-C9	120.8(4)
C8-C9-C4	121.1(4)
C12-C11-C16	117.3(3)
C12-C11-P1	120.4(3)
C16-C11-P1	122.2(3)
C13-C12-C11	121.9(3)
C12-C13-C14	120.2(3)
O5-C14-C15	125.1(4)
O5-C14-C13	115.8(3)
C15-C14-C13	119.1(4)
C14-C15-C16	120.0(3)
C15-C16-C11	121.4(3)

C23–C18–C19	118.6(3)
C23–C18–P1	120.8(3)
C19–C18–P1	120.4(3)
C20–C19–C18	120.8(3)
C19–C20–C21	119.5(3)
O6–C21–C22	116.0(3)
O6–C21–C20	123.8(3)
C22–C21–C20	120.2(3)
C21–C22–C23	119.6(3)
C18–C23–C22	121.2(3)
C26–C25–C30	117.5(3)
C26–C25–P2	119.9(3)
C30–C25–P2	122.6(3)
C25–C26–C27	122.4(3)
C28–C27–C26	119.3(3)
O7–C28–C27	124.4(3)
O7–C28–C29	115.9(3)
C27–C28–C29	119.8(3)
C30–C29–C28	119.8(3)
C29–C30–C25	121.1(3)
C33–C32–C37	117.2(3)
C33–C32–P2	121.4(3)
C37–C32–P2	121.0(3)
C34–C33–C32	121.9(3)
C35–C34–C33	119.6(3)
O8–C35–C34	125.2(3)
O8–C35–C36	115.3(3)
C34–C35–C36	119.5(3)
C37–C36–C35	120.2(4)
C36–C37–C32	121.6(3)
C40–C39–C44	117.6(3)
C40–C39–P2	124.9(3)
C44–C39–P2	117.2(3)
C39–C40–C41	121.8(3)
C42–C41–C40	119.4(3)
O9–C42–C41	125.3(3)
O9–C42–C43	114.8(3)
C41–C42–C43	119.9(3)
C44–C43–C42	119.4(3)
C43–C44–C39	121.9(3)

Symmetry transformations used to generate equivalent atoms:

Table 4. Anisotropic displacement parameters [$\text{\AA}^2 \times 10^3$]. The anisotropic displacement factor exponent takes the form: $-2\pi^2[h^2a^{*2}U^{11} + \dots + 2hk a^* b^* U^{12}]$.

Atom	U^{11}	U^{22}	U^{33}	U^{23}	U^{13}	U^{12}
Re1	20(1)	18(1)	18(1)	-1(1)	1(1)	1(1)
Br1	28(1)	40(1)	22(1)	5(1)	1(1)	-5(1)
P1	20(1)	20(1)	22(1)	-2(1)	1(1)	0(1)
P2	21(1)	21(1)	19(1)	1(1)	0(1)	0(1)
O1	30(1)	32(1)	25(2)	1(1)	1(1)	0(1)
O2	45(2)	33(2)	49(2)	0(1)	-3(2)	11(1)
O3	37(2)	24(1)	43(2)	-4(1)	-5(1)	-4(1)
O4	32(2)	37(2)	43(2)	0(1)	-4(1)	-15(1)
O5	75(2)	37(2)	29(2)	4(1)	4(1)	15(2)
O6	51(2)	28(1)	43(2)	-14(1)	3(1)	8(1)
O7	45(2)	28(1)	38(2)	12(1)	-3(1)	-2(1)
O8	65(2)	32(2)	24(2)	-10(1)	4(1)	-5(1)
O9	28(1)	48(2)	27(2)	-3(1)	4(1)	13(1)
C1	19(2)	21(2)	38(2)	-6(2)	-3(2)	1(1)
C2	28(2)	26(2)	29(2)	1(2)	1(2)	1(2)
C3	24(2)	24(2)	27(2)	0(2)	1(2)	4(1)
C4	20(2)	23(2)	29(2)	-4(1)	2(1)	0(1)
C5	25(2)	41(2)	27(2)	2(2)	-2(2)	-2(2)
C6	28(2)	35(2)	30(2)	4(2)	1(2)	0(2)
C7	24(2)	25(2)	36(2)	-2(2)	1(1)	-1(2)
C8	34(2)	40(2)	30(2)	-4(2)	-8(2)	-11(2)
C9	32(2)	31(2)	28(2)	0(2)	2(2)	-6(2)
C10	36(2)	43(3)	59(3)	15(2)	3(2)	-9(2)
C11	22(2)	22(2)	26(2)	2(1)	-1(1)	2(1)
C12	30(2)	22(2)	27(2)	-3(1)	0(2)	2(1)
C13	37(2)	30(2)	26(2)	-4(2)	-2(2)	10(2)
C14	38(2)	36(2)	23(2)	4(2)	0(2)	5(2)
C15	33(2)	26(2)	28(2)	0(2)	-4(2)	3(2)
C16	27(2)	24(2)	26(2)	-2(1)	-2(1)	5(1)
C17	86(4)	34(2)	32(2)	7(2)	5(2)	11(2)
C18	27(2)	23(2)	20(2)	-1(1)	4(1)	1(1)
C19	24(2)	34(2)	40(2)	-10(2)	-1(2)	1(2)
C20	26(2)	35(2)	42(2)	-9(2)	6(2)	7(2)
C21	35(2)	24(2)	32(2)	-5(2)	8(2)	2(2)
C22	33(2)	25(2)	29(2)	-2(2)	-1(2)	-1(2)
C23	24(2)	28(2)	24(2)	-2(2)	1(1)	1(1)
C24	50(3)	37(2)	79(4)	-22(2)	13(3)	13(2)
C25	28(2)	24(2)	21(2)	1(2)	3(1)	0(1)
C26	26(2)	28(2)	26(2)	2(2)	-1(1)	-5(1)
C27	28(2)	29(2)	32(2)	5(2)	-2(2)	1(2)
C28	39(2)	23(2)	24(2)	5(2)	3(2)	-2(2)
C29	26(2)	32(2)	48(3)	9(2)	0(2)	-7(2)
C30	27(2)	33(2)	44(3)	10(2)	-6(2)	-5(2)
C31	47(2)	34(2)	38(2)	10(2)	-2(2)	8(2)
C32	21(2)	25(2)	26(2)	-4(2)	-1(1)	-1(1)
C33	28(2)	26(2)	27(2)	2(2)	-5(2)	1(1)
C34	30(2)	24(2)	32(2)	-8(2)	0(2)	1(2)
C35	25(2)	30(2)	24(2)	-4(2)	2(1)	-1(1)
C36	31(2)	29(2)	21(2)	0(2)	2(1)	-1(1)
C37	25(2)	21(2)	25(2)	-2(1)	1(1)	1(1)
C38	88(3)	33(2)	33(3)	-14(2)	14(2)	-10(2)
C39	18(2)	23(2)	26(2)	-1(1)	0(1)	0(1)
C40	28(2)	30(2)	21(2)	1(2)	2(1)	1(2)
C41	25(2)	30(2)	23(2)	3(1)	-1(2)	4(1)
C42	24(2)	26(2)	28(2)	-2(2)	2(2)	2(1)
C43	28(2)	38(2)	17(2)	-6(2)	3(1)	1(2)
C44	25(2)	36(2)	27(2)	-1(2)	-5(2)	2(2)
C45	39(2)	58(3)	35(2)	8(2)	8(2)	25(2)

Table 5. Hydrogen coordinates [$\times 10^4$] and isotropic displacement parameters [$\text{\AA}^2 \times 10^3$].

Atom	<i>x</i>	<i>y</i>	<i>z</i>	<i>U_{eq}</i>	<i>S.o.f.</i>
H5	2592	457	6990	37	1
H6	1593	-231	7083	37	1
H8	1154	26	5376	42	1
H9	2126	729	5290	36	1
H10A	829	-1120	6920	69	1
H10B	11	-1095	6721	69	1
H10C	351	-507	7066	69	1
H12	3370	743	4879	32	1
H13	3321	1192	3961	37	1
H15	2972	2957	4673	35	1
H16	2977	2491	5597	31	1
H17A	2757	3223	3748	76	1
H17B	3229	3152	3177	76	1
H17C	3611	3239	3789	76	1
H19	2000	1944	6357	39	1
H20	1768	2883	6887	41	1
H22	3831	2868	7481	35	1
H23	4058	1936	6942	30	1
H24A	1896	3942	7087	83	1
H24B	2046	4282	7692	83	1
H24C	1651	3605	7673	83	1
H26	4410	2094	5761	32	1
H27	4384	3041	5219	36	1
H29	6493	3345	5620	42	1
H30	6507	2397	6156	42	1
H31A	4732	3728	4446	60	1
H31B	4919	4464	4557	60	1
H31C	4433	4082	5008	60	1
H33	5308	2652	7040	32	1
H34	5235	3014	8000	34	1
H36	5630	1191	8564	32	1
H37	5618	825	7612	28	1
H38A	5671	3235	8913	77	1
H38B	5349	3034	9525	77	1
H38C	4832	3107	8979	77	1
H40	6701	864	7103	31	1
H41	7768	335	6832	31	1
H43	7239	596	5129	34	1
H44	6183	1107	5410	35	1
H45A	8940	223	6383	66	1
H45B	9134	-341	5945	66	1
H45C	8507	-435	6406	66	1

Appendix C

Crystal tables for **2h**

Table 1. Crystal data and structure refinement.

Archive code	98_11IS07
Identification code	MAB1
Empirical formula	C ₄₅ H ₄₂ BrO ₃ P ₂ Re
Formula weight	958.84
Temperature	150(2) K
Wavelength	0.71073 Å [Mo-K _α]
Crystal system	Triclinic
Space group	<i>P</i> -1
Unit cell dimensions	<i>a</i> = 10.15740(10) Å α = 103.0460(6)° <i>b</i> = 10.3729(2) Å β = 94.8190(9)° <i>c</i> = 19.2892(3) Å γ = 92.1630(9)°
Volume	1969.52(5) Å ³
Z	2
Density (calculated)	1.617 Mg/m ³
Absorption coefficient	4.220 mm ⁻¹
<i>F</i> (000)	952
Crystal size	0.52 x 0.40 x 0.38 mm
Data collection range	2.06 ≤ θ ≤ 26.00°
Index ranges	-12 ≤ <i>h</i> ≤ 12, -12 ≤ <i>k</i> ≤ 12, -23 ≤ <i>l</i> ≤ 23
Reflections collected	34942
Independent reflections	7740 [<i>R</i> (int) = 0.0414]
Absorption correction	Empirical [<i>via</i> SORTAV]
Max. and min. transmission	0.2969 and 0.2176
Refinement method	Full-matrix least-squares on <i>F</i> ²
Data / restraints / parameters	7740 / 0 / 470
Goodness-of-fit on <i>F</i> ²	1.062
Final <i>R</i> indices [<i>I</i> >2σ(<i>I</i>)]	<i>R</i> ₁ = 0.0193, <i>wR</i> ₂ = 0.0476
<i>R</i> indices (all data)	<i>R</i> ₁ = 0.0201, <i>wR</i> ₂ = 0.0481
Largest diff. peak and hole	1.134 and -1.051 e.Å ⁻³
Extinction coefficient	0.0025(2)

Table 2. Atomic co-ordinates ($x \times 10^4$) and equivalent isotropic displacement parameters ($\text{\AA}^2 \times 10^3$) with estimated standard deviations (e.s.d.s) in parentheses. U_{eq} is defined as $1/3$ of the trace of the orthogonalized U_{ij} tensor.

	x	y	z	U_{eq}
Re(1)	9848.52(8)	-3.65(8)	1980.33(4)	15.33(5)
Br(1)	9753.9(2)	2259.8(2)	2938.34(14)	26.47(7)
C(1)	9973(2)	-1531(2)	1220.2(13)	19.9(5)
O(1)	10040.5(17)	-2355.7(18)	718.9(9)	27.2(4)
C(2)	9543(2)	952(3)	1227.5(14)	26.6(5)
O(2)	9264(2)	1428(2)	755.5(11)	41.6(5)
C(3)	7942(2)	-218(2)	1945.6(13)	21.4(5)
O(3)	6811.5(17)	-273.8(19)	1933.1(10)	31.8(4)
P(1)	12251.3(5)	722.8(6)	2137.9(3)	14.65(11)
C(111)	13473(2)	-346(2)	1661.9(12)	17.8(4)
C(112)	13646(2)	-1670(2)	1847.1(12)	17.5(4)
C(113)	14473(2)	-1795(2)	2442.7(12)	19.5(5)
C(114)	14645(2)	-3022(2)	2600.7(14)	24.0(5)
C(115)	14022(3)	-4149(2)	2156.0(15)	28.2(5)
C(116)	13223(3)	-4056(3)	1553.1(15)	29.9(6)
C(117)	13034(2)	-2820(2)	1404.4(13)	23.6(5)
C(121)	12983(2)	1149(2)	3085.6(12)	18.4(5)
C(122)	14007(2)	2296(2)	3297.1(11)	17.5(4)
C(123)	15326(2)	2158(2)	3169.7(13)	22.8(5)
C(124)	16236(2)	3246(3)	3350.8(14)	28.8(6)
C(125)	15836(3)	4481(3)	3670.9(14)	30.3(6)
C(126)	14531(3)	4633(2)	3807.5(14)	28.5(6)
C(127)	13624(2)	3551(2)	3616.4(13)	23.6(5)
C(131)	12505(2)	2292(2)	1825.4(12)	18.9(5)
C(132)	13309(3)	2190(2)	1196.7(13)	22.5(5)
C(133)	14661(3)	2461(3)	1294.2(17)	35.4(6)
C(134)	15378(4)	2322(4)	689(2)	60.0(11)
C(135)	14698(5)	1920(4)	10(2)	70.3(13)
C(136)	13374(5)	1691(4)	-80(2)	66.8(11)
C(137)	12669(4)	1812(3)	507.3(15)	42.7(7)
P(2)	9870.0(5)	-1352.9(6)	2899.4(3)	15.80(12)
C(211)	11422(2)	-2130(2)	3095.8(12)	20.1(5)
C(212)	11505(2)	-2774(2)	3726.2(12)	19.7(5)
C(213)	12185(2)	-2096(2)	4372.2(13)	24.4(5)
C(214)	12274(2)	-2654(3)	4963.4(14)	28.7(6)
C(215)	11671(2)	-3891(3)	4922.7(13)	26.9(5)
C(216)	10995(2)	-4578(2)	4283.8(13)	24.3(5)
C(217)	10928(2)	-4032(2)	3687.6(12)	20.4(5)
C(221)	9501(2)	-408(2)	3797.1(12)	22.3(5)

Table 2 (continued)

C(222)	8393(2)	-951(2)	4141.3(12)	19.5(5)
C(223)	8620(3)	-1775(2)	4611.5(13)	25.2(5)
C(224)	7593(3)	-2235(3)	4937.6(15)	36.5(7)
C(225)	6324(3)	-1881(3)	4805.6(15)	40.6(7)
C(226)	6075(3)	-1065(3)	4337.6(15)	39.2(7)
C(227)	7099(2)	-611(3)	4006.9(13)	27.4(5)
C(231)	8587(2)	-2737(2)	2677.1(12)	19.1(5)
C(232)	8555(2)	-3642(2)	1939.1(12)	21.9(5)
C(233)	9556(3)	-4491(2)	1738.1(13)	26.2(5)
C(234)	9500(3)	-5303(3)	1054.6(14)	32.3(6)
C(235)	8434(3)	-5286(3)	565.8(15)	37.0(7)
C(236)	7417(3)	-4471(3)	757.0(15)	37.3(7)
C(237)	7478(3)	-3652(3)	1439.7(14)	28.3(5)

Table 3. Anisotropic displacement parameters ($\text{\AA}^2 \times 10^3$). The anisotropic displacement factor exponent takes the form:

$$-2\pi^2[h^2a^{*2}U_{11} + \dots + 2hka^*b^*U_{12}]$$

	U_{11}	U_{22}	U_{33}	U_{23}	U_{13}	U_{12}
Re(1)	13.10(6)	16.40(6)	16.43(6)	3.52(4)	1.90(3)	0.54(3)
Br(1)	24.43(12)	19.02(12)	33.60(14)	-0.63(10)	6.46(10)	3.63(9)
C(1)	16.3(11)	25.4(13)	20.6(12)	10.5(10)	2.5(9)	0.5(9)
O(1)	31.8(10)	27.6(10)	20.2(9)	0.1(8)	5.3(7)	2.1(7)
C(2)	16.6(11)	27.8(13)	35.5(15)	8.2(11)	1.2(10)	-2.0(10)
O(2)	39.2(11)	48.7(13)	44.7(13)	32.1(11)	-8.7(9)	-1.7(9)
C(3)	23.7(13)	19.7(12)	19.6(12)	2.0(9)	2.4(9)	0.7(9)
O(3)	16.3(9)	39.7(11)	37.9(11)	5.4(9)	3.6(7)	1.5(7)
P(1)	13.6(3)	15.6(3)	14.8(3)	3.4(2)	2.2(2)	0.6(2)
C(111)	17.4(10)	19.8(11)	17.4(11)	5.2(9)	5.1(8)	3.1(9)
C(112)	14.8(10)	20.0(11)	18.6(11)	3.5(9)	7.9(8)	1.9(8)
C(113)	17.4(11)	19.0(11)	21.5(12)	2.8(9)	3.6(9)	1.1(9)
C(114)	22.2(12)	24.4(13)	27.5(13)	9.2(10)	4.4(10)	3.6(10)
C(115)	32.3(14)	18.3(12)	36.0(15)	7.8(11)	9.1(11)	5.3(10)
C(116)	34.3(14)	19.6(12)	31.8(14)	-2.4(10)	4.8(11)	-1.5(10)
C(117)	23.3(12)	25.7(13)	19.8(12)	0.8(10)	2.4(9)	3.2(10)
C(121)	19.2(11)	21.8(12)	14.6(11)	4.6(9)	2.0(8)	1.7(9)
C(122)	20.7(11)	21.1(11)	10.2(10)	3.4(9)	-0.9(8)	2.0(9)
C(123)	19.7(11)	23.8(12)	23.0(13)	2.3(10)	-2.0(9)	3.8(9)
C(124)	17.5(12)	35.1(15)	32.2(14)	7.3(12)	-3.8(10)	-2.0(10)
C(125)	31.6(14)	26.3(14)	30.0(14)	6.5(11)	-9.3(11)	-9.1(11)
C(126)	38.8(15)	18.9(12)	26.1(13)	1.9(10)	1.1(11)	3.6(10)
C(127)	26.9(12)	23.9(12)	20.1(12)	3.2(10)	5.4(9)	5.6(10)
C(131)	19.2(11)	17.8(11)	20.5(12)	6.9(9)	1.0(9)	-0.2(9)
C(132)	34.3(13)	15.5(11)	19.8(12)	6.8(9)	7.0(10)	1.8(9)
C(133)	31.8(14)	29.8(15)	51.9(18)	19.8(13)	16.2(13)	4.7(11)
C(134)	49(2)	48(2)	100(3)	40(2)	42(2)	13.0(16)
C(135)	109(4)	70(3)	48(2)	26(2)	52(2)	30(2)
C(136)	102(4)	71(3)	31.0(19)	13.1(18)	25(2)	8(2)
C(137)	65(2)	43.2(18)	21.1(14)	10.1(13)	3.5(13)	-0.9(15)
P(2)	17.0(3)	16.4(3)	13.0(3)	0.6(2)	4.0(2)	-0.6(2)
C(211)	21.1(11)	20.0(11)	20.4(12)	5.8(9)	5.8(9)	0(9)
C(212)	16.0(11)	24.0(12)	20.1(12)	5.3(9)	5.7(8)	4.7(9)
C(213)	21.3(12)	23.6(12)	26.7(13)	3.2(10)	0.7(9)	-0.2(9)
C(214)	26.5(13)	35.2(15)	21.9(13)	4.1(11)	-5.4(10)	2.7(11)
C(215)	28.5(13)	34.8(14)	19.9(12)	10.5(11)	2.3(10)	8.0(11)
C(216)	25.0(12)	21.7(12)	27.8(13)	6.9(10)	6.5(10)	3.3(9)
C(217)	22.6(11)	20.7(12)	17.6(12)	3.2(9)	2.6(9)	3.4(9)
C(221)	27.5(12)	20.1(12)	16.7(11)	-2.0(9)	4.8(9)	-0.6(9)
C(222)	21.2(11)	19.8(11)	14.1(11)	-3.9(9)	4.0(8)	0.5(9)
C(223)	30.8(13)	26.7(13)	18.2(12)	2.9(10)	6.1(10)	7.1(10)

Table 3 (continued)

C(224)	56.2(19)	31.3(15)	24.1(14)	6.0(11)	17.3(12)	1.3(13)
C(225)	39.6(16)	46.8(18)	29.8(15)	-5.7(13)	18.8(12)	-13.7(13)
C(226)	19.9(13)	61(2)	27.7(15)	-9.1(14)	4.4(10)	1.1(12)
C(227)	27.3(13)	36.0(15)	15.6(12)	-1.8(10)	1.1(9)	7.5(11)
C(231)	20.5(11)	19.1(11)	16.3(11)	0.6(9)	4.6(8)	-2.8(9)
C(232)	28.4(12)	17.2(11)	18.3(12)	0.3(9)	5.0(9)	-5.8(9)
C(233)	36.5(14)	21.2(12)	20.2(12)	3.5(10)	2.6(10)	2.1(10)
C(234)	45.9(16)	21.9(13)	26.0(14)	-3.5(11)	8.8(12)	3.3(11)
C(235)	52.0(18)	28.5(14)	22.0(14)	-10.0(11)	2.2(12)	-5.6(12)
C(236)	40.0(16)	38.4(16)	25.5(14)	-4.1(12)	-7.6(11)	-7.2(12)
C(237)	27.5(13)	27.2(13)	26.5(14)	-1.0(11)	2.7(10)	-4.1(10)

Table 4. Hydrogen atom co-ordinates ($\times 10^4$) and isotropic displacement parameters ($\text{\AA}^2 \times 10^3$) with e.s.d.s in parentheses.

	x	y	z	U_{eq}
H(111)	13211	-507	1142	21
H(111)	14344	154	1756	21
H(113)	14924	-1027	2745	23
H(114)	15192	-3086	3015	29
H(115)	14140	-4989	2263	34
H(116)	12806	-4833	1242	36
H(117)	12477	-2762	993	28
H(121)	12253	1348	3396	22
H(121)	13392	354	3190	22
H(123)	15611	1310	2956	27
H(124)	17132	3140	3254	35
H(125)	16457	5223	3797	36
H(126)	14255	5478	4032	34
H(127)	12725	3668	3705	28
H(131)	11626	2601	1698	23
H(131)	12945	2978	2229	23
H(133)	15102	2736	1762	42
H(134)	16310	2499	744	72
H(135)	15180	1806	-399	84
H(136)	12928	1446	-547	80
H(137)	11737	1636	443	51
H(211)	11576	-2812	2665	24
H(211)	12157	-1443	3175	24
H(213)	12593	-1241	4408	29
H(214)	12751	-2184	5397	34
H(215)	11720	-4266	5330	32
H(216)	10577	-5427	4253	29
H(217)	10483	-4521	3249	24
H(221)	10318	-328	4126	27
H(221)	9296	499	3757	27
H(223)	9493	-2026	4710	30
H(224)	7769	-2801	5255	44
H(225)	5624	-2193	5033	49
H(226)	5199	-815	4243	47
H(227)	6915	-59	3683	33
H(231)	8717	-3283	3035	23
H(231)	7711	-2359	2727	23
H(233)	10290	-4516	2074	31
H(234)	10196	-5869	925	39
H(235)	8399	-5835	97	44
H(236)	6676	-4470	422	45
H(237)	6775	-3093	1567	34

Table 5. Interatomic distances (\AA) with e.s.d.s in parentheses.

Re(1)-C(1)	1.917(2)	Re(1)-C(3)	1.935(2)
Re(1)-C(2)	1.946(3)	Re(1)-P(2)	2.4936(6)
Re(1)-P(1)	2.5000(5)	Re(1)-Br(1)	2.6504(3)
C(1)-O(1)	1.146(3)	C(2)-O(2)	1.150(3)
C(3)-O(3)	1.145(3)		
P(1)-C(111)	1.857(2)	P(1)-C(121)	1.863(2)
P(1)-C(131)	1.875(2)	C(111)-C(112)	1.507(3)
C(112)-C(117)	1.391(3)	C(112)-C(113)	1.398(3)
C(113)-C(114)	1.388(3)	C(114)-C(115)	1.380(4)
C(115)-C(116)	1.385(4)	C(116)-C(117)	1.392(4)
C(121)-C(122)	1.510(3)	C(122)-C(123)	1.389(3)
C(122)-C(127)	1.394(3)	C(123)-C(124)	1.393(3)
C(124)-C(125)	1.383(4)	C(125)-C(126)	1.381(4)
C(126)-C(127)	1.386(4)	C(131)-C(132)	1.505(3)
C(132)-C(133)	1.380(4)	C(132)-C(137)	1.394(4)
C(133)-C(134)	1.410(5)	C(134)-C(135)	1.397(6)
C(135)-C(136)	1.347(6)	C(136)-C(137)	1.375(5)
P(2)-C(211)	1.847(2)	P(2)-C(231)	1.852(2)
P(2)-C(221)	1.863(2)	C(211)-C(212)	1.512(3)
C(212)-C(217)	1.394(3)	C(212)-C(213)	1.396(3)
C(213)-C(214)	1.389(4)	C(214)-C(215)	1.383(4)
C(215)-C(216)	1.387(4)	C(216)-C(217)	1.390(3)
C(221)-C(222)	1.507(3)	C(222)-C(223)	1.392(3)
C(222)-C(227)	1.392(3)	C(223)-C(224)	1.386(4)
C(224)-C(225)	1.373(5)	C(225)-C(226)	1.386(5)
C(226)-C(227)	1.386(4)	C(231)-C(232)	1.515(3)
C(232)-C(233)	1.393(4)	C(232)-C(237)	1.394(4)
C(233)-C(234)	1.390(4)	C(234)-C(235)	1.378(4)
C(235)-C(236)	1.381(4)	C(236)-C(237)	1.392(4)

Table 6. Angles between interatomic vectors ($^{\circ}$) with e.s.d.s in parentheses

C(1)-Re(1)-C(3)	93.78(10)	C(1)-Re(1)-C(2)	85.67(10)
C(3)-Re(1)-C(2)	86.18(10)	C(1)-Re(1)-P(2)	92.59(7)
C(3)-Re(1)-P(2)	85.19(7)	C(2)-Re(1)-P(2)	171.07(7)
C(1)-Re(1)-P(1)	96.38(7)	C(3)-Re(1)-P(1)	169.06(7)
C(2)-Re(1)-P(1)	90.57(7)	P(2)-Re(1)-P(1)	98.34(2)
C(1)-Re(1)-Br(1)	173.99(7)	C(3)-Re(1)-Br(1)	88.44(7)
C(2)-Re(1)-Br(1)	88.91(8)	P(2)-Re(1)-Br(1)	93.157(14)
P(1)-Re(1)-Br(1)	81.048(14)		
O(1)-C(1)-Re(1)	172.8(2)	O(2)-C(2)-Re(1)	173.4(2)
O(3)-C(3)-Re(1)	176.4(2)		
C(111)-P(1)-C(121)	103.72(10)	C(111)-P(1)-C(131)	102.08(10)
C(121)-P(1)-C(131)	104.14(10)	C(111)-P(1)-Re(1)	120.69(7)
C(121)-P(1)-Re(1)	114.15(7)	C(131)-P(1)-Re(1)	110.25(7)
C(112)-C(111)-P(1)	116.9(2)	C(117)-C(112)-C(113)	117.8(2)
C(117)-C(112)-C(111)	120.5(2)	C(113)-C(112)-C(111)	121.6(2)
C(114)-C(113)-C(112)	121.2(2)	C(115)-C(114)-C(113)	119.9(2)
C(114)-C(115)-C(116)	120.0(2)	C(115)-C(116)-C(117)	119.8(2)
C(112)-C(117)-C(116)	121.2(2)	C(122)-C(121)-P(1)	117.0(2)
C(123)-C(122)-C(127)	118.1(2)	C(123)-C(122)-C(121)	122.3(2)
C(127)-C(122)-C(121)	119.5(2)	C(122)-C(123)-C(124)	120.8(2)
C(125)-C(124)-C(123)	120.1(2)	C(126)-C(125)-C(124)	119.8(2)
C(125)-C(126)-C(127)	120.0(2)	C(126)-C(127)-C(122)	121.2(2)
C(132)-C(131)-P(1)	115.6(2)	C(133)-C(132)-C(137)	120.0(3)
C(133)-C(132)-C(131)	121.0(2)	C(137)-C(132)-C(131)	119.0(2)
C(132)-C(133)-C(134)	119.0(3)	C(135)-C(134)-C(133)	119.0(3)
C(136)-C(135)-C(134)	121.5(3)	C(135)-C(136)-C(137)	119.8(4)
C(136)-C(137)-C(132)	120.7(4)		
C(211)-P(2)-C(231)	104.73(11)	C(211)-P(2)-C(221)	103.11(11)
C(231)-P(2)-C(221)	103.43(10)	C(211)-P(2)-Re(1)	117.48(7)
C(231)-P(2)-Re(1)	112.77(8)	C(221)-P(2)-Re(1)	113.83(8)
C(212)-C(211)-P(2)	117.5(2)	C(217)-C(212)-C(213)	118.3(2)
C(217)-C(212)-C(211)	122.4(2)	C(213)-C(212)-C(211)	119.4(2)
C(214)-C(213)-C(212)	120.9(2)	C(215)-C(214)-C(213)	120.2(2)
C(214)-C(215)-C(216)	119.5(2)	C(215)-C(216)-C(217)	120.3(2)
C(216)-C(217)-C(212)	120.7(2)	C(222)-C(221)-P(2)	117.9(2)
C(223)-C(222)-C(227)	117.8(2)	C(223)-C(222)-C(221)	121.9(2)
C(227)-C(222)-C(221)	120.3(2)	C(224)-C(223)-C(222)	121.1(2)
C(225)-C(224)-C(223)	120.5(3)	C(224)-C(225)-C(226)	119.4(3)
C(225)-C(226)-C(227)	120.2(3)	C(226)-C(227)-C(222)	121.1(3)
C(232)-C(231)-P(2)	116.3(2)	C(233)-C(232)-C(237)	118.0(2)
C(233)-C(232)-C(231)	122.6(2)	C(237)-C(232)-C(231)	119.4(2)
C(234)-C(233)-C(232)	121.1(2)	C(235)-C(234)-C(233)	120.0(3)
C(234)-C(235)-C(236)	120.0(2)	C(235)-C(236)-C(237)	120.0(3)
C(236)-C(237)-C(232)	120.9(3)		

Appendix D

Crystal tables for **2j**

Table 1. Crystal data and structure refinement for $\text{Mn}(\text{CO})_3\text{Br}(\text{dppe})\text{CHCl}_3$.

Identification code	99SRC056
Empirical formula	$\text{C}_{30}\text{H}_{25}\text{BrCl}_3\text{MnO}_3\text{P}_2$
Formula weight	736.64
Temperature	150(2) K
Wavelength	0.71073 Å
Crystal system	Monoclinic
Space group	$\text{P}2_1/c$
Unit cell dimensions	$a = 11.2561(7)$ Å $b = 19.5844(11)$ Å $c = 14.7549(9)$ Å $\beta = 108.075(3)^\circ$.
Volume	3092.1(3) Å ³
Z	4
Density (calculated)	1.582 Mg/m ³
Absorption coefficient	2.113 mm ⁻¹
F(000)	1480
Crystal size	0.20 x 0.05 x 0.05 mm ³
Theta range for data collection	2.92 to 24.71°.
Index ranges	-13 <= h <= 13, -23 <= k <= 23, -17 <= l <= 17
Reflections collected	49193
Independent reflections	5257 [R(int) = 0.1412]
Completeness to theta = 24.71°	96.6 %
Max. and min. transmission	0.9017 and 0.6773
Refinement method	Full-matrix least-squares on F ²
Data / restraints / parameters	5257 / 0 / 361
Goodness-of-fit on F ²	1.040
Final R indices [I>2sigma(I)]	R1 = 0.0567, wR2 = 0.1357
R indices (all data)	R1 = 0.1023, wR2 = 0.1574
Largest diff. peak and hole	1.133 and -0.531 e.Å ⁻³

Table 3. Bond lengths [Å] and angles [°] for Mn(CO)₃Br(dppe)CHCl₃.

Br(1)-Mn(1)	2.5198(10)	C(16)-C(17)	1.398(8)
Mn(1)-C(2)	1.818(7)	C(8)-C(9)	1.366(10)
Mn(1)-C(1)	1.827(6)	C(8)-C(7)	1.374(9)
Mn(1)-C(3)	1.953(9)	Cl(3)-C(30)	1.736(7)
Mn(1)-P(1)	2.3206(17)	C(23)-C(22)	1.397(8)
Mn(1)-P(2)	2.3325(17)	C(19)-C(20)	1.374(9)
P(2)-C(5)	1.821(6)	C(22)-C(21)	1.370(9)
P(2)-C(12)	1.830(5)	C(20)-C(21)	1.381(9)
P(2)-C(6)	1.832(6)	O(3)-C(3)	0.955(7)
P(1)-C(24)	1.823(6)		
P(1)-C(4)	1.828(5)	C(2)-Mn(1)-C(1)	93.0(2)
P(1)-C(18)	1.836(6)	C(2)-Mn(1)-C(3)	90.1(2)
Cl(1)-C(30)	1.761(7)	C(1)-Mn(1)-C(3)	90.7(2)
Cl(2)-C(30)	1.767(6)	C(2)-Mn(1)-P(1)	90.06(17)
O(1)-C(1)	1.121(6)	C(1)-Mn(1)-P(1)	90.56(18)
O(2)-C(2)	1.126(7)	C(3)-Mn(1)-P(1)	178.69(17)
C(11)-C(10)	1.372(9)	C(2)-Mn(1)-P(2)	92.72(17)
C(11)-C(6)	1.377(8)	C(1)-Mn(1)-P(2)	172.58(19)
C(18)-C(23)	1.369(8)	C(3)-Mn(1)-P(2)	93.96(17)
C(18)-C(19)	1.382(8)	P(1)-Mn(1)-P(2)	84.74(6)
C(5)-C(4)	1.528(8)	C(2)-Mn(1)-Br(1)	177.56(17)
C(25)-C(24)	1.382(8)	C(1)-Mn(1)-Br(1)	89.26(18)
C(25)-C(26)	1.392(8)	C(3)-Mn(1)-Br(1)	90.70(16)
C(24)-C(29)	1.395(8)	P(1)-Mn(1)-Br(1)	89.05(5)
C(6)-C(7)	1.384(9)	P(2)-Mn(1)-Br(1)	84.94(5)
C(26)-C(27)	1.377(9)	C(5)-P(2)-C(12)	105.9(3)
C(12)-C(17)	1.388(8)	C(5)-P(2)-C(6)	104.2(3)
C(12)-C(13)	1.397(8)	C(12)-P(2)-C(6)	101.4(3)
C(29)-C(28)	1.376(9)	C(5)-P(2)-Mn(1)	107.05(19)
C(15)-C(14)	1.372(8)	C(12)-P(2)-Mn(1)	113.74(18)
C(15)-C(16)	1.379(8)	C(6)-P(2)-Mn(1)	123.11(19)
C(10)-C(9)	1.370(9)	C(24)-P(1)-C(4)	106.8(3)
C(14)-C(13)	1.382(8)	C(24)-P(1)-C(18)	100.5(3)
C(27)-C(28)	1.380(9)	C(4)-P(1)-C(18)	103.6(3)

C(24)-P(1)-Mn(1)	117.08(19)	C(14)-C(15)-C(16)	120.0(6)
C(4)-P(1)-Mn(1)	107.80(19)	C(9)-C(10)-C(11)	119.6(6)
C(18)-P(1)-Mn(1)	119.75(19)	C(15)-C(14)-C(13)	120.7(6)
C(10)-C(11)-C(6)	122.1(6)	C(14)-C(13)-C(12)	120.4(5)
C(23)-C(18)-C(19)	119.4(5)	C(26)-C(27)-C(28)	120.1(6)
C(23)-C(18)-P(1)	121.3(4)	C(5)-C(4)-P(1)	110.4(4)
C(19)-C(18)-P(1)	119.2(4)	C(29)-C(28)-C(27)	119.4(6)
C(4)-C(5)-P(2)	109.8(4)	C(15)-C(16)-C(17)	119.8(6)
O(1)-C(1)-Mn(1)	179.0(5)	C(9)-C(8)-C(7)	120.8(7)
C(24)-C(25)-C(26)	120.1(6)	C(12)-C(17)-C(16)	120.7(6)
O(2)-C(2)-Mn(1)	179.0(5)	C(8)-C(9)-C(10)	119.4(6)
C(25)-C(24)-C(29)	118.5(5)	C(8)-C(7)-C(6)	120.8(7)
C(25)-C(24)-P(1)	122.6(4)	C(18)-C(23)-C(22)	120.3(6)
C(29)-C(24)-P(1)	118.8(5)	C(20)-C(19)-C(18)	120.6(6)
C(11)-C(6)-C(7)	117.3(6)	C(21)-C(22)-C(23)	119.6(6)
C(11)-C(6)-P(2)	120.9(5)	C(19)-C(20)-C(21)	119.9(6)
C(7)-C(6)-P(2)	121.8(5)	C(22)-C(21)-C(20)	120.2(6)
C(27)-C(26)-C(25)	120.4(6)	Cl(3)-C(30)-Cl(1)	111.5(4)
C(17)-C(12)-C(13)	118.4(5)	Cl(3)-C(30)-Cl(2)	110.6(4)
C(17)-C(12)-P(2)	124.0(4)	Cl(1)-C(30)-Cl(2)	108.9(4)
C(13)-C(12)-P(2)	117.5(4)	O(3)-C(3)-Mn(1)	176.6(6)
C(28)-C(29)-C(24)	121.5(6)		

Symmetry transformations used to generate equivalent atoms:

Appendix E

Crystal tables for **2m**



Table 1. Crystal data and structure refinement.

Identification code	99src306
Empirical formula	C ₃₇ H ₂₈ BrFeMnO ₃ P ₂
Formula weight	773.23
Temperature	150(2) K
Wavelength	0.71073 Å
Crystal system	Monoclinic
Space group	P2 ₁ /c
Unit cell dimensions	$a = 11.515(2)$ Å $\alpha = 90^\circ$ $b = 19.546(4)$ Å $\beta = 93.26(3)^\circ$ $c = 14.169(3)$ Å $\gamma = 90^\circ$
Volume	3183.9(11) Å ³
Z	4
Density (calculated)	1.613 Mg / m ³
Absorption coefficient	2.245 mm ⁻¹
$F(000)$	1560
Crystal	Block; orange
Crystal size	0.15 × 0.125 × 0.1 mm ³
θ range for data collection	1.77 – 27.49°
Index ranges	$-14 \leq h \leq 14, -21 \leq k \leq 25, -18 \leq l \leq 17$
Reflections collected	36700
Independent reflections	7273 [$R_{int} = 0.0652$]
Completeness to $\theta = 27.49^\circ$	96.8 %
Absorption correction	Semi-empirical from equivalents
Max. and min. transmission	0.804 and 0.668
Refinement method	Full-matrix least-squares on F^2
Data / restraints / parameters	7273 / 0 / 406
Goodness-of-fit on F^2	1.099
Final R indices [$F^2 > 2\sigma(F^2)$]	$RI = 0.0494, wR2 = 0.1433$
R indices (all data)	$RI = 0.0663, wR2 = 0.1549$
Largest diff. peak and hole	1.049 and -1.726 e Å ⁻³

Diffractometer: *Enraf Nonius KappaCCD* area detector (ϕ scans and ω scans to fill Ewald sphere). Data collection and cell refinement: *Denzo* (Z. Otwinowski & W. Minor, *Methods in Enzymology* (1997) Vol. 276: *Macromolecular Crystallography*, part A, pp. 307–326; C. W. Carter, Jr. & R. M. Sweet, Eds., Academic Press). Absorption correction: *SORTAV* (R. H. Blessing, *Acta Cryst. A51* (1995) 33–37; R. H. Blessing, *J. Appl. Cryst.* 30 (1997) 421–426). Program used to solve structure: *SHELXS97* (G. M. Sheldrick, *Acta Cryst.* (1990) A46 467–473). Program used to refine structure: *SHELXL97* (G. M. Sheldrick (1997), University of Göttingen, Germany).

Further information: <http://www.soton.ac.uk/~xservice/strat.htm>

Special details:

Table 2. Atomic coordinates [$\times 10^4$], equivalent isotropic displacement parameters [$\text{\AA}^2 \times 10^3$] and site occupancy factors. U_{eq} is defined as one third of the trace of the orthogonalized U^{ij} tensor.

Atom	x	y	z	U_{eq}	S.o.f.
br1	2534(1)	2387(1)	7072(1)	36(1)	1
fe1	3382(1)	1017(1)	9575(1)	18(1)	1
mn1	2037(1)	1187(1)	6572(1)	18(1)	1
p1	996(1)	886(1)	7932(1)	17(1)	1
p2	3886(1)	853(1)	7250(1)	16(1)	1
o1	2985(2)	1661(2)	4787(2)	41(1)	1
o2	-136(2)	1764(2)	5685(2)	42(1)	1
o3	1604(3)	-98(2)	5685(2)	38(1)	1
c1	4937(3)	690(2)	9127(2)	20(1)	1
c2	5118(3)	1063(2)	9982(2)	24(1)	1
c3	4677(3)	1734(2)	9830(2)	26(1)	1
c4	4191(3)	1777(2)	8885(2)	24(1)	1
c5	4347(3)	1124(2)	8439(2)	18(1)	1
c6	1715(3)	1329(2)	9788(2)	25(1)	1
c7	2268(3)	1088(2)	10646(2)	31(1)	1
c8	2601(3)	402(2)	10518(2)	26(1)	1
c9	2275(3)	208(2)	9572(2)	23(1)	1
c10	1703(3)	783(2)	9106(2)	20(1)	1
c11	165(3)	99(2)	7675(2)	21(1)	1
c12	314(3)	-525(2)	8143(2)	23(1)	1
c13	-301(3)	-1098(2)	7836(3)	28(1)	1
c14	-1105(3)	-1062(2)	7067(3)	27(1)	1
c15	-1302(3)	-441(2)	6629(3)	33(1)	1
c16	-675(3)	135(2)	6922(3)	29(1)	1
c17	-205(3)	1444(2)	8270(2)	21(1)	1
c18	-1085(3)	1155(2)	8780(3)	29(1)	1
c19	-1979(3)	1556(2)	9086(3)	33(1)	1
c20	-1996(3)	2253(2)	8888(3)	32(1)	1
c21	-1126(3)	2545(2)	8415(3)	30(1)	1
c22	-228(3)	2137(2)	8086(3)	26(1)	1
c23	4186(3)	-72(2)	7326(2)	18(1)	1
c24	5300(3)	-338(2)	7243(2)	23(1)	1
c25	5507(3)	-1034(2)	7314(2)	28(1)	1
c26	4608(3)	-1479(2)	7493(3)	28(1)	1
c27	3504(3)	-1225(2)	7586(2)	27(1)	1
c28	3285(3)	-527(2)	7496(2)	19(1)	1
c29	5102(3)	1123(2)	6561(2)	20(1)	1
c30	5999(3)	1527(2)	6938(2)	23(1)	1
c31	6959(3)	1669(2)	6412(3)	30(1)	1
c32	7017(3)	1397(2)	5512(3)	30(1)	1
c33	6114(3)	1001(2)	5126(2)	28(1)	1
c34	5162(3)	868(2)	5647(2)	24(1)	1
c35	2678(3)	1472(2)	5494(2)	26(1)	1
c36	675(3)	1532(2)	6051(2)	26(1)	1
c37	1758(3)	311(2)	5960(3)	26(1)	1

Table 3. Bond lengths [\AA] and angles [$^\circ$].

br1-mn1	2.5068(8)
fe1-c5	2.018(3)
fe1-c4	2.032(4)
fe1-c9	2.031(3)
fe1-c1	2.037(3)
fe1-c8	2.044(3)
fe1-c7	2.047(4)
fe1-c2	2.051(3)
fe1-c6	2.052(3)
fe1-c10	2.059(3)
fe1-c3	2.063(4)
mn1-c35	1.821(4)
mn1-c36	1.824(4)
mn1-c37	1.938(5)
mn1-p2	2.3769(11)
mn1-p1	2.4000(11)
p1-c10	1.822(3)
p1-c11	1.837(3)
p1-c17	1.846(3)
p2-c5	1.817(3)
p2-c29	1.829(3)
p2-c23	1.842(3)
o1-c35	1.143(4)
o2-c36	1.136(4)
o3-c37	0.903(4)
c1-c2	1.420(5)
c1-c5	1.435(5)
c2-c3	1.418(5)
c3-c4	1.424(5)
c4-c5	1.438(5)
c6-c7	1.421(5)
c6-c10	1.439(5)
c7-c8	1.409(6)
c8-c9	1.422(5)
c9-c10	1.443(5)
c11-c12	1.394(5)
c11-c16	1.400(5)
c12-c13	1.381(5)
c13-c14	1.391(5)
c14-c15	1.376(6)
c15-c16	1.389(5)
c17-c22	1.381(5)
c17-c18	1.395(5)
c18-c19	1.383(5)
c19-c20	1.391(6)
c20-c21	1.362(6)
c21-c22	1.406(5)
c23-c24	1.396(5)
c23-c28	1.397(5)
c24-c25	1.383(5)
c25-c26	1.386(5)
c26-c27	1.378(5)
c27-c28	1.393(5)
c29-c30	1.383(5)
c29-c34	1.394(5)
c30-c31	1.397(5)
c31-c32	1.387(5)
c32-c33	1.384(5)
c33-c34	1.381(5)

c5-fe1-c4	41.61(13)
c5-fe1-c9	116.92(14)
c4-fe1-c9	150.74(14)
c5-fe1-c1	41.44(13)
c4-fe1-c1	69.16(14)
c9-fe1-c1	108.49(14)
c5-fe1-c8	149.88(14)
c4-fe1-c8	167.19(14)
c9-fe1-c8	40.86(14)
c1-fe1-c8	116.48(14)
c5-fe1-c7	168.88(15)
c4-fe1-c7	129.17(16)
c9-fe1-c7	68.56(15)
c1-fe1-c7	148.34(14)
c8-fe1-c7	40.29(16)
c5-fe1-c2	69.37(13)
c4-fe1-c2	68.71(14)
c9-fe1-c2	129.52(14)
c1-fe1-c2	40.65(13)
c8-fe1-c2	107.46(14)
c7-fe1-c2	115.48(14)
c5-fe1-c6	130.42(14)
c4-fe1-c6	108.20(15)
c9-fe1-c6	68.87(14)
c1-fe1-c6	170.15(13)
c8-fe1-c6	68.21(15)
c7-fe1-c6	40.57(15)
c2-fe1-c6	148.26(14)
c5-fe1-c10	108.38(13)
c4-fe1-c10	117.07(14)
c9-fe1-c10	41.29(13)
c1-fe1-c10	130.94(13)
c8-fe1-c10	68.89(13)
c7-fe1-c10	68.77(14)
c2-fe1-c10	169.26(14)
c6-fe1-c10	40.96(13)
c5-fe1-c3	69.16(13)
c4-fe1-c3	40.69(14)
c9-fe1-c3	167.55(14)
c1-fe1-c3	68.21(14)
c8-fe1-c3	128.73(14)
c7-fe1-c3	107.54(15)
c2-fe1-c3	40.33(15)
c6-fe1-c3	116.44(15)
c10-fe1-c3	149.70(14)
c35-mn1-c36	85.85(16)
c35-mn1-c37	87.71(17)
c36-mn1-c37	91.62(15)
c35-mn1-p2	91.50(11)
c36-mn1-p2	174.17(12)
c37-mn1-p2	93.46(10)
c35-mn1-p1	173.36(11)
c36-mn1-p1	87.62(11)
c37-mn1-p1	93.72(12)
p2-mn1-p1	94.88(4)
c35-mn1-br1	81.56(12)
c36-mn1-br1	86.90(12)
c37-mn1-br1	169.25(12)
p2-mn1-br1	87.58(3)
p1-mn1-br1	96.85(3)

c10-p1-c11	106.84(16)
c10-p1-c17	97.49(15)
c11-p1-c17	99.02(15)
c10-p1-mn1	122.86(11)
c11-p1-mn1	108.95(11)
c17-p1-mn1	118.65(11)
c5-p2-c29	102.61(15)
c5-p2-c23	100.87(14)
c29-p2-c23	99.67(15)
c5-p2-mn1	120.16(11)
c29-p2-mn1	113.60(11)
c23-p2-mn1	116.96(11)
c2-c1-c5	108.4(3)
c2-c1-fe1	70.21(19)
c5-c1-fe1	68.57(18)
c3-c2-c1	108.2(3)
c3-c2-fe1	70.3(2)
c1-c2-fe1	69.14(19)
c2-c3-c4	108.3(3)
c2-c3-fe1	69.4(2)
c4-c3-fe1	68.5(2)
c3-c4-c5	108.0(3)
c3-c4-fe1	70.8(2)
c5-c4-fe1	68.66(19)
c1-c5-c4	107.0(3)
c1-c5-p2	124.0(2)
c4-c5-p2	129.0(3)
c1-c5-fe1	69.99(18)
c4-c5-fe1	69.73(18)
p2-c5-fe1	124.37(17)
c7-c6-c10	108.4(3)
c7-c6-fe1	69.5(2)
c10-c6-fe1	69.81(19)
c8-c7-c6	108.5(3)
c8-c7-fe1	69.8(2)
c6-c7-fe1	69.9(2)
c7-c8-c9	108.4(3)
c7-c8-fe1	69.9(2)
c9-c8-fe1	69.08(19)
c8-c9-c10	108.2(3)
c8-c9-fe1	70.1(2)
c10-c9-fe1	70.41(19)
c6-c10-c9	106.5(3)
c6-c10-p1	121.2(3)
c9-c10-p1	132.2(3)
c6-c10-fe1	69.23(19)
c9-c10-fe1	68.30(18)
p1-c10-fe1	129.25(17)
c12-c11-c16	117.9(3)
c12-c11-p1	126.1(3)
c16-c11-p1	116.0(3)
c13-c12-c11	120.8(3)
c12-c13-c14	120.8(3)
c15-c14-c13	118.9(3)
c14-c15-c16	120.7(4)
c15-c16-c11	120.8(4)
c22-c17-c18	119.2(3)
c22-c17-p1	122.5(3)
c18-c17-p1	118.2(3)
c19-c18-c17	120.6(3)
c18-c19-c20	119.6(3)

c21–c20–c19	120.6(3)
c20–c21–c22	120.0(4)
c17–c22–c21	120.0(3)
c24–c23–c28	118.2(3)
c24–c23–p2	122.1(3)
c28–c23–p2	119.7(2)
c25–c24–c23	121.0(3)
c24–c25–c26	120.2(3)
c27–c26–c25	119.6(3)
c26–c27–c28	120.4(3)
c27–c28–c23	120.5(3)
c30–c29–c34	119.2(3)
c30–c29–p2	122.5(3)
c34–c29–p2	118.2(3)
c29–c30–c31	120.3(3)
c32–c31–c30	119.7(3)
c33–c32–c31	120.3(3)
c32–c33–c34	119.7(3)
c33–c34–c29	120.8(3)
o1–c35–mn1	174.1(3)
o2–c36–mn1	175.9(3)
o3–c37–mn1	178.0(4)

Symmetry transformations used to generate equivalent atoms:

Table 4. Anisotropic displacement parameters [$\text{\AA}^2 \times 10^3$]. The anisotropic displacement factor exponent takes the form: $-2\pi^2[h^2a^{*2}U^{11} + \dots + 2hk a^* b^* U^{12}]$.

Atom	U^{11}	U^{22}	U^{33}	U^{23}	U^{13}	U^{12}
br1	34(1)	24(1)	50(1)	2(1)	0(1)	-1(1)
fe1	19(1)	19(1)	16(1)	-2(1)	2(1)	0(1)
mn1	17(1)	18(1)	20(1)	4(1)	1(1)	0(1)
p1	16(1)	14(1)	19(1)	1(1)	2(1)	0(1)
p2	16(1)	16(1)	17(1)	0(1)	2(1)	-1(1)
o1	38(2)	56(2)	29(1)	16(1)	3(1)	-4(1)
o2	26(1)	51(2)	47(2)	18(2)	-7(1)	5(1)
o3	29(2)	68(2)	15(1)	2(1)	3(1)	20(2)
c1	17(2)	23(2)	21(2)	0(1)	3(1)	1(1)
c2	20(2)	32(2)	20(2)	2(1)	0(1)	-3(1)
c3	30(2)	24(2)	25(2)	-8(2)	3(1)	-7(2)
c4	28(2)	21(2)	23(2)	-3(1)	4(1)	-3(1)
c5	18(2)	19(2)	18(2)	0(1)	2(1)	-2(1)
c6	24(2)	26(2)	27(2)	-7(2)	5(1)	2(1)
c7	24(2)	49(2)	19(2)	-9(2)	5(1)	-1(2)
c8	22(2)	33(2)	22(2)	8(2)	2(1)	-2(1)
c9	19(2)	24(2)	24(2)	5(1)	2(1)	-4(1)
c10	16(2)	23(2)	20(2)	0(1)	4(1)	1(1)
c11	18(2)	19(2)	25(2)	-2(1)	5(1)	-4(1)
c12	23(2)	18(2)	30(2)	3(1)	1(1)	-1(1)
c13	29(2)	19(2)	38(2)	0(2)	8(2)	-1(1)
c14	29(2)	25(2)	28(2)	-9(2)	9(1)	-11(2)
c15	35(2)	39(2)	26(2)	1(2)	-4(2)	-17(2)
c16	32(2)	26(2)	28(2)	7(2)	-6(1)	-12(2)
c17	18(2)	19(2)	24(2)	-2(1)	1(1)	2(1)
c18	28(2)	23(2)	37(2)	4(2)	7(2)	1(2)
c19	24(2)	39(2)	37(2)	-1(2)	14(2)	1(2)
c20	24(2)	33(2)	37(2)	-12(2)	4(2)	7(2)
c21	28(2)	21(2)	40(2)	-1(2)	0(2)	6(2)
c22	24(2)	22(2)	31(2)	1(2)	5(1)	0(1)
c23	23(2)	17(2)	14(1)	-3(1)	1(1)	1(1)
c24	23(2)	23(2)	24(2)	0(1)	1(1)	3(1)
c25	28(2)	30(2)	24(2)	-3(2)	-3(1)	9(2)
c26	38(2)	19(2)	26(2)	-3(1)	-5(2)	2(2)
c27	32(2)	22(2)	26(2)	-1(1)	-1(1)	-5(2)
c28	17(2)	22(2)	18(2)	-3(1)	1(1)	0(1)
c29	19(2)	21(2)	20(2)	2(1)	0(1)	0(1)
c30	24(2)	22(2)	24(2)	-1(1)	5(1)	-1(1)
c31	24(2)	32(2)	35(2)	1(2)	2(2)	-10(2)
c32	24(2)	37(2)	31(2)	7(2)	9(1)	-5(2)
c33	28(2)	37(2)	19(2)	0(2)	5(1)	0(2)
c34	26(2)	27(2)	19(2)	-1(1)	1(1)	-5(1)
c35	24(2)	31(2)	24(2)	3(2)	-3(1)	3(2)
c36	28(2)	26(2)	25(2)	4(2)	2(1)	-2(2)
c37	3(2)	22(2)	51(3)	31(2)	-8(1)	-6(1)

Appendix F

Crystal tables for **2r**



Table 1. Crystal data and structure refinement.

Identification code	00src068		
Empirical formula	$C_{37}H_{28}BrFeO_3P_2Re$		
Formula weight	904.49		
Temperature	150(2) K		
Wavelength	0.71073 Å		
Crystal system	Monoclinic		
Space group	$P2_1/c$		
Unit cell dimensions	$a = 9.21530(1)$ Å	$\alpha = 90^\circ$	
	$b = 54.1758(3)$ Å	$\beta = 111.999(3)^\circ$	
	$c = 21.76700(2)$ Å	$\gamma = 90^\circ$	
Volume	10075.9(6) Å ³		
Z	12		
Density (calculated)	1.789 Mg / m ³		
Absorption coefficient	5.353 mm ⁻¹		
$F(000)$	5280		
Crystal	Block; yellow		
Crystal size	0.07 × 0.07 × 0.05 mm ³		
θ range for data collection	2.94 – 25.05°		
Index ranges	–10 ≤ h ≤ 10, –64 ≤ k ≤ 64, –25 ≤ l ≤ 25		
Reflections collected	56559		
Independent reflections	17103 [$R_{int} = 0.0604$]		
Completeness to $\theta = 25.05^\circ$	96.1 %		
Max. and min. transmission	0.7756 and 0.7057		
Refinement method	Full-matrix least-squares on F^2		
Data / restraints / parameters	17103 / 1 / 1240		
Goodness-of-fit on F^2	1.000		
Final R indices [$F^2 > 2\sigma(F^2)$]	$RI = 0.0454$, $wR2 = 0.0928$		
R indices (all data)	$RI = 0.0715$, $wR2 = 0.1007$		
Largest diff. peak and hole	1.758 and –1.287 e Å ^{–3}		

Diffractometer: *Enraf Nonius KappaCCD* area detector (ϕ scans and ω scans to fill *Ewald* sphere). **Data collection and cell refinement:** *Denzo* (Z. Otwinowski & W. Minor, *Methods in Enzymology* (1997) Vol. 276: *Macromolecular Crystallography*, part A, pp. 307–326; C. W. Carter, Jr. & R. M. Sweet, Eds., Academic Press). **Absorption correction:** *SORTAV* (R. H. Blessing, *Acta Cryst. A51* (1995) 33–37; R. H. Blessing, *J. Appl. Cryst.* **30** (1997) 421–426). **Program used to solve structure:** *SHELXS97* (G. M. Sheldrick, *Acta Cryst.* (1990) **A46** 467–473). **Program used to refine structure:** *SHELXL97* (G. M. Sheldrick (1997), University of Göttingen, Germany).

Further information: <http://www.soton.ac.uk/~xservice/strat.htm>

Special details:

The asymmetric unit contains 3 independent molecules. The final structure was checked for additional crystallographic symmetry using the *Platon* program package. The comparison of the three independent molecules **I** (Re1), **II** (Re2) and **III** (Re3) shows that **I** and **II**_{inverted} have approximate the same geometry. In contrast, there are considerable geometric differences between **I** and **III**_{inverted} and between **III** and **II**. In each molecule the axial positions of the Re co-ordination occupied by Br and CO was found to be disordered. Partial occupancies for the major components were refined to 0.59, 0.56 and 0.75. The CHCl₃ solvate (19 e/cell) was treated in the manner described by Sluis and Spek (*Acta Cryst. A46* (1990), 194).

Table 2. Atomic coordinates [$\times 10^4$], equivalent isotropic displacement parameters [$\text{\AA}^2 \times 10^3$] and site occupancy factors. U_{eq} is defined as one third of the trace of the orthogonalized U^{ij} tensor.

Atom	x	y	z	U_{eq}	S.o.f.
Re1	3205(1)	-1095(1)	3304(1)	18(1)	1
Fe1	-453(1)	-541(1)	2504(1)	22(1)	1
Br1	4624(2)	-965(1)	2530(1)	25(1)	0.586(4)
C1	2330(16)	-1201(3)	3899(8)	42(4)	0.586(4)
O1	1717(13)	-1264(2)	4277(5)	32(3)	0.586(4)
Br1A	2176(3)	-1259(1)	4187(1)	27(1)	0.414(4)
C1A	4180(30)	-1004(5)	2745(13)	48(9)	0.414(4)
O1A	4810(20)	-923(4)	2383(10)	34(8)	0.414(4)
P2	708(2)	-1105(1)	2265(1)	19(1)	1
P1	2958(2)	-670(1)	3728(1)	19(1)	1
O2	6519(6)	-1144(1)	4373(3)	57(2)	1
O3	3860(6)	-1628(1)	3004(2)	33(1)	1
C2	5273(9)	-1111(1)	3986(3)	31(2)	1
C3	3531(8)	-1434(2)	3093(3)	22(2)	1
C21	-91(7)	-810(1)	1918(3)	20(2)	1
C22	813(8)	-598(1)	1934(3)	24(2)	1
C11	987(7)	-554(1)	3467(3)	21(2)	1
C12	-374(8)	-703(2)	3360(3)	32(2)	1
C13	-1698(8)	-548(2)	3110(3)	34(2)	1
C14	-1195(8)	-304(2)	3061(3)	31(2)	1
C15	482(8)	-306(1)	3291(3)	25(2)	1
C23	-189(8)	-393(1)	1679(3)	26(2)	1
C24	-1742(8)	-473(1)	1526(3)	28(2)	1
C25	-1706(8)	-731(1)	1660(3)	30(2)	1
C31	3972(7)	-391(1)	3611(3)	20(2)	1
C32	4170(8)	-193(1)	4029(3)	30(2)	1
C33	4769(9)	25(1)	3916(4)	39(2)	1
C34	5177(8)	52(2)	3377(4)	36(2)	1
C35	4969(8)	-140(2)	2948(4)	31(2)	1
C36	4415(7)	-365(1)	3063(3)	25(2)	1
C41	3635(8)	-673(1)	4640(3)	20(2)	1
C42	5252(9)	-692(1)	5012(3)	36(2)	1
C43	5761(10)	-692(1)	5697(4)	42(2)	1
C44	4742(10)	-683(1)	6015(4)	41(2)	1
C45	3179(10)	-660(1)	5651(4)	38(2)	1
C46	2632(8)	-658(1)	4962(3)	27(2)	1
C51	1142(7)	-1253(1)	1595(3)	18(2)	1
C52	1399(7)	-1119(1)	1095(3)	23(2)	1
C53	1799(8)	-1241(2)	616(3)	28(2)	1
C54	1944(7)	-1489(2)	632(3)	30(2)	1
C55	1703(8)	-1629(1)	1124(3)	27(2)	1
C56	1307(8)	-1507(1)	1596(3)	25(2)	1
C61	-1064(7)	-1275(1)	2201(3)	19(2)	1
C62	-2212(8)	-1313(1)	1575(3)	25(2)	1
C63	-3606(8)	-1428(1)	1501(3)	32(2)	1
C64	-3880(8)	-1515(1)	2037(3)	29(2)	1
C65	-2720(8)	-1488(1)	2664(3)	29(2)	1
C66	-1341(7)	-1366(1)	2743(3)	23(2)	1
Re2	2114(1)	-698(1)	-1732(1)	19(1)	1
Fe2	5932(1)	-1245(1)	-1099(1)	21(1)	1
Br2	2900(2)	-543(1)	-2697(1)	30(1)	0.562(4)
C1'	1320(20)	-777(3)	-1074(8)	43(5)	0.562(4)
O1'	782(16)	-830(3)	-673(7)	37(4)	0.562(4)
Br2A	865(4)	-811(1)	-882(2)	25(1)	0.438(4)
C1'A	2830(20)	-611(4)	-2417(10)	25(5)	0.438(4)
O1'A	3250(20)	-564(4)	-2852(9)	42(7)	0.438(4)
P1'	2289(2)	-1122(1)	-2171(1)	19(1)	1

P2'	4753(2)	-693(1)	-774(1)	19(1)	1
O1'	-1349(6)	-646(1)	-2664(3)	51(2)	1
O2'	1852(7)	-141(1)	-1516(2)	47(2)	1
C1'	-80(9)	-675(1)	-2344(4)	33(2)	1
C2'	1973(8)	-350(2)	-1563(3)	32(2)	1
C11'	5701(8)	-987(1)	-475(3)	20(2)	1
C12'	7321(8)	-1054(1)	-287(3)	25(2)	1
C13'	7457(8)	-1308(2)	-140(3)	33(2)	1
C14'	5971(8)	-1405(1)	-234(3)	23(2)	1
C15'	4872(8)	-1208(1)	-440(3)	23(2)	1
C21'	4243(7)	-1227(1)	-2020(3)	18(2)	1
C22'	4826(8)	-1475(1)	-1886(3)	25(2)	1
C23'	6453(8)	-1467(2)	-1754(3)	29(2)	1
C24'	6908(8)	-1220(2)	-1806(3)	29(2)	1
C25'	5553(7)	-1068(1)	-1968(3)	27(2)	1
C31'	1393(7)	-1397(1)	-1960(3)	22(2)	1
C32'	1025(7)	-1403(1)	-1397(3)	23(2)	1
C33'	452(8)	-1621(1)	-1235(3)	30(2)	1
C34'	196(8)	-1828(1)	-1628(4)	31(2)	1
C35'	524(8)	-1817(1)	-2202(3)	30(2)	1
C36'	1125(7)	-1605(1)	-2369(3)	25(2)	1
C41'	1408(8)	-1134(1)	-3084(3)	20(2)	1
C42'	-212(8)	-1108(1)	-3393(3)	29(2)	1
C43'	-873(9)	-1109(1)	-4084(3)	35(2)	1
C44'	30(10)	-1134(1)	-4456(3)	37(2)	1
C45'	1616(9)	-1166(1)	-4146(3)	30(2)	1
C46'	2310(8)	-1170(1)	-3461(3)	26(2)	1
C51'	4443(7)	-568(1)	-57(3)	18(2)	1
C52'	4172(8)	-317(1)	-18(3)	28(2)	1
C53'	3810(8)	-218(1)	489(3)	31(2)	1
C54'	3726(8)	-377(2)	984(3)	34(2)	1
C55'	4044(8)	-621(2)	977(3)	30(2)	1
C56'	4398(7)	-719(1)	457(3)	25(2)	1
C61'	6399(8)	-502(1)	-784(3)	22(2)	1
C62'	6437(8)	-402(1)	-1359(3)	28(2)	1
C63'	7713(9)	-269(1)	-1355(4)	34(2)	1
C64'	9017(9)	-241(1)	-764(4)	35(2)	1
C65'	8958(8)	-337(1)	-183(4)	33(2)	1
C66'	7659(8)	-467(1)	-194(3)	28(2)	1
Re3	2581(1)	-2572(1)	-461(1)	20(1)	1
Fe3	-820(1)	-3068(1)	-1(1)	19(1)	1
Br3	3142(2)	-2973(1)	-1004(1)	28(1)	0.750(4)
C1"	2367(13)	-2251(3)	-144(5)	27(3)	0.750(4)
O1"	2239(12)	-2058(2)	64(5)	48(4)	0.750(4)
Br3A	2508(7)	-2119(1)	-63(3)	33(2)	0.250(4)
C1"A	2850(50)	-2880(4)	-820(20)	59(14)	0.250(4)
O1"A	3240(40)	-3071(6)	-1002(16)	42(14)	0.250(4)
P1"	-245(2)	-2665(1)	-1087(1)	19(1)	1
P2"	2708(2)	-2755(1)	624(1)	20(1)	1
O2"	2529(5)	-2301(1)	-1713(2)	40(1)	1
O3"	6176(6)	-2517(1)	136(2)	38(1)	1
C2"	2552(8)	-2408(1)	-1250(4)	27(2)	1
C3"	4854(8)	-2534(1)	-65(3)	25(2)	1
C11"	-1053(7)	-2944(1)	-917(3)	19(2)	1
C12"	-304(8)	-3184(1)	-787(3)	19(2)	1
C14"	-2730(8)	-3227(1)	-718(3)	24(2)	1
C13"	-1332(8)	-3354(1)	-672(3)	23(2)	1
C15"	-2573(7)	-2975(1)	-881(3)	22(2)	1
C21"	1023(7)	-2899(1)	713(3)	16(2)	1
C22"	935(7)	-3152(1)	895(3)	22(2)	1
C23"	-575(8)	-3188(1)	931(3)	23(2)	1

C24"	-1414(8)	-2964(1)	774(3)	23(2)	1
C25"	-436(7)	-2783(1)	638(3)	20(2)	1
C31"	-1655(7)	-2426(1)	-1065(3)	21(2)	1
C32"	-1273(8)	-2276(1)	-522(3)	24(2)	1
C33"	-2322(8)	-2088(1)	-493(4)	30(2)	1
C34"	-3710(8)	-2060(1)	-1015(4)	32(2)	1
C35"	-4097(8)	-2212(2)	-1570(4)	35(2)	1
C36"	-3084(8)	-2394(1)	-1588(3)	25(2)	1
C41"	-674(7)	-2701(1)	-1975(3)	17(2)	1
C42"	-944(7)	-2493(1)	-2396(3)	25(2)	1
C43"	-1274(8)	-2522(1)	-3064(3)	27(2)	1
C44"	-1298(8)	-2753(2)	-3333(4)	32(2)	1
C45"	-1008(8)	-2958(1)	-2919(3)	27(2)	1
C46"	-696(7)	-2932(1)	-2248(3)	24(2)	1
C51"	3270(7)	-2524(1)	1292(3)	20(2)	1
C52"	2480(8)	-2496(1)	1715(3)	28(2)	1
C53"	2925(8)	-2313(1)	2207(3)	31(2)	1
C54"	4159(8)	-2162(1)	2276(3)	27(2)	1
C55"	4964(8)	-2190(1)	1867(3)	29(2)	1
C56"	4507(8)	-2364(1)	1362(3)	27(2)	1
C61"	4188(8)	-2994(1)	963(3)	24(2)	1
C62"	4167(8)	-3207(1)	592(3)	31(2)	1
C63"	5210(9)	-3399(2)	858(4)	40(2)	1
C64"	6294(9)	-3384(2)	1498(4)	39(2)	1
C65"	6351(8)	-3175(2)	1862(4)	39(2)	1
C66"	5306(8)	-2981(2)	1610(3)	32(2)	1

Table 3. Bond lengths [Å] and angles [°].

Re1-C1A	1.83(3)
Re1-C1	1.855(19)
Re1-C2	1.930(7)
Re1-C3	1.943(8)
Re1-P1	2.5180(18)
Re1-P2	2.5520(16)
Re1-Br1	2.586(3)
Re1-Br1A	2.597(3)
Fe1-C22	2.018(7)
Fe1-C11	2.020(6)
Fe1-C12	2.035(7)
Fe1-C25	2.043(7)
Fe1-C21	2.044(6)
Fe1-C24	2.046(6)
Fe1-C15	2.049(6)
Fe1-C13	2.047(7)
Fe1-C14	2.055(7)
Fe1-C23	2.063(7)
C1-O1	1.21(2)
C1A-O1A	1.23(3)
P2-C21	1.803(7)
P2-C51	1.833(6)
P2-C61	1.833(7)
P1-C11	1.802(7)
P1-C41	1.846(6)
P1-C31	1.847(7)
O2-C2	1.155(7)
O3-C3	1.135(7)
C21-C22	1.411(9)
C21-C25	1.446(9)
C22-C23	1.419(9)
C22-H22	0.9500
C11-C15	1.426(9)
C11-C12	1.434(9)
C12-C13	1.413(10)
C12-H12	0.9500
C13-C14	1.418(10)
C13-H13	0.9500
C14-C15	1.436(9)
C14-H14	0.9500
C15-H15	0.9500
C23-C24	1.410(9)
C23-H23	0.9500
C24-C25	1.425(9)
C24-H24	0.9500
C25-H25	0.9500
C31-C32	1.373(9)
C31-C36	1.405(8)
C32-C33	1.362(9)
C32-H32	0.9500
C33-C34	1.368(9)
C33-H33	0.9500
C34-C35	1.361(10)
C34-H34	0.9500
C35-C36	1.380(9)
C35-H35	0.9500
C36-H36	0.9500
C41-C46	1.355(9)
C41-C42	1.408(9)

C42–C43	1.386(9)
C42–H42	0.9500
C43–C44	1.362(11)
C43–H43	0.9500
C44–C45	1.365(10)
C44–H44	0.9500
C45–C46	1.391(9)
C45–H45	0.9500
C46–H46	0.9500
C51–C56	1.386(9)
C51–C52	1.400(9)
C52–C53	1.396(9)
C52–H52	0.9500
C53–C54	1.351(9)
C53–H53	0.9500
C54–C55	1.397(9)
C54–H54	0.9500
C55–C56	1.382(9)
C55–H55	0.9500
C56–H56	0.9500
C61–C66	1.387(8)
C61–C62	1.391(8)
C62–C63	1.382(9)
C62–H62	0.9500
C63–C64	1.366(9)
C63–H63	0.9500
C64–C65	1.390(9)
C64–H64	0.9500
C65–C66	1.384(9)
C65–H65	0.9500
C66–H66	0.9500
Re2–C1'A	1.90(2)
Re2–C2'	1.932(9)
Re2–C1'	1.89(2)
Re2–C1'	1.965(8)
Re2–P1'	2.5191(18)
Re2–P2'	2.5428(17)
Re2–Br2A	2.591(3)
Re2–Br2	2.604(2)
Fe2–C11'	2.018(7)
Fe2–C21'	2.027(6)
Fe2–C15'	2.027(7)
Fe2–C25'	2.032(7)
Fe2–C12'	2.037(6)
Fe2–C22'	2.052(7)
Fe2–C23'	2.054(7)
Fe2–C24'	2.057(7)
Fe2–C14'	2.060(6)
Fe2–C13'	2.062(6)
C1'–O1'	1.19(3)
C1'A–O1'A	1.17(3)
P1'–C21'	1.797(7)
P1'–C31'	1.841(7)
P1'–C41'	1.846(6)
P2'–C11'	1.815(7)
P2'–C51'	1.817(7)
P2'–C61'	1.844(7)
O1'–C1'	1.126(8)
O2'–C2'	1.148(8)
C11'–C15'	1.437(9)
C11'–C12'	1.439(9)

C12'–C13'	1.410(10)
C12'–H12'	0.9500
C13'–C14'	1.408(9)
C13'–H13'	0.9500
C14'–C15'	1.422(9)
C14'–H14'	0.9500
C15'–H15'	0.9500
C21'–C22'	1.437(9)
C21'–C25'	1.454(9)
C22'–C23'	1.418(9)
C22'–H22'	0.9500
C23'–C24'	1.421(10)
C23'–H23'	0.9500
C24'–C25'	1.427(9)
C24'–H24'	0.9500
C25'–H25'	0.9500
C31'–C32'	1.389(8)
C31'–C36'	1.399(9)
C32'–C33'	1.394(9)
C32'–H32'	0.9500
C33'–C34'	1.377(10)
C33'–H33'	0.9500
C34'–C35'	1.394(9)
C34'–H34'	0.9500
C35'–C36'	1.382(9)
C35'–H35'	0.9500
C36'–H36'	0.9500
C41'–C46'	1.383(9)
C41'–C42'	1.396(9)
C42'–C43'	1.397(9)
C42'–H42'	0.9500
C43'–C44'	1.367(10)
C43'–H43'	0.9500
C44'–C45'	1.372(10)
C44'–H44'	0.9500
C45'–C46'	1.384(8)
C45'–H45'	0.9500
C46'–H46'	0.9500
C51'–C52'	1.393(9)
C51'–C56'	1.398(9)
C52'–C53'	1.375(9)
C52'–H52'	0.9500
C53'–C54'	1.403(10)
C53'–H53'	0.9500
C54'–C55'	1.360(10)
C54'–H54'	0.9500
C55'–C56'	1.395(9)
C55'–H55'	0.9500
C56'–H56'	0.9500
C61'–C62'	1.377(9)
C61'–C66'	1.385(9)
C62'–C63'	1.375(9)
C62'–H62'	0.9500
C63'–C64'	1.402(10)
C63'–H63'	0.9500
C64'–C65'	1.387(9)
C64'–H64'	0.9500
C65'–C66'	1.382(9)
C65'–H65'	0.9500
C66'–H66'	0.9500
Re3–Cl" A	1.900(3)

Re3-C2"	1.927(8)
Re3-C1"	1.909(14)
Re3-C3"	1.954(7)
Re3-P1"	2.4961(17)
Re3-P2"	2.5223(17)
Re3-Br3	2.6171(18)
Re3-Br3A	2.615(7)
Fe3-C25"	2.022(6)
Fe3-C12"	2.037(6)
Fe3-C11"	2.036(6)
Fe3-C24"	2.038(7)
Fe3-C21"	2.040(6)
Fe3-C15"	2.052(6)
Fe3-C14"	2.052(6)
Fe3-C13"	2.056(6)
Fe3-C23"	2.061(6)
Fe3-C22"	2.064(6)
C1"-O1"	1.16(2)
C1"A-O1"A	1.21(3)
P1"-C11"	1.788(7)
P1"-C41"	1.832(6)
P1"-C31"	1.845(7)
P2"-C21"	1.812(7)
P2"-C61"	1.824(7)
P2"-C51"	1.840(7)
O2"-C2"	1.154(8)
O3"-C3"	1.134(7)
C11"-C15"	1.441(9)
C11"-C12"	1.446(9)
C12"-C13"	1.409(9)
C12"-H12"	0.9500
C14"-C15"	1.427(9)
C14"-C13"	1.430(9)
C14"-H13"	0.9500
C13"-H14"	0.9500
C15"-H15"	0.9500
C21"-C22"	1.436(9)
C21"-C25"	1.438(9)
C22"-C23"	1.437(9)
C22"-H22"	0.9500
C23"-C24"	1.409(9)
C23"-H23"	0.9500
C24"-C25"	1.436(9)
C24"-H24"	0.9500
C25"-H25"	0.9500
C31"-C32"	1.371(9)
C31"-C36"	1.392(8)
C32"-C33"	1.420(9)
C32"-H32"	0.9500
C33"-C34"	1.364(9)
C33"-H33"	0.9500
C34"-C35"	1.393(10)
C34"-H34"	0.9500
C35"-C36"	1.371(9)
C35"-H35"	0.9500
C36"-H36"	0.9500
C41"-C46"	1.383(9)
C41"-C42"	1.414(9)
C42"-C43"	1.380(9)
C42"-H42"	0.9500
C43"-C44"	1.378(9)

C43"-H43"	0.9500
C44"-C45"	1.391(9)
C44"-H44"	0.9500
C45"-C46"	1.387(8)
C45"-H45"	0.9500
C46"-H46"	0.9500
C51"-C52"	1.379(9)
C51"-C56"	1.394(9)
C52"-C53"	1.400(9)
C52"-H52"	0.9500
C53"-C54"	1.363(9)
C53"-H53"	0.9500
C54"-C55"	1.365(9)
C54"-H54"	0.9500
C55"-C56"	1.387(9)
C55"-H55"	0.9500
C56"-H56"	0.9500
C61"-C66"	1.401(9)
C61"-C62"	1.405(9)
C62"-C63"	1.387(9)
C62"-H62"	0.9500
C63"-C64"	1.380(10)
C63"-H63"	0.9500
C64"-C65"	1.371(10)
C64"-H64"	0.9500
C65"-C66"	1.392(10)
C65"-H65"	0.9500
C66"-H66"	0.9500
C1A-Re1-C1	176.1(9)
C1A-Re1-C2	86.4(8)
C1-Re1-C2	90.6(5)
C1A-Re1-C3	86.5(8)
C1-Re1-C3	91.0(5)
C2-Re1-C3	86.7(3)
C1A-Re1-P1	97.7(8)
C1-Re1-P1	84.6(5)
C2-Re1-P1	87.7(2)
C3-Re1-P1	172.76(19)
C1A-Re1-P2	85.4(7)
C1-Re1-P2	97.4(4)
C2-Re1-P2	169.6(2)
C3-Re1-P2	86.42(19)
P1-Re1-P2	99.79(6)
C1A-Re1-Br1	1.0(8)
C1-Re1-Br1	175.4(5)
C2-Re1-Br1	85.4(2)
C3-Re1-Br1	86.7(2)
P1-Re1-Br1	97.33(6)
P2-Re1-Br1	86.41(6)
C1A-Re1-Br1A	172.0(8)
C1-Re1-Br1A	4.2(5)
C2-Re1-Br1A	86.7(2)
C3-Re1-Br1A	89.0(2)
P1-Re1-Br1A	86.15(6)
P2-Re1-Br1A	100.95(6)
Br1-Re1-Br1A	171.25(6)
C22-Fe1-C11	109.0(3)
C22-Fe1-C12	131.7(3)
C11-Fe1-C12	41.4(3)
C22-Fe1-C25	68.5(3)

C11–Fe1–C25	147.9(3)
C12–Fe1–C25	114.9(3)
C22–Fe1–C21	40.6(3)
C11–Fe1–C21	115.2(3)
C12–Fe1–C21	107.8(3)
C25–Fe1–C21	41.4(2)
C22–Fe1–C24	68.4(3)
C11–Fe1–C24	170.5(3)
C12–Fe1–C24	147.0(3)
C25–Fe1–C24	40.8(3)
C21–Fe1–C24	69.3(3)
C22–Fe1–C15	116.7(3)
C11–Fe1–C15	41.0(3)
C12–Fe1–C15	69.0(3)
C25–Fe1–C15	169.7(3)
C21–Fe1–C15	148.1(3)
C24–Fe1–C15	131.0(3)
C22–Fe1–C13	170.1(3)
C11–Fe1–C13	68.8(3)
C12–Fe1–C13	40.5(3)
C25–Fe1–C13	107.9(3)
C21–Fe1–C13	130.7(3)
C24–Fe1–C13	115.3(3)
C15–Fe1–C13	68.5(3)
C22–Fe1–C14	148.8(3)
C11–Fe1–C14	69.0(3)
C12–Fe1–C14	68.6(3)
C25–Fe1–C14	130.2(3)
C21–Fe1–C14	169.6(3)
C24–Fe1–C14	108.0(3)
C15–Fe1–C14	41.0(3)
C13–Fe1–C14	40.4(3)
C22–Fe1–C23	40.7(2)
C11–Fe1–C23	132.2(3)
C12–Fe1–C23	171.5(3)
C25–Fe1–C23	68.0(3)
C21–Fe1–C23	68.6(3)
C24–Fe1–C23	40.1(3)
C15–Fe1–C23	109.6(3)
C13–Fe1–C23	147.6(3)
C14–Fe1–C23	116.3(3)
O1–C1–Re1	177.6(14)
O1A–C1A–Re1	175(2)
C21–P2–C51	103.2(3)
C21–P2–C61	101.6(3)
C51–P2–C61	100.0(3)
C21–P2–Re1	116.3(2)
C51–P2–Re1	108.8(2)
C61–P2–Re1	124.1(2)
C11–P1–C41	103.6(3)
C11–P1–C31	99.9(3)
C41–P1–C31	99.8(3)
C11–P1–Re1	115.0(2)
C41–P1–Re1	110.2(2)
C31–P1–Re1	125.4(2)
O2–C2–Re1	173.4(6)
O3–C3–Re1	173.9(6)
C22–C21–C25	106.2(6)
C22–C21–P2	124.5(5)
C25–C21–P2	128.7(6)
C22–C21–Fe1	68.7(4)

C25–C21–Fe1	69.2(4)
P2–C21–Fe1	120.4(3)
C21–C22–C23	109.7(6)
C21–C22–Fe1	70.7(4)
C23–C22–Fe1	71.4(4)
C21–C22–H22	125.2
C23–C22–H22	125.2
Fe1–C22–H22	124.4
C15–C11–C12	108.0(6)
C15–C11–P1	127.0(5)
C12–C11–P1	124.8(6)
C15–C11–Fe1	70.6(4)
C12–C11–Fe1	69.8(4)
P1–C11–Fe1	122.1(3)
C13–C12–C11	107.7(7)
C13–C12–Fe1	70.2(4)
C11–C12–Fe1	68.7(4)
C13–C12–H12	126.2
C11–C12–H12	126.2
Fe1–C12–H12	126.5
C12–C13–C14	109.0(7)
C12–C13–Fe1	69.3(4)
C14–C13–Fe1	70.1(4)
C12–C13–H13	125.5
C14–C13–H13	125.5
Fe1–C13–H13	126.7
C13–C14–C15	107.7(6)
C13–C14–Fe1	69.5(4)
C15–C14–Fe1	69.3(4)
C13–C14–H14	126.2
C15–C14–H14	126.2
Fe1–C14–H14	126.6
C11–C15–C14	107.6(6)
C11–C15–Fe1	68.4(4)
C14–C15–Fe1	69.7(4)
C11–C15–H15	126.2
C14–C15–H15	126.2
Fe1–C15–H15	127.2
C24–C23–C22	107.8(7)
C24–C23–Fe1	69.3(4)
C22–C23–Fe1	68.0(4)
C24–C23–H23	126.1
C22–C23–H23	126.1
Fe1–C23–H23	128.2
C23–C24–C25	108.0(6)
C23–C24–Fe1	70.6(4)
C25–C24–Fe1	69.5(4)
C23–C24–H24	126.0
C25–C24–H24	126.0
Fe1–C24–H24	125.5
C24–C25–C21	108.2(6)
C24–C25–Fe1	69.7(4)
C21–C25–Fe1	69.4(4)
C24–C25–H25	125.9
C21–C25–H25	125.9
Fe1–C25–H25	126.6
C32–C31–C36	118.3(7)
C32–C31–P1	119.9(5)
C36–C31–P1	121.5(5)
C33–C32–C31	121.2(7)
C33–C32–H32	119.4

C31–C32–H32	119.4
C32–C33–C34	120.7(7)
C32–C33–H33	119.7
C34–C33–H33	119.7
C35–C34–C33	119.4(7)
C35–C34–H34	120.3
C33–C34–H34	120.3
C34–C35–C36	121.1(7)
C34–C35–H35	119.5
C36–C35–H35	119.5
C35–C36–C31	119.2(7)
C35–C36–H36	120.4
C31–C36–H36	120.4
C46–C41–C42	119.2(6)
C46–C41–P1	122.3(5)
C42–C41–P1	118.5(5)
C43–C42–C41	118.4(7)
C43–C42–H42	120.8
C41–C42–H42	120.8
C44–C43–C42	121.9(8)
C44–C43–H43	119.1
C42–C43–H43	119.1
C43–C44–C45	119.1(7)
C43–C44–H44	120.4
C45–C44–H44	120.5
C44–C45–C46	120.3(7)
C44–C45–H45	119.8
C46–C45–H45	119.8
C41–C46–C45	121.0(7)
C41–C46–H46	119.5
C45–C46–H46	119.5
C56–C51–C52	117.7(6)
C56–C51–P2	119.2(5)
C52–C51–P2	123.0(5)
C53–C52–C51	120.4(7)
C53–C52–H52	119.8
C51–C52–H52	119.8
C54–C53–C52	120.1(7)
C54–C53–H53	119.9
C52–C53–H53	119.9
C53–C54–C55	121.3(7)
C53–C54–H54	119.4
C55–C54–H54	119.4
C56–C55–C54	118.1(7)
C56–C55–H55	120.9
C54–C55–H55	120.9
C55–C56–C51	122.4(7)
C55–C56–H56	118.8
C51–C56–H56	118.8
C66–C61–C62	117.7(6)
C66–C61–P2	123.7(5)
C62–C61–P2	118.5(5)
C63–C62–C61	120.9(6)
C63–C62–H62	119.5
C61–C62–H62	119.5
C64–C63–C62	121.0(6)
C64–C63–H63	119.5
C62–C63–H63	119.5
C63–C64–C65	118.9(7)
C63–C64–H64	120.6
C65–C64–H64	120.6

C66–C65–C64	120.3(7)
C66–C65–H65	119.9
C64–C65–H65	119.9
C65–C66–C61	121.1(6)
C65–C66–H66	119.5
C61–C66–H66	119.5
C1'A–Re2–C2'	88.6(6)
C1'A–Re2–C1'	177.6(7)
C2'–Re2–C1'	90.3(5)
C1'A–Re2–C1'	91.5(6)
C2'–Re2–C1'	86.8(3)
C1'–Re2–C1'	86.3(5)
C1'A–Re2–P1'	80.7(6)
C2'–Re2–P1'	168.6(2)
C1'–Re2–P1'	100.2(5)
C1'–Re2–P1'	89.7(2)
C1'A–Re2–P2'	97.6(5)
C2'–Re2–P2'	87.0(2)
C1'–Re2–P2'	84.5(5)
C1'–Re2–P2'	168.8(2)
P1'–Re2–P2'	98.16(6)
C1'A–Re2–Br2A	174.6(6)
C2'–Re2–Br2A	91.0(2)
C1'–Re2–Br2A	3.3(5)
C1'–Re2–Br2A	83.1(2)
P1'–Re2–Br2A	99.32(9)
P2'–Re2–Br2A	87.77(9)
C1'A–Re2–Br2	5.7(6)
C2'–Re2–Br2	84.2(2)
C1'–Re2–Br2	172.1(5)
C1'–Re2–Br2	87.7(2)
P1'–Re2–Br2	84.85(6)
P2'–Re2–Br2	100.90(6)
Br2A–Re2–Br2	169.80(9)
C11'–Fe2–C21'	113.3(3)
C11'–Fe2–C15'	41.6(3)
C21'–Fe2–C15'	107.4(3)
C11'–Fe2–C25'	105.9(3)
C21'–Fe2–C25'	42.0(3)
C15'–Fe2–C25'	130.7(3)
C11'–Fe2–C12'	41.6(2)
C21'–Fe2–C12'	146.4(3)
C15'–Fe2–C12'	69.3(3)
C25'–Fe2–C12'	113.5(3)
C11'–Fe2–C22'	146.9(3)
C21'–Fe2–C22'	41.3(2)
C15'–Fe2–C22'	115.5(3)
C25'–Fe2–C22'	69.7(3)
C12'–Fe2–C22'	171.0(3)
C11'–Fe2–C23'	170.0(3)
C21'–Fe2–C23'	68.7(3)
C15'–Fe2–C23'	148.2(3)
C25'–Fe2–C23'	68.6(3)
C12'–Fe2–C23'	131.8(3)
C22'–Fe2–C23'	40.4(3)
C11'–Fe2–C24'	130.1(3)
C21'–Fe2–C24'	69.3(3)
C15'–Fe2–C24'	170.1(3)
C25'–Fe2–C24'	40.8(3)
C12'–Fe2–C24'	107.8(3)
C22'–Fe2–C24'	68.7(3)

C23'-Fe2-C24'	40.4(3)
C11'-Fe2-C14'	69.2(3)
C21'-Fe2-C14'	131.9(3)
C15'-Fe2-C14'	40.7(2)
C25'-Fe2-C14'	170.9(3)
C12'-Fe2-C14'	68.3(3)
C22'-Fe2-C14'	109.9(3)
C23'-Fe2-C14'	117.4(3)
C24'-Fe2-C14'	148.1(3)
C11'-Fe2-C13'	68.6(3)
C21'-Fe2-C13'	171.3(3)
C15'-Fe2-C13'	68.0(3)
C25'-Fe2-C13'	146.6(3)
C12'-Fe2-C13'	40.2(3)
C22'-Fe2-C13'	133.0(3)
C23'-Fe2-C13'	111.0(3)
C24'-Fe2-C13'	116.4(3)
C14'-Fe2-C13'	39.9(3)
O1'-C1'-Re2	178.2(14)
O1'A-C1'A-Re2	177.5(19)
C21'-P1'-C31'	102.2(3)
C21'-P1'-C41'	101.1(3)
C31'-P1'-C41'	100.5(3)
C21'-P1'-Re2	114.9(2)
C31'-P1'-Re2	123.0(2)
C41'-P1'-Re2	112.0(2)
C11'-P2'-C51'	103.2(3)
C11'-P2'-C61'	102.1(3)
C51'-P2'-C61'	101.3(3)
C11'-P2'-Re2	118.0(2)
C51'-P2'-Re2	107.3(2)
C61'-P2'-Re2	122.2(2)
O1'-C1'-Re2	174.0(7)
O2'-C2'-Re2	174.7(6)
C15'-C11'-C12'	107.0(6)
C15'-C11'-P2'	123.8(5)
C12'-C11'-P2'	129.0(5)
C15'-C11'-Fe2	69.5(4)
C12'-C11'-Fe2	69.9(4)
P2'-C11'-Fe2	121.6(3)
C13'-C12'-C11'	107.6(7)
C13'-C12'-Fe2	70.8(4)
C11'-C12'-Fe2	68.5(4)
C13'-C12'-H12'	126.2
C11'-C12'-H12'	126.2
Fe2-C12'-H12'	126.1
C14'-C13'-C12'	109.4(7)
C14'-C13'-Fe2	70.0(4)
C12'-C13'-Fe2	68.9(4)
C14'-C13'-H13'	125.3
C12'-C13'-H13'	125.3
Fe2-C13'-H13'	127.4
C13'-C14'-C15'	107.8(6)
C13'-C14'-Fe2	70.1(4)
C15'-C14'-Fe2	68.4(4)
C13'-C14'-H14'	126.1
C15'-C14'-H14'	126.1
Fe2-C14'-H14'	127.0
C14'-C15'-C11'	108.1(6)
C14'-C15'-Fe2	70.9(4)
C11'-C15'-Fe2	68.9(4)

C14'-C15'-H15'	125.9
C11'-C15'-H15'	125.9
Fe2-C15'-H15'	125.9
C22'-C21'-C25'	107.6(6)
C22'-C21'-P1'	127.2(5)
C25'-C21'-P1'	125.0(5)
C22'-C21'-Fe2	70.3(3)
C25'-C21'-Fe2	69.2(3)
P1'-C21'-Fe2	122.9(3)
C23'-C22'-C21'	107.4(6)
C23'-C22'-Fe2	69.9(4)
C21'-C22'-Fe2	68.4(3)
C23'-C22'-H22'	126.3
C21'-C22'-H22'	126.3
Fe2-C22'-H22'	127.0
C24'-C23'-C22'	109.5(6)
C24'-C23'-Fe2	69.9(4)
C22'-C23'-Fe2	69.7(4)
C24'-C23'-H23'	125.2
C22'-C23'-H23'	125.2
Fe2-C23'-H23'	126.7
C23'-C24'-C25'	107.9(7)
C23'-C24'-Fe2	69.7(4)
C25'-C24'-Fe2	68.6(4)
C23'-C24'-H24'	126.0
C25'-C24'-H24'	126.0
Fe2-C24'-H24'	127.2
C24'-C25'-C21'	107.5(7)
C24'-C25'-Fe2	70.5(4)
C21'-C25'-Fe2	68.8(4)
C24'-C25'-H25'	126.3
C21'-C25'-H25'	126.3
Fe2-C25'-H25'	126.0
C32'-C31'-C36'	120.0(7)
C32'-C31'-P1'	121.2(5)
C36'-C31'-P1'	118.7(5)
C31'-C32'-C33'	118.9(7)
C31'-C32'-H32'	120.6
C33'-C32'-H32'	120.6
C34'-C33'-C32'	121.9(7)
C34'-C33'-H33'	119.0
C32'-C33'-H33'	119.0
C33'-C34'-C35'	118.4(7)
C33'-C34'-H34'	120.8
C35'-C34'-H34'	120.8
C36'-C35'-C34'	121.2(7)
C36'-C35'-H35'	119.4
C34'-C35'-H35'	119.4
C35'-C36'-C31'	119.6(7)
C35'-C36'-H36'	120.2
C31'-C36'-H36'	120.2
C46'-C41'-C42'	120.1(6)
C46'-C41'-P1'	121.6(5)
C42'-C41'-P1'	118.3(5)
C41'-C42'-C43'	118.3(7)
C41'-C42'-H42'	120.9
C43'-C42'-H42'	120.9
C44'-C43'-C42'	121.5(7)
C44'-C43'-H43'	119.3
C42'-C43'-H43'	119.3
C45'-C44'-C43'	119.5(6)

C45'-C44'-H44'	120.2
C43'-C44'-H44'	120.2
C44'-C45'-C46'	120.6(7)
C44'-C45'-H45'	119.7
C46'-C45'-H45'	119.7
C45'-C46'-C41'	119.9(7)
C45'-C46'-H46'	120.0
C41'-C46'-H46'	120.0
C52'-C51'-C56'	117.4(6)
C52'-C51'-P2'	120.5(5)
C56'-C51'-P2'	122.0(5)
C53'-C52'-C51'	122.3(7)
C53'-C52'-H52'	118.8
C51'-C52'-H52'	118.8
C52'-C53'-C54'	118.4(7)
C52'-C53'-H53'	120.8
C54'-C53'-H53'	120.8
C55'-C54'-C53'	121.0(7)
C55'-C54'-H54'	119.5
C53'-C54'-H54'	119.5
C54'-C55'-C56'	119.7(7)
C54'-C55'-H55'	120.2
C56'-C55'-H55'	120.2
C55'-C56'-C51'	121.0(7)
C55'-C56'-H56'	119.5
C51'-C56'-H56'	119.5
C62'-C61'-C66'	119.4(6)
C62'-C61'-P2'	122.3(5)
C66'-C61'-P2'	118.2(5)
C61'-C62'-C63'	120.9(6)
C61'-C62'-H62'	119.6
C63'-C62'-H62'	119.6
C62'-C63'-C64'	120.0(7)
C62'-C63'-H63'	120.0
C64'-C63'-H63'	120.0
C65'-C64'-C63'	119.0(7)
C65'-C64'-H64'	120.5
C63'-C64'-H64'	120.5
C66'-C65'-C64'	120.3(7)
C66'-C65'-H65'	119.9
C64'-C65'-H65'	119.9
C65'-C66'-C61'	120.4(7)
C65'-C66'-H66'	119.8
C61'-C66'-H66'	119.8
C1"A-Re3-C2"	89.9(14)
C1"A-Re3-C1"	175.7(14)
C2"-Re3-C1"	86.1(4)
C1"A-Re3-C3"	89.3(13)
C2"-Re3-C3"	90.0(3)
C1"-Re3-C3"	89.1(4)
C1"A-Re3-P1"	82.6(13)
C2"-Re3-P1"	86.7(2)
C1"-Re3-P1"	98.8(3)
C3"-Re3-P1"	171.3(2)
C1"A-Re3-P2"	94.3(14)
C2"-Re3-P2"	175.2(2)
C1"-Re3-P2"	89.6(3)
C3"-Re3-P2"	87.8(2)
P1"-Re3-P2"	96.05(6)
C1"A-Re3-Br3	5.7(14)
C2"-Re3-Br3	85.5(2)

C1"-Re3-Br3	170.1(4)
C3"-Re3-Br3	85.7(2)
P1"-Re3-Br3	85.93(5)
P2"-Re3-Br3	98.59(6)
C1"A-Re3-Br3A	170.3(14)
C2"-Re3-Br3A	82.3(3)
C1"-Re3-Br3A	5.6(4)
C3"-Re3-Br3A	84.9(2)
P1"-Re3-Br3A	102.62(14)
P2"-Re3-Br3A	93.24(15)
Br3-Re3-Br3A	164.62(14)
C25"-Fe3-C12"	141.0(3)
C25"-Fe3-C11"	110.4(3)
C12"-Fe3-C11"	41.6(2)
C25"-Fe3-C24"	41.4(3)
C12"-Fe3-C24"	177.4(3)
C11"-Fe3-C24"	139.1(3)
C25"-Fe3-C21"	41.5(2)
C12"-Fe3-C21"	112.8(3)
C11"-Fe3-C21"	110.5(3)
C24"-Fe3-C21"	69.5(3)
C25"-Fe3-C15"	109.2(3)
C12"-Fe3-C15"	69.0(3)
C11"-Fe3-C15"	41.3(2)
C24"-Fe3-C15"	110.0(3)
C21"-Fe3-C15"	137.8(3)
C25"-Fe3-C14"	136.2(3)
C12"-Fe3-C14"	68.7(3)
C11"-Fe3-C14"	69.4(3)
C24"-Fe3-C14"	109.0(3)
C21"-Fe3-C14"	177.7(3)
C15"-Fe3-C14"	40.7(2)
C25"-Fe3-C13"	177.0(3)
C12"-Fe3-C13"	40.3(2)
C11"-Fe3-C13"	69.0(3)
C24"-Fe3-C13"	137.2(3)
C21"-Fe3-C13"	141.5(3)
C15"-Fe3-C13"	68.3(3)
C14"-Fe3-C13"	40.7(3)
C25"-Fe3-C23"	68.6(3)
C12"-Fe3-C23"	139.2(3)
C11"-Fe3-C23"	179.0(3)
C24"-Fe3-C23"	40.2(2)
C21"-Fe3-C23"	68.8(3)
C15"-Fe3-C23"	138.9(3)
C14"-Fe3-C23"	111.3(3)
C13"-Fe3-C23"	112.0(3)
C25"-Fe3-C22"	69.2(3)
C12"-Fe3-C22"	112.3(3)
C11"-Fe3-C22"	139.0(3)
C24"-Fe3-C22"	68.7(3)
C21"-Fe3-C22"	41.0(2)
C15"-Fe3-C22"	178.3(3)
C14"-Fe3-C22"	140.5(3)
C13"-Fe3-C22"	113.3(3)
C23"-Fe3-C22"	40.8(2)
O1"-C1"-Re3	178.3(11)
O1"A-C1"A-Re3	171(4)
C11"-P1"-C41"	100.8(3)
C11"-P1"-C31"	103.6(3)
C41"-P1"-C31"	103.1(3)

C11"-P1"-Re3	119.2(2)
C41"-P1"-Re3	111.5(2)
C31"-P1"-Re3	116.5(2)
C21"-P2"-C61"	101.0(3)
C21"-P2"-C51"	102.0(3)
C61"-P2"-C51"	102.4(3)
C21"-P2"-Re3	121.89(19)
C61"-P2"-Re3	115.0(2)
C51"-P2"-Re3	112.0(2)
O2"-C2"-Re3	177.5(7)
O3"-C3"-Re3	176.6(6)
C15"-C11"-C12"	106.6(6)
C15"-C11"-P1"	126.8(5)
C12"-C11"-P1"	126.5(5)
C15"-C11"-Fe3	69.9(4)
C12"-C11"-Fe3	69.2(3)
P1"-C11"-Fe3	125.7(3)
C13"-C12"-C11"	108.5(6)
C13"-C12"-Fe3	70.6(4)
C11"-C12"-Fe3	69.2(4)
C13"-C12"-H12"	125.8
C11"-C12"-H12"	125.8
Fe3-C12"-H12"	126.0
C15"-C14"-C13"	107.7(6)
C15"-C14"-Fe3	69.7(4)
C13"-C14"-Fe3	69.8(4)
C15"-C14"-H13"	126.2
C13"-C14"-H13"	126.2
Fe3-C14"-H13"	126.0
C12"-C13"-C14"	108.7(6)
C12"-C13"-Fe3	69.1(4)
C14"-C13"-Fe3	69.5(4)
C12"-C13"-H14"	125.6
C14"-C13"-H14"	125.6
Fe3-C13"-H14"	127.3
C14"-C15"-C11"	108.4(6)
C14"-C15"-Fe3	69.6(4)
C11"-C15"-Fe3	68.8(3)
C14"-C15"-H15"	125.8
C11"-C15"-H15"	125.8
Fe3-C15"-H15"	127.4
C22"-C21"-C25"	107.6(6)
C22"-C21"-P2"	125.4(5)
C25"-C21"-P2"	126.9(5)
C22"-C21"-Fe3	70.4(3)
C25"-C21"-Fe3	68.6(3)
P2"-C21"-Fe3	127.9(3)
C23"-C22"-C21"	107.5(6)
C23"-C22"-Fe3	69.5(3)
C21"-C22"-Fe3	68.6(3)
C23"-C22"-H22"	126.3
C21"-C22"-H22"	126.3
Fe3-C22"-H22"	127.2
C24"-C23"-C22"	109.0(6)
C24"-C23"-Fe3	69.0(4)
C22"-C23"-Fe3	69.7(3)
C24"-C23"-H23"	125.5
C22"-C23"-H23"	125.5
Fe3-C23"-H23"	127.3
C23"-C24"-C25"	108.0(6)
C23"-C24"-Fe3	70.8(4)

C25"-C24"-Fe3	68.7(4)
C23"-C24"-H24"	126.0
C25"-C24"-H24"	126.0
Fe3-C24"-H24"	126.1
C24"-C25"-C21"	108.0(6)
C24"-C25"-Fe3	69.9(4)
C21"-C25"-Fe3	69.9(4)
C24"-C25"-H25"	126.0
C21"-C25"-H25"	126.0
Fe3-C25"-H25"	125.8
C32"-C31"-C36"	119.3(6)
C32"-C31"-P1"	118.9(5)
C36"-C31"-P1"	121.7(5)
C31"-C32"-C33"	120.4(6)
C31"-C32"-H32"	119.8
C33"-C32"-H32"	119.8
C34"-C33"-C32"	118.9(7)
C34"-C33"-H33"	120.5
C32"-C33"-H33"	120.5
C33"-C34"-C35"	120.9(7)
C33"-C34"-H34"	119.6
C35"-C34"-H34"	119.6
C36"-C35"-C34"	119.6(7)
C36"-C35"-H35"	120.2
C34"-C35"-H35"	120.2
C35"-C36"-C31"	120.9(7)
C35"-C36"-H36"	119.6
C31"-C36"-H36"	119.6
C46"-C41"-C42"	118.3(6)
C46"-C41"-P1"	120.8(5)
C42"-C41"-P1"	120.9(5)
C43"-C42"-C41"	120.4(7)
C43"-C42"-H42"	119.8
C41"-C42"-H42"	119.8
C44"-C43"-C42"	121.0(7)
C44"-C43"-H43"	119.5
C42"-C43"-H43"	119.5
C43"-C44"-C45"	118.7(7)
C43"-C44"-H44"	120.6
C45"-C44"-H44"	120.6
C46"-C45"-C44"	121.0(7)
C46"-C45"-H45"	119.5
C44"-C45"-H45"	119.5
C41"-C46"-C45"	120.6(7)
C41"-C46"-H46"	119.7
C45"-C46"-H46"	119.7
C52"-C51"-C56"	118.2(6)
C52"-C51"-P2"	122.7(5)
C56"-C51"-P2"	119.0(5)
C51"-C52"-C53"	120.8(7)
C51"-C52"-H52"	119.6
C53"-C52"-H52"	119.6
C54"-C53"-C52"	120.2(7)
C54"-C53"-H53"	119.9
C52"-C53"-H53"	119.9
C55"-C54"-C53"	119.6(7)
C55"-C54"-H54"	120.2
C53"-C54"-H54"	120.2
C54"-C55"-C56"	121.0(7)
C54"-C55"-H55"	119.5
C56"-C55"-H55"	119.5

C55"--C56"--C51"	120.1(7)
C55"--C56"--H56"	119.9
C51"--C56"--H56"	119.9
C66"--C61"--C62"	117.7(7)
C66"--C61"--P2"	121.9(6)
C62"--C61"--P2"	120.2(5)
C63"--C62"--C61"	121.2(7)
C63"--C62"--H62"	119.4
C61"--C62"--H62"	119.4
C64"--C63"--C62"	120.2(8)
C64"--C63"--H63"	119.9
C62"--C63"--H63"	119.9
C65"--C64"--C63"	119.3(7)
C65"--C64"--H64"	120.4
C63"--C64"--H64"	120.4
C64"--C65"--C66"	121.7(7)
C64"--C65"--H65"	119.2
C66"--C65"--H65"	119.2
C65"--C66"--C61"	119.8(7)
C65"--C66"--H66"	120.1
C61"--C66"--H66"	120.1

Symmetry transformations used to generate equivalent atoms:

Table 4. Anisotropic displacement parameters [$\text{\AA}^2 \times 10^3$]. The anisotropic displacement factor exponent takes the form: $-2\pi^2[h^2a^*{}^2U^{11} + \dots + 2hk a^* b^* U^{12}]$.

Atom	U^{11}	U^{22}	U^{33}	U^{23}	U^{13}	U^{12}
Re1	21(1)	20(1)	13(1)	0(1)	4(1)	1(1)
Fe1	18(1)	24(1)	20(1)	-1(1)	3(1)	2(1)
Br1	23(1)	26(1)	25(1)	1(1)	9(1)	-2(1)
P2	21(1)	22(1)	14(1)	0(1)	5(1)	0(1)
P1	19(1)	22(1)	15(1)	-2(1)	6(1)	0(1)
O2	36(3)	62(5)	45(4)	-20(3)	-17(3)	22(3)
O3	46(3)	27(4)	27(3)	0(2)	14(2)	2(3)
C2	33(5)	30(5)	20(4)	-12(3)	-2(3)	14(4)
C3	24(4)	30(5)	11(4)	0(3)	8(3)	0(4)
C21	23(4)	21(5)	13(4)	-3(3)	4(3)	2(3)
C22	28(4)	24(5)	16(4)	0(3)	5(3)	3(3)
C11	17(4)	27(5)	17(4)	-8(3)	5(3)	-2(3)
C12	30(4)	42(6)	24(4)	-5(4)	12(3)	-3(4)
C13	21(4)	49(6)	33(4)	-12(4)	11(3)	-1(4)
C14	28(4)	30(5)	34(4)	-6(4)	12(4)	7(4)
C15	25(4)	24(5)	22(4)	-8(3)	4(3)	-1(3)
C23	34(4)	22(5)	25(4)	0(3)	15(3)	1(3)
C24	29(4)	24(5)	24(4)	3(3)	2(3)	3(3)
C25	21(4)	37(6)	25(4)	-4(3)	1(3)	-2(4)
C31	15(4)	20(5)	23(4)	-3(3)	6(3)	4(3)
C32	35(5)	22(5)	33(4)	-1(4)	13(4)	-4(4)
C33	46(5)	23(5)	46(5)	-7(4)	16(4)	-10(4)
C34	40(5)	28(5)	46(5)	6(4)	25(4)	-5(4)
C35	22(4)	41(6)	33(4)	3(4)	14(3)	-3(4)
C36	10(4)	35(5)	28(4)	-5(3)	6(3)	-2(3)
C41	23(4)	17(4)	16(4)	-4(3)	2(3)	0(3)
C42	38(5)	42(6)	19(4)	-11(3)	0(4)	7(4)
C43	52(6)	36(6)	22(4)	-7(4)	-7(4)	19(4)
C44	69(6)	36(6)	16(4)	0(4)	13(4)	13(5)
C45	54(6)	38(6)	28(5)	-2(4)	23(4)	-9(4)
C46	30(4)	30(5)	19(4)	-4(3)	7(3)	-5(4)
C51	13(3)	25(5)	15(4)	-7(3)	5(3)	-2(3)
C52	23(4)	29(5)	16(4)	7(3)	5(3)	-3(3)
C53	32(4)	33(5)	18(4)	1(3)	10(3)	-9(4)
C54	18(4)	51(6)	20(4)	-7(4)	6(3)	-3(4)
C55	26(4)	24(5)	24(4)	-9(3)	1(3)	2(3)
C56	29(4)	29(5)	17(4)	0(3)	10(3)	0(3)
C61	18(4)	18(4)	22(4)	-1(3)	9(3)	2(3)
C62	30(4)	36(5)	17(4)	2(3)	17(3)	-6(4)
C63	28(4)	37(5)	22(4)	-2(3)	-2(3)	-5(4)
C64	21(4)	31(5)	30(4)	2(3)	5(3)	-7(3)
C65	29(4)	36(5)	19(4)	8(3)	7(3)	0(4)
C66	19(4)	28(5)	18(4)	-1(3)	4(3)	-2(3)
Re2	20(1)	21(1)	15(1)	1(1)	5(1)	1(1)
Fe2	18(1)	25(1)	15(1)	-2(1)	3(1)	2(1)
Br2	40(1)	32(1)	21(1)	1(1)	13(1)	-5(1)
O1'	33(7)	43(8)	30(9)	-3(7)	5(7)	-8(5)
P1'	17(1)	24(1)	13(1)	-1(1)	3(1)	-1(1)
P2'	21(1)	22(1)	14(1)	-1(1)	6(1)	0(1)
O1'	28(3)	64(5)	45(4)	-10(3)	-5(3)	12(3)
O2'	63(4)	28(4)	43(3)	1(3)	12(3)	8(3)
C1'	42(5)	31(5)	27(4)	-6(3)	13(4)	12(4)
C2'	32(5)	45(6)	19(4)	7(4)	9(3)	6(4)
C11'	24(4)	26(5)	5(3)	-3(3)	0(3)	-6(3)
C12'	25(4)	28(5)	14(4)	-4(3)	0(3)	6(3)
C13'	31(5)	46(6)	10(4)	-7(3)	-4(3)	11(4)
C14'	38(5)	18(5)	13(4)	-3(3)	9(3)	-3(3)
C15'	27(4)	30(5)	12(4)	1(3)	5(3)	3(4)

C21'	19(4)	24(5)	8(3)	-5(3)	1(3)	1(3)
C22'	18(4)	26(5)	24(4)	-7(3)	2(3)	5(3)
C23'	28(4)	38(6)	19(4)	-11(3)	7(3)	8(4)
C24'	19(4)	44(6)	25(4)	-7(4)	11(3)	3(4)
C25'	20(4)	44(5)	13(4)	-6(3)	3(3)	1(4)
C31'	17(4)	28(5)	19(4)	4(3)	4(3)	-1(3)
C32'	18(4)	28(5)	22(4)	2(3)	7(3)	2(3)
C33'	31(4)	40(6)	19(4)	8(4)	7(3)	-2(4)
C34'	23(4)	27(5)	36(5)	6(4)	4(4)	-3(3)
C35'	36(5)	21(5)	29(4)	-2(3)	6(4)	-2(4)
C36'	24(4)	33(5)	16(4)	-2(3)	7(3)	-4(3)
C41'	24(4)	15(4)	15(4)	-1(3)	3(3)	-4(3)
C42'	32(4)	30(5)	18(4)	-5(3)	2(3)	-5(4)
C43'	31(4)	35(5)	22(4)	-7(3)	-11(4)	-2(4)
C44'	63(6)	25(5)	8(4)	-4(3)	-3(4)	0(4)
C45'	46(5)	28(5)	13(4)	-5(3)	9(4)	-9(4)
C46'	27(4)	28(5)	22(4)	0(3)	8(3)	2(3)
C51'	16(4)	24(5)	11(3)	-2(3)	1(3)	-2(3)
C52'	30(4)	30(5)	20(4)	-2(3)	6(3)	-4(4)
C53'	41(5)	22(5)	32(4)	-10(3)	16(4)	-7(4)
C54'	29(4)	55(6)	22(4)	-7(4)	15(3)	-3(4)
C55'	35(5)	38(6)	19(4)	4(4)	12(3)	0(4)
C56'	25(4)	27(5)	17(4)	-3(3)	2(3)	-5(3)
C61'	27(4)	18(4)	26(4)	-3(3)	15(3)	1(3)
C62'	29(4)	33(5)	18(4)	3(3)	4(3)	-2(4)
C63'	54(5)	34(5)	25(4)	2(4)	25(4)	-11(4)
C64'	37(5)	30(5)	50(5)	-9(4)	30(4)	-9(4)
C65'	26(4)	33(5)	38(5)	-7(4)	8(4)	3(4)
C66'	32(4)	35(5)	19(4)	-8(3)	14(3)	-10(4)
Re3	16(1)	26(1)	17(1)	0(1)	7(1)	0(1)
Fe3	20(1)	23(1)	13(1)	-1(1)	5(1)	-2(1)
Br3	26(1)	33(1)	29(1)	-4(1)	13(1)	6(1)
C1"	23(6)	34(9)	18(6)	6(6)	2(4)	15(6)
O1"	41(6)	62(9)	44(6)	3(5)	18(5)	22(5)
P1"	19(1)	24(1)	13(1)	1(1)	6(1)	0(1)
P2"	15(1)	26(1)	16(1)	-1(1)	4(1)	1(1)
O2"	31(3)	60(4)	31(3)	14(3)	15(3)	2(3)
O3"	21(3)	55(4)	35(3)	0(3)	9(2)	0(3)
C2"	17(4)	36(5)	29(4)	-6(4)	11(3)	-1(3)
C3"	23(4)	30(5)	27(4)	-4(3)	14(3)	-11(4)
C11"	18(4)	23(5)	9(3)	-1(3)	-2(3)	-1(3)
C12"	22(4)	25(5)	10(3)	5(3)	5(3)	-3(3)
C14"	28(4)	31(5)	11(3)	-3(3)	3(3)	-15(4)
C13"	31(4)	22(5)	15(4)	-7(3)	9(3)	-2(3)
C15"	20(4)	25(5)	16(4)	-1(3)	1(3)	0(3)
C21"	16(4)	25(5)	5(3)	-1(3)	2(3)	1(3)
C22"	19(4)	26(5)	18(4)	4(3)	3(3)	6(3)
C23"	35(4)	30(5)	6(3)	1(3)	9(3)	-9(4)
C24"	24(4)	31(5)	15(4)	-1(3)	8(3)	2(4)
C25"	22(4)	24(5)	8(3)	-1(3)	-1(3)	1(3)
C31"	22(4)	18(4)	26(4)	2(3)	14(3)	3(3)
C32"	28(4)	24(5)	23(4)	1(3)	13(3)	5(3)
C33"	34(5)	24(5)	36(5)	-2(3)	17(4)	0(4)
C34"	34(5)	31(5)	37(5)	9(4)	20(4)	17(4)
C35"	21(4)	54(6)	33(5)	20(4)	13(4)	10(4)
C36"	22(4)	31(5)	21(4)	5(3)	9(3)	-1(3)
C41"	10(3)	27(5)	14(4)	-1(3)	6(3)	-5(3)
C42"	21(4)	31(5)	26(4)	1(3)	14(3)	-7(3)
C43"	35(4)	29(5)	18(4)	8(3)	13(3)	2(4)
C44"	30(4)	45(6)	25(4)	1(4)	18(3)	2(4)
C45"	33(4)	28(5)	22(4)	-4(3)	11(3)	8(4)
C46"	26(4)	28(5)	17(4)	4(3)	7(3)	4(3)

C51"	15(4)	25(5)	15(4)	-2(3)	0(3)	2(3)
C52"	21(4)	42(6)	19(4)	-6(3)	5(3)	0(3)
C53"	29(4)	50(6)	13(4)	-10(3)	8(3)	-2(4)
C54"	30(4)	21(5)	22(4)	-11(3)	0(3)	2(4)
C55"	29(4)	24(5)	34(4)	-7(4)	11(4)	-11(3)
C56"	26(4)	34(5)	23(4)	-4(3)	11(3)	-4(4)
C61"	24(4)	27(5)	21(4)	0(3)	10(3)	-3(3)
C62"	28(4)	34(5)	28(4)	9(4)	6(3)	4(4)
C63"	48(5)	46(6)	33(5)	4(4)	24(4)	14(4)
C64"	34(5)	45(6)	47(5)	21(4)	25(4)	16(4)
C65"	28(5)	52(6)	32(5)	18(4)	7(4)	14(4)
C66"	26(4)	44(6)	23(4)	7(4)	7(3)	7(4)

Table 5. Hydrogen coordinates [$\times 10^4$] and isotropic displacement parameters [$\text{\AA}^2 \times 10^3$].

Atom	<i>x</i>	<i>y</i>	<i>z</i>	<i>U_{eq}</i>	<i>S.o.f.</i>
H22	1923	-594	2093	28	1
H12	-383	-875	3442	38	1
H13	-2754	-599	2993	41	1
H14	-1850	-164	2905	37	1
H15	1138	-168	3321	30	1
H23	130	-231	1622	31	1
H24	-2652	-372	1362	34	1
H25	-2591	-833	1591	36	1
H32	3885	-208	4404	36	1
H33	4905	158	4214	46	1
H34	5603	204	3302	43	1
H35	5208	-118	2563	37	1
H36	4335	-500	2776	30	1
H42	5978	-704	4797	43	1
H43	6853	-699	5951	51	1
H44	5113	-693	6485	49	1
H45	2461	-645	5869	45	1
H46	1540	-645	4714	33	1
H52	1301	-944	1082	28	1
H53	1971	-1149	278	33	1
H54	2214	-1570	303	36	1
H55	1808	-1804	1134	33	1
H56	1141	-1600	1933	30	1
H62	-2034	-1260	1194	30	1
H63	-4387	-1447	1070	38	1
H64	-4846	-1592	1982	34	1
H65	-2875	-1553	3039	35	1
H66	-572	-1344	3175	27	1
H12'	8151	-946	-266	29	1
H13'	8404	-1400	0	39	1
H14'	5743	-1572	-172	28	1
H15'	3780	-1221	-537	28	1
H22'	4230	-1618	-1886	29	1
H23'	7133	-1606	-1647	35	1
H24'	7934	-1166	-1744	34	1
H25'	5515	-894	-2031	32	1
H32'	1161	-1260	-1127	27	1
H33'	232	-1627	-843	36	1
H34'	-195	-1976	-1510	37	1
H35'	330	-1957	-2484	36	1
H36'	1355	-1600	-2760	30	1
H42'	-849	-1089	-3139	35	1
H43'	-1974	-1091	-4302	43	1
H44'	-438	-1129	-4926	44	1
H45'	2244	-1186	-4403	35	1
H46'	3404	-1197	-3251	31	1
H52'	4240	-210	-352	33	1
H53'	3620	-46	503	37	1
H54'	3443	-312	1329	40	1
H55'	4025	-726	1325	36	1
H56'	4613	-890	452	30	1
H62'	5571	-425	-1764	33	1
H63'	7712	-197	-1753	41	1
H64'	9925	-157	-761	42	1
H65'	9814	-313	225	40	1
H66'	7631	-533	206	33	1
H12"	710	-3220	-780	23	1

H13"	-3605	-3297	-652	29	I
H14"	-1131	-3524	-579	27	I
H15"	-3340	-2850	-953	26	I
H22"	1730	-3273	976	26	I
H23"	-948	-3338	1044	28	I
H24"	-2446	-2938	759	28	I
H25"	-706	-2615	521	23	I
H32"	-300	-2296	-163	29	I
H33"	-2061	-1984	-116	36	I
H34"	-4422	-1936	-999	38	I
H35"	-5058	-2188	-1935	42	I
H36"	-3360	-2500	-1962	30	I
H42"	-899	-2331	-2217	30	I
H43"	-1487	-2381	-3343	32	I
H44"	-1508	-2772	-3792	38	I
H45"	-1025	-3118	-3099	33	I
H46"	-495	-3074	-1973	29	I
H52"	1623	-2601	1672	34	I
H53"	2365	-2295	2492	37	I
H54"	4456	-2037	2608	33	I
H55"	5852	-2090	1929	35	I
H56"	5037	-2374	1064	32	I
H62"	3424	-3220	151	37	I
H63"	5177	-3541	598	48	I
H64"	6995	-3516	1684	47	I
H65"	7122	-3162	2297	46	I
H66"	5352	-2840	1877	38	I

Appendix G

Crystal tables for **3b**



Table 1. Crystal data and structure refinement.

Identification code	s92 49SRC 307
Empirical formula	C ₂₈ H ₃₂ B ₃ MnO ₂ P ₂
Formula weight	549.85
Temperature	150(2) K
Wavelength	0.71073 Å
Crystal system	Orthorhombic
Space group	Pbca
Unit cell dimensions	$a = 17.123(3)$ Å $\alpha = 90^\circ$ $b = 12.328(2)$ Å $\beta = 90^\circ$ $c = 26.170(5)$ Å $\gamma = 90^\circ$
Volume	5524.3(17) Å ³
Z	8
Density (calculated)	1.322 Mg / m ³
Absorption coefficient	0.618 mm ⁻¹
$F(000)$	2288
Crystal	Plate; orange
Crystal size	0.2 × 0.15 × 0.02 mm ³
θ range for data collection	1.96 – 27.45°
Index ranges	−16 ≤ h ≤ 22, −13 ≤ k ≤ 15, −33 ≤ l ≤ 25
Reflections collected	37761
Independent reflections	6296 [$R_{int} = 0.0810$]
Completeness to $\theta = 27.45^\circ$	90.7 %
Absorption correction	Semi-empirical from equivalents
Max. and min. transmission	0.992 and 0.925
Refinement method	Full-matrix least-squares on F^2
Data / restraints / parameters	6296 / 0 / 357
Goodness-of-fit on F^2	0.830
Final R indices [$F^2 > 2\sigma(F^2)$]	$R_I = 0.0432$, $wR2 = 0.1112$
R indices (all data)	$R_I = 0.0774$, $wR2 = 0.1326$
Largest diff. peak and hole	0.434 and −0.391 e Å ^{−3}

Diffractometer: *Enraf Nonius KappaCCD* area detector (ϕ scans and ω scans to fill *Ewald* sphere). Data collection and cell refinement: *Denzo* (Z. Otwinowski & W. Minor, *Methods in Enzymology* (1997) Vol. 276: *Macromolecular Crystallography*, part A, pp. 307–326; C. W. Carter, Jr. & R. M. Sweet, Eds., Academic Press). Absorption correction: *SORTAV* (R. H. Blessing, *Acta Cryst. A*51 (1995) 33–37; R. H. Blessing, *J. Appl. Cryst.* 30 (1997) 421–426). Program used to solve structure: *SHELXS97* (G. M. Sheldrick, *Acta Cryst.* (1990) A46 467–473). Program used to refine structure: *SHELXL97* (G. M. Sheldrick (1997), University of Göttingen, Germany).

Further information: <http://www.soton.ac.uk/~xservice/strat.htm>

Special details:

Table 2. Atomic coordinates [$\times 10^4$], equivalent isotropic displacement parameters [$\text{\AA}^2 \times 10^3$] and site occupancy factors. U_{eq} is defined as one third of the trace of the orthogonalized U^{ij} tensor.

Atom	<i>x</i>	<i>y</i>	<i>z</i>	U_{eq}	S.o.f.
Mn1	-56(1)	3860(1)	3647(1)	19(1)	1
P1	-238(1)	3376(1)	2827(1)	21(1)	1
P2	-677(1)	2312(1)	3851(1)	20(1)	1
O1	1459(1)	2681(1)	3640(1)	31(1)	1
O2	-1623(1)	4911(1)	3687(1)	34(1)	1
B1	509(2)	4790(2)	4328(1)	27(1)	1
B2	681(2)	5443(2)	3742(1)	29(1)	1
B3	188(2)	6161(2)	4255(1)	35(1)	1
C1	590(1)	3405(2)	2384(1)	21(1)	1
C2	575(2)	2793(2)	1934(1)	29(1)	1
C3	1186(2)	2820(2)	1594(1)	33(1)	1
C4	1829(2)	3473(2)	1690(1)	30(1)	1
C5	1856(2)	4085(2)	2131(1)	27(1)	1
C6	1244(2)	4047(2)	2477(1)	24(1)	1
C7	-982(1)	4079(2)	2448(1)	25(1)	1
C8	-1422(2)	3581(2)	2065(1)	33(1)	1
C9	-1928(2)	4181(2)	1764(1)	41(1)	1
C10	-2006(2)	5285(2)	1840(1)	42(1)	1
C11	-1587(2)	5789(2)	2221(1)	36(1)	1
C12	-1079(2)	5190(2)	2522(1)	28(1)	1
C13	-544(2)	1942(2)	2827(1)	24(1)	1
C14	-1123(2)	1781(2)	3263(1)	24(1)	1
C15	-1490(1)	2316(2)	4304(1)	22(1)	1
C16	-2031(2)	1466(2)	4308(1)	31(1)	1
C17	-2626(2)	1447(2)	4660(1)	36(1)	1
C18	-2700(2)	2260(2)	5018(1)	35(1)	1
C19	-2170(2)	3109(2)	5018(1)	38(1)	1
C20	-1576(2)	3138(2)	4663(1)	28(1)	1
C21	-77(1)	1207(2)	4101(1)	21(1)	1
C22	373(2)	1418(2)	4531(1)	32(1)	1
C23	842(2)	612(2)	4745(1)	37(1)	1
C24	859(2)	-401(2)	4525(1)	39(1)	1
C25	415(2)	-623(2)	4101(1)	39(1)	1
C26	-51(2)	176(2)	3885(1)	31(1)	1
C27	882(2)	3125(2)	3635(1)	22(1)	1
C28	-1012(2)	4530(2)	3676(1)	22(1)	1

Table 3. Bond lengths [\AA] and angles [$^\circ$].

Mn1–C28	1.835(3)
Mn1–C27	1.844(3)
Mn1–P1	2.2480(8)
Mn1–P2	2.2495(7)
Mn1–B1	2.330(3)
Mn1–B2	2.336(3)
P1–C1	1.831(3)
P1–C7	1.832(3)
P1–C13	1.843(2)
P2–C15	1.827(2)
P2–C21	1.828(2)
P2–C14	1.840(2)
O1–C27	1.130(3)
O2–C28	1.147(3)
B1–B2	1.756(4)
B1–B3	1.788(4)
B2–B3	1.815(5)
C1–C6	1.394(3)
C1–C2	1.398(3)
C2–C3	1.376(4)
C3–C4	1.387(4)
C4–C5	1.381(4)
C5–C6	1.386(3)
C7–C12	1.393(3)
C7–C8	1.398(3)
C8–C9	1.384(4)
C9–C10	1.381(4)
C10–C11	1.377(4)
C11–C12	1.386(4)
C13–C14	1.525(3)
C15–C20	1.390(3)
C15–C16	1.399(3)
C16–C17	1.373(4)
C17–C18	1.380(4)
C18–C19	1.384(4)
C19–C20	1.379(4)
C21–C22	1.389(4)
C21–C26	1.391(3)
C22–C23	1.395(4)
C23–C24	1.375(4)
C24–C25	1.374(4)
C25–C26	1.387(4)
C28–Mn1–C27	176.96(10)
C28–Mn1–P1	91.99(7)
C27–Mn1–P1	88.55(7)
C28–Mn1–P2	87.10(7)
C27–Mn1–P2	89.95(7)
P1–Mn1–P2	86.34(3)
C28–Mn1–B1	96.76(11)
C27–Mn1–B1	83.86(11)
P1–Mn1–B1	156.69(8)
P2–Mn1–B1	115.57(8)
C28–Mn1–B2	95.84(11)
C27–Mn1–B2	86.69(11)
P1–Mn1–B2	113.50(8)
P2–Mn1–B2	159.75(8)
B1–Mn1–B2	44.22(11)
C1–P1–C7	100.73(11)

C1—P1—C13	103.76(11)
C7—P1—C13	104.83(12)
C1—P1—Mn1	119.42(8)
C7—P1—Mn1	119.17(9)
C13—P1—Mn1	107.14(8)
C15—P2—C21	101.50(10)
C15—P2—C14	103.12(11)
C21—P2—C14	105.46(11)
C15—P2—Mn1	120.82(8)
C21—P2—Mn1	116.83(8)
C14—P2—Mn1	107.42(8)
B2—B1—B3	61.59(18)
B2—B1—Mn1	68.08(14)
B3—B1—Mn1	104.78(17)
B1—B2—B3	60.07(17)
B1—B2—Mn1	67.70(14)
B3—B2—Mn1	103.64(18)
B1—B3—B2	58.34(17)
C6—C1—C2	117.9(2)
C6—C1—P1	121.50(18)
C2—C1—P1	120.55(19)
C3—C2—C1	121.2(2)
C2—C3—C4	120.1(2)
C5—C4—C3	119.7(2)
C4—C5—C6	120.3(2)
C5—C6—C1	120.8(2)
C12—C7—C8	117.7(2)
C12—C7—P1	118.30(19)
C8—C7—P1	123.8(2)
C9—C8—C7	120.8(3)
C10—C9—C8	120.3(3)
C11—C10—C9	119.9(3)
C10—C11—C12	119.9(3)
C11—C12—C7	121.4(3)
C14—C13—P1	108.02(16)
C13—C14—P2	108.05(17)
C20—C15—C16	118.1(2)
C20—C15—P2	121.37(19)
C16—C15—P2	120.52(18)
C17—C16—C15	120.7(2)
C16—C17—C18	120.7(2)
C17—C18—C19	119.3(3)
C20—C19—C18	120.3(2)
C19—C20—C15	121.0(2)
C22—C21—C26	118.8(2)
C22—C21—P2	117.47(18)
C26—C21—P2	123.7(2)
C21—C22—C23	120.7(2)
C24—C23—C22	119.5(3)
C25—C24—C23	120.4(3)
C24—C25—C26	120.4(3)
C25—C26—C21	120.1(3)
O1—C27—Mn1	178.3(2)
O2—C28—Mn1	177.3(2)

Symmetry transformations used to generate equivalent atoms:

Table 4. Anisotropic displacement parameters [$\text{\AA}^2 \times 10^3$]. The anisotropic displacement factor exponent takes the form: $-2\pi^2[h^2a^{*2}U^{11} + \dots + 2hk a^* b^* U^{12}]$.

Atom	U^{11}	U^{22}	U^{33}	U^{23}	U^{13}	U^{12}
Mn1	18(1)	19(1)	19(1)	0(1)	0(1)	-2(1)
P1	19(1)	23(1)	20(1)	-1(1)	-1(1)	-4(1)
P2	18(1)	20(1)	21(1)	0(1)	1(1)	-2(1)
O1	24(1)	32(1)	37(1)	-1(1)	0(1)	3(1)
O2	25(1)	37(1)	39(1)	-2(1)	0(1)	6(1)
B1	28(2)	29(2)	24(2)	0(1)	-6(1)	0(1)
B2	25(2)	22(1)	41(2)	-4(1)	-7(1)	-4(1)
B3	46(2)	25(2)	33(2)	-2(1)	-11(2)	1(1)
C1	21(1)	23(1)	19(1)	2(1)	-2(1)	-1(1)
C2	28(2)	30(1)	28(2)	-6(1)	0(1)	-7(1)
C3	35(2)	36(1)	28(2)	-8(1)	5(1)	-5(1)
C4	24(2)	36(1)	29(2)	1(1)	6(1)	1(1)
C5	21(1)	33(1)	28(1)	3(1)	0(1)	-5(1)
C6	24(1)	25(1)	24(1)	-1(1)	-2(1)	-1(1)
C7	17(1)	35(1)	23(1)	6(1)	1(1)	-5(1)
C8	26(2)	43(2)	29(2)	-1(1)	-3(1)	-5(1)
C9	24(2)	67(2)	30(2)	4(1)	-10(1)	-13(1)
C10	24(2)	59(2)	43(2)	23(1)	-7(1)	-3(1)
C11	27(2)	36(1)	45(2)	17(1)	-2(1)	-1(1)
C12	21(1)	34(1)	30(1)	6(1)	-1(1)	-5(1)
C13	27(1)	23(1)	22(1)	-3(1)	0(1)	-5(1)
C14	23(1)	22(1)	25(1)	-1(1)	0(1)	-5(1)
C15	18(1)	28(1)	22(1)	2(1)	0(1)	-1(1)
C16	29(2)	31(1)	32(2)	-2(1)	3(1)	-6(1)
C17	26(2)	41(2)	39(2)	3(1)	6(1)	-10(1)
C18	29(2)	43(2)	35(2)	5(1)	11(1)	3(1)
C19	38(2)	37(2)	37(2)	-5(1)	12(1)	4(1)
C20	25(2)	29(1)	30(1)	-2(1)	2(1)	-2(1)
C21	17(1)	22(1)	23(1)	7(1)	5(1)	-2(1)
C22	30(2)	29(1)	35(2)	5(1)	-3(1)	-6(1)
C23	29(2)	44(2)	39(2)	15(1)	-7(1)	-6(1)
C24	34(2)	37(2)	47(2)	16(1)	7(1)	12(1)
C25	47(2)	30(1)	38(2)	3(1)	6(1)	13(1)
C26	35(2)	29(1)	29(2)	0(1)	2(1)	4(1)
C27	24(1)	24(1)	18(1)	-2(1)	0(1)	-6(1)
C28	24(1)	20(1)	23(1)	0(1)	-4(1)	-4(1)

Appendix H

Crystal tables for **3m**



Table 1. Crystal data and structure refinement.

Identification code	99src443
Empirical formula	C ₃₆ H ₃₆ B ₃ FeO ₂ P ₂ Re
Formula weight	837.07
Temperature	150(2) K
Wavelength	0.71073 Å
Crystal system	Monoclinic
Space group	C2/c
Unit cell dimensions	$a = 13.2009(3)$ Å $\alpha = 90^\circ$ $b = 15.8108(4)$ Å $\beta = 91.0570(10)^\circ$ $c = 16.0822(3)$ Å $\gamma = 90^\circ$
Volume	3356.05(13) Å ³
Z	4
Density (calculated)	1.657 Mg / m ³
Absorption coefficient	4.163 mm ⁻¹
$F(000)$	1656
Crystal	tabular; orange
Crystal size	0.25 × 0.10 × 0.10 mm ³
θ range for data collection	2.01 – 26.02°
Index ranges	$-16 \leq h \leq 16, -19 \leq k \leq 19, -19 \leq l \leq 19$
Reflections collected	12891
Independent reflections	3274 [$R_{int} = 0.0361$]
Completeness to $\theta = 26.02^\circ$	98.8 %
Max. and min. transmission	0.6809 and 0.4225
Refinement method	Full-matrix least-squares on F^2
Data / restraints / parameters	3274 / 2 / 285
Goodness-of-fit on F^2	1.060
Final R indices [$F^2 > 2\sigma(F^2)$]	$R_I = 0.0228, wR2 = 0.0534$
R indices (all data)	$R_I = 0.0249, wR2 = 0.0543$
Extinction coefficient	0.00103(8)
Largest diff. peak and hole	1.693 and -0.980 e Å ⁻³

Diffractometer: *Enraf Nonius KappaCCD* area detector (ϕ scans and ω scans to fill *Ewald* sphere). Data collection and cell refinement: *Denzo* (Z. Otwinowski & W. Minor, *Methods in Enzymology* (1997) Vol. 276: *Macromolecular Crystallography*, part A, pp. 307–326; C. W. Carter, Jr. & R. M. Sweet, Eds., Academic Press). Absorption correction: *SORTAV* (R. H. Blessing, *Acta Cryst. A51* (1995) 33–37; R. H. Blessing, *J. Appl. Cryst.* 30 (1997) 421–426). Program used to solve structure: *DIRDIF-96* (P. T. Beurskens, G. Beurskens, W. P. Bosman, R. de Gelder, S. Garcia-Granda, R. O. Gould, R. Israël & J. M. M. Smits (1996). Crystallography Laboratory, University of Nijmegen, The Netherlands. Program used to refine structure: *SHELXL97* (G. M. Sheldrick (1997), University of Göttingen, Germany).

Further information: <http://www.soton.ac.uk/~xservice/strat.htm>

Special details:

The two alternative positions of the disordered B2 atom are related by $-x, y, -z + 1/2$

Table 2. Atomic coordinates [$\times 10^4$], equivalent isotropic displacement parameters [$\text{\AA}^2 \times 10^3$] and site occupancy factors. U_{eq} is defined as one third of the trace of the orthogonalized U^{ij} tensor.

Atom	x	y	z	U_{eq}	S.o.f.
Re1	0	1836(1)	2500	24(1)	1
Fe1	0	-886(1)	2500	26(1)	1
P1	1400(1)	878(1)	2471(1)	22(1)	1
O1	-72(2)	1772(2)	573(2)	59(1)	1
B1	-663(4)	3271(3)	2530(4)	54(1)	1
B2	-163(8)	3832(6)	1774(7)	64(3)	0.50
C1	1216(2)	-189(2)	2846(2)	27(1)	1
C2	1544(2)	-1003(2)	2558(2)	36(1)	1
C3	1090(3)	-1631(2)	3052(2)	45(1)	1
C4	511(3)	-1231(2)	3662(2)	41(1)	1
C5	584(2)	-348(2)	3547(2)	31(1)	1
C6	-46(3)	1805(2)	1277(2)	37(1)	1
C11	2518(2)	1199(2)	3110(2)	33(1)	1
C12	3385(3)	710(3)	3086(2)	52(1)	1
C13	4224(3)	940(5)	3576(3)	80(2)	1
C14	4204(4)	1617(4)	4090(3)	78(2)	1
C15	3355(4)	2101(4)	4112(3)	64(1)	1
C16	2510(3)	1901(2)	3626(2)	42(1)	1
C21	1982(2)	794(2)	1446(2)	25(1)	1
C22	1890(2)	108(2)	908(2)	33(1)	1
C23	2347(3)	122(2)	142(2)	41(1)	1
C24	2883(3)	825(3)	-106(2)	47(1)	1
C25	2958(3)	1512(3)	407(2)	43(1)	1
C26	2505(2)	1502(2)	1176(2)	34(1)	1

Table 3. Bond lengths [Å] and angles [°].

Re1-C6 ⁱ	1.968(4)
Re1-C6	1.968(4)
Re1-P1 ⁱ	2.3911(7)
Re1-P1	2.3911(7)
Re1-B1 ⁱ	2.432(4)
Re1-B1	2.432(4)
Re1-H1B	1.83(3)
Fe1-C1 ⁱ	2.017(3)
Fe1-C1	2.017(3)
Fe1-C5 ⁱ	2.026(3)
Fe1-C5	2.026(3)
Fe1-C2 ⁱ	2.046(3)
Fe1-C2	2.046(3)
Fe1-C4 ⁱ	2.048(3)
Fe1-C4	2.048(3)
Fe1-C3 ⁱ	2.049(3)
Fe1-C3	2.049(3)
P1-C1	1.809(3)
P1-C21	1.837(3)
P1-C11	1.853(3)
O1-C6	1.134(4)
B1-B2	1.653(11)
B1-B1 ⁱ	1.754(10)
B1-H1B	1.21(3)
B1-H2B	1.06(5)
B1-H3B	1.10(5)
B2-B1 ⁱ	1.784(12)
B2-H3B	1.31(5)
B2-H4B	1.258(8)
B2-H5B	1.247(8)
C1-C2	1.437(4)
C1-C5	1.437(4)
C2-C3	1.412(5)
C2-H2	0.96(4)
C3-C4	1.404(5)
C3-H3	0.93(4)
C4-C5	1.412(5)
C4-H4	0.87(4)
C5-H5	0.89(3)
C11-C12	1.382(5)
C11-C16	1.385(5)
C12-C13	1.396(6)
C12-H12	0.88(3)
C13-C14	1.353(8)
C13-H13	0.82(4)
C14-C15	1.359(8)
C14-H14	0.91(6)
C15-C16	1.386(5)
C15-H15	0.80(4)
C16-H16	0.92(4)
C21-C26	1.389(4)
C21-C22	1.392(4)
C22-C23	1.381(4)
C22-H22	0.93(3)
C23-C24	1.381(6)
C23-H23	0.97(4)
C24-C25	1.366(6)
C24-H24	0.91(4)
C25-C26	1.384(5)

C25–H25	0.92(4)
C26–H26	0.90(3)
C6 ⁱ –Re1–C6	177.17(17)
C6 ⁱ –Re1–P1 ⁱ	88.57(9)
C6–Re1–P1 ⁱ	89.64(10)
C6 ⁱ –Re1–P1	89.64(10)
C6–Re1–P1	88.57(9)
P1 ⁱ –Re1–P1	101.34(3)
C6 ⁱ –Re1–B1 ⁱ	92.19(17)
C6–Re1–B1 ⁱ	90.45(17)
P1 ⁱ –Re1–B1 ⁱ	150.46(12)
P1–Re1–B1 ⁱ	108.20(12)
C6 ⁱ –Re1–B1	90.45(17)
C6–Re1–B1	92.19(17)
P1 ⁱ –Re1–B1	108.20(12)
P1–Re1–B1	150.46(12)
B1 ⁱ –Re1–B1	42.3(2)
C6 ⁱ –Re1–H1B	89.4(10)
C6–Re1–H1B	92.4(10)
P1 ⁱ –Re1–H1B	79.3(10)
P1–Re1–H1B	178.9(10)
B1 ⁱ –Re1–H1B	71.2(10)
B1–Re1–H1B	28.9(10)
C1 ⁱ –Fe1–C1	113.79(17)
C1 ⁱ –Fe1–C5 ⁱ	41.63(12)
C1–Fe1–C5 ⁱ	106.77(13)
C1 ⁱ –Fe1–C5	106.77(13)
C1–Fe1–C5	41.63(12)
C5 ⁱ –Fe1–C5	130.31(18)
C1 ⁱ –Fe1–C2 ⁱ	41.40(12)
C1–Fe1–C2 ⁱ	148.08(12)
C5 ⁱ –Fe1–C2 ⁱ	68.71(14)
C5–Fe1–C2 ⁱ	116.04(13)
C1 ⁱ –Fe1–C2	148.08(12)
C1–Fe1–C2	41.40(12)
C5 ⁱ –Fe1–C2	116.04(13)
C5–Fe1–C2	68.71(14)
C2 ⁱ –Fe1–C2	169.63(18)
C1 ⁱ –Fe1–C4 ⁱ	69.30(12)
C1–Fe1–C4 ⁱ	130.11(14)
C5 ⁱ –Fe1–C4 ⁱ	40.55(13)
C5–Fe1–C4 ⁱ	169.57(14)
C2 ⁱ –Fe1–C4 ⁱ	67.87(14)
C2–Fe1–C4 ⁱ	109.18(14)
C1 ⁱ –Fe1–C4	130.11(14)
C1–Fe1–C4	69.30(12)
C5 ⁱ –Fe1–C4	169.57(14)
C5–Fe1–C4	40.55(13)
C2 ⁱ –Fe1–C4	109.18(14)
C2–Fe1–C4	67.87(14)
C4 ⁱ –Fe1–C4	149.1(2)
C1 ⁱ –Fe1–C3 ⁱ	69.23(13)
C1–Fe1–C3 ⁱ	169.27(14)
C5 ⁱ –Fe1–C3 ⁱ	68.18(15)
C5–Fe1–C3 ⁱ	148.75(14)
C2 ⁱ –Fe1–C3 ⁱ	40.34(14)
C2–Fe1–C3 ⁱ	131.17(14)
C4 ⁱ –Fe1–C3 ⁱ	40.09(15)
C4–Fe1–C3 ⁱ	117.33(15)
C1 ⁱ –Fe1–C3	169.27(14)

C1–Fe1–C3	69.23(13)
C5 ⁱ –Fe1–C3	148.75(14)
C5–Fe1–C3	68.18(15)
C2 ⁱ –Fe1–C3	131.17(14)
C2–Fe1–C3	40.34(14)
C4 ⁱ –Fe1–C3	117.33(15)
C4–Fe1–C3	40.09(15)
C3 ⁱ –Fe1–C3	109.8(2)
C1–P1–C21	107.03(13)
C1–P1–C11	100.43(13)
C21–P1–C11	100.10(13)
C1–P1–Re1	118.43(9)
C21–P1–Re1	113.52(9)
C11–P1–Re1	115.06(11)
B2–B1–B1 ⁱ	63.1(5)
B2–B1–Re1	109.74(4)
B1 ⁱ –B1–Re1	68.86(12)
B2–B1–H1B	132.3(16)
B1 ⁱ –B1–H1B	115.8(15)
Re1–B1–H1B	46.9(15)
B2–B1–H2B	122(3)
B1 ⁱ –B1–H2B	119(3)
Re1–B1–H2B	125(3)
H1B–B1–H2B	100(3)
B2–B1–H3B	52(3)
B1 ⁱ –B1–H3B	114(3)
Re1–B1–H3B	120(3)
H1B–B1–H3B	99(3)
H2B–B1–H3B	107(4)
B1–B2–B1 ⁱ	61.3(5)
B1–B2–H3B	41(2)
B1 ⁱ –B2–H3B	102(2)
B1–B2–H4B	88(3)
B1 ⁱ –B2–H4B	87(3)
H3B–B2–H4B	100(4)
B1–B2–H5B	120(4)
B1 ⁱ –B2–H5B	113(4)
H3B–B2–H5B	97(5)
H4B–B2–H5B	151(5)
C2–C1–C5	106.2(3)
C2–C1–P1	133.2(2)
C5–C1–P1	120.5(2)
C2–C1–Fe1	70.40(18)
C5–C1–Fe1	69.52(17)
P1–C1–Fe1	121.88(14)
C3–C2–C1	108.4(3)
C3–C2–Fe1	69.9(2)
C1–C2–Fe1	68.20(17)
C3–C2–H2	127(2)
C1–C2–H2	125(2)
Fe1–C2–H2	126(2)
C4–C3–C2	108.5(3)
C4–C3–Fe1	69.94(19)
C2–C3–Fe1	69.74(19)
C4–C3–H3	127(2)
C2–C3–H3	124(2)
Fe1–C3–H3	122(2)
C3–C4–C5	108.4(3)
C3–C4–Fe1	70.0(2)
C5–C4–Fe1	68.88(18)
C3–C4–H4	129(3)

C5–C4–H4	122(3)
Fe1–C4–H4	125(3)
C4–C5–C1	108.5(3)
C4–C5–Fe1	70.57(19)
C1–C5–Fe1	68.84(17)
C4–C5–H5	127(2)
C1–C5–H5	124(2)
Fe1–C5–H5	124(2)
O1–C6–R ₁	178.7(3)
C12–C11–C16	118.7(3)
C12–C11–P1	118.8(3)
C16–C11–P1	122.5(3)
C11–C12–C13	119.2(5)
C11–C12–H12	120(2)
C13–C12–H12	121(2)
C14–C13–C12	121.8(5)
C14–C13–H13	128(3)
C12–C13–H13	110(3)
C13–C14–C15	119.1(4)
C13–C14–H14	120(3)
C15–C14–H14	121(3)
C14–C15–C16	120.8(5)
C14–C15–H15	118(3)
C16–C15–H15	121(3)
C11–C16–C15	120.4(4)
C11–C16–H16	119(2)
C15–C16–H16	121(2)
C26–C21–C22	118.1(3)
C26–C21–P1	116.2(2)
C22–C21–P1	125.6(2)
C23–C22–C21	120.5(3)
C23–C22–H22	117.7(19)
C21–C22–H22	121.8(19)
C24–C23–C22	120.3(3)
C24–C23–H23	121(2)
C22–C23–H23	119(2)
C25–C24–C23	119.9(3)
C25–C24–H24	121(3)
C23–C24–H24	119(3)
C24–C25–C26	120.2(3)
C24–C25–H25	121(3)
C26–C25–H25	119(3)
C25–C26–C21	121.0(3)
C25–C26–H26	120(2)
C21–C26–H26	119(2)

Symmetry transformations used to generate equivalent atoms:
 (i) $-x, y, -z + \frac{1}{2}$

Table 4. Anisotropic displacement parameters [$\text{\AA}^2 \times 10^3$]. The anisotropic displacement factor exponent takes the form: $-2\pi^2[h^2a^{*2}U^{11} + \dots + 2hk a^* b^* U^{12}]$.

Atom	U^{11}	U^{22}	U^{33}	U^{23}	U^{13}	U^{12}
Re1	28(1)	22(1)	20(1)	0	6(1)	0
Fe1	29(1)	23(1)	27(1)	0	-1(1)	0
P1	21(1)	26(1)	19(1)	1(1)	2(1)	-2(1)
O1	71(2)	86(2)	22(1)	10(1)	10(1)	38(2)
B1	55(3)	25(2)	81(4)	-5(2)	8(3)	6(2)
B2	65(6)	31(4)	98(8)	20(5)	37(6)	12(4)
C1	22(1)	32(2)	26(1)	4(1)	-3(1)	1(1)
C2	31(2)	33(2)	44(2)	9(1)	-1(1)	10(1)
C3	46(2)	29(2)	58(2)	13(2)	-5(2)	6(2)
C4	45(2)	42(2)	37(2)	17(2)	-6(2)	-10(2)
C5	32(2)	38(2)	23(2)	5(1)	-2(1)	-5(1)
C6	34(2)	40(2)	37(2)	7(1)	10(1)	15(1)
C11	27(2)	47(2)	24(1)	4(1)	1(1)	-12(1)
C12	30(2)	89(3)	36(2)	-5(2)	-5(1)	1(2)
C13	28(2)	151(6)	59(3)	6(3)	-11(2)	4(3)
C14	47(3)	144(5)	42(2)	4(3)	-17(2)	-42(3)
C15	62(3)	94(3)	37(2)	-5(2)	-10(2)	-47(3)
C16	42(2)	51(2)	33(2)	1(2)	0(2)	-22(2)
C21	21(1)	33(2)	21(1)	2(1)	2(1)	2(1)
C22	32(2)	35(2)	31(2)	-2(1)	4(1)	2(1)
C23	42(2)	53(2)	28(2)	-9(2)	7(1)	5(2)
C24	41(2)	72(3)	27(2)	4(2)	13(1)	3(2)
C25	37(2)	55(2)	36(2)	12(2)	9(1)	-9(2)
C26	34(2)	40(2)	29(2)	-2(2)	4(1)	-6(2)

Table 5. Hydrogen coordinates [$\times 10^4$] and isotropic displacement parameters [$\text{\AA}^2 \times 10^3$].

Atom	<i>x</i>	<i>y</i>	<i>z</i>	<i>U</i> _{eq}	S.o.f.
H2	1980(30)	-1090(20)	2100(20)	53(11)	1
H3	1130(30)	-2210(20)	2950(20)	40(9)	1
H4	140(30)	-1450(30)	4040(20)	49(11)	1
H5	280(20)	50(20)	3837(19)	26(8)	1
H12	3410(20)	280(20)	2740(20)	33(9)	1
H13	4660(30)	570(20)	3550(30)	49(12)	1
H14	4740(40)	1730(30)	4430(40)	99(19)	1
H15	3340(30)	2480(30)	4440(30)	57(13)	1
H16	1940(30)	2240(20)	3630(20)	40(10)	1
H22	1530(20)	-370(20)	1047(19)	24(8)	1
H23	2260(30)	-360(20)	-230(20)	40(9)	1
H24	3140(30)	840(30)	-620(30)	62(12)	1
H25	3280(30)	2000(20)	240(20)	52(11)	1
H26	2540(20)	1960(19)	1510(20)	24(8)	1
H1B	-1060(20)	2580(20)	2541(19)	35(8)	1
H2B	-1000(30)	3560(30)	3060(30)	82(14)	1
H3B	-1050(40)	3530(30)	1980(30)	94(16)	1
H4B	-100(60)	4440(20)	2270(30)	30	0.50
H5B	-160(70)	3540(60)	1050(20)	80(30)	0.50

Appendix I

Crystal tables for **4c**

PSB



University of Southampton · Department of Chemistry

EPSRC National Crystallography Service



Table 1. Crystal data and structure refinement.

Identification code	00src161		
Empirical formula	$C_{24}H_{15}BF_{15}OP$		
Formula weight	646.14		
Temperature	150(2) K		
Wavelength	0.71073 Å		
Crystal system	Triclinic		
Space group	$P\bar{1}$		
Unit cell dimensions	$a = 10.344(2)$ Å	$\alpha = 74.39(3)^\circ$	
	$b = 11.174(2)$ Å	$\beta = 89.09(3)^\circ$	
	$c = 11.553(2)$ Å	$\gamma = 84.29(3)^\circ$	
Volume	1279.5(4) Å ³		
Z	2		
Density (calculated)	1.677 Mg / m ³		
Absorption coefficient	0.236 mm ⁻¹		
$F(000)$	644		
Crystal	Prism; colourless		
Crystal size	0.30 × 0.15 × 0.15 mm ³		
θ range for data collection	2.26 – 27.55°		
Index ranges	−13 ≤ h ≤ 11, −14 ≤ k ≤ 14, −15 ≤ l ≤ 15		
Reflections collected	19170		
Independent reflections	5853 [$R_{int} = 0.0499$]		
Completeness to $\theta = 27.55^\circ$	99.1 %		
Absorption correction	Semi-empirical from equivalents		
Max. and min. transmission	0.9655 and 0.9327		
Refinement method	Full-matrix least-squares on F^2		
Data / restraints / parameters	5853 / 0 / 382		
Goodness-of-fit on F^2	0.891		
Final R indices [$F^2 > 2\sigma(F^2)$]	$R_I = 0.0506$, $wR_2 = 0.1286$		
R indices (all data)	$R_I = 0.1150$, $wR_2 = 0.1604$		
Largest diff. peak and hole	0.296 and −0.303 e Å ^{−3}		

Diffractometer: *Enraf Nonius KappaCCD* area detector (ϕ scans and ω scans to fill *Ewald sphere*). Data collection and cell refinement: *Denzo* (Z. Otwinowski & W. Minor, *Methods in Enzymology* (1997) Vol. 276: *Macromolecular Crystallography*, part A, pp. 307–326; C. W. Carter, Jr. & R. M. Sweet, Eds., Academic Press). Absorption correction: *SORTAV* (R. H. Blessing, *Acta Cryst. A*51 (1995) 33–37; R. H. Blessing, *J. Appl. Cryst.* **30** (1997) 421–426). Program used to solve structure: *SHELXS97* (G. M. Sheldrick, *Acta Cryst. (1990) A46* 467–473). Program used to refine structure: *SHELXL97* (G. M. Sheldrick (1997), University of Göttingen, Germany).

Further information: <http://www.soton.ac.uk/~xservice/strat.htm>

Special details:

Table 2. Atomic coordinates [$\times 10^4$], equivalent isotropic displacement parameters [$\text{\AA}^2 \times 10^3$] and site occupancy factors. U_{eq} is defined as one third of the trace of the orthogonalized U^{ij} tensor.

Atom	x	y	z	U_{eq}	S.o.f.
P1	3407(1)	6943(1)	1423(1)	52(1)	1
F1	5573(1)	9003(2)	1411(1)	68(1)	1
F2	8132(2)	8627(2)	1702(2)	97(1)	1
F3	9193(2)	7636(2)	3941(2)	99(1)	1
F4	7621(2)	7040(2)	5863(2)	90(1)	1
F5	5077(2)	7405(2)	5602(1)	76(1)	1
F6	3037(2)	5824(1)	4494(2)	81(1)	1
F7	1391(2)	5191(2)	6274(2)	96(1)	1
F8	219(2)	6925(2)	7304(2)	94(1)	1
F9	727(2)	9334(2)	6471(2)	101(1)	1
F10	2332(2)	10008(2)	4663(2)	93(1)	1
F11	4855(2)	10831(1)	2826(2)	76(1)	1
F12	3872(2)	13048(1)	1526(2)	85(1)	1
F13	1539(2)	13334(2)	412(2)	99(1)	1
F14	161(2)	11318(2)	682(2)	94(1)	1
F15	1107(1)	9093(1)	2008(2)	71(1)	1
O1	3369(2)	7520(2)	2453(1)	52(1)	1
B1	3606(3)	8403(2)	3222(2)	46(1)	1
C1	6044(2)	8494(2)	2550(2)	52(1)	1
C2	7366(3)	8316(3)	2668(2)	62(1)	1
C3	7910(3)	7821(3)	3797(3)	67(1)	1
C4	7103(3)	7526(2)	4758(2)	60(1)	1
C5	5775(2)	7727(2)	4592(2)	54(1)	1
C6	5168(2)	8218(2)	3488(2)	47(1)	1
C7	2710(2)	7973(2)	4414(2)	48(1)	1
C8	2434(2)	6762(2)	4907(2)	54(1)	1
C9	1613(3)	6395(3)	5854(2)	62(1)	1
C10	1027(3)	7259(3)	6375(2)	64(1)	1
C11	1284(3)	8467(3)	5951(2)	65(1)	1
C12	2106(3)	8796(2)	5006(2)	58(1)	1
C13	3067(2)	9819(2)	2437(2)	46(1)	1
C14	3688(2)	10883(2)	2287(2)	54(1)	1
C15	3194(3)	12046(2)	1621(2)	61(1)	1
C16	2025(3)	12204(2)	1073(2)	65(1)	1
C17	1339(3)	11183(3)	1203(2)	63(1)	1
C18	1857(2)	10042(2)	1881(2)	53(1)	1
C19	5010(3)	6186(3)	1276(3)	80(1)	1
C20	5548(4)	5278(3)	2411(4)	104(1)	1
C21	2324(3)	5778(3)	1680(3)	80(1)	1
C22	964(3)	6216(3)	1885(4)	102(1)	1
C23	3030(3)	8082(3)	38(2)	66(1)	1
C24	2881(3)	7594(4)	-1061(3)	93(1)	1

Table 3. Bond lengths [\AA] and angles [°].

P1–O1	1.4973(17)
P1–C21	1.763(3)
P1–C23	1.776(3)
P1–C19	1.811(3)
F1–C1	1.361(3)
F2–C2	1.347(3)
F3–C3	1.329(3)
F4–C4	1.343(3)
F5–C5	1.346(3)
F6–C8	1.358(3)
F7–C9	1.344(3)
F8–C10	1.344(3)
F9–C11	1.350(3)
F10–C12	1.348(3)
F11–C14	1.356(3)
F12–C15	1.358(3)
F13–C16	1.340(3)
F14–C17	1.344(3)
F15–C18	1.351(3)
O1–B1	1.533(3)
B1–C6	1.632(4)
B1–C7	1.636(4)
B1–C13	1.645(3)
C1–C2	1.366(4)
C1–C6	1.391(3)
C2–C3	1.377(4)
C3–C4	1.366(4)
C4–C5	1.377(4)
C5–C6	1.379(3)
C7–C8	1.376(3)
C7–C12	1.384(3)
C8–C9	1.373(4)
C9–C10	1.359(4)
C10–C11	1.358(4)
C11–C12	1.366(4)
C13–C14	1.376(3)
C13–C18	1.384(3)
C14–C15	1.373(3)
C15–C16	1.348(4)
C16–C17	1.376(4)
C17–C18	1.366(4)
C19–C20	1.501(4)
C21–C22	1.479(4)
C23–C24	1.526(4)
O1–P1–C21	109.81(13)
O1–P1–C23	111.50(12)
C21–P1–C23	110.52(15)
O1–P1–C19	110.97(13)
C21–P1–C19	106.86(15)
C23–P1–C19	107.07(15)
P1–O1–B1	161.04(16)
O1–B1–C6	105.70(19)
O1–B1–C7	105.30(18)
C6–B1–C7	114.79(19)
O1–B1–C13	106.79(18)
C6–B1–C13	113.8(2)
C7–B1–C13	109.66(19)
F1–C1–C2	115.9(2)

F1-C1-C6	118.8(2)
C2-C1-C6	125.4(2)
F2-C2-C1	120.8(2)
F2-C2-C3	120.2(2)
C1-C2-C3	119.0(3)
F3-C3-C4	121.1(3)
F3-C3-C2	120.4(3)
C4-C3-C2	118.6(2)
F4-C4-C3	119.1(2)
F4-C4-C5	120.6(3)
C3-C4-C5	120.3(2)
F5-C5-C4	115.1(2)
F5-C5-C6	120.8(2)
C4-C5-C6	124.1(2)
C5-C6-C1	112.7(2)
C5-C6-B1	126.5(2)
C1-C6-B1	120.7(2)
C8-C7-C12	112.7(2)
C8-C7-B1	123.6(2)
C12-C7-B1	123.6(2)
F6-C8-C9	115.3(2)
F6-C8-C7	120.0(2)
C9-C8-C7	124.6(2)
F7-C9-C10	119.8(2)
F7-C9-C8	120.6(3)
C10-C9-C8	119.6(2)
F8-C10-C9	120.8(3)
F8-C10-C11	120.4(3)
C9-C10-C11	118.8(2)
F9-C11-C10	119.6(2)
F9-C11-C12	120.5(3)
C10-C11-C12	119.9(3)
F10-C12-C11	115.9(2)
F10-C12-C7	119.7(2)
C11-C12-C7	124.4(2)
C14-C13-C18	113.1(2)
C14-C13-B1	126.4(2)
C18-C13-B1	120.4(2)
F11-C14-C15	115.5(2)
F11-C14-C13	120.4(2)
C15-C14-C13	124.1(2)
C16-C15-F12	119.6(2)
C16-C15-C14	120.2(3)
F12-C15-C14	120.2(3)
F13-C16-C15	120.7(3)
F13-C16-C17	120.6(3)
C15-C16-C17	118.8(2)
F14-C17-C18	120.6(3)
F14-C17-C16	120.0(2)
C18-C17-C16	119.3(3)
F15-C18-C17	116.0(2)
F15-C18-C13	119.6(2)
C17-C18-C13	124.4(3)
C20-C19-P1	114.5(3)
C22-C21-P1	114.5(2)
C24-C23-P1	116.5(2)

Symmetry transformations used to generate equivalent atoms:

Table 4. Anisotropic displacement parameters [$\text{\AA}^2 \times 10^3$]. The anisotropic displacement factor exponent takes the form: $-2\pi^2[h^2a^{*2}U^{11} + \dots + 2hk a^* b^* U^{12}]$.

Atom	U^{11}	U^{22}	U^{33}	U^{23}	U^{13}	U^{12}
P1	61(1)	49(1)	46(1)	-16(1)	-3(1)	-2(1)
F1	61(1)	91(1)	44(1)	-6(1)	3(1)	-9(1)
F2	57(1)	148(2)	82(1)	-25(1)	19(1)	-15(1)
F3	50(1)	134(2)	108(1)	-30(1)	-14(1)	0(1)
F4	84(1)	108(1)	68(1)	-5(1)	-30(1)	-4(1)
F5	73(1)	105(1)	45(1)	-7(1)	-1(1)	-15(1)
F6	120(1)	47(1)	71(1)	-12(1)	27(1)	0(1)
F7	123(2)	77(1)	85(1)	-6(1)	31(1)	-40(1)
F8	83(1)	129(2)	67(1)	-18(1)	31(1)	-22(1)
F9	130(2)	101(1)	73(1)	-37(1)	37(1)	11(1)
F10	157(2)	60(1)	71(1)	-31(1)	37(1)	-21(1)
F11	73(1)	56(1)	99(1)	-21(1)	-16(1)	-10(1)
F12	99(1)	47(1)	106(1)	-12(1)	14(1)	-12(1)
F13	115(2)	63(1)	99(1)	4(1)	-8(1)	23(1)
F14	67(1)	103(1)	101(1)	-20(1)	-24(1)	22(1)
F15	50(1)	72(1)	91(1)	-24(1)	-1(1)	-7(1)
O1	61(1)	54(1)	46(1)	-20(1)	2(1)	-7(1)
B1	54(2)	44(1)	41(1)	-13(1)	1(1)	-6(1)
C1	53(2)	57(1)	47(1)	-14(1)	-2(1)	-4(1)
C2	55(2)	74(2)	60(2)	-22(1)	8(1)	-8(1)
C3	47(2)	72(2)	84(2)	-25(2)	-9(1)	1(1)
C4	62(2)	59(2)	59(2)	-13(1)	-18(1)	-2(1)
C5	61(2)	51(1)	50(1)	-14(1)	-2(1)	-6(1)
C6	51(1)	43(1)	47(1)	-13(1)	-1(1)	-3(1)
C7	51(1)	52(1)	41(1)	-14(1)	1(1)	-7(1)
C8	59(2)	52(2)	51(1)	-13(1)	3(1)	-5(1)
C9	65(2)	65(2)	53(2)	-5(1)	6(1)	-17(1)
C10	54(2)	92(2)	46(1)	-13(1)	11(1)	-14(2)
C11	71(2)	77(2)	50(2)	-24(1)	11(1)	2(2)
C12	74(2)	52(2)	50(1)	-16(1)	8(1)	-7(1)
C13	49(1)	49(1)	40(1)	-13(1)	7(1)	-3(1)
C14	58(2)	49(1)	54(1)	-14(1)	3(1)	-3(1)
C15	73(2)	46(2)	62(2)	-12(1)	14(1)	-3(1)
C16	76(2)	51(2)	57(2)	-2(1)	6(1)	12(1)
C17	56(2)	72(2)	58(2)	-16(1)	-2(1)	14(1)
C18	50(1)	59(2)	53(1)	-21(1)	8(1)	-2(1)
C19	85(2)	80(2)	80(2)	-37(2)	-1(2)	14(2)
C20	100(3)	91(3)	117(3)	-37(2)	-31(2)	33(2)
C21	100(2)	65(2)	79(2)	-24(2)	-3(2)	-17(2)
C22	80(2)	95(3)	126(3)	-20(2)	5(2)	-18(2)
C23	67(2)	79(2)	49(1)	-10(1)	-4(1)	-9(1)
C24	84(2)	141(3)	56(2)	-35(2)	-10(2)	5(2)

Table 5. Hydrogen coordinates [$\times 10^4$] and isotropic displacement parameters [$\text{\AA}^2 \times 10^3$].

Atom	<i>x</i>	<i>y</i>	<i>z</i>	<i>U</i> _{eq}	<i>S.o.f.</i>
H19A	4975	5748	660	96	1
H19B	5603	6823	1007	96	1
H20A	5584	5700	3030	156	1
H20B	6407	4939	2268	156	1
H20C	4997	4614	2660	156	1
H21A	2341	5434	993	95	1
H21B	2629	5109	2375	95	1
H22A	902	6380	2659	153	1
H22B	410	5584	1856	153	1
H22C	699	6968	1273	153	1
H23A	2227	8570	135	79	1
H23B	3708	8643	-123	79	1
H24A	3683	7144	-1198	140	1
H24B	2664	8283	-1752	140	1
H24C	2202	7047	-924	140	1

Appendix J

Crystal tables for **4f**



Table 1. Crystal data and structure refinement.

Identification code	00SRC095	
Empirical formula	$C_{36}H_{15}BF_{15}OP$	
Formula weight	790.26	
Temperature	150(2) K	
Wavelength	0.71073 Å	
Crystal system	Monoclinic	
Space group	$C2/c$	
Unit cell dimensions	$a = 31.0247(4)$ Å	
	$b = 9.4124(2)$ Å	$\beta = 105.9570(9)^\circ$
	$c = 22.5961(3)$ Å	
Volume	$6344.19(18)$ Å ³	
Z	8	
Density (calculated)	1.655 Mg / m ³	
Absorption coefficient	0.207 mm ⁻¹	
$F(000)$	3152	
Crystal	Colourless block	
Crystal size	$0.10 \times 0.10 \times 0.05$ mm ³	
θ range for data collection	2.95 – 25.03°	
Index ranges	$-36 \leq h \leq 36, -11 \leq k \leq 11, -26 \leq l \leq 25$	
Reflections collected	31694	
Independent reflections	5572 [$R_{int} = 0.0690$]	
Completeness to $\theta = 25.03^\circ$	99.5 %	
Absorption correction	Multiscan, SORTAV	
Max. and min. transmission	0.9897 and 0.9796	
Refinement method	Full-matrix least-squares on F^2	
Data / restraints / parameters	5572 / 0 / 548	
Goodness-of-fit on F^2	1.036	
Final R indices [$F^2 > 2\sigma(F^2)$]	$RI = 0.0395, wR2 = 0.0934$	
R indices (all data)	$RI = 0.0620, wR2 = 0.1031$	
Extinction coefficient	0.00049(11)	
Largest diff. peak and hole	0.265 and -0.381 e Å ⁻³	

Diffractometer: *Enraf Nonius KappaCCD* area detector (ϕ scans and ω scans to fill *Ewald* sphere). **Data collection and cell refinement:** *Denzo* (Z. Otwinowski & W. Minor, *Methods in Enzymology* (1997) Vol. 276: *Macromolecular Crystallography*, part A, pp. 307–326; C. W. Carter, Jr. & R. M. Sweet, Eds., Academic Press). **Absorption correction:** *SORTAV* (R. H. Blessing, *Acta Cryst. A*51 (1995) 33–37; R. H. Blessing, *J. Appl. Cryst.* 30 (1997) 421–426). **Program used to solve structure:** *SHELXS97* (G. M. Sheldrick, *Acta Cryst.* (1990) A46 467–473). **Program used to refine structure:** *SHELXL97* (G. M. Sheldrick (1997), University of Göttingen, Germany).

Further information: <http://www.soton.ac.uk/~xservice/strat.htm>

Special details: All hydrogen atoms were located from the difference map and fully refined.

Table 3. Bond lengths [\AA] and angles [$^\circ$].

P1–O1	1.4971(15)	C1–C6	1.388(3)
P1–C13	1.783(2)	C1–C2	1.390(3)
P1–C1	1.791(2)	C24–C23	1.368(3)
P1–C7	1.791(2)	C33–C32	1.373(3)
F11–C32	1.355(2)	C33–C34	1.374(3)
F12–C33	1.345(2)	C36–C35	1.382(3)
F14–C35	1.345(3)	C13–C14	1.390(3)
F5–C24	1.357(3)	C13–C18	1.398(3)
F6–C26	1.353(2)	C30–C29	1.375(3)
F15–C36	1.357(2)	C30–C25	1.388(3)
O1–B1	1.538(3)	C34–C35	1.365(3)
F9–C29	1.346(3)	C18–C17	1.375(3)
F1–C20	1.353(2)	C25–B1	1.639(3)
F2–C21	1.346(3)	C28–C27	1.374(3)
F8–C28	1.347(3)	C28–C29	1.374(4)
F7–C27	1.345(3)	C23–C22	1.376(4)
F10–C30	1.355(3)	C9–C10	1.371(4)
F4–C23	1.347(3)	C9–C8	1.393(3)
F13–C34	1.350(2)	C20–C21	1.381(3)
F3–C22	1.347(3)	C12–C11	1.380(3)
C26–C27	1.375(3)	C21–C22	1.368(3)
C26–C25	1.389(3)	C6–C5	1.392(4)
C7–C8	1.383(3)	C10–C11	1.381(4)
C7–C12	1.395(3)	C3–C2	1.379(4)
C31–C36	1.382(3)	C3–C4	1.388(4)
C31–C32	1.393(3)	C16–C15	1.380(3)
C31–B1	1.643(3)	C16–C17	1.384(3)
C19–C20	1.385(3)	C15–C14	1.383(4)
C19–C24	1.395(3)	C4–C5	1.369(4)
C19–B1	1.632(3)		
O1–P1–C13	109.85(9)	C36–C31–C32	113.50(18)
O1–P1–C1	109.52(9)	C36–C31–B1	126.09(19)
C13–P1–C1	108.89(10)	C32–C31–B1	120.39(19)
O1–P1–C7	109.63(9)	C20–C19–C24	113.3(2)
C13–P1–C7	108.70(10)	C20–C19–B1	126.15(18)
C1–P1–C7	110.23(10)	C24–C19–B1	120.49(19)
P1–O1–B1	178.66(16)	C6–C1–C2	120.2(2)
F6–C26–C27	116.4(2)	C6–C1–P1	120.99(19)
F6–C26–C25	119.37(19)	C2–C1–P1	118.70(17)
C27–C26–C25	124.3(2)	F5–C24–C23	116.46(19)
C8–C7–C12	120.3(2)	F5–C24–C19	118.90(19)
C8–C7–P1	122.12(17)	C23–C24–C19	124.6(2)
C12–C7–P1	117.60(17)	F12–C33–C32	121.2(2)

F12–C33–C34	119.73(18)	C21–C20–C19	124.0(2)
C32–C33–C34	119.1(2)	C11–C12–C7	119.6(2)
F15–C36–C31	120.96(18)	F7–C27–C28	119.7(2)
F15–C36–C35	115.03(19)	F7–C27–C26	121.0(2)
C31–C36–C35	124.0(2)	C28–C27–C26	119.3(2)
C14–C13–C18	119.3(2)	F2–C21–C22	120.1(2)
C14–C13–P1	121.66(16)	F2–C21–C20	120.4(2)
C18–C13–P1	119.03(17)	C22–C21–C20	119.5(2)
F10–C30–C29	115.52(19)	F3–C22–C21	120.1(2)
F10–C30–C25	120.7(2)	F3–C22–C23	120.5(2)
C29–C30–C25	123.8(2)	C21–C22–C23	119.4(2)
F13–C34–C35	120.2(2)	C1–C6–C5	119.0(3)
F13–C34–C33	120.3(2)	F9–C29–C28	119.5(2)
C35–C34–C33	119.49(19)	F9–C29–C30	120.8(2)
C17–C18–C13	120.2(2)	C28–C29–C30	119.7(2)
F11–C32–C33	116.11(19)	C9–C10–C11	120.3(2)
F11–C32–C31	119.53(18)	C7–C8–C9	119.2(2)
C33–C32–C31	124.4(2)	C2–C3–C4	119.5(3)
C30–C25–C26	113.7(2)	C3–C2–C1	120.2(3)
C30–C25–B1	126.03(19)	O1–B1–C19	104.91(17)
C26–C25–B1	120.12(18)	O1–B1–C25	105.12(17)
F8–C28–C27	119.9(2)	C19–B1–C25	113.67(17)
F8–C28–C29	121.0(2)	O1–B1–C31	105.06(16)
C27–C28–C29	119.1(2)	C19–B1–C31	112.69(18)
F14–C35–C34	119.99(19)	C25–B1–C31	114.21(18)
F14–C35–C36	120.5(2)	C15–C16–C17	120.4(2)
C34–C35–C36	119.5(2)	C18–C17–C16	120.0(2)
F4–C23–C24	121.2(2)	C16–C15–C14	119.9(2)
F4–C23–C22	119.6(2)	C15–C14–C13	120.2(2)
C24–C23–C22	119.1(2)	C12–C11–C10	120.2(3)
C10–C9–C8	120.5(2)	C5–C4–C3	120.5(3)
F1–C20–C21	115.3(2)	C4–C5–C6	120.6(3)
F1–C20–C19	120.69(19)		

Symmetry transformations used to generate equivalent atoms:
